

The Palaeolithic of the Avon valley

**A geoarchaeological approach to the hominin
colonisation of Britain**

Volume II of II

Ella Egberts

Dissertation submitted in partial fulfilment of the requirements for the degree 'Doctor of
Philosophy', awarded by Bournemouth University

October 2016

Table of Contents Volume II

Appendix 1	Artefact numbers.....	1
Appendix 2	Artefact data collection.....	1
Appendix 3	Bemerton site recordings	6
Appendix 4	Bemerton sediment logs.....	13
Appendix 5	Hatchet Gate Farm site recordings.....	14
Appendix 6	Hatchet Gate Farm sediment log.....	25
Appendix 7	Woodriding site recordings.....	26
Appendix 8	Woodriding sediment log.....	34
Appendix 9	Woodgreen site recordings	35
Appendix 10	Woodgreen sediment logs.....	44
Appendix 11	Somerley site recordings.....	47
Appendix 12	Somerley sediment logs	59
Appendix 13	Ashley site recordings.....	62
Appendix 14	Ashley sediment log.....	67
Appendix 15	Bickton site recordings	70
Appendix 16	Bemerton clast size distributions	74
Appendix 17	Bemerton clast size distribution statistics	79
Appendix 18	Hatchet Gate Farm clast size distribution	83
Appendix 19	Hatchet Gate Farm clast size distribution statistics	88
Appendix 20	Image-based automated grain-sizing at Hatchet Gate Farm	92
Appendix 21	Woodriding clast size distributions.....	96
Appendix 22	Woodriding clast size distribution statistics	102
Appendix 23	Woodgreen clast size distributions	106
Appendix 24	Woodgreen clast size distribution statistics	113
Appendix 25	Image-based automated grain-sizing at Woodgreen.....	117

Appendix 26	Somerley clast size distributions.....	124
Appendix 27	Somerley clast size distribution statistics.....	132
Appendix 28	Image-based automated grain-sizing at Somerley	136
Appendix 29	Ashely clast size distributions.....	144
Appendix 30	Ashley clast size distribution statistics.....	149
Appendix 31	Image-based automated grain-sizing at Ashley	153
Appendix 32	Clast lithology of all size fractions.....	159
Appendix 33	Clast angularity-roundedness	162
Appendix 34	Details on equivalent dose and dose rate estimation for OSL dating	163
34.1	Introduction.....	163
34.2	Specifications of D_e acquisition.....	163
34.3	Test procedures	163
34.3.1	Laboratory factors.....	163
34.3.2	Environmental factors	165
Appendix 35	Details of OSL dating results	166
35.1	Explanation of diagnostic diagrams.....	166
Appendix 36	Diagnostics of OSL results presented per site.....	169
	Bemerton GL14038	169
	Bemerton GL14039	172
	Bemerton GL14040	175
	Bemerton GL14041	178
	Hatchet Gate Farm GL14045	181
	Hatchet Gate Farm GL14046	184
	Woodriding GL14047	187
	Woodriding GL14048	190
	Woodgreen GL14042	193

Woodgreen GL14043	196
Woodgreen GL14044	199
Somerley GL15038	202
Somerley GL15039	205
Somerley GL15040	208
Somerley GL15041	211
Somerley GL15042	214
Ashley GL15033	217
Ashley GL15034	220
Ashley GL15035	223
Ashley GL15036	226
Ashley GL15037	229
Bickton GL15075	232
Bickton GL15076	235
Bickton GL15077	238
Bickton GL15078	241
Appendix 37 Table summarising the number of artefacts studied per site and their current location.	244
Appendix 38 Possible Levallois artefacts from Bemerton	245
Appendix 39 Possible Levallois artefacts from Milford Hill	246
Appendix 40 Possible Levallois artefacts from Woodgreen	248
Appendix 41 Comparison of the condition of biface types	251
Appendix 42 Statistical analysis of artefact data for the comparison of the sites.....	255
Appendix 43 Average artefact size and shape of per abrasion category	269
Appendix 44 Groups of artefacts from Bemerton, Milford Hill and Woodgreen in various conditions	273

List of Figures Volume II

Figure A3.1 Map showing the location of the site of Bemerton pit in relationship to the local bedrock and superficial geology (based upon 1:10000 scale geology data with permission of the British Geological Survey and 1:10000 scale OS VectorMap Local [shape file], Digimap Licence).....	7
Figure A3.2 Terrestrial laser scan of Bemerton pit, providing an overview of the site and the locations of section 2 and pit 1.....	8
Figure A3.3 Annotated photograph of section 2 at Bemerton pit.....	9
Figure A3.4 Drawing of section 2 at Bemerton pit.....	10
Figure A3.5 Drawing of pit 1 at Bemerton pit.....	11
Figure A3.6 Detailed laser scan of section 2 at Bemerton.....	12
Figure A5.1 Map showing the location of the site of Hatchet Gate Farm pit in relationship to the local bedrock and superficial geology (based upon 1:10000 scale geology data with permission of the British Geological Survey and 1:10000 scale OS VectorMap Local [shape file], Digimap Licence).....	15
Figure A5.2 Terrestrial laser scan of Hatchet Gate Farm pit, providing an overview of the north, east and south sections of the pit.....	16
Figure A5.3 Drawing of Hatchet Gate Farm pit, providing an overview of the north, east and south sections of the pit.....	17
Figure A5.4 Overview annotated photograph of Hatchet Gate Farm pit.....	18
Figure A5.5 Annotated photograph of the south section at Hatchet Gate Farm pit.....	19
Figure A5.6 Annotated photograph of the north section at Hatchet Gate Farm pit.....	20
Figure A5.7 Drawing of the south section at Hatchet Gate Farm pit.....	21
Figure A5.8 Drawing of the north section at Hatchet Gate Farm pit.....	22
Figure A5.9 Detailed laser scan of the south section at Hatchet Gate Farm.....	23
Figure A5.10 Detailed scan of north section at Hatchet Gate Farm.....	24

Figure A7.1 Map showing the location of the site of Woodriding pit in relationship to the local bedrock and superficial geology (based upon 1:10000 scale geology data with permission of the British Geological Survey and 1:10000 scale OS VectorMap Local [shape file], Digimap Licence).....	27
Figure A7.2 Terrestrial laser scan of Woodriding pit.	28
Figure A7.3 Overview annotated photograph of Woodriding pit.	29
Figure A7.4 Drawing of Woodriding pit providing an overview of the northeast, middle, and southwest part of the section.	30
Figure A7.5 Drawing of the northeast part of the section at Woodriding pit.	31
Figure A7.6 Drawing of the southwest part of the section at Woodriding pit.	32
Figure A7.7 Detailed scan of section at Woodriding.....	33
Figure A9.1 Map showing the location of the site of Woodgreen pit in relationship to the local bedrock and superficial geology (based upon 1:10000 scale geology data with permission of the British Geological Survey and 1:10000 scale OS VectorMap Local [shape file], Digimap Licence).....	36
Figure A9.2 Terrestrial laser scan of Woodgreen pit, providing an overview of the site and the locations of sections 1 and 2.....	37
Figure A9.3 Annotated photograph of the section 1 at Woodgreen pit.	38
Figure A9.4 Annotated photograph of the section 2 at Woodgreen pit.	39
Figure A9.5 Drawing of section 1 at Woodgreen pit.....	40
Figure A9.6 Drawing of section 2 at Woodgreen pit.....	41
Figure A9.7 Detailed laser scan of section 1 at Woodgreen.	42
Figure A9.8 Detailed laser scan of section 2 at Woodgreen.	43
Figure A11.1 Map showing the location of the site of Somerley pit in relationship to the local bedrock and superficial geology (based upon 1:10000 scale geology data with permission of the British Geological Survey and 1:10000 scale OS VectorMap Local [shape file], Digimap Licence).....	48

Figure A11.2 Terrestrial laser scan of Somerley pit, providing an overview of the site and the locations of sections 1-3.	49
Figure A11.3 Annotated photograph of the section 1 at Somerley pit.....	50
Figure A11.4 Annotated photograph of the section 2 at Somerley pit.....	51
Figure A11.5 Annotated photograph of the section 3 at Somerley pit.....	52
Figure A11.6 Drawing of section 1 at Somerley pit.	53
Figure A11.7 Drawing of section 2 at Somerley pit.	54
Figure A11.8 Drawing of section 3 at Somerley pit.	55
Figure A11.9 Detailed laser scan of section 1 at Somerley.	56
Figure A11.10 Detailed laser scan of section 2 at Somerley.	57
Figure A11.11 Detailed laser scan of section 3 at Somerley.	58
Figure A13.1 Map showing the location of the site of Asheley pit in relationship to the local bedrock and superficial geology (based upon 1:10000 scale geology data with permission of the British Geological Survey and 1:10000 scale OS VectorMap Local [shape file], Digimap Licence).	63
Figure A13.2 Terrestrial laser scan of section 1 at Asheley pit.	64
Figure A13.3 Annotated photograph of the section 1 at Ashley pit.....	65
Figure A13.4 Drawing of section 1 at Ashley pit.	66
Figure A15.1 Map showing the location of the site of Bickton pit in relationship to the local bedrock and superficial geology (based upon 1:10000 scale geology data with permission of the British Geological Survey and 1:10000 scale OS VectorMap Local [shape file], Digimap Licence).	71
Figure A15.2 Annotated photograph of Bickton pit showing the OSL sample locations in the western and northern walls of the pit.	72
Figure A15.3 Schematic representation of the western and northern walls of Bickton pit....	73

Figure A16.1 Section in the undifferentiated terrace deposit at Bemerton showing gravel sample locations and the main stratigraphic units. 1= BEM2.2; 2=BEM2.3; 3=BEM2.4a; 4=BEM2.4b. 74

Figure A16.2 Percentage frequency and cumulative percentage frequency of sediment fractions present in sample BEM2.2 (top) and BEM2.3 (bottom). 75

Figure A16.3 Percentage frequency and cumulative percentage frequency of sediment fractions present in sample BEM2.4a (top) and BEM2.4b (bottom)..... 76

Figure A16.4. Particle size distribution of the <63µm fraction of BEM2.2 (a), BEM2.3 (b), BEM2.4a (c) and BEM2.4b (d). 77

Figure A16.5 Comparison of the integrated particle size distribution curves of the four gravel samples from Bemerton showing weight in percentages of each size fraction (top) and the cumulative percentage of the weight in percentages (bottom)..... 78

Figure A18.1 Section in terrace 10 at Hatchet Gate Farm showing gravel sample locations and the main stratigraphic units. 1= HA1.1; 2=HA1.3..... 84

Figure A18.2 Percentage frequency and cumulative percentage frequency of sediment fractions present in sample HA1.1 (top) and HA1.3 (bottom). 85

Figure A18.3 Particle size distribution of the <63µm fraction of HA1.1 (a) and HA1.3 (b). 86

Figure A18.4 Comparison of the integrated particle size distribution curves of the two gravel samples from Hatchet Gate Farm showing weight in percentages of each size fraction (top) and the cumulative percentage of the weight in percentages (bottom). 87

Figure A20.1 Section in terrace 10 at Hatchet Gate Farm showing image locations and the main stratigraphic units. 1= HA1.1; 2=HA1.2; 3=HA1.3. 92

Figure A20.2 Photographs used for image-based automated grainsizing of HA1.1 (a), HA1.2 (b), and HA1.3 (c) and the resulting grain size distributions..... 93

Figure A20.3 Comparison of percentage frequency (left) and cumulative percentage frequency (right) of the grain size distributions of HA1.1, HA1.2 and HA1.3 obtained from image-based automated grainsizing. 94

Figure A20.4 Comparison of sieving and IBAG results from HA1.1 and HA1.3. 95

Figure A21.1 Section in terrace 10 at Woodriding showing gravel sample locations and the main stratigraphic units. 1= HB1.1; 2=HB1.2; 3=HB1.9.....	97
Figure A21.2 Percentage frequency and cumulative percentage frequency of sediment fractions present in sample HB1.1 (top) and HB1.2 (bottom).....	98
Figure A21.3 Percentage frequency and cumulative percentage frequency of sediment fractions present in sample HB1.9.....	99
Figure A21.4 Particle size distribution of the <63µm fraction of HB1.1 (a), HB1.2 (b) and HB1.9 (c).....	100
Figure A21.5 Comparison if the ntegrated particle size distribution curves of the three gravel samples from Woodriding showing weight in percentages of each size fraction (top) and the cumulative percentage of the weight in percentages (bottom)...	101
Figure A23.1 Two sections in terrace 7 at Woodgreen showing gravel sample locations and the main stratigraphic units. 1= WG1.11; 2=WG2.3; 3=WG2.7.4a; 4=WG2.8.	107
Figure A23.2 Percentage frequency and cumulative percentage frequency of sediment fractions present in sample WG1.11.	108
Figure A23.3 Percentage frequency and cumulative percentage frequency of sediment fractions present in sample WG2.3 (top) and WG2.7 (bottom).	109
Figure A23.4 Percentage frequency and cumulative percentage frequency of sediment fractions present in sample WG2.8.	110
Figure A23.5 Particle size distribution of the <63µm fraction of WG1.11 (a), WG2.3 (b), WG2.7 (c) and WG2.8 (d).....	111
Figure A23.6 Comparison if the integrated particle size distribution curves of the four gravel samples from Woodgreen showing weight in percentages of each size fraction (top) and the cumulative percentage of the weight in percentages (bottom)...	112
Figure A25.1 Two sections in terrace 7 at Woodgreen showing image locations and the main stratigraphic units.	117
Figure A25.2 Woodgreen frame 1-4.	118

Figure A25.3 Woodgreen frame 5-8.	119
Figure A25.4 Comparison of percentage frequencies obtained from IBAG in Woodgreen section 1 (left) and section 2 (right).	120
Figure A25.5 Comparison of percentage frequencies obtained from IBAG from both sections at Woodgreen.....	121
Figure A25.6 Comparison of sieving and IBAG results from WG1.11 and frame 4 and WG2.3 and frame 6.	122
Figure A25.7 Comparison of sieving and IBAG results from WG2.8up and frame 7 and WG28low and frame 8.	123
Figure A26.1 Two sections in terrace 6 in Somerley pit showing gravel sample locations and the main stratigraphic units. 1= SOM1.5; 2=SOM1.8; 3=SOM3.1; 4=SOM3.2; 5=SOM3.7.	125
Figure A26.2 Percentage frequency and cumulative percentage frequency of sediment fractions present in sample SOM1.5 (top) and SOM1.8 (bottom).	126
Figure A26.3 Percentage frequency and cumulative percentage frequency of sediment fractions present in sample SOM3.1 (top) and SOM3.2 (bottom).	127
Figure A26.4 Percentage frequency and cumulative percentage frequency of sediment fractions present in sample SOM3.7.	128
Figure A26.5 Particle size distribution of the <63µm fraction of SOM1.5 (a) and SOM1.8 (b).	129
Figure A26.6 Particle size distribution of the <63µm fraction of SOM3.1 (a), SOM3.2 (b) and SOM3.7 (c).	130
Figure A26.7 Comparison if the integrated particle size distribution curves of the five gravel samples from Somerley Pit showing weight in percentages of each size fraction (top) and the cumulative percentage of the weight in percentages (bottom)...	131
Figure A28.1 Two sections in terrace 6 in Somerley pit showing photograph locations for image-based automated grainsizing and the main stratigraphic units.	136

Figure A28.2 Photographs and the resulting grain size distributions of frames 1-4 (previous page) and 3-7 (this page) at Somerley pit.....	138
Figure A28.3 Photographs and the resulting grain size distributions of frame 8 and 9 at Somerley pit.	139
Figure A28.4 Comparison of percentage frequencies obtained from IBAG from both sections at Somerley pit.....	140
Figure A28.5 Comparison of sieving and IBAG results from SOM1.5 and frame 2 and SOM1.8up and frame 3.	141
Figure A28.6 Comparison of sieving and IBAG results from SOM1.8low and frame 4.....	142
Figure A28.7 Comparison of sieving and IBAG results from SOM3.2 and frame 5 and SOM3.7 and frame 9.	143
Figure A29.1 Section in terrace 5 at Ashley Pit showing gravel sample locations and the main stratigraphic units. 1= ASH1.6; 2=ASH1.11; 3=ASH1.13.	144
Figure A29.2 Percentage frequency and cumulative percentage frequency of sediment fractions present in sample ASH1.6.	145
Figure A29.3 Percentage frequency and cumulative percentage frequency of sediment fractions present in sample ASH1.11 (top) and ASH1.13 (bottom).....	146
Figure A29.4 Particle size distribution of the <63µm fraction of ASH1.6 (a), ASH1.11 (b) and ASH1.13 (c).....	147
Figure A29.5 Comparison if the integrated particle size distribution curves of the three gravel samples from Ashley Pit showing weight in percentages of each size fraction (top) and the cumulative percentage of the weight in percentages (bottom).....	148
Figure A31.1 Section drawing of terrace 5 at Ashley Pit showing photograph locations for image-based automated grainsizing and the main stratigraphic units.	154
Figure A31.2 Photographs and the resulting grain size distributions of frames 1-3 at Ashley pit.....	155

Figure A31.3 Comparison of percentage frequency (left) and cumulative percentage frequency (right) of the grain size distributions of ASH1.6, ASH1.11 and ASH1.13 obtained from image-based automated grainsizing.	156
Figure A31.4 Comparison of sieving and IBAG results from ASH1.6 and frame 1 and ASH1.11 and frame 2.	157
Figure A31.5 Comparison of sieving and IBAG results from ASH1.13 and frame 3.	158
Figure A41.1 Patination, staining, abrasion and iron-manganese concretion of pointed, ovate and cleaver type bifaces from Bemerton.	252
Figure A41.2 Patination, staining, abrasion and iron-manganese concretion of pointed, ovate and cleaver type bifaces from Milford Hill.	253
Figure A41.3 Patination, staining, abrasion and iron-manganese concretion of pointed, ovate and cleaver type bifaces from Woodgreen.	254

List of Tables Volume II

Table A32.1 Clast size lithology of all size fractions (cont. below)	159
Table A33.1 Clast angularity-roundness of deposits from all sites.	162
Table A35.1 Summary laboratory procedures, applied Dr values and the results of the analytical tests per sample.	168
Table A37.1 Table summarising the number of artefacts studied per site and their current location.	244
Table A43.1 Average size and shape of artefacts from Bemerton (the significance was tested using one-way ANOVA. Results with *are analysed using Kruskal-Wallis test).	270
Table A43.2 Average size and shape of artefacts from Milford Hill (the significance was tested using one-way ANOVA. Results with *are analysed using Kruskal-Wallis test).	271
Table A43.3 Average size and shape of artefacts from Woodgreen (the significance was tested using one-way ANOVA. Results with *are analysed using Kruskal-Wallis test).	272

Appendix 1 Artefact numbers

Many of the artefacts analysed for this research were unnumbered in which case the artefacts were numbered and bagged so that the artefacts can be retraced. The majority of artefacts are stored in numbered boxes, per site, that is included in the here adapted numbering of artefacts. The numbers include a reference to the site (B=Bemerton, M=Milford Hill, W=Woodgreen), the number of the box, the number of the artefact in that box and the number of the artefact as part of the total assemblage for continuity over various museums. For example artefact W4.46.178 is the 178th artefact studied from Woodgreen. It is stored in box 4 where it is the 46th artefact. In the data base this artefact can be found to be stored in Salisbury Museum. These artefact codes are also used to number the photos. The coding allows results from statistical analyses and geometric morphometrics to be reviewed, e.g. outliers can be viewed in the photo data base and revisited in the museum.

Appendix 2 Artefact data collection

The following data were recorded for all artefacts from Bemerton, Milford Hill and Woodgreen:

Type of artefact (after Andrefsky 2005)

1. Biface (*'...have two sides that meet to form a single edge that circumscribes the entire artefact.'* (Andrefsky 2005, p.22))
2. Flake (Striking platform and/or dorsal face intact)
3. Core (*'... is a mass of homogeneous lithic material that has had flakes removed from its surface.'* Andrefsky 2005, p.14))
4. Miscellaneous
5. Other

Roughout (for bifaces only)

1. No
2. Yes

Raw material

1. Flint
2. Chert
3. Other (defined in comments)

Patination

1. No
2. 0-25%
3. 25-50%
4. 50-75%
5. >75%

Location of Patination

1. N/A
2. Entirely
3. One side partly
4. One side totally
5. Two sides partly
6. One side totally, one side partly

Multiple phases of patination?

This can be recognised in flake scars and breakage scars that are less patinated than the rest of the implement.

1. No
2. Yes
3. NID

Staining

1. Not stained
2. Lightly stained
3. Moderately stained
4. Stained
5. Heavily stained

Staining location

1. N/A
2. Entirely
3. One side partly
4. One side totally
5. Two sides partly
6. One side totally, one side partly

Colour description

1. White (light grey/light blue)
2. Orange (buff brown to yellow)
3. Black/grey
4. Dark mottled blue
5. Olive/dark grey/black

Manganese

1. N/A
2. Entirely
3. One side partly
4. One side totally
5. Two sides partly
6. One side totally, one side partly

Broken

1. No
2. Yes
3. NID

Location

1. N/A
2. Butt
3. Tip
4. Side
5. Body
6. Multiple
7. NID

Breakage

1. N/A
2. Patinated/stained/rolled comparable to state of worked surface
3. Fresh
4. Neither fresh nor comparable to the state of the worked surface
5. NID
6. 1 and 2
7. 1 and 3

Cortex (For flakes: dorsal side plus platform total cortex = 100%)

1. No
2. 0-25%
3. 25-50%
4. 50-75%
5. >75%
6. NID

Location

1. N/A
2. Butt
3. Tip
4. Butt/tip
5. Side
6. Body
7. Multiple

Abrasion of the intentionally knapped surface (after Ashton 1998)

1. Fresh condition. Sharp edges, no evidence of abrasion to the scar ridges.
2. Slightly rolled. Occasional edge damage and/or abrasion to scar ridges.
3. Rolled. Frequent damage to edges and slight rounding of scar ridges.
4. Very rolled. Considerable damage to edges and clear rounding of scar ridges.

Rolling natural surface

Following Power's scale (1982)

Blank type

1. NID
2. Possible cobble (well-rounded surface, chatter-marked, no nodular surface (cf. White 1998)
3. Nodule (more or less friable white rind, characteristically shaped)
4. Flake (identification of (part of) striking platform/bulb of percussion/ventral face)

Metric measurements

Measurement of the dimensions of the artefacts are based on Roe (1968), that also allow ratios describing biface shape to be calculated (ibid.). Weight, as an indication of size and a technique to identify artefacts, was obtained using the Salter Brecknell ESA 6000 (6000x0.1g capacity and resolution) electronic balance.

Evidence of burning

1. No
2. Yes

Appendix 3 Bemerton site recordings



Figure A3.1 Map showing the location of the site of Bemerton pit in relationship to the local bedrock and superficial geology (based upon 1:10000 scale geology data with permission of the British Geological Survey and 1:10000 scale OS VectorMap Local [shape file], Digimap Licence).

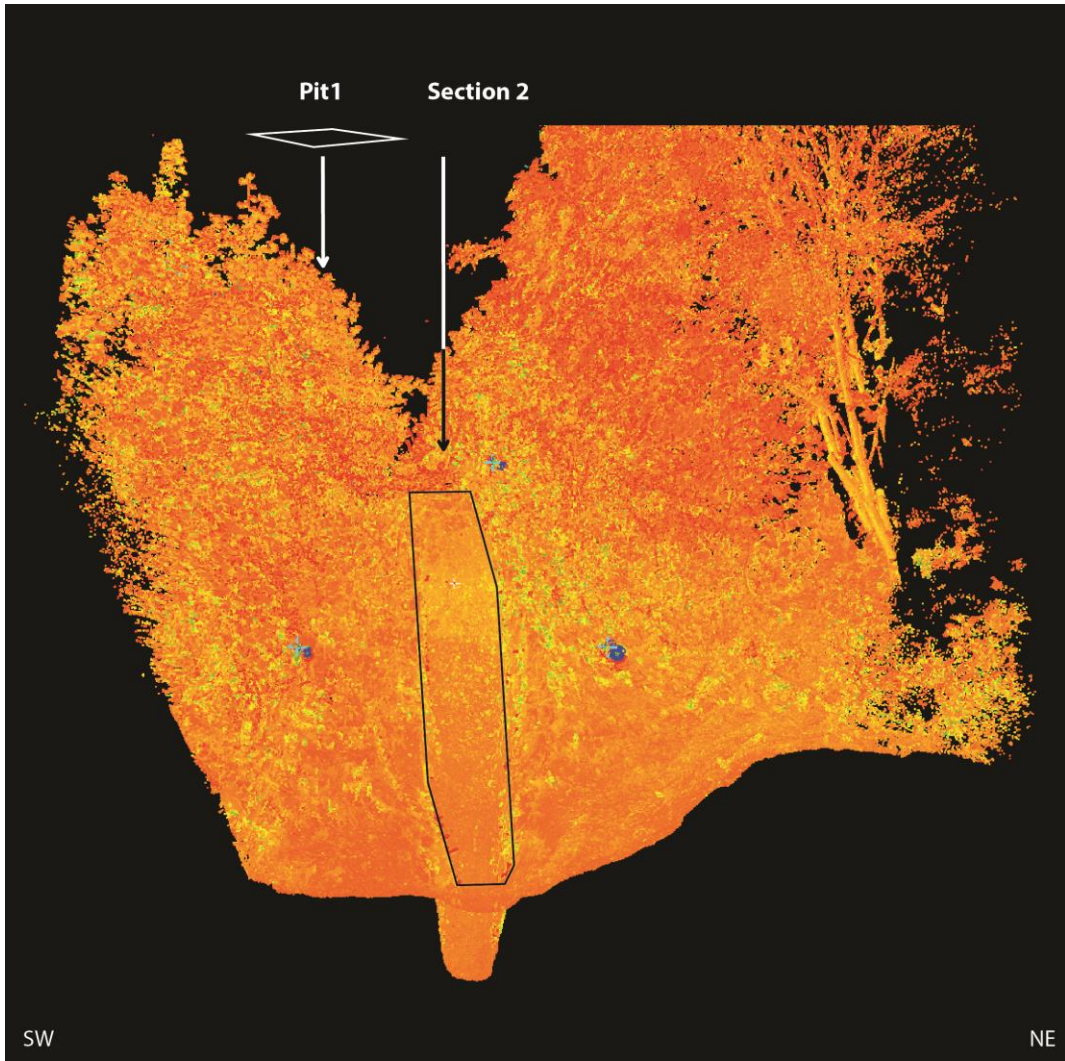


Figure A3.2 Terrestrial laser scan of Bemerton pit, providing an overview of the site and the locations of section 2 and pit 1.

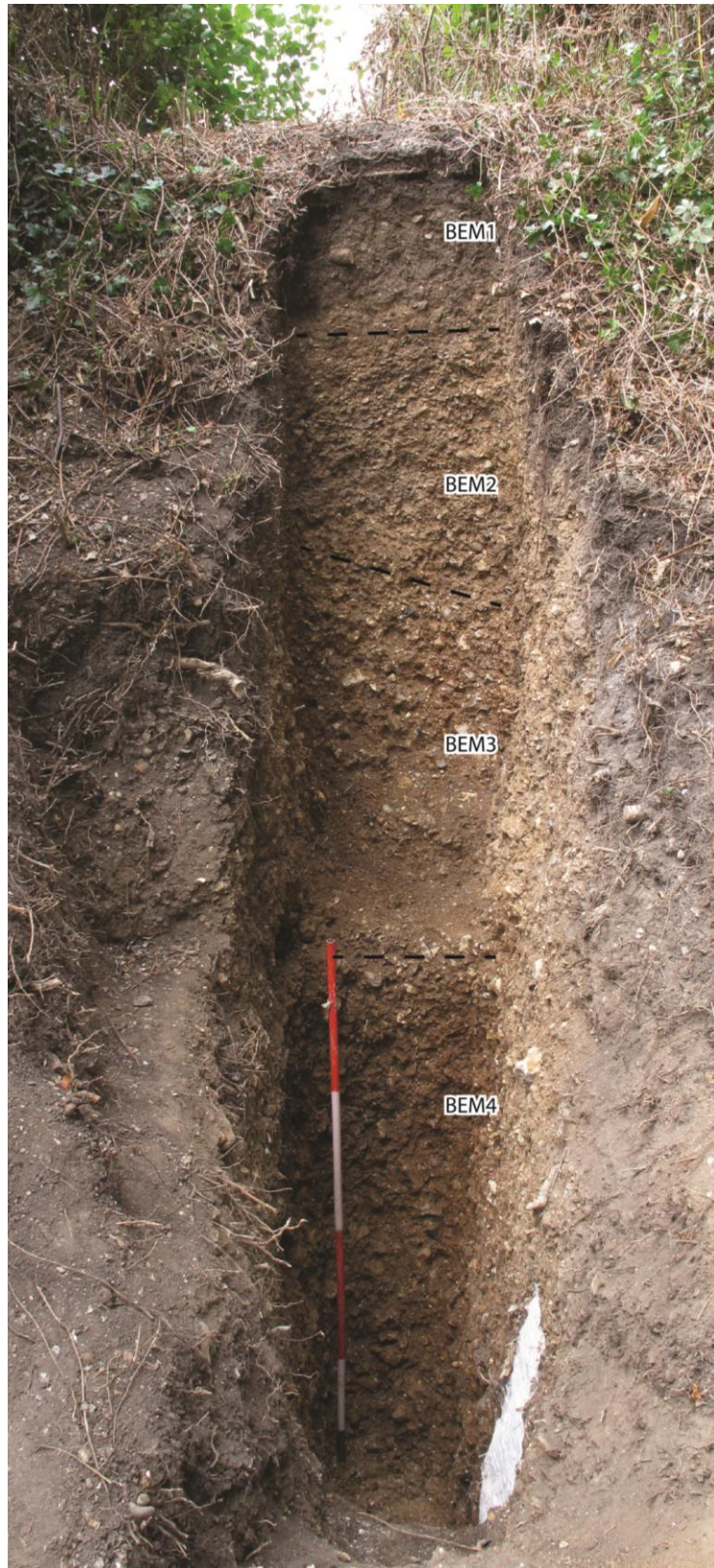


Figure A3.3 Annotated photograph of section 2 at Bemerton pit.

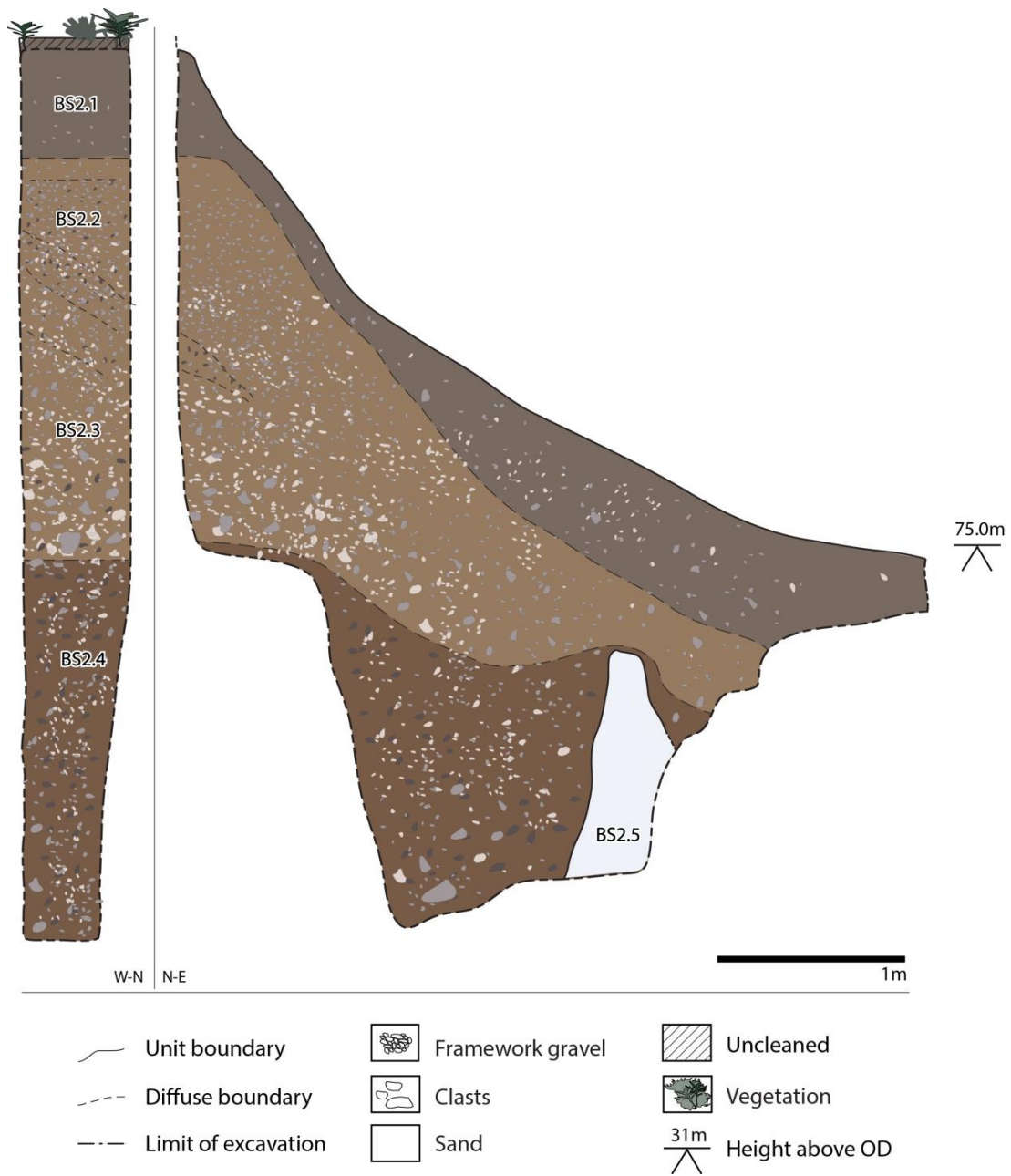


Figure A3.4 Drawing of section 2 at Bemerton pit.

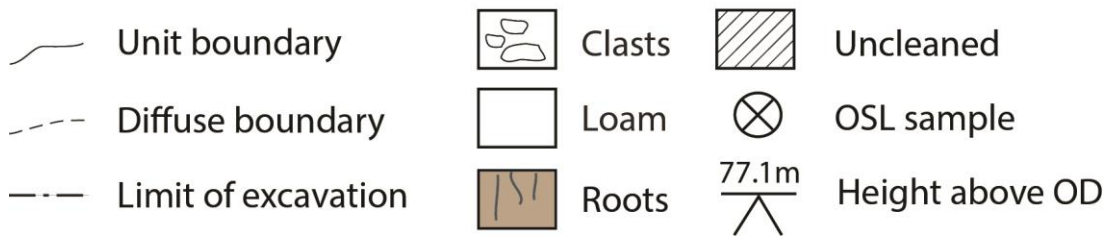
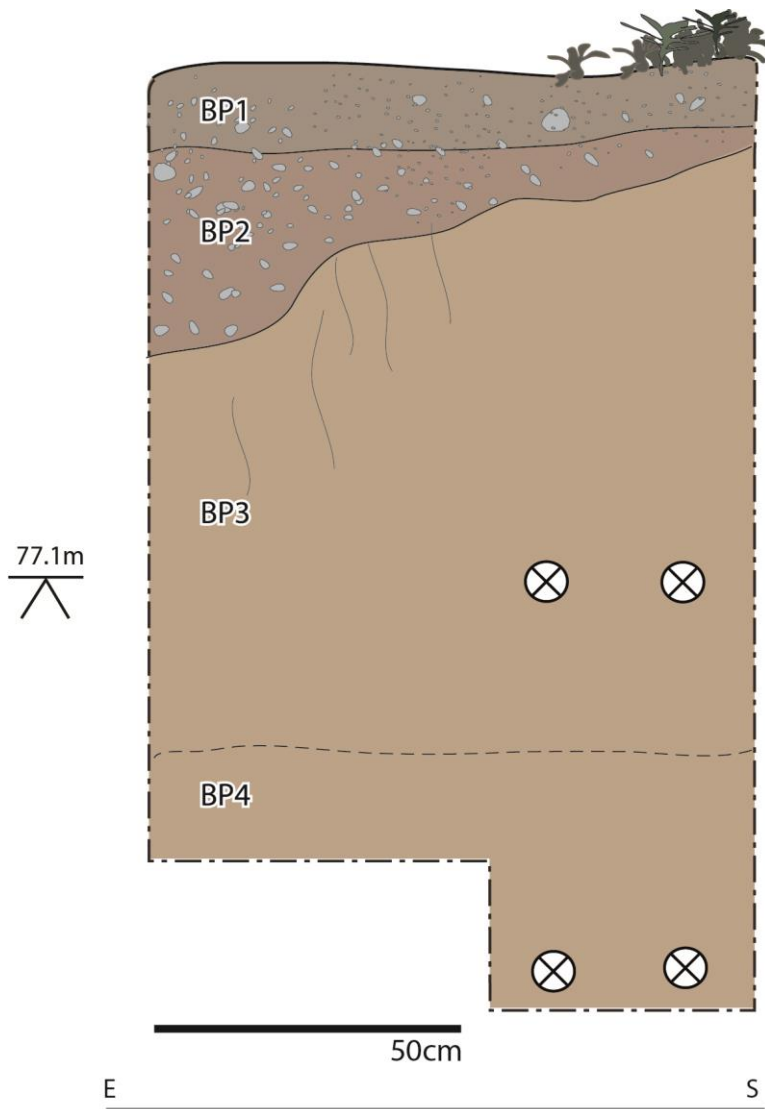


Figure A3.5 Drawing of pit 1 at Bemerton pit.



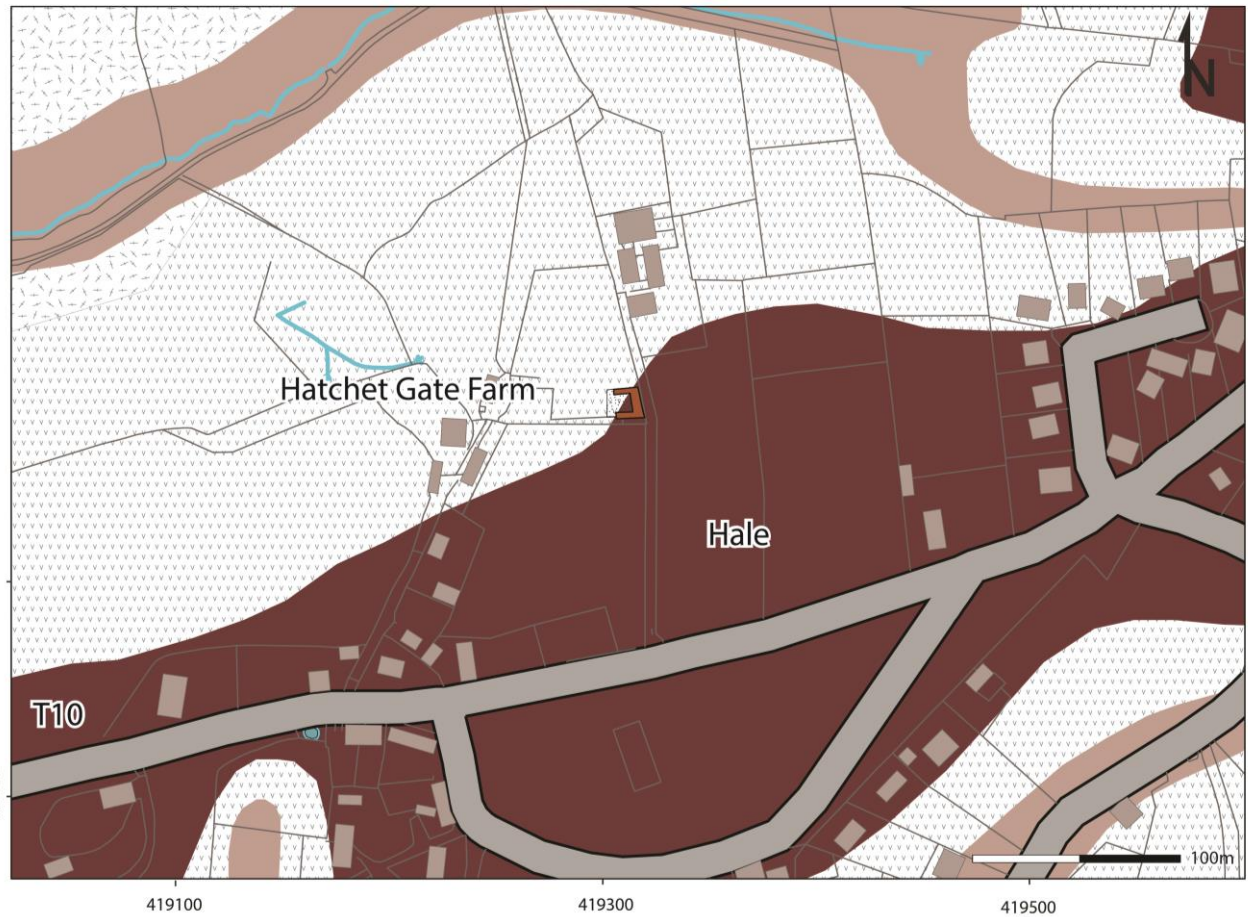
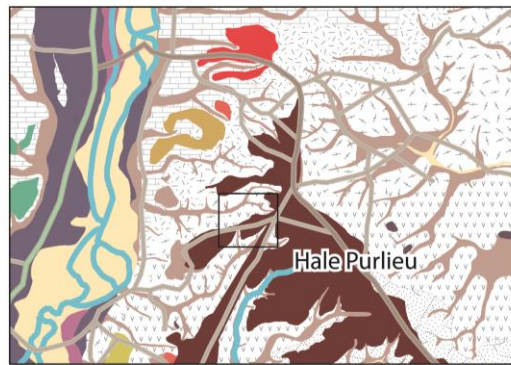
Figure A3.6 Detailed laser scan of section 2 at Bemerton.

Appendix 4 Bemerton sediment logs

BEMERTON SECTION 2		
Unit	Description	Lithofacies
BEM2.1	TOPSOIL. Dark grey brown, sandy, silty and some clay (2.5Y 3/3). Abundant sub-rounded to angular gravel. Includes roots.	
BEM2.2	GRAVEL. Very poorly sorted, clast supported, crudely bedded, yellow, light brown, medium gravel (10YR 6/6 - 10YR 6/4). Diffuse bands of framework gravel. Dominant clast size is 1-3cm with occasional larger clasts.	Gh
BEM2.3	GRAVEL. Poorly sorted, matrix supported, crudely graded, yellow brown, very coarse gravel (7.5YR 5/8 - 10YR 5/8). Clasts up to 20cm. The larger clasts form a crude band. Matrix is sandy, clayey, silt with fine and coarse quartz sand.	Gmg
BEM2.4	GRAVEL. Very poorly sorted, clast supported, crudely graded, dark yellow brown, very coarse gravel (10YR 4/4). Clasts up to 20cm. The matrix is sandy, clayey silt with fine and coarse sand and some clayey patches.	Gcg

BEMERTON PIT 1		
Unit	Description	Lithofacies
BP1	Per BEM2.1	
BP2	GRAVELLY SILT. Massive, yellow brown, clayey, sandy, silt. Contains frequent, isolated, small, angular to subrounded stones. Blocky fabric.	Fm
BP3	SILT. Massive, yellow brown, sandy, clayey silt. Contains occasional small sub-angular fine (2-3mm); very occasional larger stones. Honeycomb fabric.	Fm
BP4	SILT. Massive, yellowish, grey, sandy, clayey, silt. Includes some granules. Honeycomb fabric.	Fm

Appendix 5 Hatchet Gate Farm site recordings



- | | |
|-------------------|-----------------------|
| Quarry | Buildings |
| Sections | Water |
| Road | River |
| Alluvium | Terrace 8-9 |
| Terrace 3 | Terrace 9 |
| Terrace 4 | Undiff. Terrace |
| Terrace 5 | Head |
| Terrace 7 | |
| Barton Group | London Clay Formation |
| Bracklesham Group | Reading Formation |
| Bagshot Formation | Chalk |

Figure A5.1 Map showing the location of the site of Hatchet Gate Farm pit in relationship to the local bedrock and superficial geology (based upon 1:10000 scale geology data with permission of the British Geological Survey and 1:10000 scale OS VectorMap Local [shape file], Digimap Licence).



Figure A5.2 Terrestrial laser scan of Hatchet Gate Farm pit, providing an overview of the north, east and south sections of the pit.

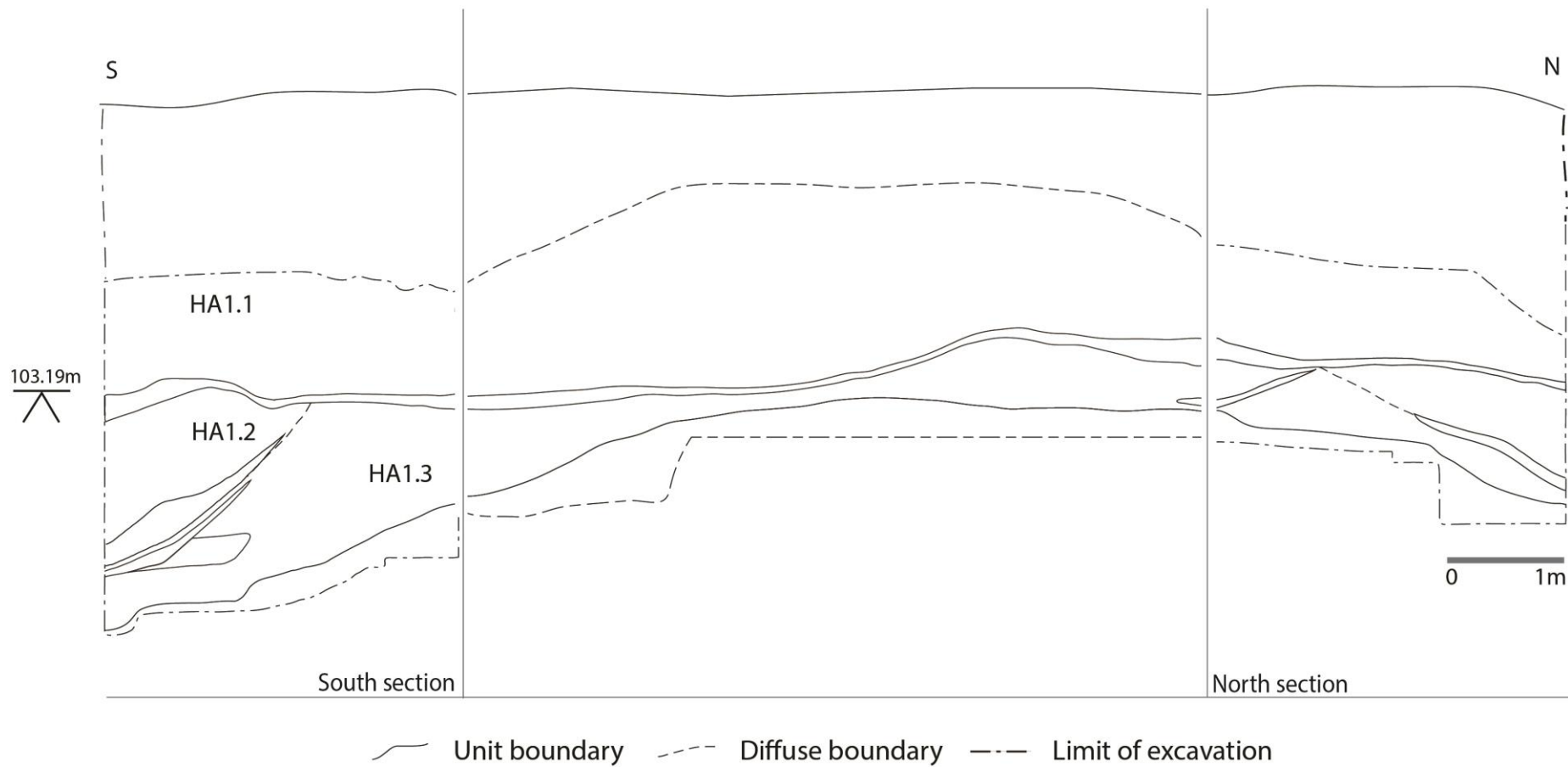


Figure A5.3 Drawing of Hatchet Gate Farm pit, providing an overview of the north, east and south sections of the pit.



Figure A5.4 Overview annotated photograph of Hatchet Gate Farm pit.

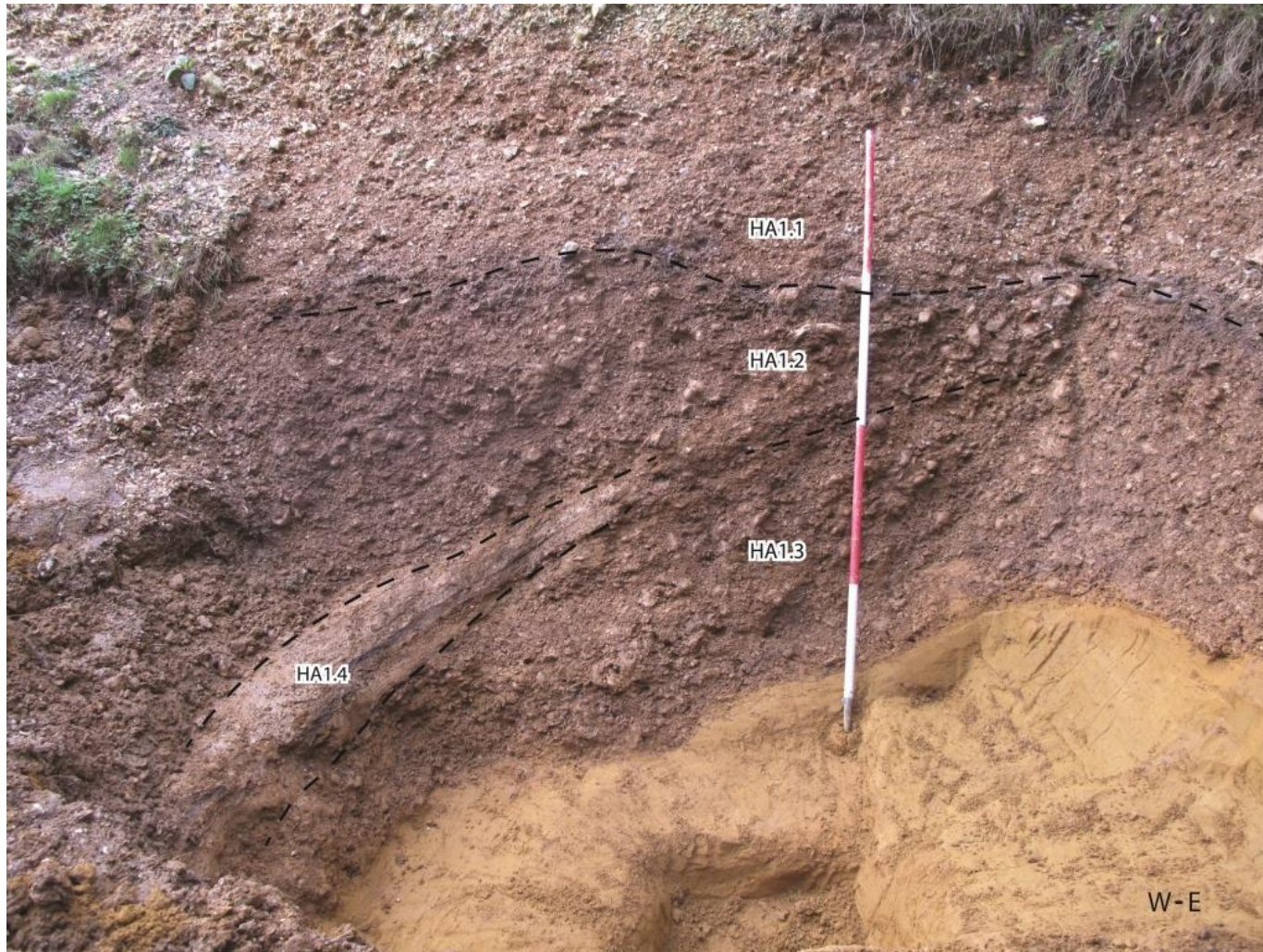


Figure A5.5 Annotated photograph of the south section at Hatchet Gate Farm pit.



Figure A5.6 Annotated photograph of the north section at Hatchet Gate Farm pit.

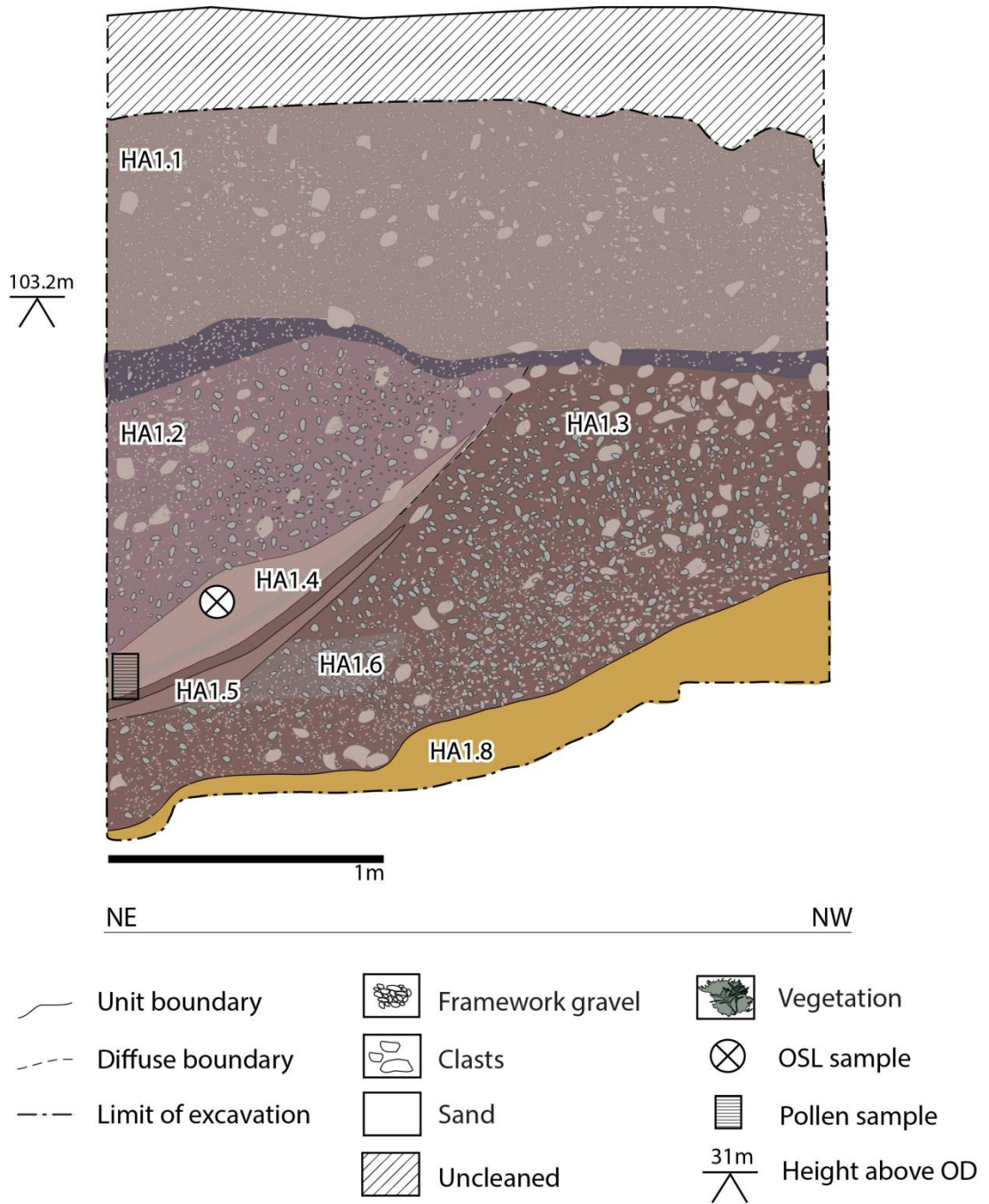


Figure A5.7 Drawing of the south section at Hatchet Gate Farm pit.

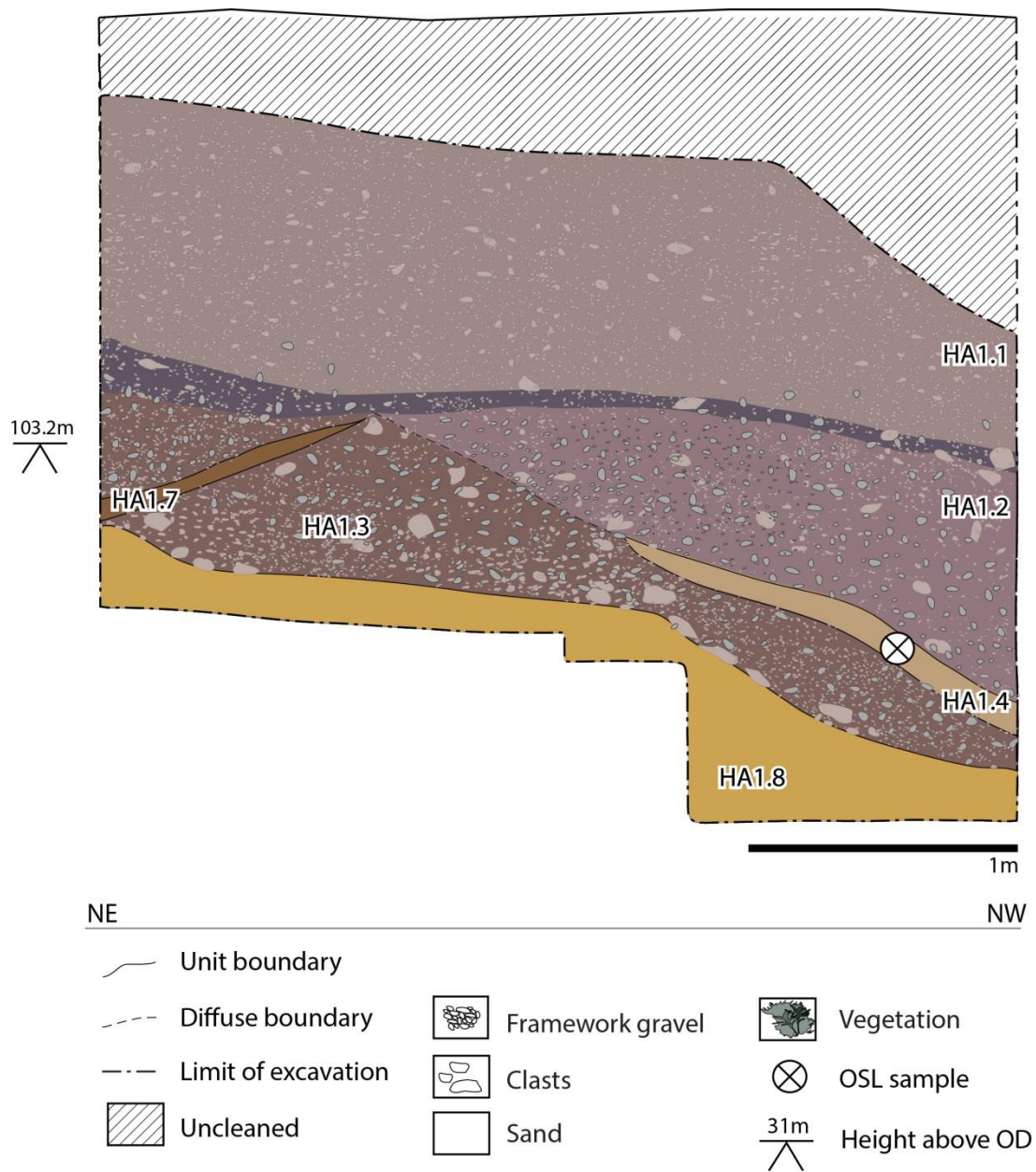


Figure A5.8 Drawing of the north section at Hatchet Gate Farm pit.

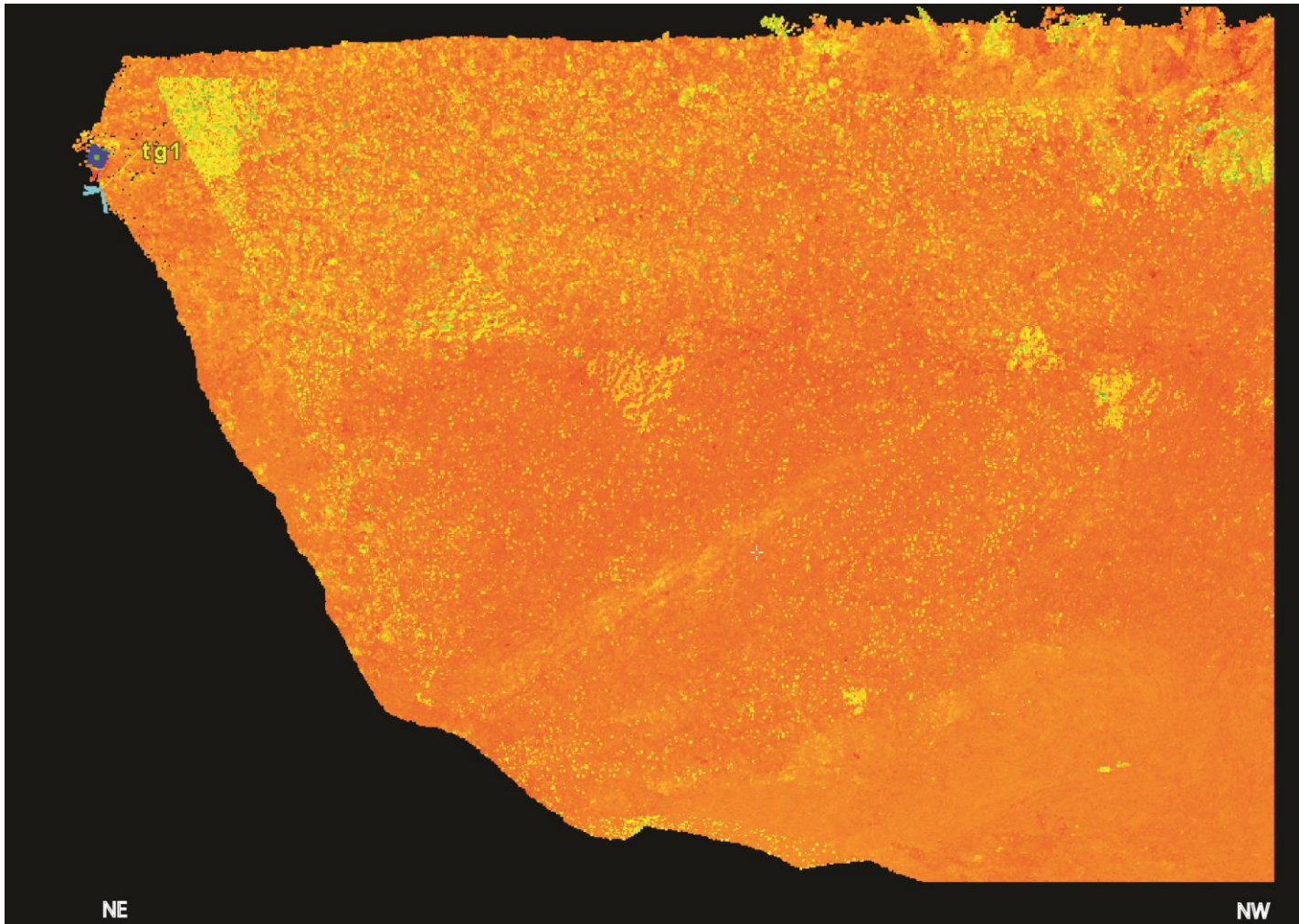


Figure A5.9 Detailed laser scan of the south section at Hatchet Gate Farm.

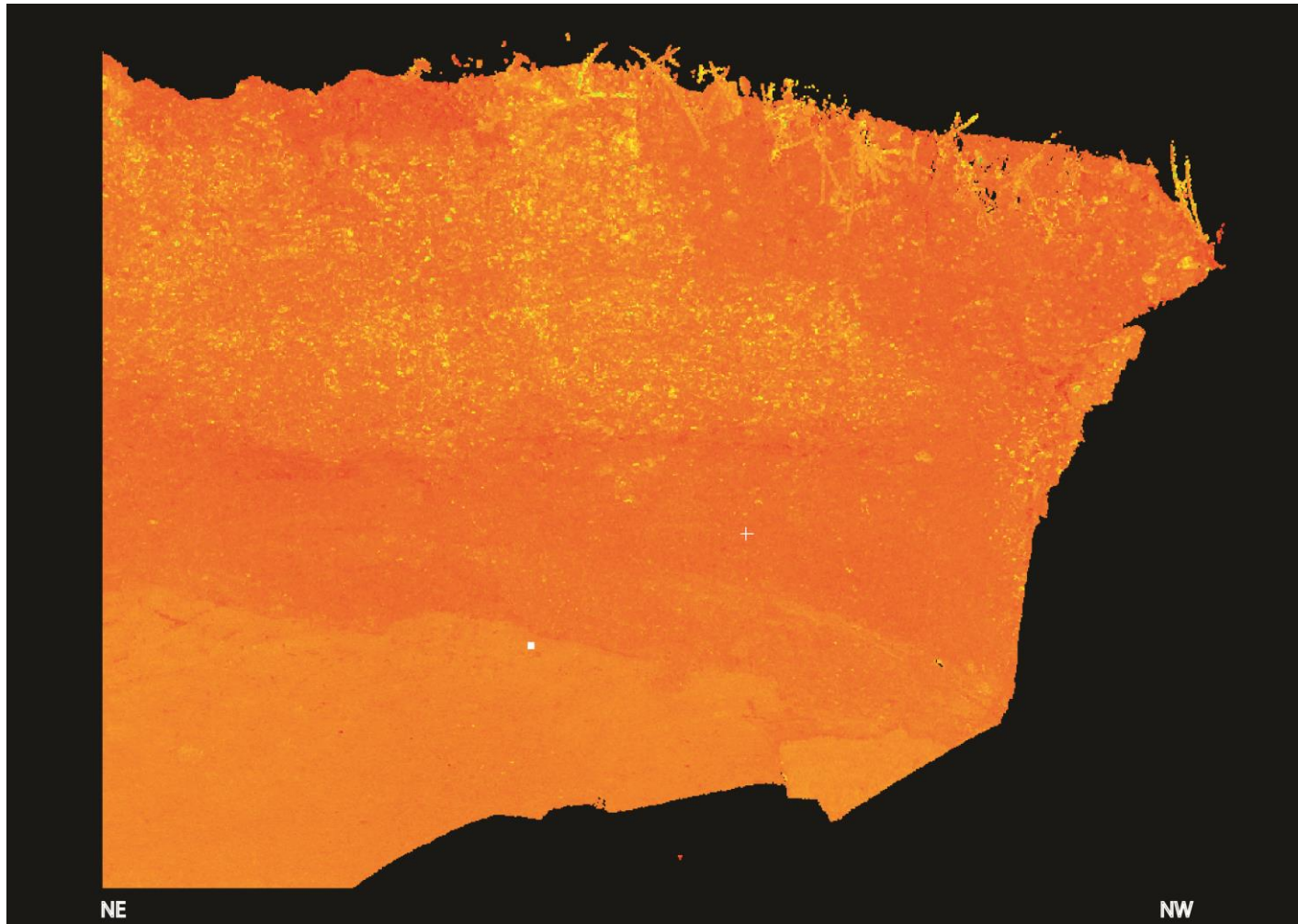


Figure A5.10 Detailed scan of north section at Hatchet Gate Farm.

Appendix 6 Hatchet Gate Farm sediment log

HATCHET GATE FARM		
Unit	Description	Lithofacies
HA1.1	SILTY, SANDY GRAVEL. Poorly sorted, matrix supported, massive, orange-grey, medium gravel (5YR 4/6; 7.5YR 6/2). Coarse silty sandy matrix with granules, grid and coarse quartz sand.	Gmm
HA1.2	SILTY GRAVEL. Poorly sorted, matrix supported, massive, dark orange, red-brown, medium coarse gravel (2.5YR 2.5/10). The deposit is compact; includes large clasts. The matrix is clayey silt.	Gmm
HA1.3	SILTY GRAVEL. Very poorly sorted, matrix supported, crudely bedded, orange-brown, very coarse gravel (5YR 4/6). The matrix is clayey silt with grid, granules and coarse sand.	Gmh
HA1.4	SILTY-CLAY. Compact, light grey, orange and black, horizontally bedded silty clay with beds of fine sand and clayey silt (7.5YR 5/8; 7.5YR 3/2; 7.5YR 8/1).	Fl
HA1.5	SAND. Compact, well sorted, horizontally bedded, yellow, orange-brown, fine to medium sand (7.5YR 4/6).	Sh
HA1.6	SILTY GRAVEL. Poorly sorted, matrix supported, horizontally bedded, yellow orange, silty clayey gravel (7.5YR 5/8).	Gm
HA1.7	SAND. Compact, well sorted, horizontally bedded, yellow and bright orange, medium to fine sand (5YR 4/6). Iron concreted; beds of clay.	Sh
HA1.8	SAND. Very compact, well-sorted, horizontally bedded, medium to fine sand (7.5YR 5/8). Bands clay present (Poole Formation).	Sh

Appendix 7 Woodriding site recordings



Figure A7.1 Map showing the location of the site of Woodriding pit in relationship to the local bedrock and superficial geology (based upon 1:10000 scale geology data with permission of the British Geological Survey and 1:10000 scale OS VectorMap Local [shape file], Digimap Licence).

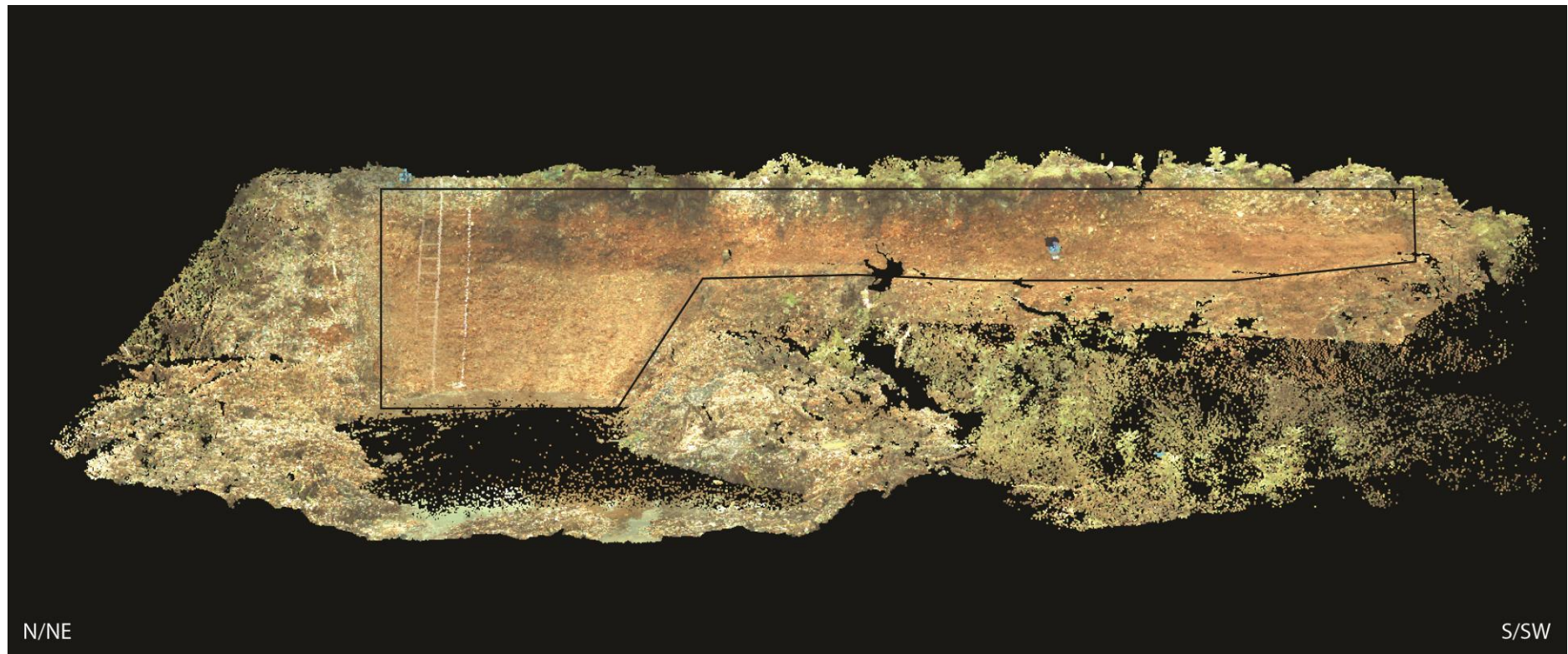


Figure A7.2 Terrestrial laser scan of Woodriding pit.



Figure A7.3 Overview annotated photograph of Woodriding pit.

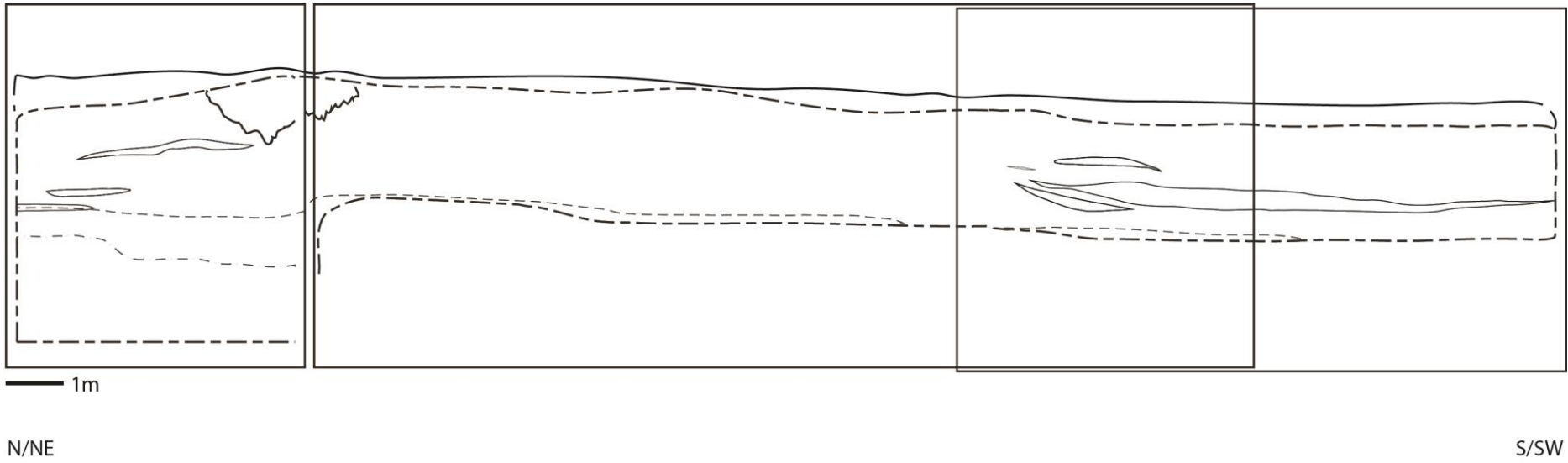


Figure A7.4 Drawing of Woodriding pit providing an overview of the northeast, middle, and southwest part of the section.

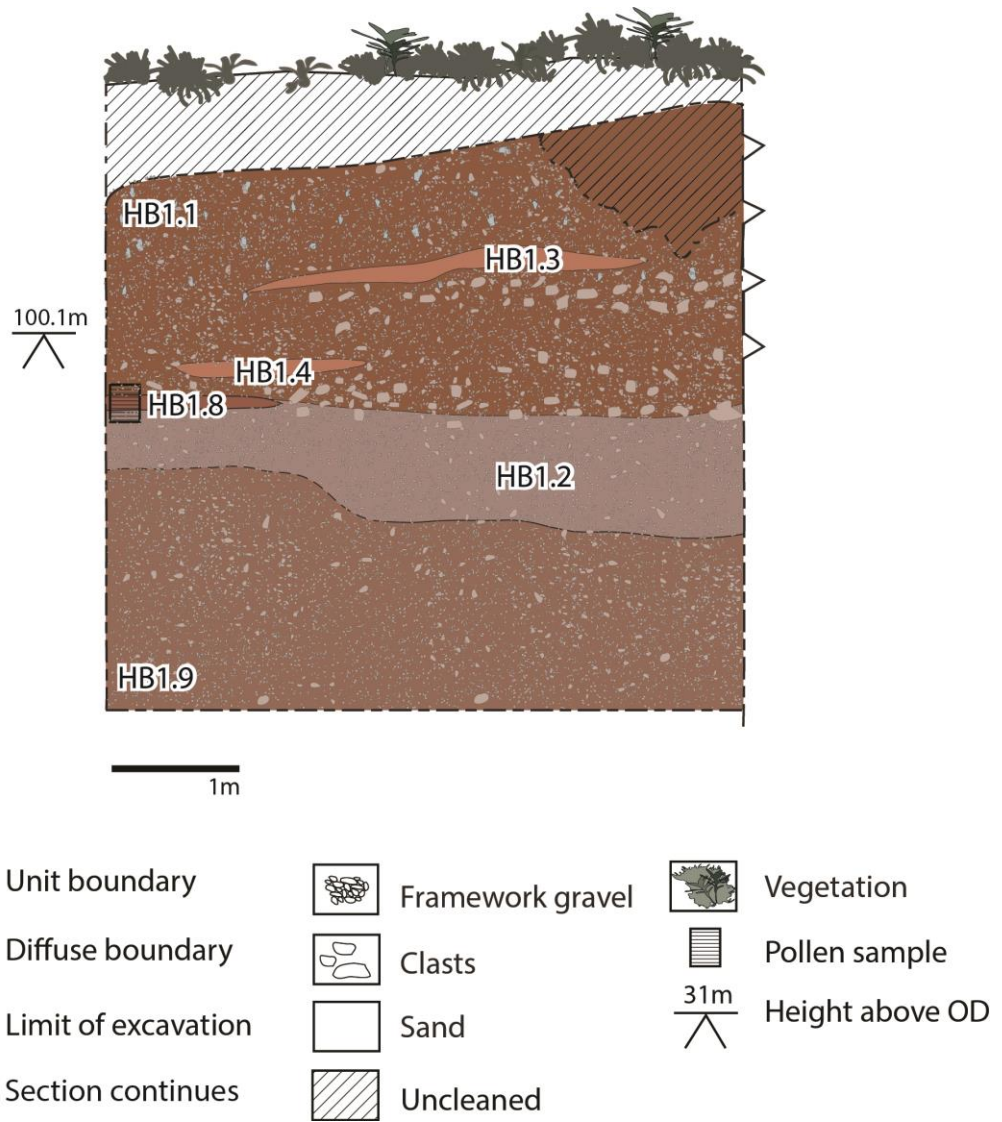
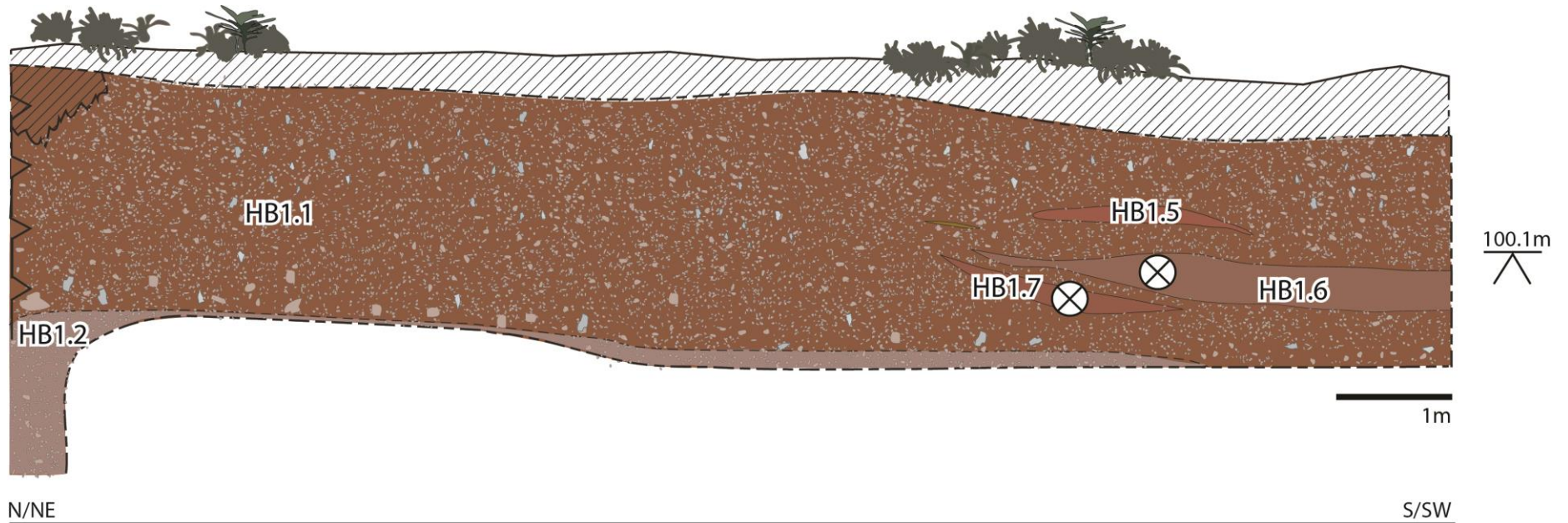


Figure A7.5 Drawing of the northeast part of the section at Woodriding pit.



- | | | | |
|---------------------|------------------|------------|-----------------|
| Unit boundary | Framework gravel | Uncleaned | OSL sample |
| Diffuse boundary | Clasts | Vegetation | Height above OD |
| Limit of excavation | Sand | | |
| Section continues | | | |

Figure A7.6 Drawing of the southwest part of the section at Woodriding pit.

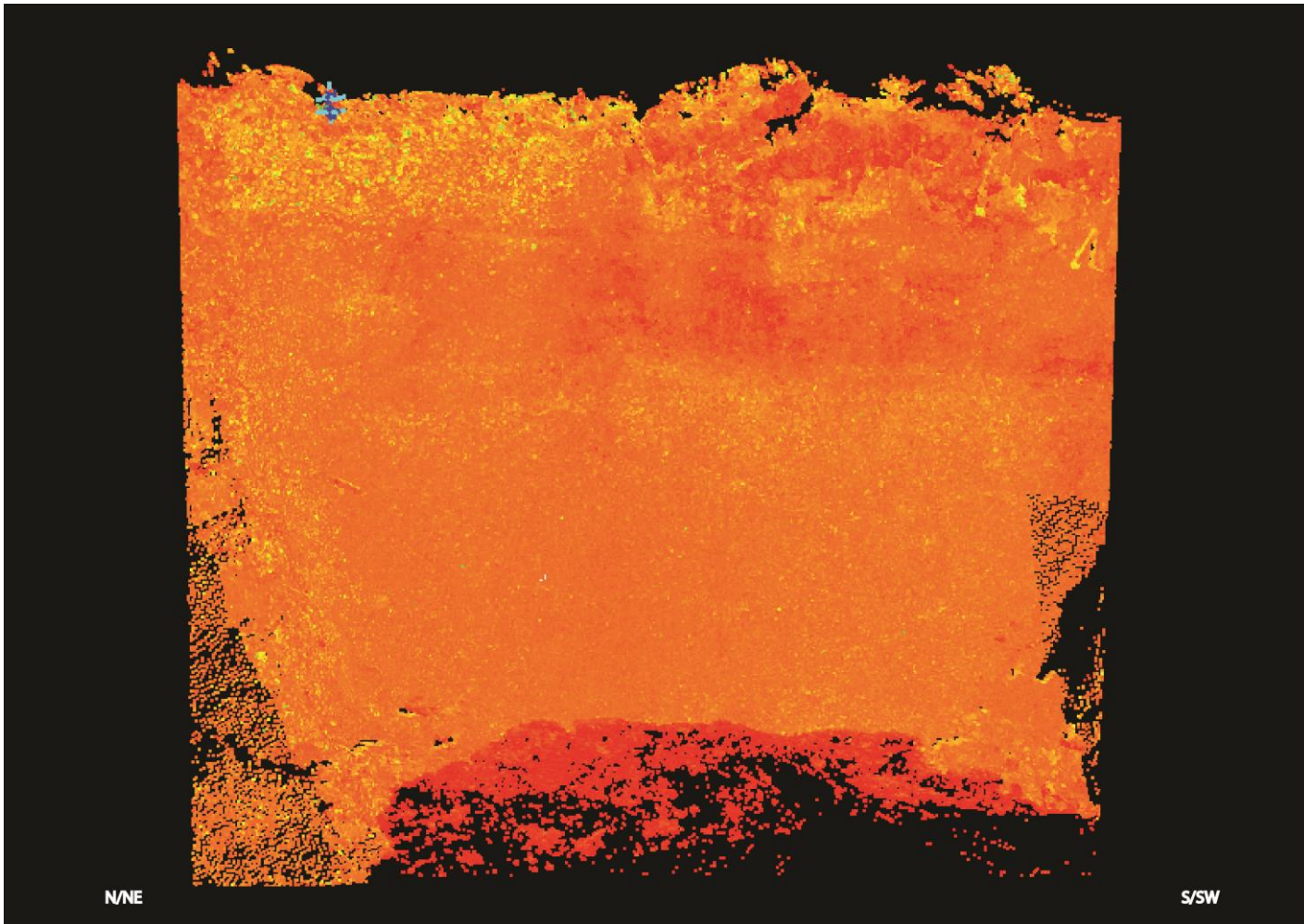


Figure A7.7 Detailed scan of section at Woodriding.

Appendix 8 Woodriding sediment log

WOODRIDING SECTION 1		
Unit	Description	Lithofacies
HB1.1	GRAVEL. Poorly sorted, matrix supported, crudely bedded, crudely graded, orange, medium gravel (7.5YR 4/6). High concentration of clasts and little matrix; pockets of framework gravel. Interbedded with sand and silty lenses. Large clasts (up to 30cm) present towards the lower boundary.	Gmg
HB1.2	SILTY GRAVEL. Very poorly sorted, matrix supported, massive, grey with orange, coarse silty medium gravel.	Gmm
HB1.3	SAND. Well-sorted, horizontally bedded, inversely graded, orange-red, medium to fine sand (2.5YR 4/6).	Sh
HB1.4	SAND. Well-sorted, horizontally bedded, inversely graded, orange-red, silty medium to fine sand (2.5YR 4/6).	Sh
HB1.5	SAND. Moderately sorted, horizontally bedded, graded, red-orange, clayey very coarse to coarse sand (2.5YR 4/6).	Sh
HB1.6	SAND. Moderately sorted, horizontally bedded, red silty coarse and medium sand (5YR 4/6).	Sh
HB1.7	SAND. Moderately sorted, horizontally bedded, graded, red, silty medium fine sand (5YR 4/6).	Sh
HB1.8	SAND. Moderately sorted horizontally bedded, orange-red silty clayey sand (2.5YR 4/6).	Sh
HB1.9	GRAVEL. Very poorly sorted, matrix supported, very crudely bedded, yellow-orange grey, coarse gravel (5YR 4/6). Band of larger clasts present towards the upper boundary. Here the matrix becomes more sandy. Clasts up to 20cm. The matrix is clayey sandy with much grit and granules. Bands of sandier matrix are present and a sand layer was identified towards to bottom of the section before obscuration by the water.	Gmh

Appendix 9 Woodgreen site recordings

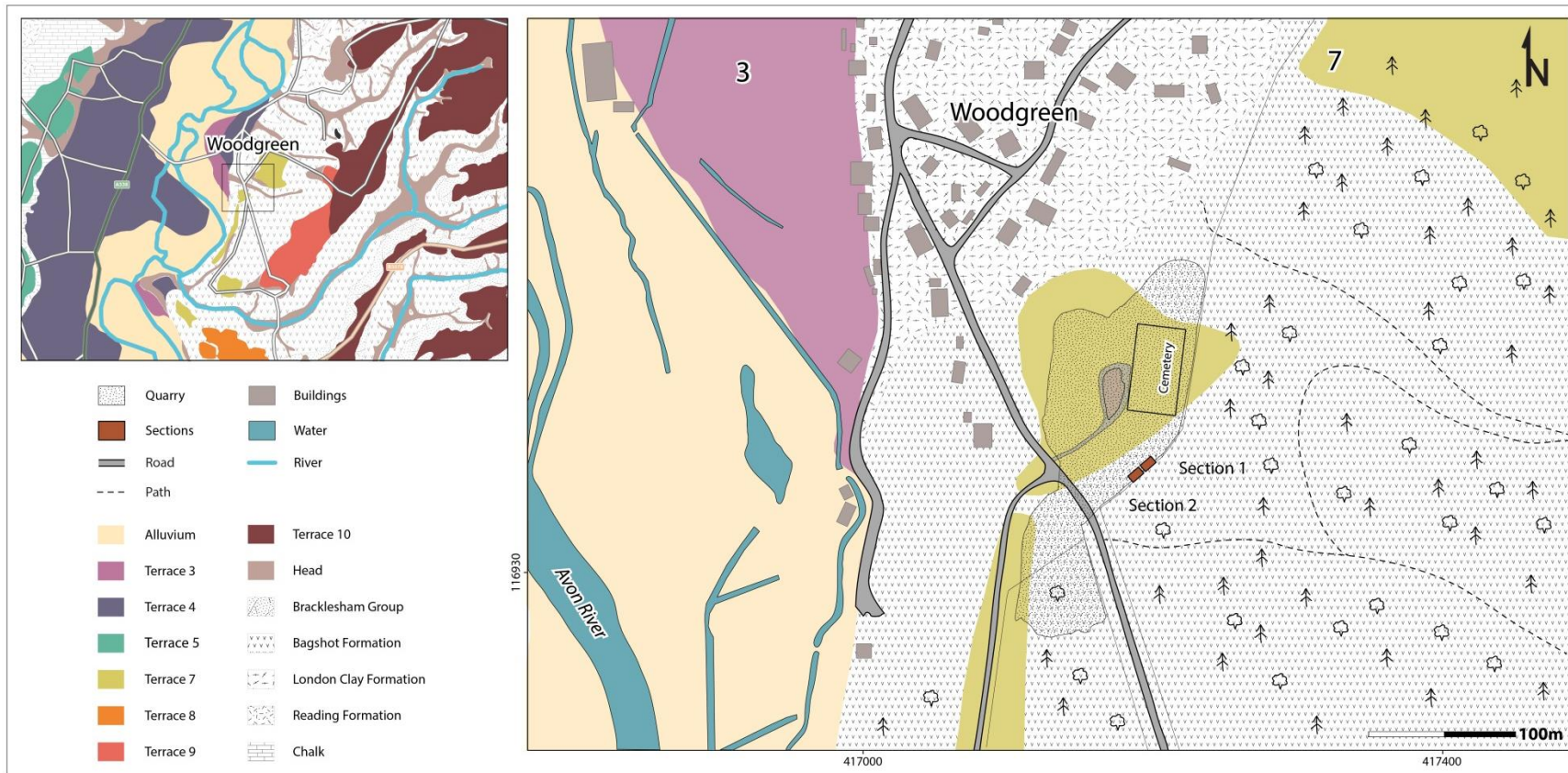


Figure A9.1 Map showing the location of the site of Woodgreen pit in relationship to the local bedrock and superficial geology (based upon 1:10000 scale geology data with permission of the British Geological Survey and 1:10000 scale OS VectorMap Local [shape file], Digimap Licence).

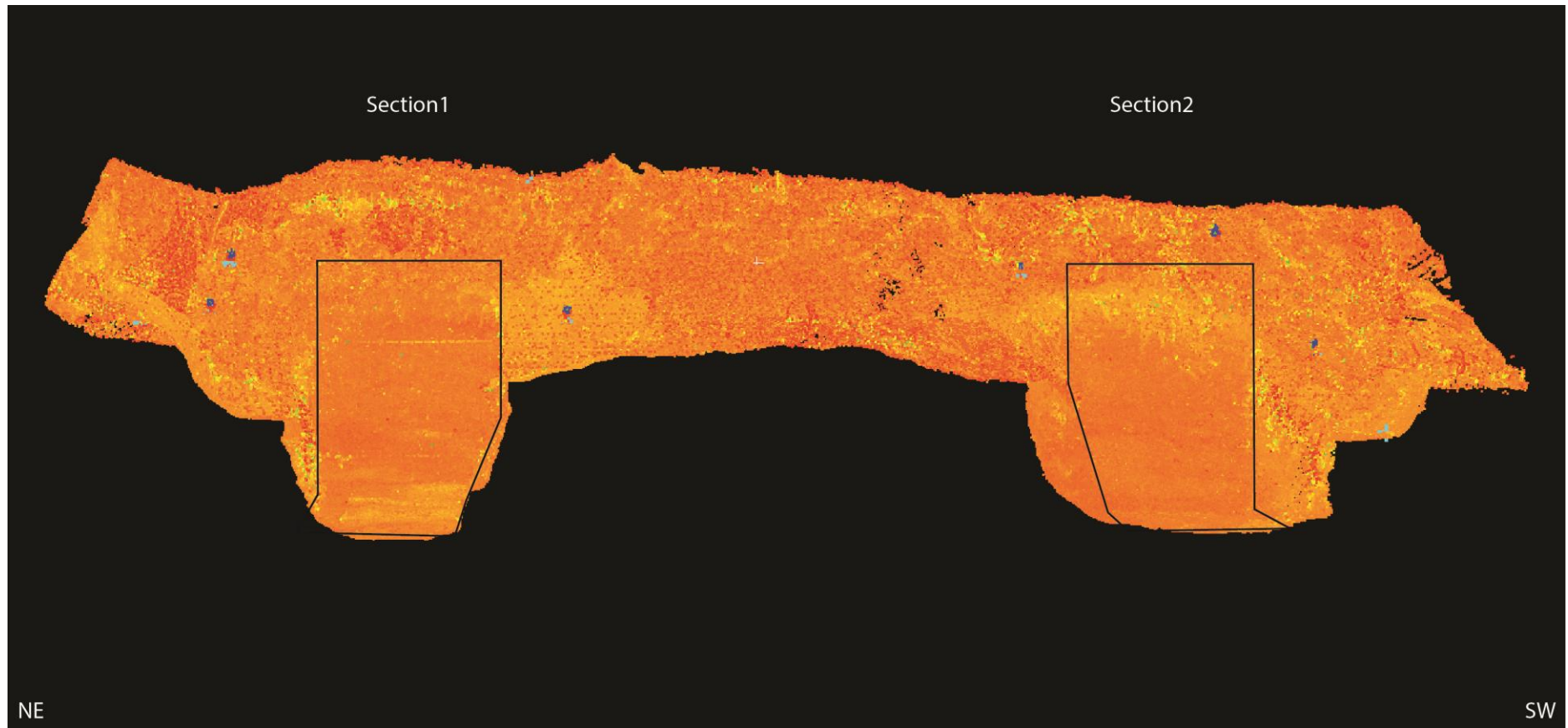


Figure A9.2 Terrestrial laser scan of Woodgreen pit, providing an overview of the site and the locations of sections 1 and 2.

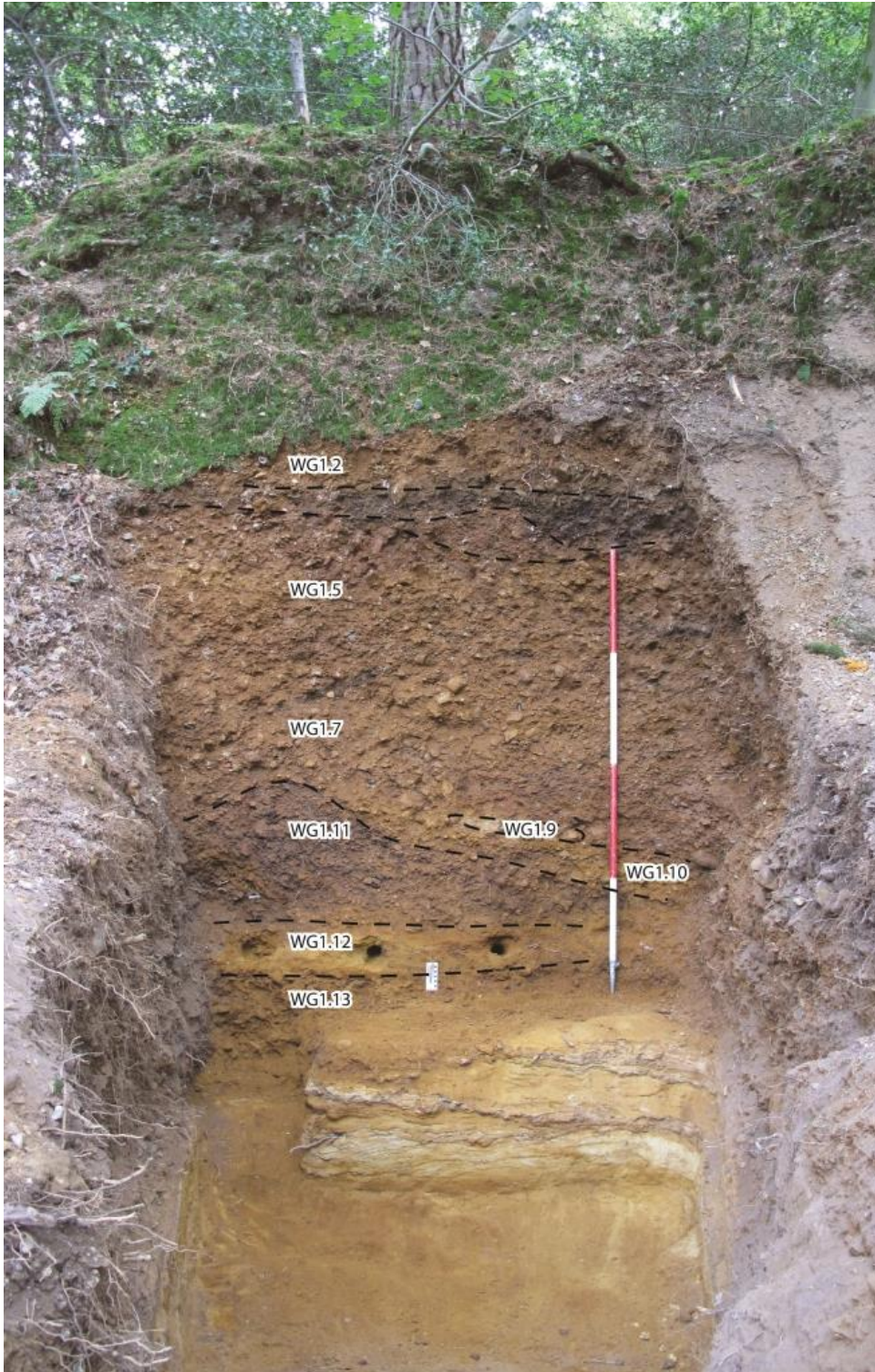


Figure A9.3 Annotated photograph of the section 1 at Woodgreen pit.



Figure A9.4 Annotated photograph of the section 2 at Woodgreen pit.

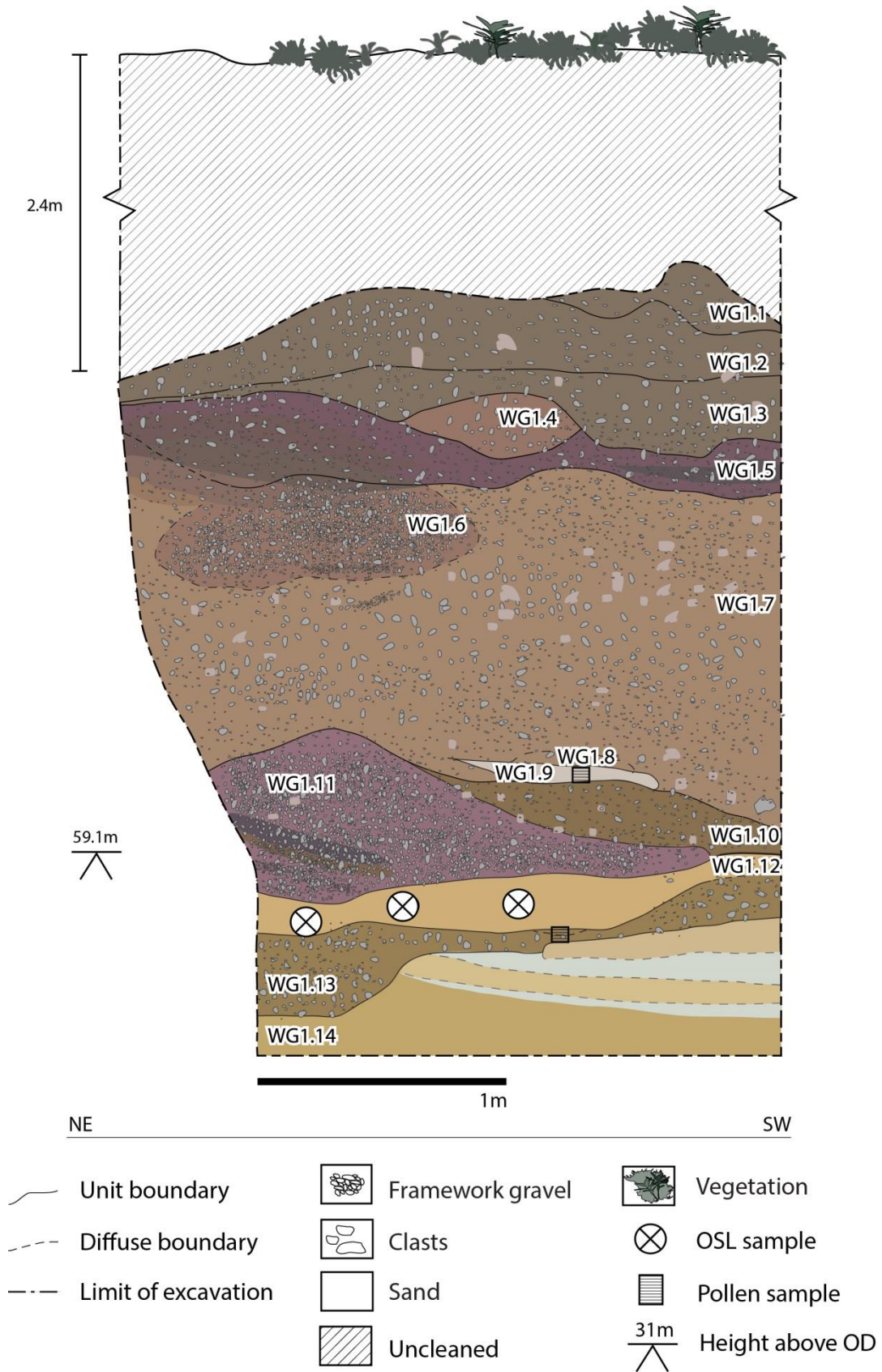


Figure A9.5 Drawing of section 1 at Woodgreen pit.

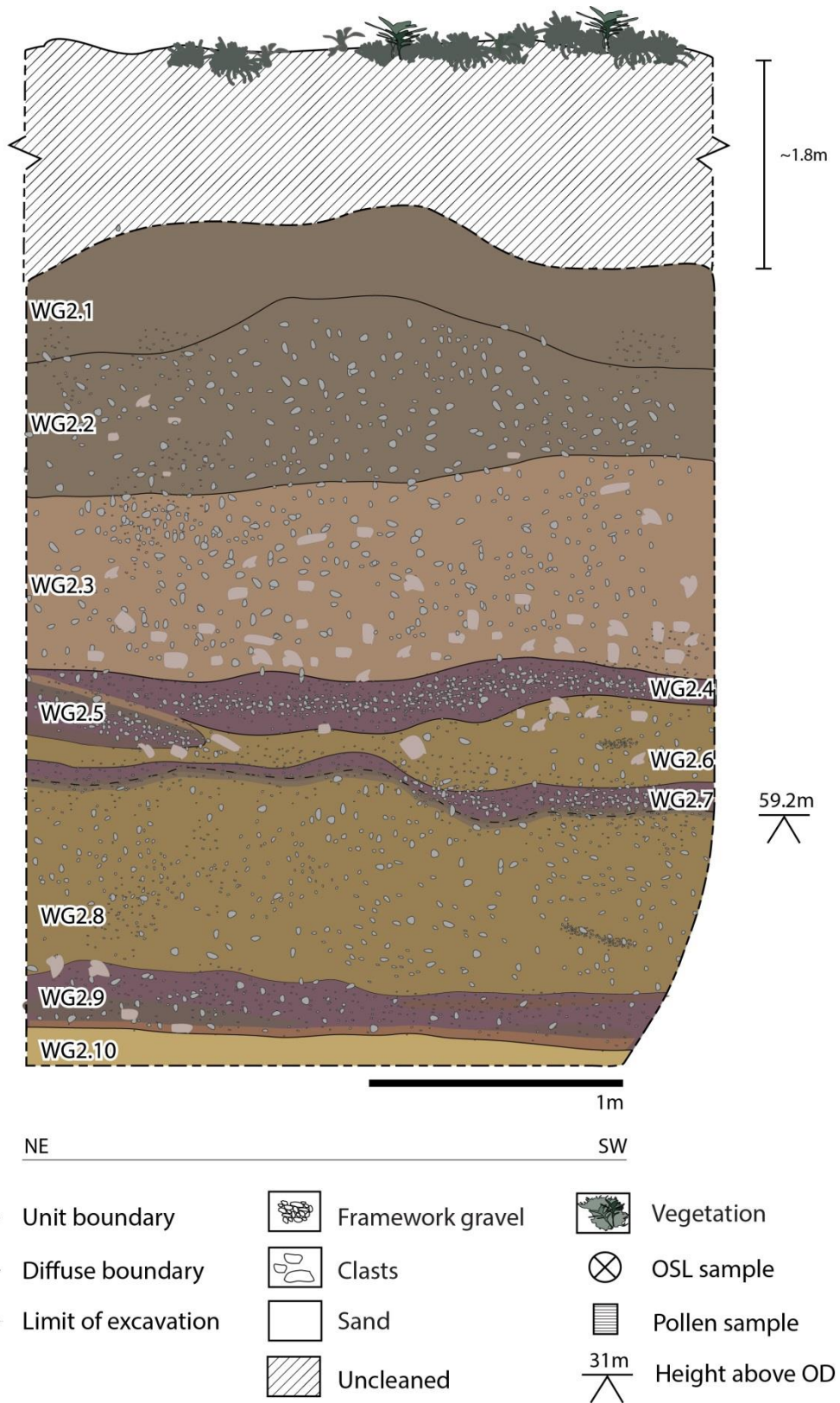


Figure A9.6 Drawing of section 2 at Woodgreen pit.

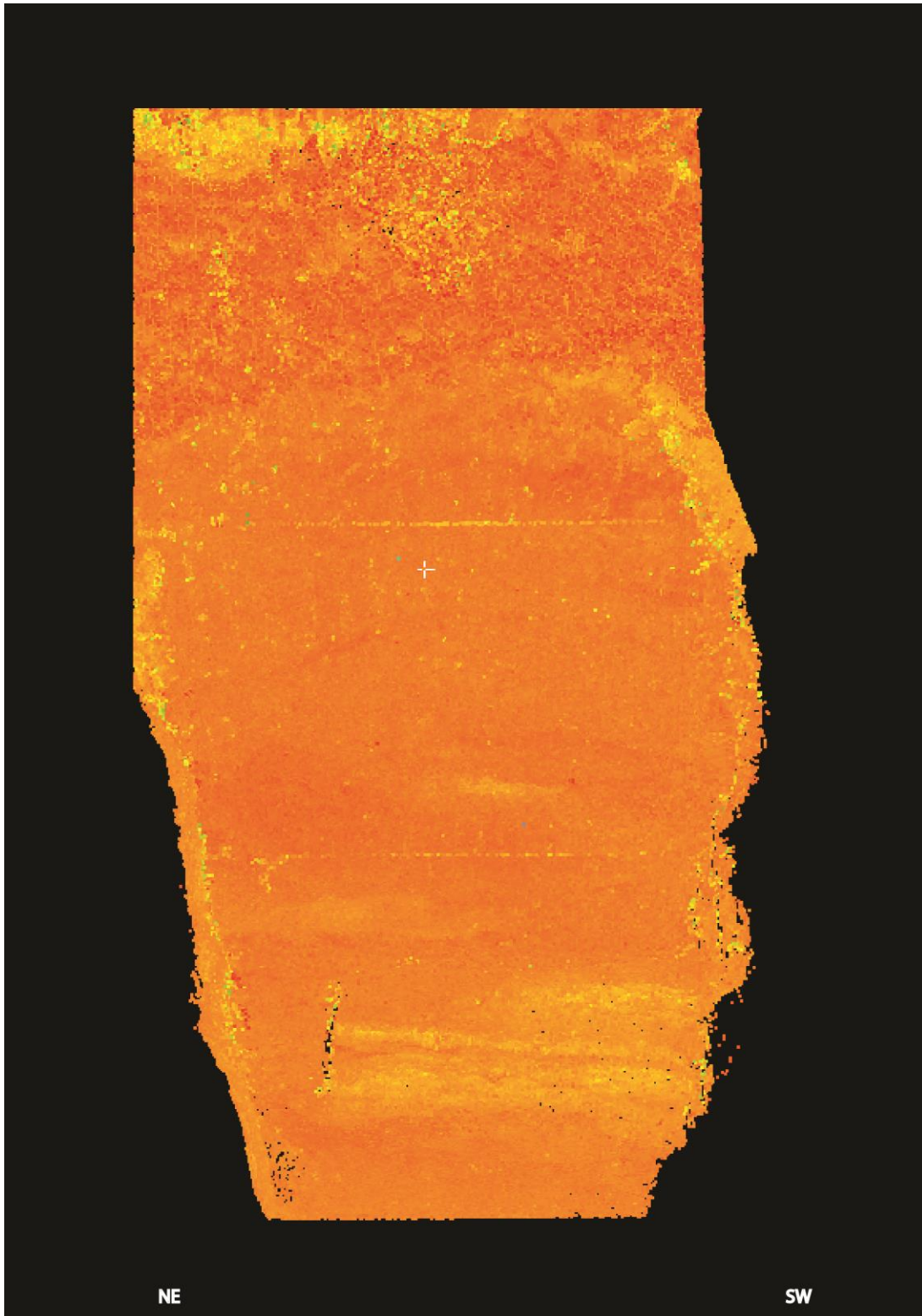


Figure A9.7 Detailed laser scan of section 1 at Woodgreen.

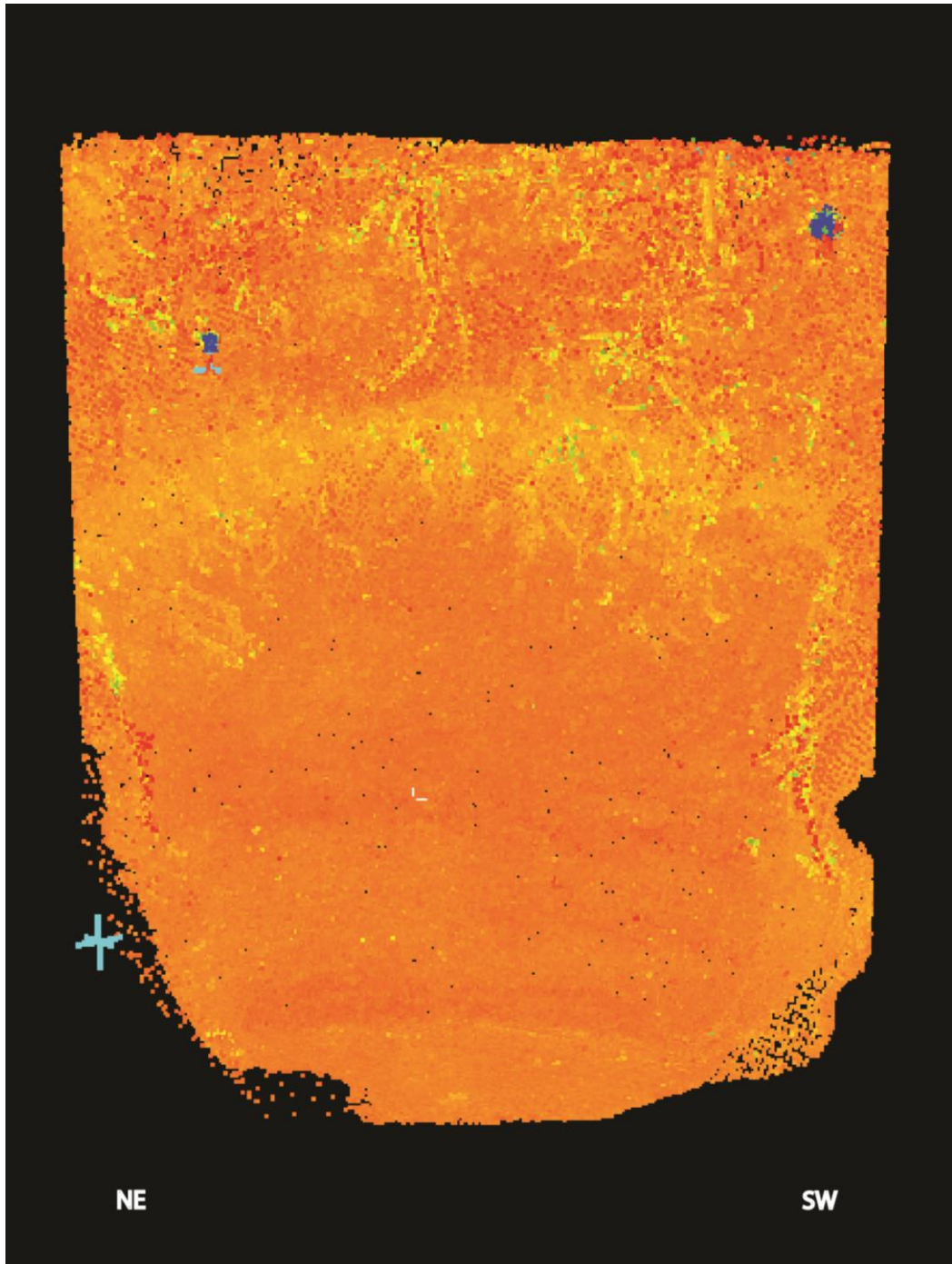


Figure A9.8 Detailed laser scan of section 2 at Woodgreen.

Appendix 10 Woodgreen sediment logs

WOODGREEN SECTION 1		
Unit	Description	Lithofacies
WG1.1	TOPSOIL. Topsoil and uncleaned section.	
WG1.2	GRAVEL. Poorly sorted, matrix supported, crudely graded gravel (7.5YR 4/6; top 7.5YR 5/8). The matrix is silt with coarse sand and granules.	Gmg
WG1.3	GRAVEL. Manganese and iron stained, clast supported, moderately sorted flint gravel (7.5YR 2.5/3). Dominant clasts are subangular and of an average size of 2cm.	Gc
WG1.4	GRAVEL. Pocket of moderately sorted, medium flint gravel (5YR 4/6). Clasts are angular to subangular on average 1cm.	Gc
WG1.5	GRAVEL. Poorly sorted, clast supported, flint gravel (5YR 4/6). Larger clasts (ranging up to 8cm) are dominant and subrounded, other clasts range from well-rounded to subangular clasts. Matrix is clayey, including silt and granules. In some places the deposit is manganese concreted.	Gc
WG1.6	GRAVEL. Pocket of moderately sorted, clast supported flint gravel (5YR 4/6). Dominant clast size 1-2cm.	Gc
WG1.7	SANDY GRAVEL. Poorly to very poorly sorted, matrix supported sandy gravel (7.5YR 4/6 higher: 7.5YR 5/8). Some cross-bedding. Largest clasts ca. 9cm, smallest ca. 0.5cm. Dominant clast size falls between 1-3cm. Clasts are well-round to subrounded and rolled(?) but unbroken flint nodules. Majority of the smaller clasts are sub-angular.	Gp
WG1.8	GRAVELLY SAND. Coarse, horizontally-bedded gravelly sand (5YR 4/6). Larger clasts up to 2.5cm and are well-rounded to sub-angular. The deposit is crudely graded to the left and inversely graded into clast supported gravel.	Sh
WG1.9	SILT. Horizontally-bedded, compact silt (10YR 6/6). Crudely graded to the left, getting more clayey, silt deposited around clasts up to 5cm.	Fl

WG1.10	GRAVEL. Poorly sorted, matrix supported flint gravel (7.5YR 5/8 some bands more red). Largest clasts are ca. 9cm and subrounded. The average clast size is ca. 3cm, mainly angular. Smallest clasts are 0.5cm. Some crude grading towards the left. The matrix is sandy silt.	Gmg
WG1.11	GRAVEL. Bedded matrix and clast supported gravel, moderately sorted gravel (lower layer: 5YR 4/6 FG: 2.5YR 4/8 and some purple). Average clast size ca. 2cm. Bands of framework gravel present in the upper part of the unit, dipping NE to SW. Framework gravel is moderately to well sorted with an average clast size of ca. 1cm; layers interspersed with coarser gravel. Clasts are angular to subangular.	Gh
WG1.12	SAND. Horizontally-bedded coarse sand (10YR 5/8). Some grading. Largest clasts are ca. 2.4cm.	Sh
WG1.13	GRAVEL. Clast supported, moderately sorted, compact flint gravel (5YR 4/6). Some bedding and some grading. Dominant clast size is ca. 1cm, smallest clasts are 0.5cm. Both are angular, larger clasts are sub-angular and subrounded. Bands of framework gravel dip towards the NE.	Gcg
WG1.14	SAND. Horizontally-(slightly wavy)bedded, very compact medium sand and fine sand deposit, interspersed with compact clay (clay: 7.5YR 6/4 and 8/1 sand: 10YR 5/8 and black and orange). Dipping south and east (Bagshot Formation).	Sh

WOODGREEN SECTION 2		
Unit	Description	Lithofacies
WG2.1	TOPSOIL. Topsoil and uncleaned section. Par WG1.1	
WG2.2	GRAVEL. Par WG1.2	Gmg
WG2.3	Par WG1.7	Gc
WG2.4	GRAVEL. is a greyish brown and purple orange, clast supported, moderately sorted flint gravel deposit. The larger clasts, some rounded and many sub-rounded to sub-angular, measure 4cm, the smaller clasts are mainly sub-angular and 1cm. the average clast size is 1.5-2cm. The matrix consists of granules and coarse sand with a trace of clay.	Gc
WG2.5	GRAVEL. Dark patch of moderately sorted, sub-horizontally bedded, graded, gravel. Layer of framework with gravel with an average size of 0.5cm the clasts become grid sized and matrix supported in a lighter yellow deposit. Abrupt upper boundary, gradual lower boundary. Largest clasts 6cm. Sub-angular to rounded.	Gc
WG2.6	GRAVEL. Poorly sorted, matrix supported, inversely graded, flint gravel. Largest clast 12cm, average clast is 2cm. Sub-angular to sub-rounded clasts. Silty matrix including granules, grid and coarse sand.	Gm
WG2.7	Par WG1.11	
WG2.8	GRAVEL. Poorly sorted, matrix supported, orange, crudely bedded, flint gravel. Iron-manganese stained and indurated. Largest clast 10cm. Clasts are subangular, some sub-rounded.	Gm
WG2.9	GRAVEL. Poorly sorted, clast supported, grey and purple red, compact flint gravel. Iron-manganese stained and indurated. Largest clast 10cm. Clasts are subangular, some sub-rounded.	Gc
WG2.10	SAND. Par WG1.14	Sh

Appendix 11 Somerley site recordings

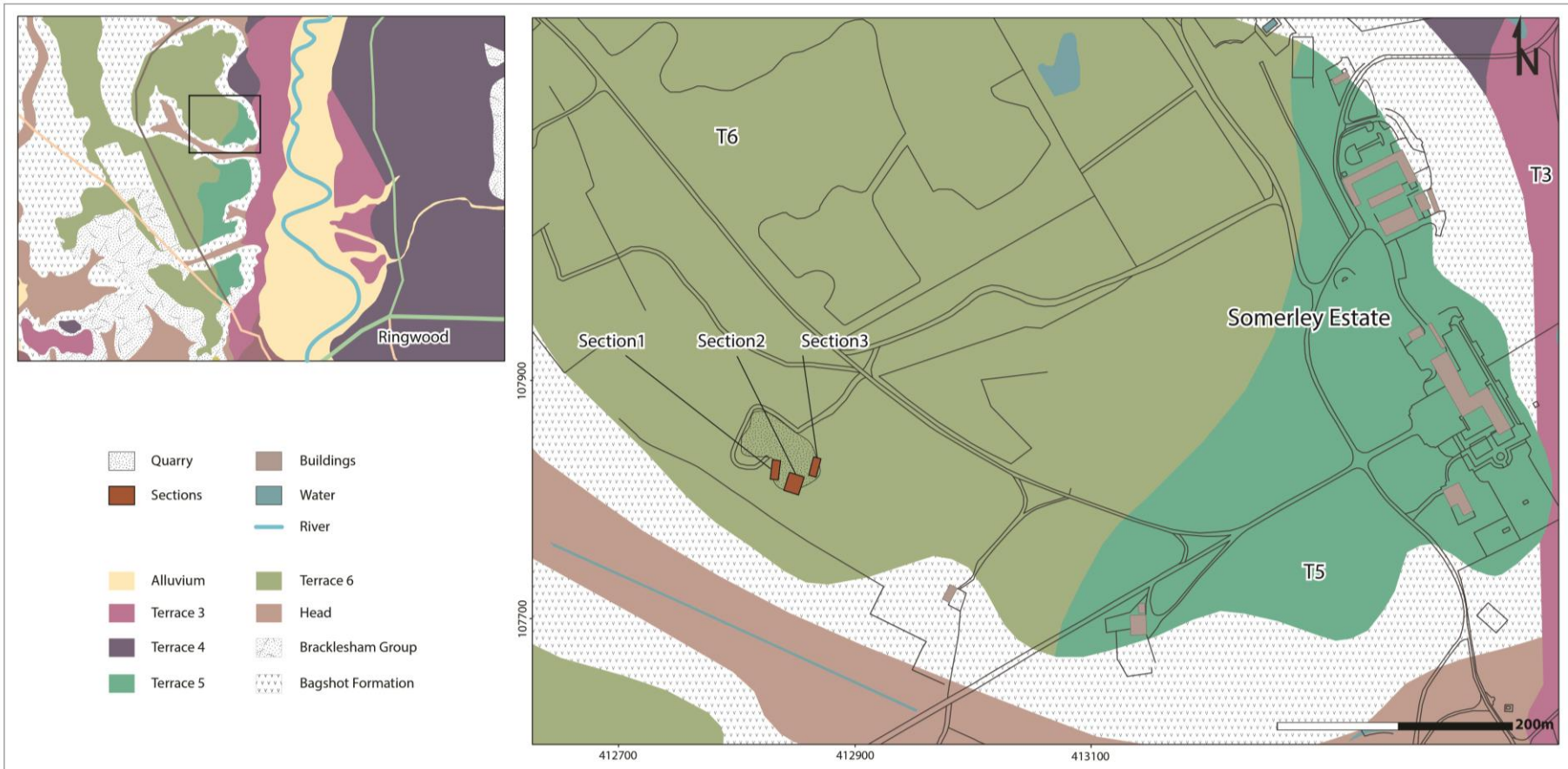


Figure A11.1 Map showing the location of the site of Somerley pit in relationship to the local bedrock and superficial geology (based upon 1:10000 scale geology data with permission of the British Geological Survey and 1:10000 scale OS VectorMap Local [shape file], Digimap Licence).

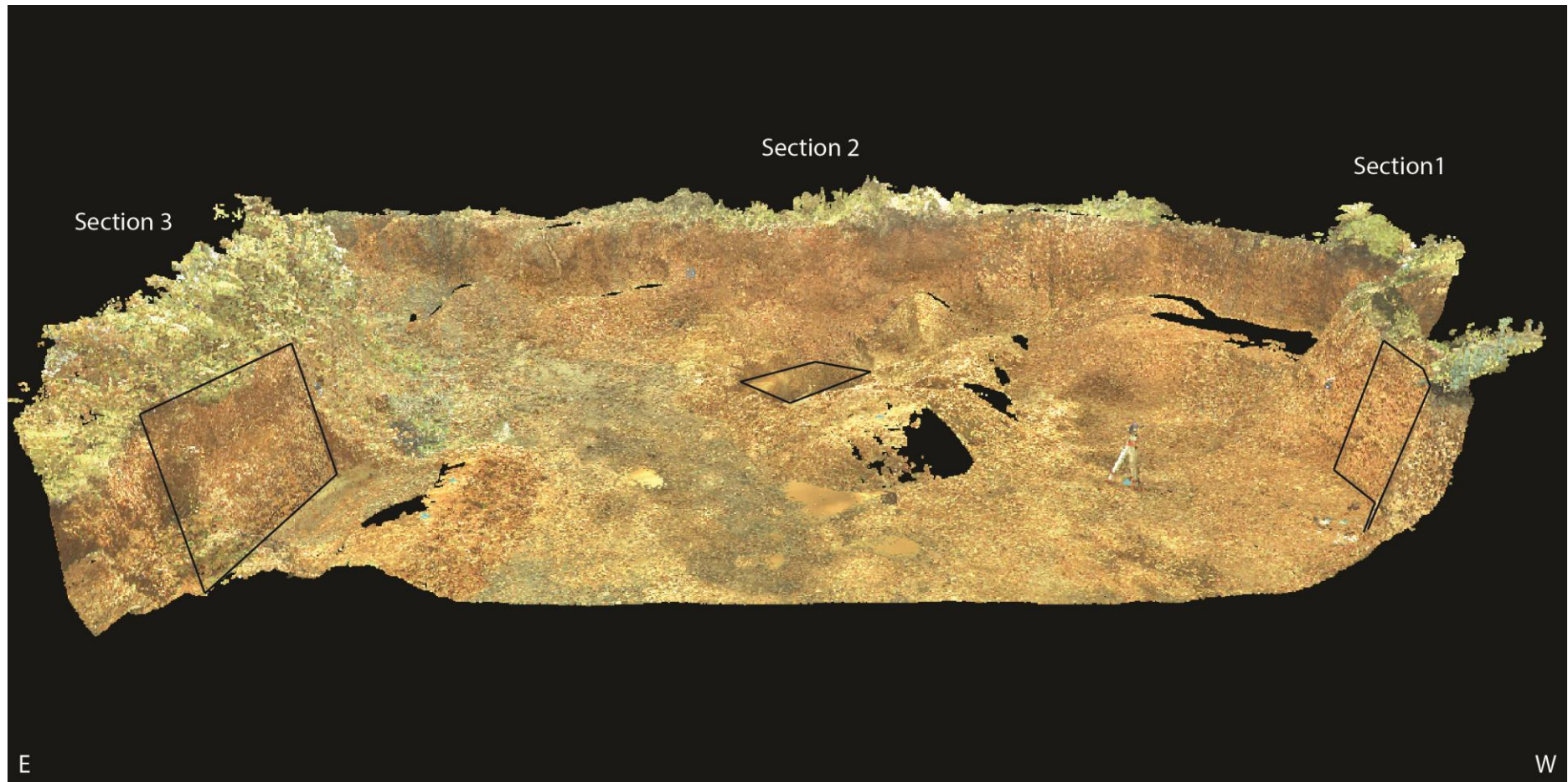


Figure A11.2 Terrestrial laser scan of Somerley pit, providing an overview of the site and the locations of sections 1-3.

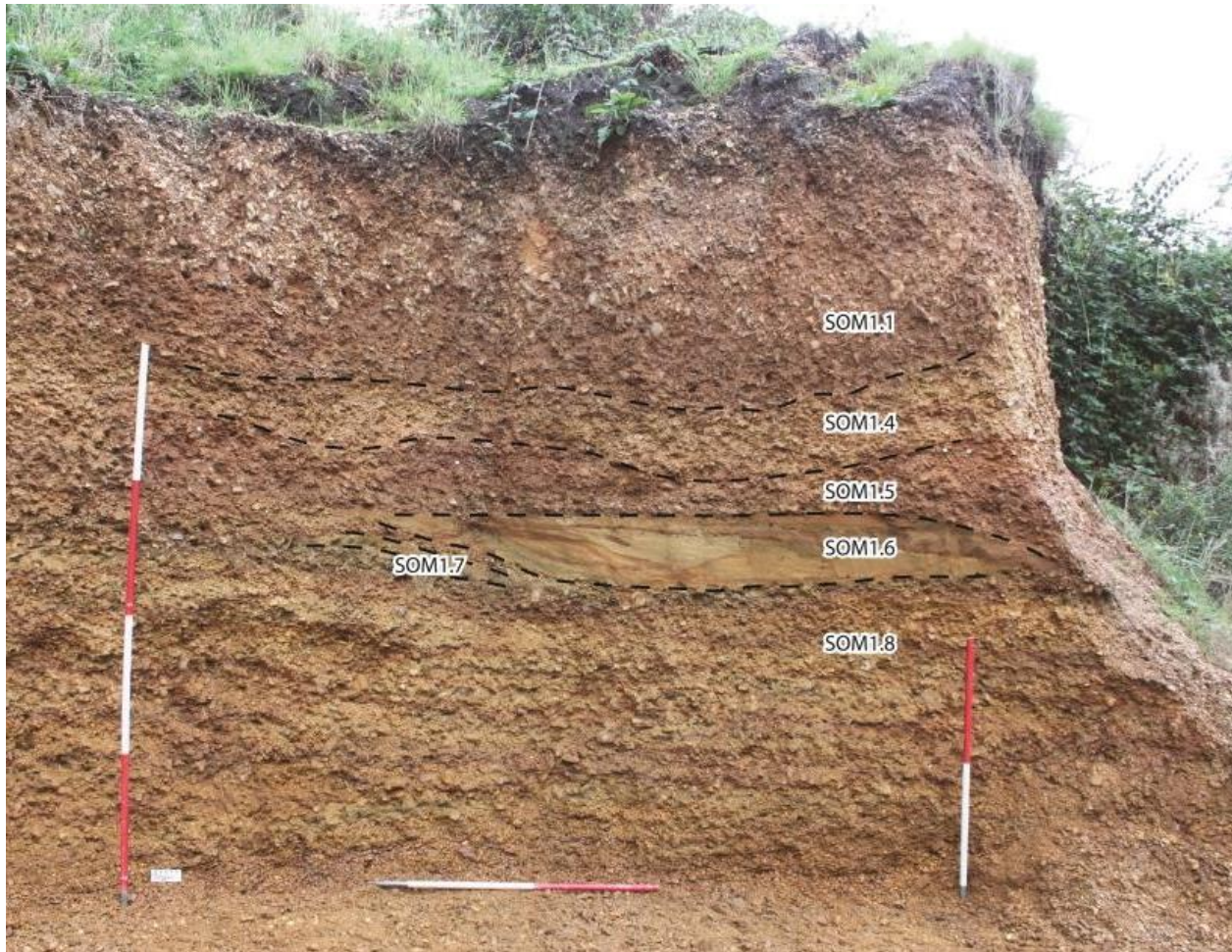


Figure A11.3 Annotated photograph of the section 1 at Somerley pit.

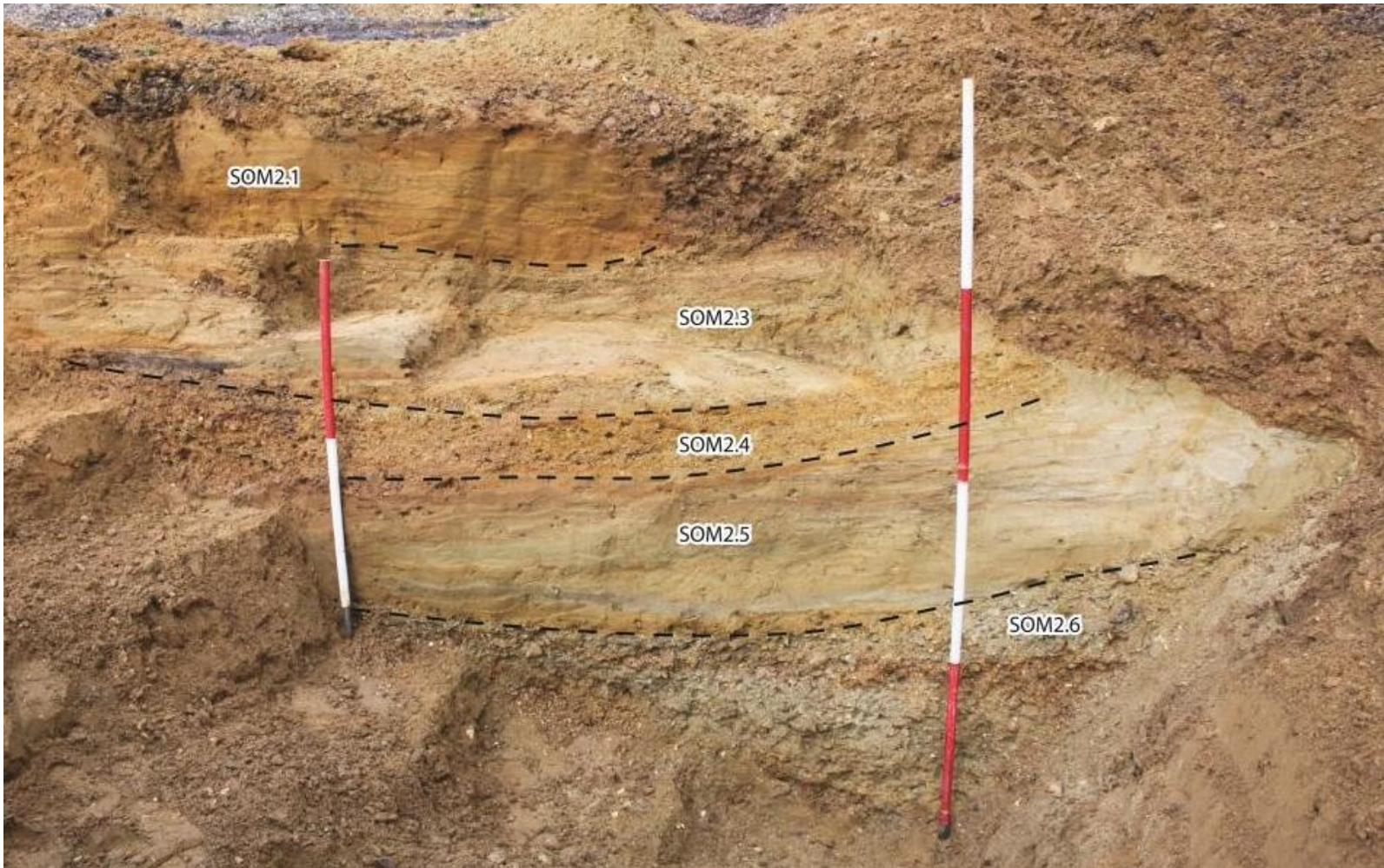


Figure A11.4 Annotated photograph of the section 2 at Somerley pit.

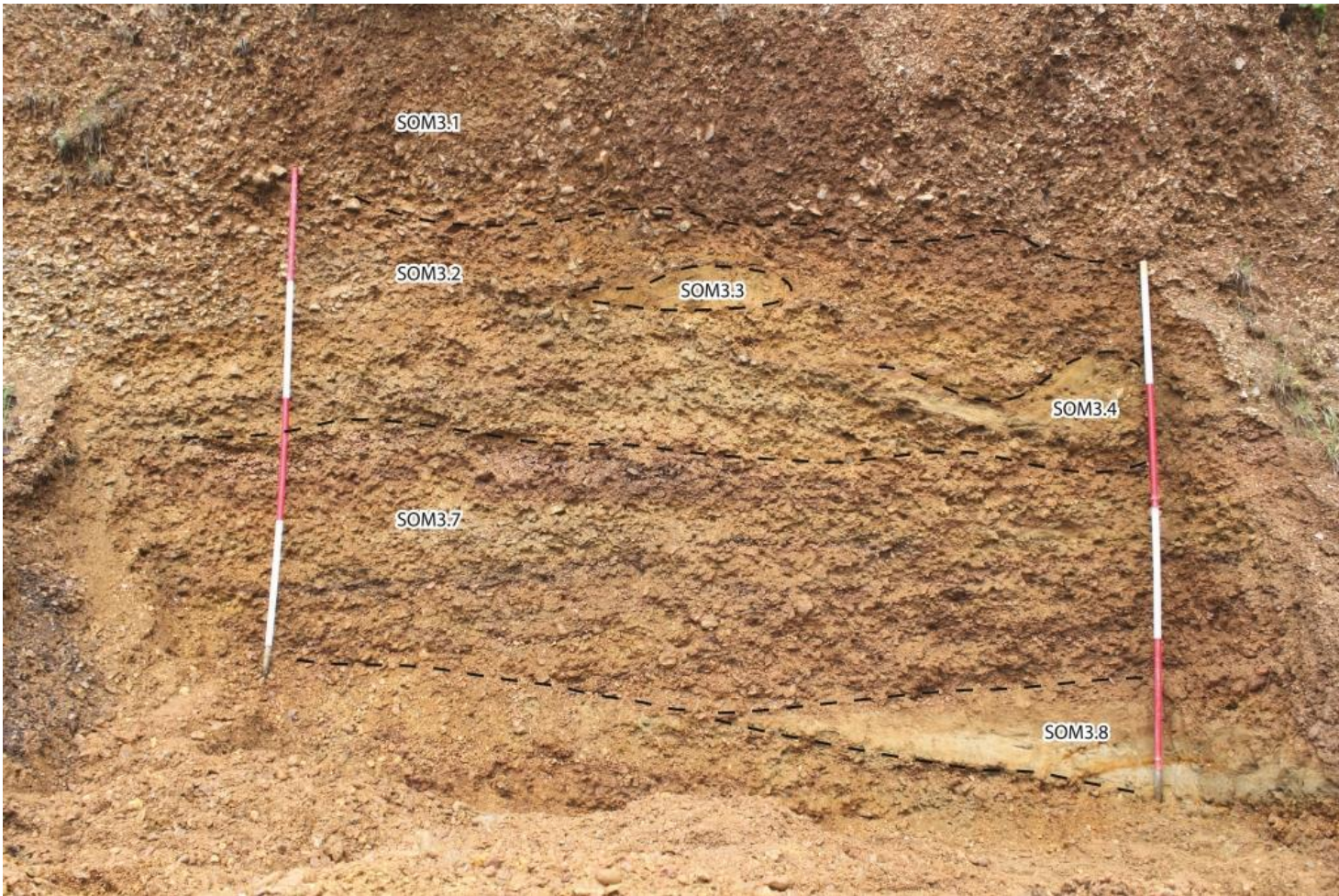


Figure A11.5 Annotated photograph of the section 3 at Somerley pit.

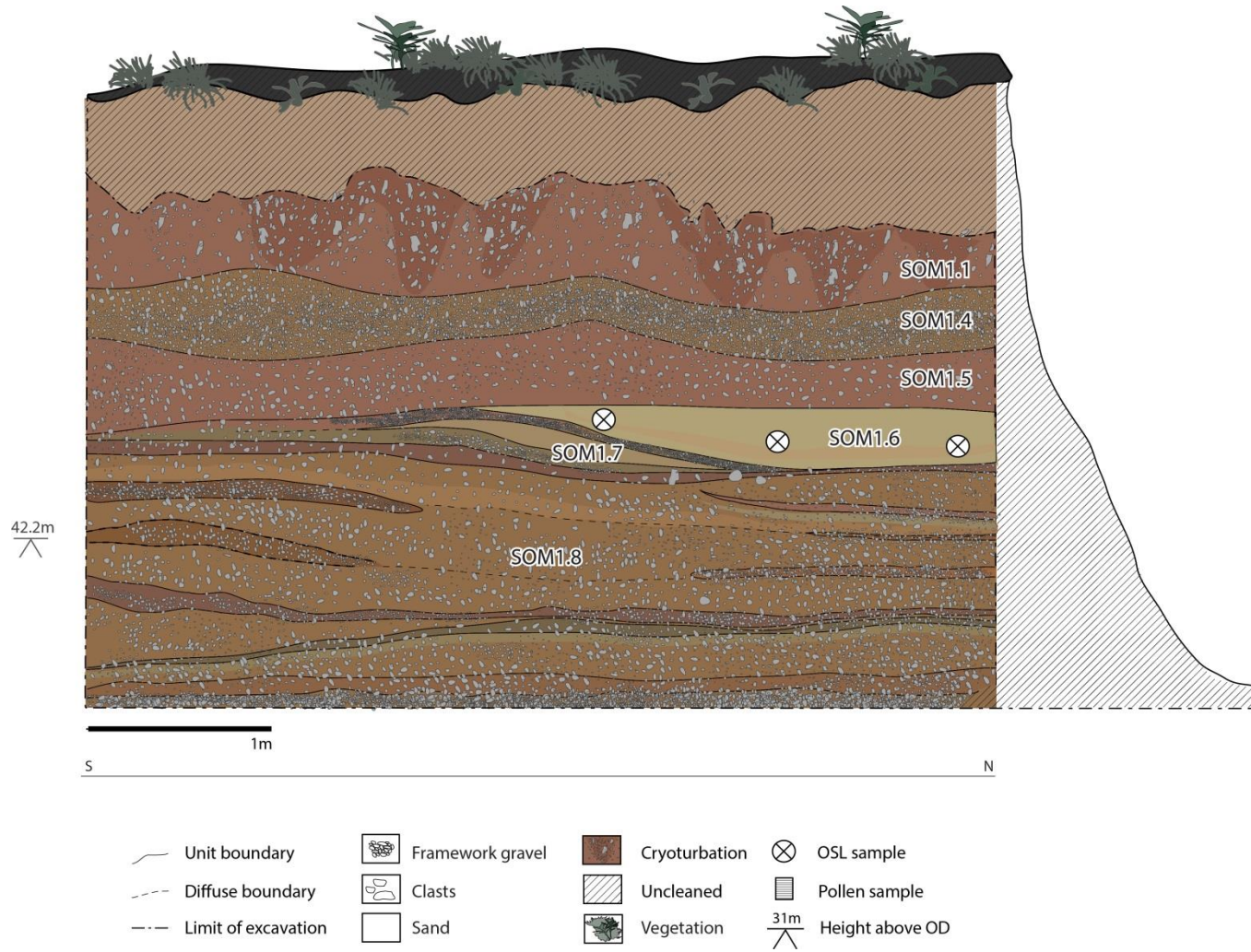


Figure A11.6 Drawing of section 1 at Somerley pit.

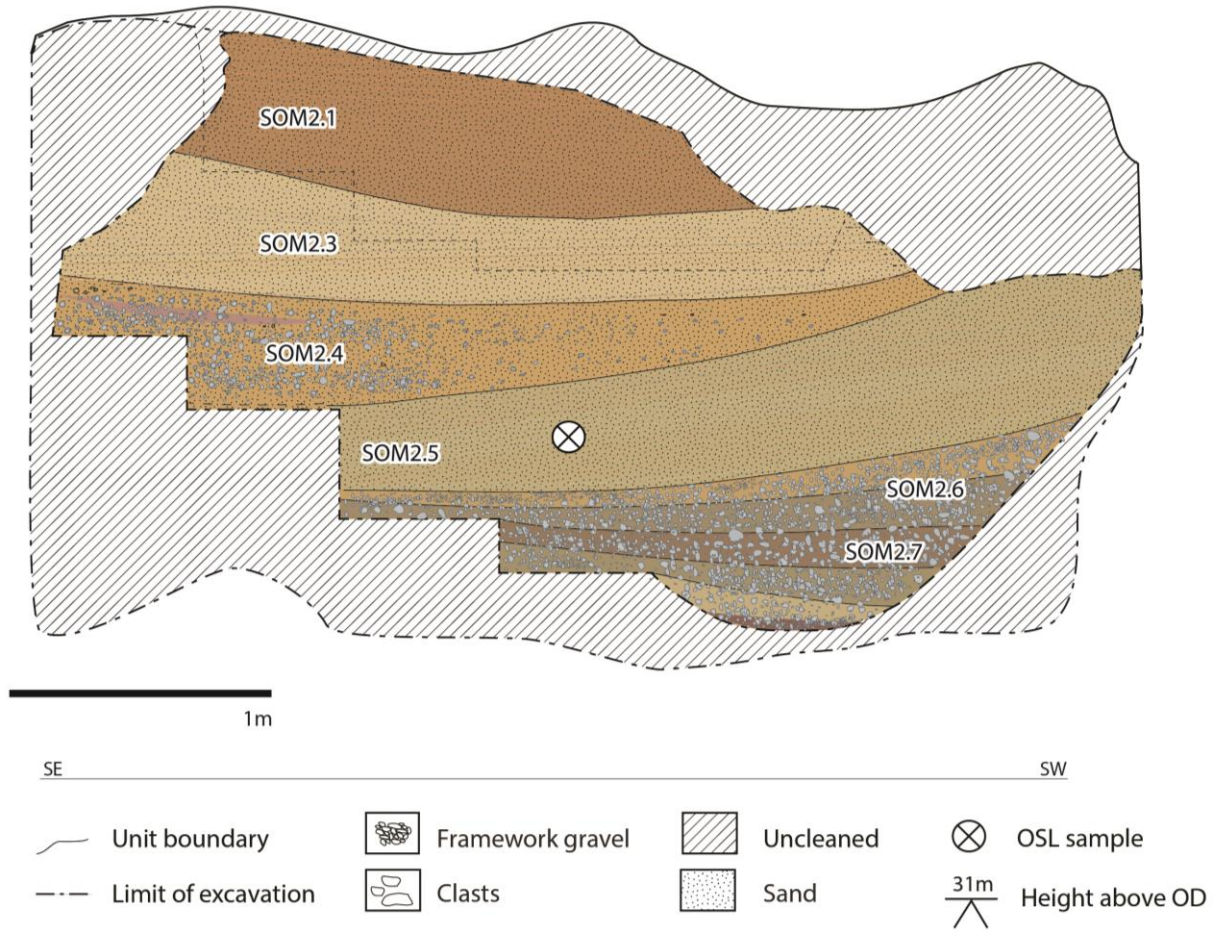


Figure A11.7 Drawing of section 2 at Somerley pit.

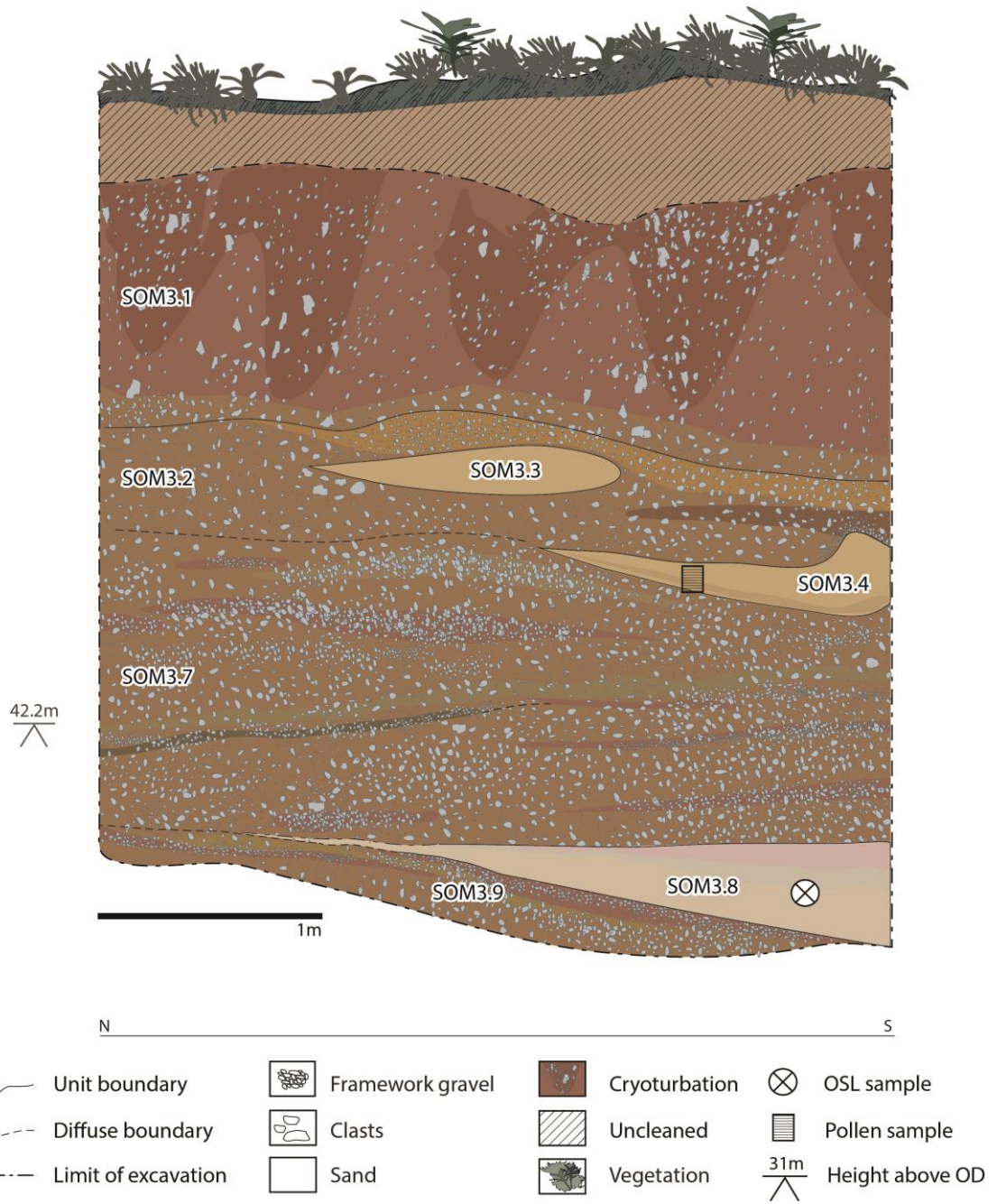


Figure A11.8 Drawing of section 3 at Somerley pit.

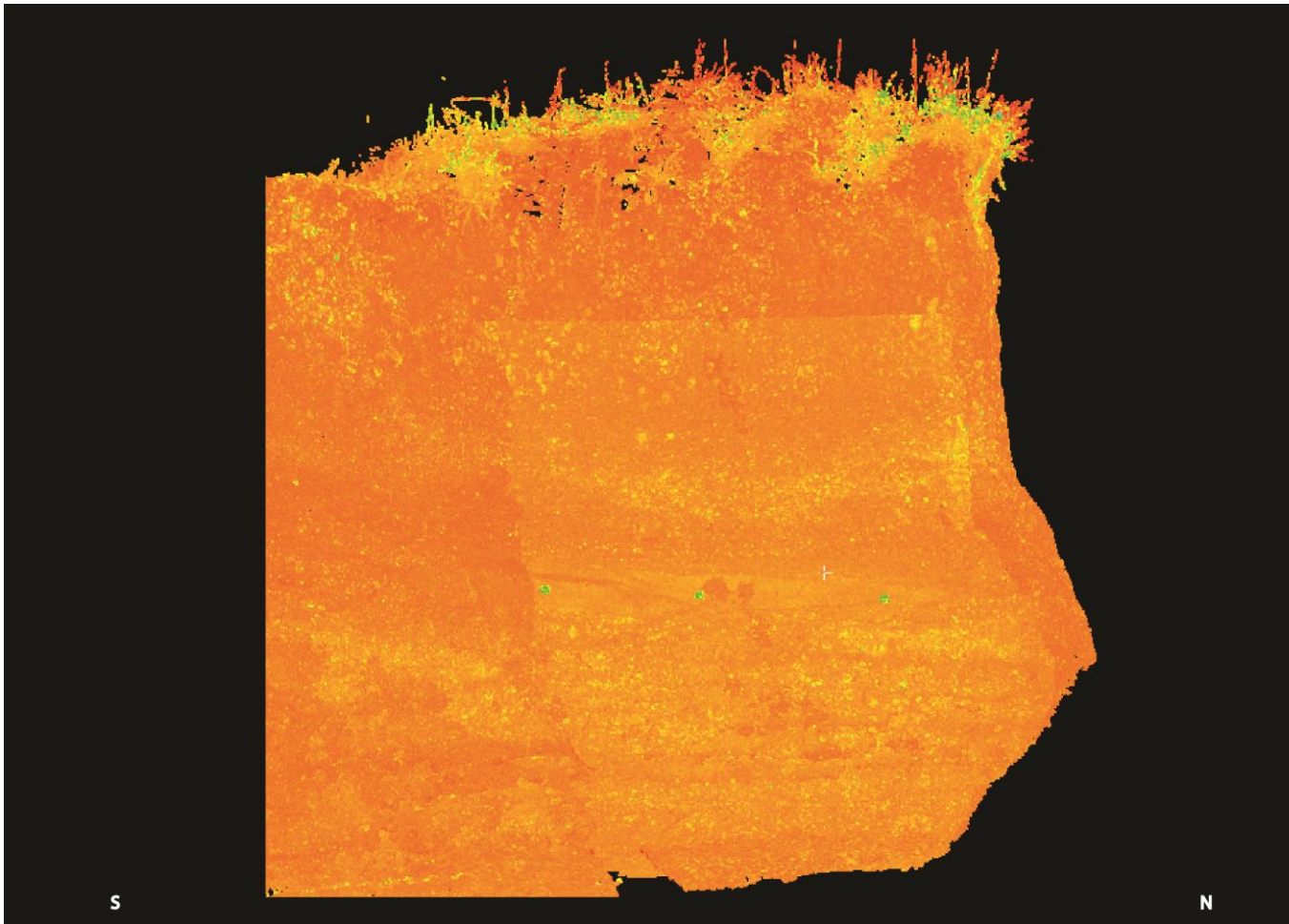


Figure A11.9 Detailed laser scan of section 1 at Somerley.



Figure A11.10 Detailed laser scan of section 2 at Somerley.

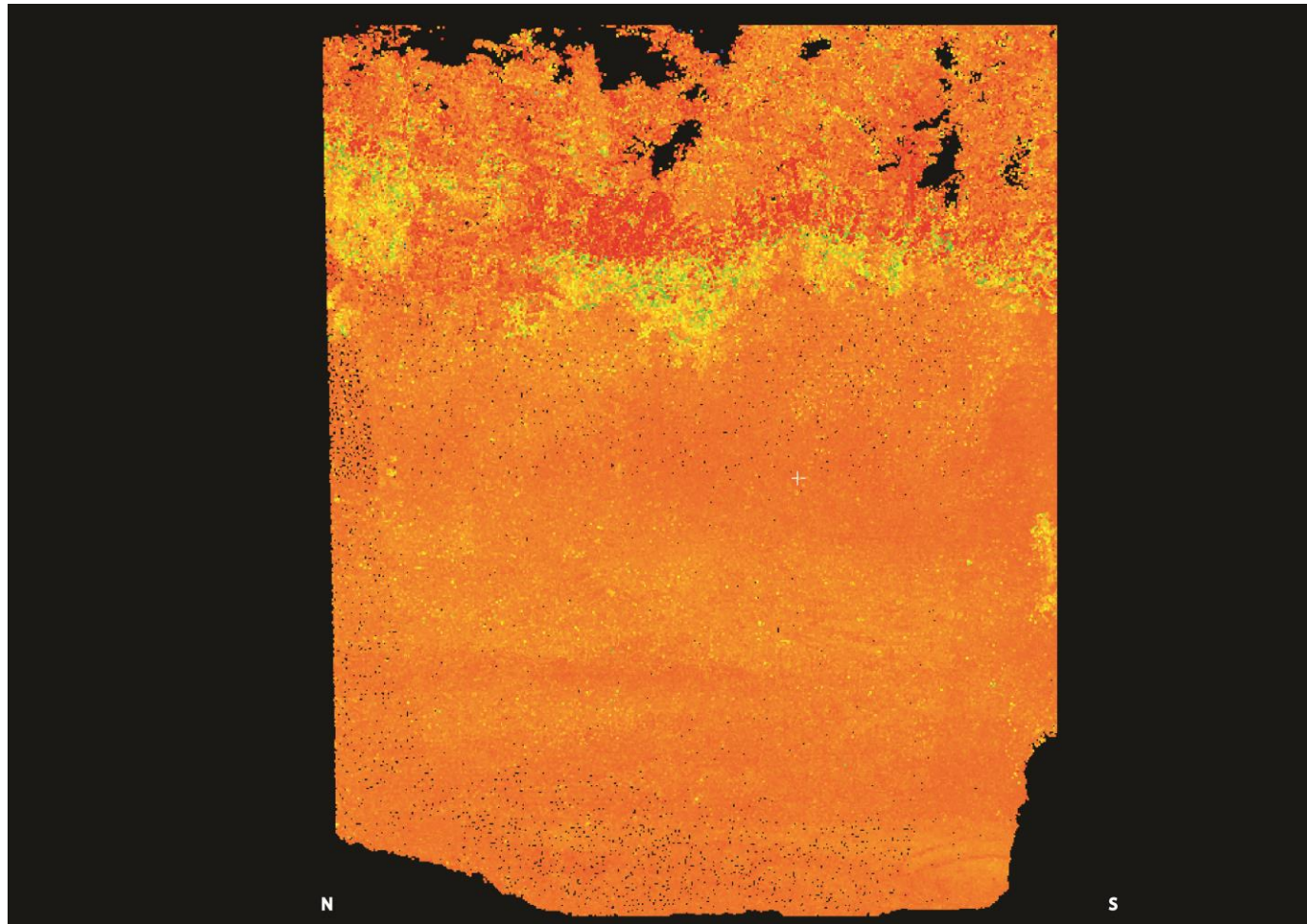


Figure A11.11 Detailed laser scan of section 3 at Somerley.

Appendix 12 Somerley sediment logs

SOMERLEY SECTION 1		
Unit	Description	Lithofacies
SOM1.1	GRAVEL. Very poorly sorted, matrix supported, red-orange coarse gravel (7.5YR 5/8). Clasts are sub angular to (well) rounded of which the largest measures 11cm and the smallest 0.5cm. Clasts of over 3cm are dominant. Some cryoturbation features present. The matrix is clayey silt with little inclusions of larger size.	Gm
SOM1.4	SANDY GRAVEL. Poorly sorted, matrix supported, yellow orange, horizontally-bedded, yellow orange, medium gravel. The matrix is very sandy including coarse sand, grid and granules.	Gh
SOM1.5	SANDY GRAVEL. Poorly sorted, matrix supported, red-orange coarse gravel (7.5YR 5/8). Clasts of over 3cm are dominant. The matrix is clayey silty coarse to medium sand.	Gh
SOM1.6	SAND. Compact, moderately sorted, cross-bedded, graded, yellow, orange and grey, medium sand (10YR 5/6). The sand includes quartz and black grains.	Sp
SOM1.7	SAND. Compact, well-sorted, bedded, inversely graded, dark grey, yellow-brown, medium to fine sand (10YR 5/6; 10YR 5/8). Some silt towards the bottom of the deposit.	Sh
SOM1.8	GRAVEL. Poorly sorted, horizontally-bedded, alternatingly sandy matrix supported and clast supported to open framework gravel (Sandy gravel 10YR 5/8; framework gravel 7.5YR 5/8). Bands of open-framework gravel are overlain with clast supported gravel sandy, matrix supported gravel.	Gh

SOMERLEY SECTION 2		
Unit	Description	Lithofacies
SOM2.1	SAND. Well-sorted, nearly horizontally-bedded, bright orange, medium sand (7.5YR 5/8). Red/pink/purple layers and some grey bands with a higher silt content. The bedding is dipping towards the right of the section. The sand includes quartz grains and black grains. This sand unit includes some small, subrounded, flint clasts of 0.5cm.	Sh
SOM2.3	SILTY SAND. Moderately sorted, horizontally-bedded, pink and grey, medium fine sand with granules (10YR 5/8; 2.5Y 5/4; 7.5YR 5/8). Grey-yellow and very yellow layers appear towards the bottom of the unit. Here the sand includes more black grains.	Sh
SOM2.4	SAND. Loose, finely bedded, red grey, coarse sand with some gravel of 1cm (10YR 5/8). Coarser layers with granules alternate with finer, reddish, deposits. The layers dip towards the left of the section. Towards the lower boundary the unit becomes really gravelly, especially in the left of the section. Here the clasts are sub-angular, 1cm/0.5cm up to 3cm.	Sh
SOM2.5	SILTY SAND. Moderately sorted, horizontally-bedded, pink and grey, medium fine sand (10YR 5/8; 2.5Y 5/4; 7.5YR 5/8). Grey-yellow and very yellow layers appear towards the bottom of the unit. Here the sand includes more black grains.	Sh
SOM2.6	SANDY GRAVEL. Poorly sorted, matrix supported, horizontally-bedded, grey sandy medium to fine gravel.	Gh
SOM2.7	CLAYEY GRAVEL. Poorly sorted, matrix supported, orange, medium gravel. A similar sequence of bedding as described in SOM1.8 was observed here when the trench was temporarily further opened to establish bedrock height.	Gh
SOM2.8	SAND. Well-sorted, light-grey medium sand with silt and clay (Parkstone Sand).	Sh

SOMERLEY SECTION 3		
Unit	Description	Lithofacies
SOM3.1	Par SOM1.1	
SOM3.2	Par SOM1.4	
SOM3.3	SAND. Poorly sorted, cross-bedded, horizontally graded, coarse to medium sand. To the right the deposit is coarser, yellow-orange and gritty and to the left it contains some silt and clay and is orange-red (10YR 5/8; 7.5YR 5/6 and 4/6).	Sp
SOM3.4	SAND. Moderately sorted, horizontally-bedded, yellow grey, medium to fine sand with some silt and clay. Multiple phases of inverse grading. At the top the sand grades into a gravelly sand that again grades into sand. Cryoturbation features present in the right of the deposit.	Sh
SOM3.7	Par SOM1.8	
SOM3.8	SAND. Moderately sorted, horizontally-bedded, inversely graded, orange and light grey yellow, coarse to medium sand (10YR 6/6).	Sh

Appendix 13 Ashley site recordings

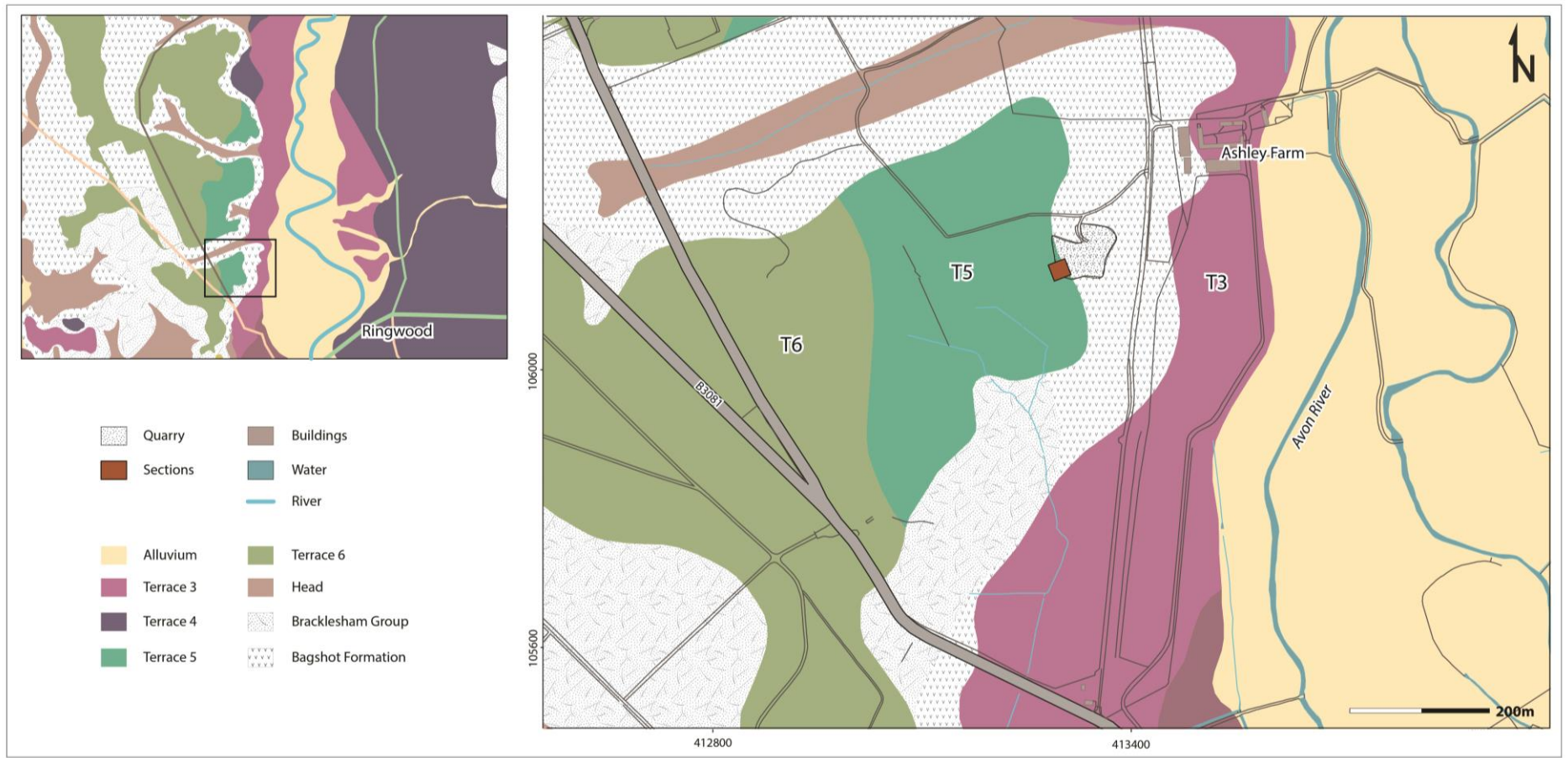


Figure A13.1 Map showing the location of the site of Ashley pit in relationship to the local bedrock and superficial geology (based upon 1:10000 scale geology data with permission of the British Geological Survey and 1:10000 scale OS VectorMap Local [shape file], Digimap Licence).

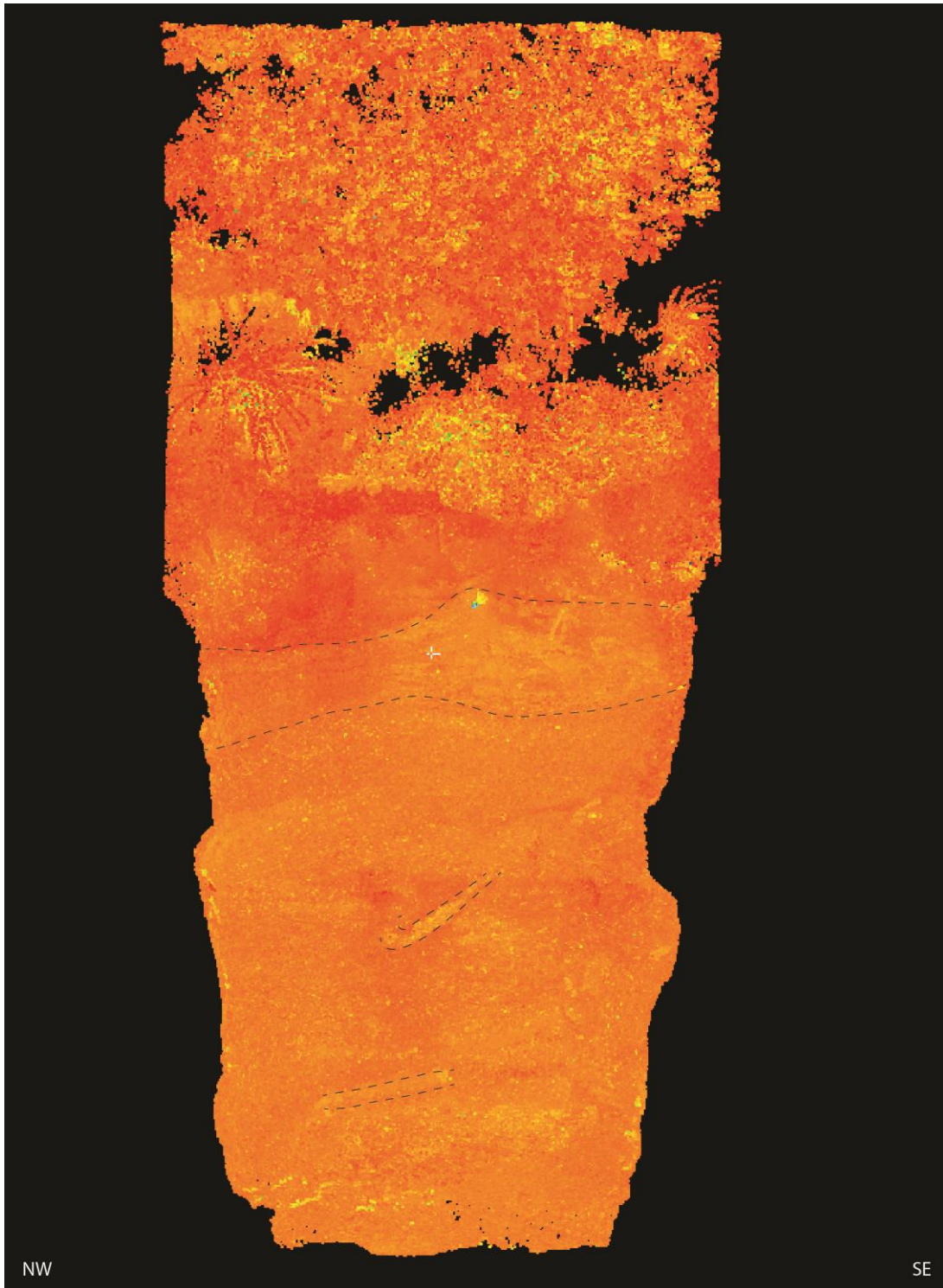


Figure A13.2 Terrestrial laser scan of section 1 at Asheley pit.

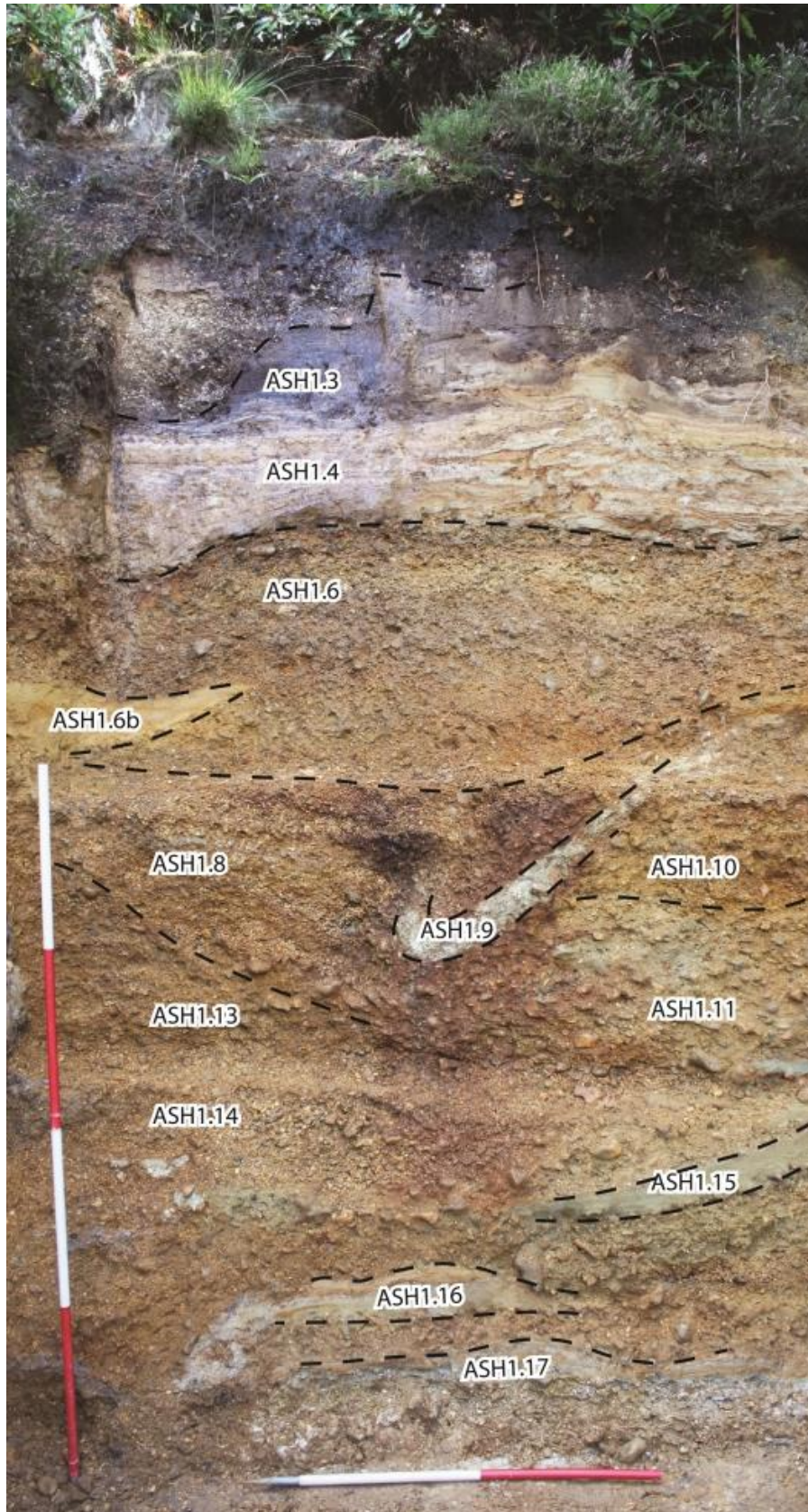


Figure A13.3 Annotated photograph of the section 1 at Ashley pit.

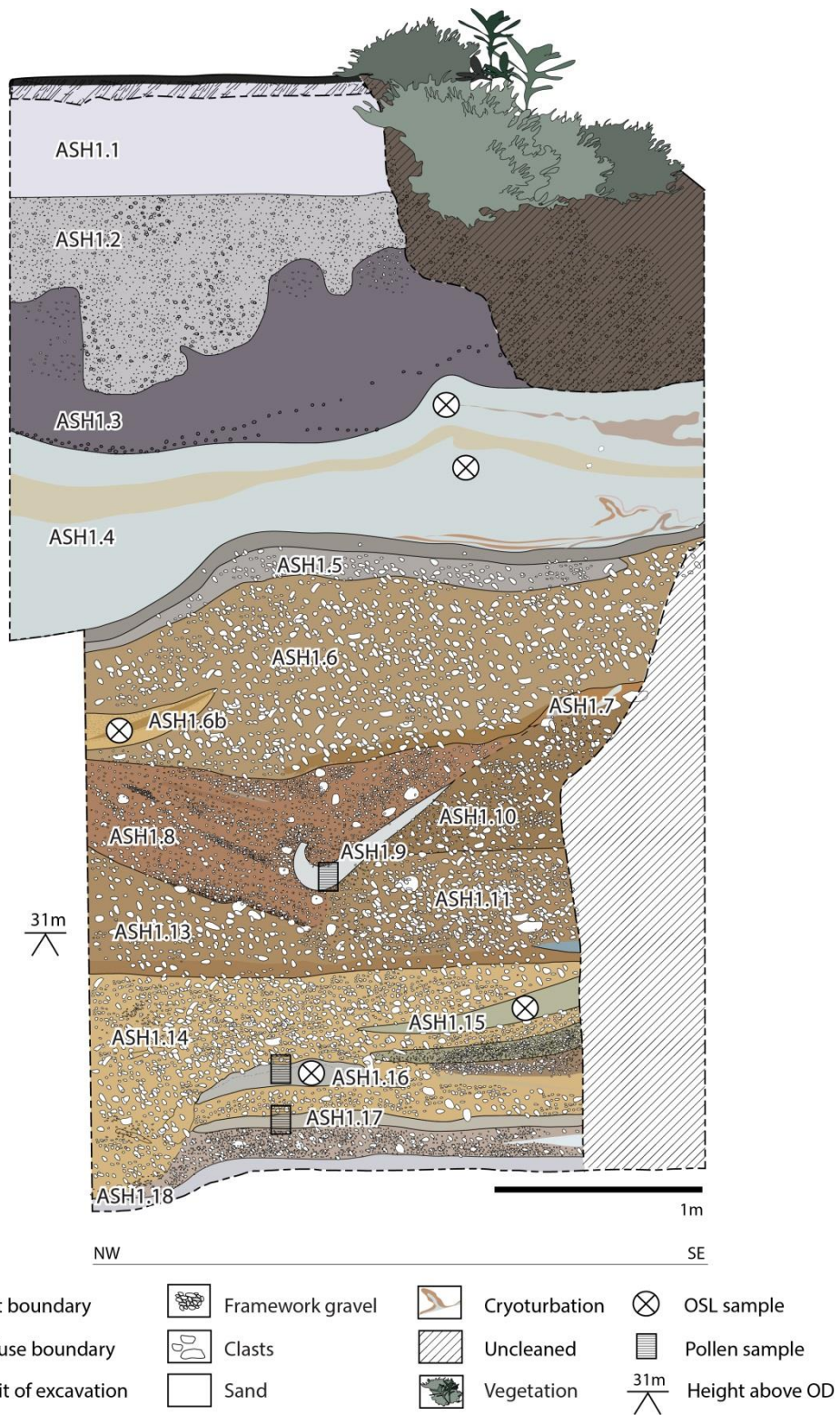


Figure A13.4 Drawing of section 1 at Ashley pit.

Appendix 14 Ashley sediment log

ASHLEY SECTION 1		
Unit	Description	Lithofacies
ASH1.1	SAND. Well-sorted, massive, loose, light grey medium sand.	Sm
ASH1.2	SANDY GRAVEL. Poorly sorted, matrix supported, massive orange and brown medium gravel. The matrix is very sandy and abundant. Pockets of more clayey matrix. A band of iron concretion runs through the deposit in a very irregular pattern.	Gm
ASH1.3	SAND. Well-sorted, massive, compact, pale yellow to red-brown medium to fine sand. Towards the bottom of the deposit some wavy clayey bands appear.	Sm
ASH1.4	CLAYEY SAND. Well-sorted, bedded, vaguely inversely graded, light grey, pink and orange, medium to fine sand and clayey sand (2.5YR 6/4). The clayey sand (light grey and pink) appears in wavy bands within the less clayey, fine/medium sand (yellow-grey and orange and red staining). The sand gets coarser towards the top of the unit, here it shows limited bedding and the silt and clay component is limited. Load features and drop stones.	Sh
ASH1.5	SANDY GRAVEL. Moderately sorted, matrix supported, yellow-orange, medium gravel (2.5YR 6/8). The matrix is light grey sand, including many quartz grains, granules and grit and some black grains.	Gh
ASH1.6	GRAVEL. Very poorly sorted, matrix supported, crudely bedded, crudely inversely graded, red orange, coarse gravel (7.5YR 5/8). The matrix is silty and clayey but towards the lower boundary more gritty with limited clay and silt content grading into a clast supported deposit.	Gh

ASH1.6b	SAND. Moderately sorted, horizontally-bedded, yellow-orange, medium to fine sand (2.5Y 5/6). The lower part of the unit consists of fine/medium sand, well sorted and compact including many quartz grains and very few black grains. It is overlain by slightly coarser sand with some grit inclusions and less compact sand followed by a finer pinkish sand with some silt and some fine black grains. Above that the sand gets coarser again including grit and white cortex particles. The silt and clay content is again less resulting in an almost pure sand deposit. The sand further coarsens upwards until the top of the unit.	Sh
ASH1.7	SAND. Well-sorted, horizontally bedded, grey-yellow and orange, medium sand (7.5YR 5/8). It overlies the tail end of ASH1.9. The sand includes quartz and some black grains and bands within the sand contain more granules and grit. The lower part of the unit is light grey alternating with red bands and is clayey.	Sh
ASH1.8	GRAVEL. Cross-bedded deposits of poorly sorted, matrix supported coarse gravel and moderately sorted, clast supported medium to fine gravel (7.5YR 5/8). The matrix supported poorly sorted flint gravel is yellow-orange, consists of a coarse sandy matrix including much grit and granules and flint splinters. Finer sand is also present in the matrix as are quartz grains and fine black sand grains. The clast supported gravel is orange-red, in parts open-framework gravel.	Gp
ASH1.9	CLAY. Grey and orange mottled clay (2.5Y 6/4). Includes a few quartz and black sand grains. Clay shows a honeycombe structure.	Fm
ASH1.10	GRAVEL. Poorly sorted, matrix supported, poorly bedded, orange yellow coarse gravel (10YR 5/8). The matrix is very sandy and heterogeneous, including coarse sand, granules, grit, flint splinters, quartz grains, orange and black grains.	Gh
ASH1.11	GRAVEL. Poorly sorted, matrix supported, poorly bedded, light grey and yellow coarse gravel (10YR 5/8). The matrix is very sandy and heterogeneous,	Gh

	including coarse sand, granules, grit, flint splinters, quartz grains, orange and black grains.	
ASH1.12	SAND. Thin, moderately sorted, crudely inversely graded, dark grey/blue grey medium to fine sand. Includes quartz and fine black grains.	Sh
ASH1.13	Par ASH1.11	
ASH1.14	SANDY GRAVEL. Poorly sorted, matrix supported, poorly bedded, yellow orange medium gravel. Diagonal band of larger cobbles and bands of clst supported medium gravel towards the top. The bottom left shows no bedding and crude clay-rich patches.	Gh
ASH1.15	SAND. Moderately sorted, horizontally-bedded, dark grey yellow, medium sand (2.5Y 5/6). Almost pure sand with the exception of a more clayey band in the upper part. Sand includes quartz, black grains and occasionally very coarse sand grains.	Sh
ASH1.16	CLAYEY SAND. Moderately sorted, horizontally-bedded, inversely graded, grey, yellow and orange medium to fine sand (2.5Y 5/6). Towards to lower boundary almost pure sand with high quartz content, more silty and finer sand towards the upper boundary.	Sh
ASH1.17	CLAYEY SAND. Well-sorted, horizontally-bedded, grey and orange, medium to fine sand. Horizontal beds of clay with very limited sand.	Sh
ASH1.18	SANDY CLAY. Horizontally bedded, light grey with pink and orange mottling, fine clayey sand and clay (2.5Y 7/4) (Parkstone Sand).	Fl

Appendix 15 Bickton site recordings

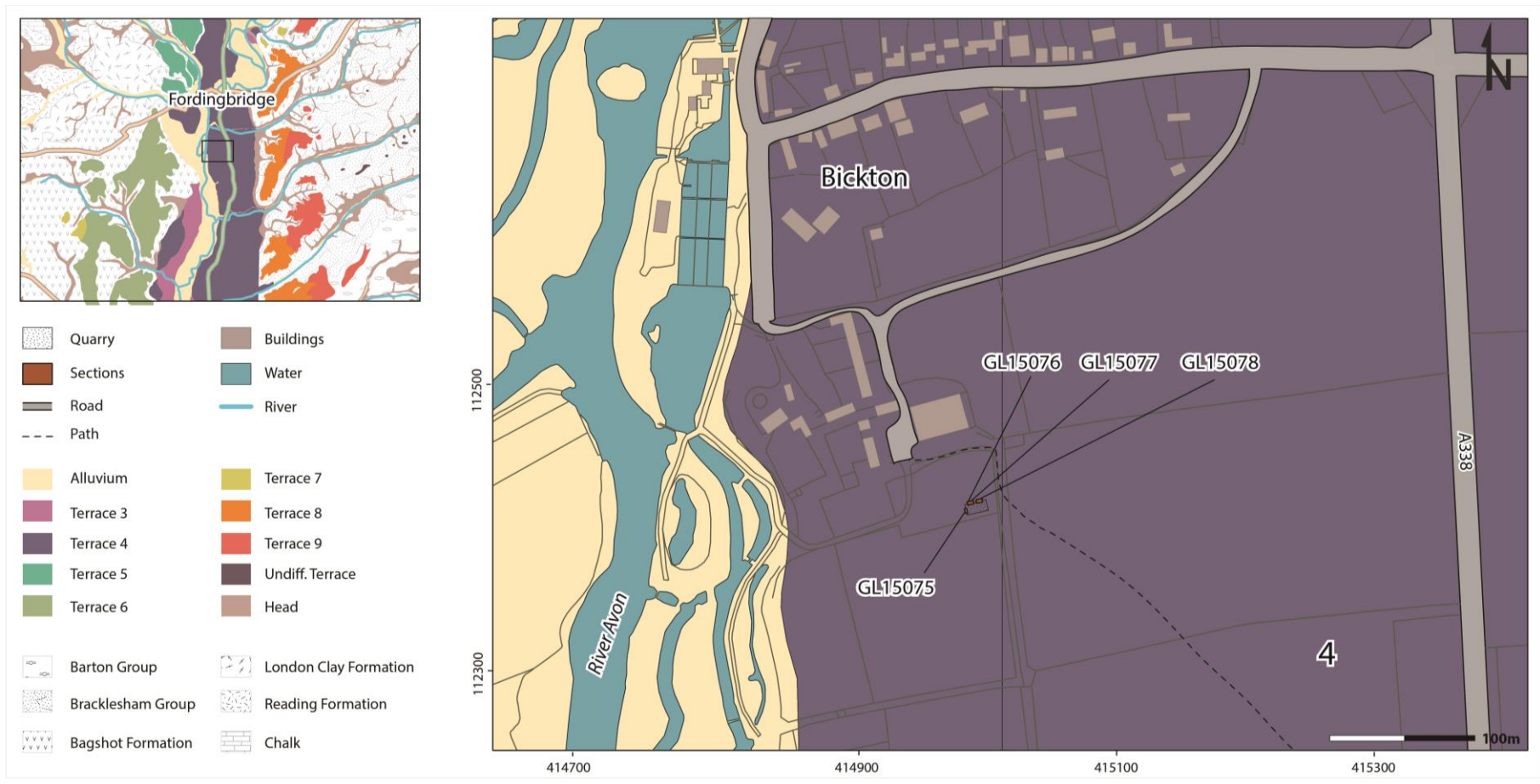


Figure A15.1 Map showing the location of the site of Bickton pit in relationship to the local bedrock and superficial geology (based upon 1:10000 scale geology data with permission of the British Geological Survey and 1:10000 scale OS VectorMap Local [shape file], Digimap Licence).



Figure A15.2 Annotated photograph of Bickton pit showing the OSL sample locations in the western and northern walls of the pit.

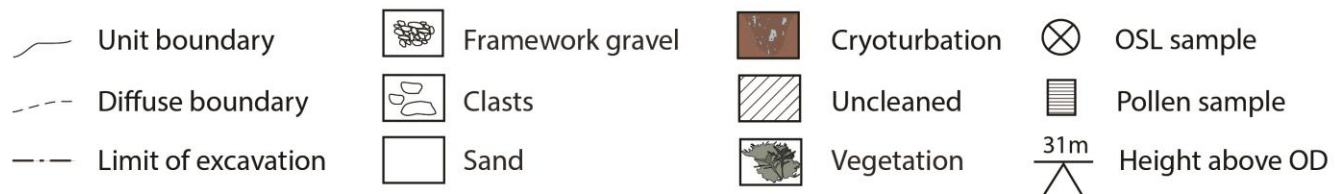
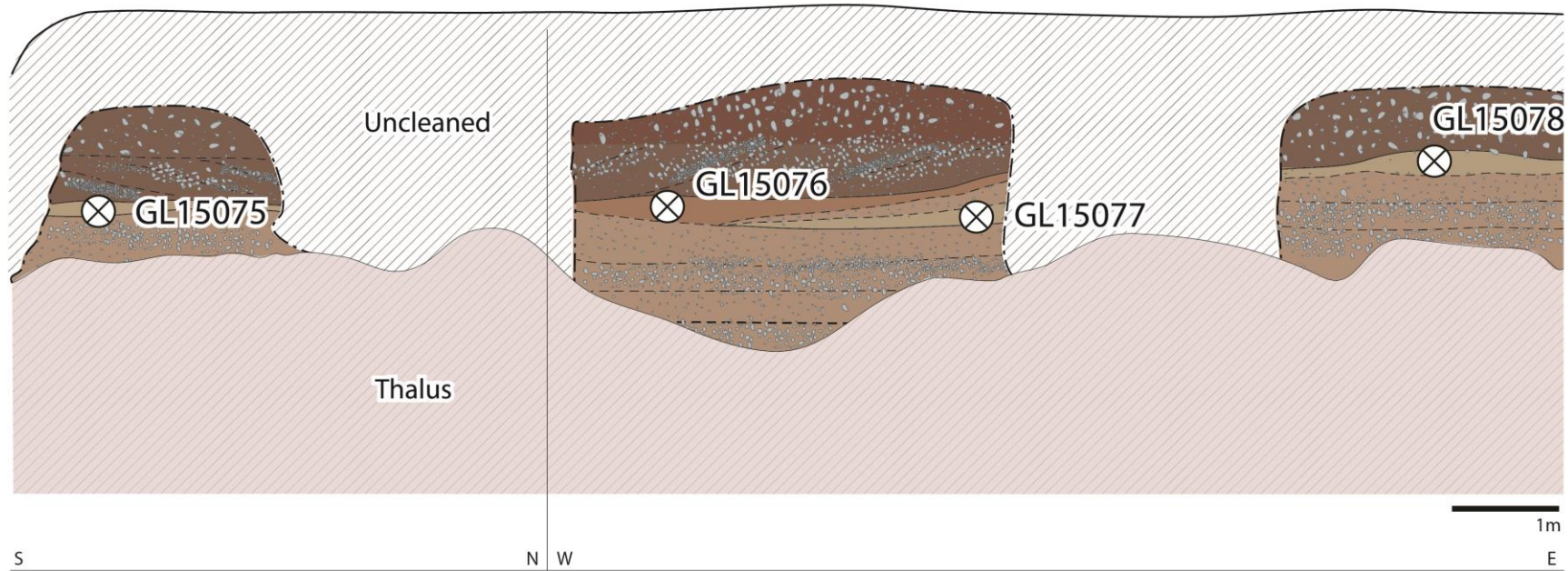


Figure A15.3 Schematic representation of the western and northern walls of Bickton pit.

Appendix 16 Bemerton clast size distributions

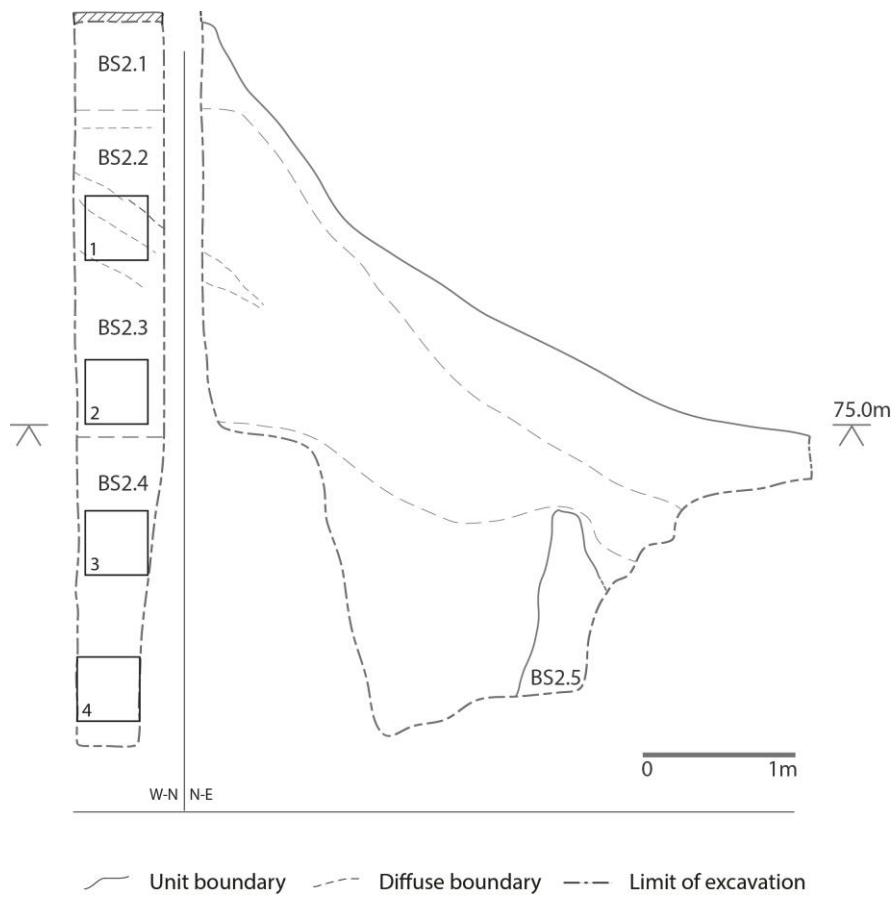


Figure A16.1 Section in the undifferentiated terrace deposit at Bemerton showing gravel sample locations and the main stratigraphic units. 1= BEM2.2; 2=BEM2.3; 3=BEM2.4a; 4=BEM2.4b.

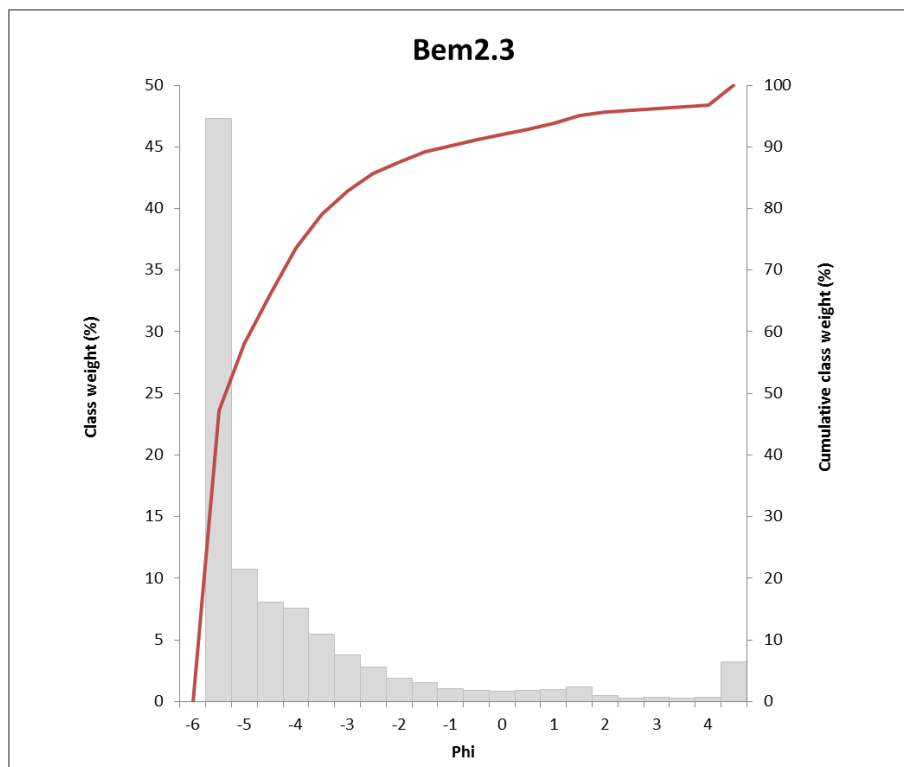
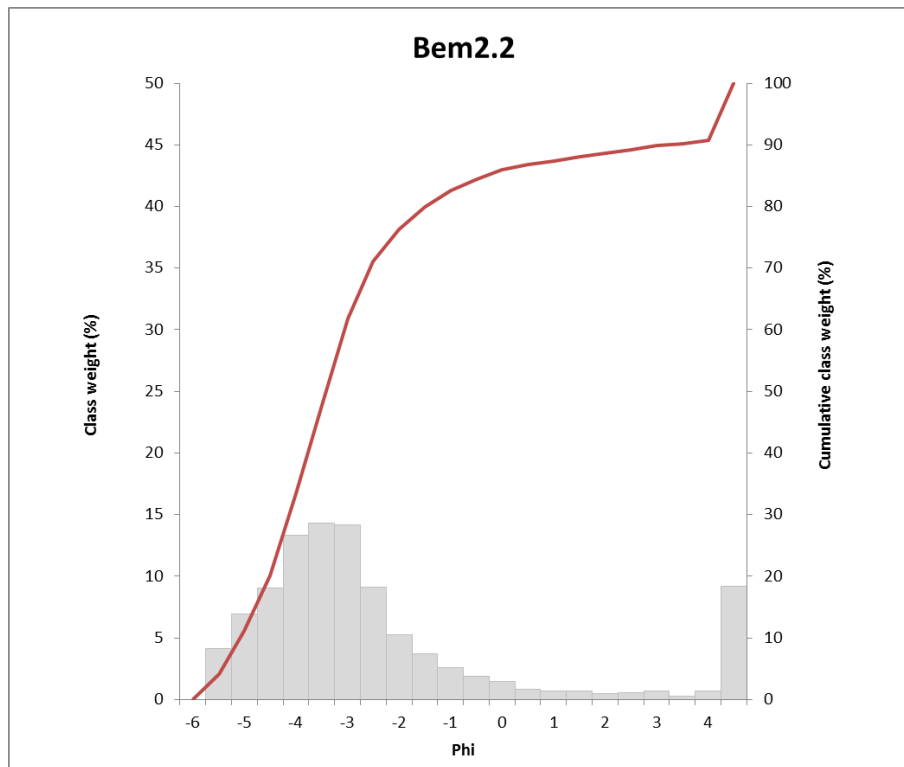


Figure A16.2 Percentage frequency and cumulative percentage frequency of sediment fractions present in sample BEM2.2 (top) and BEM2.3 (bottom).

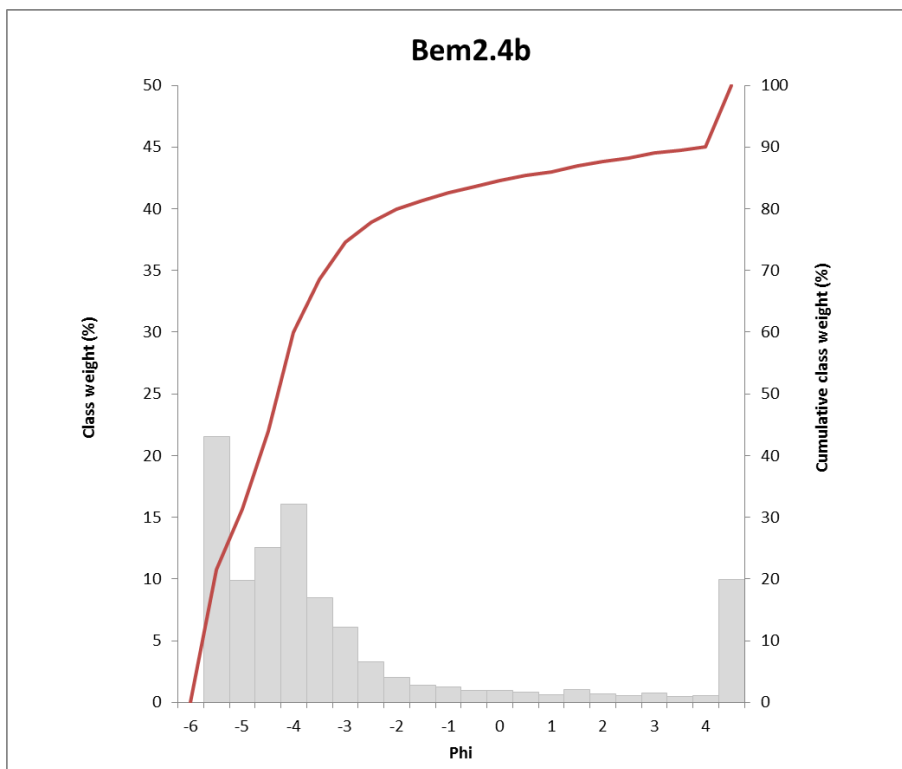
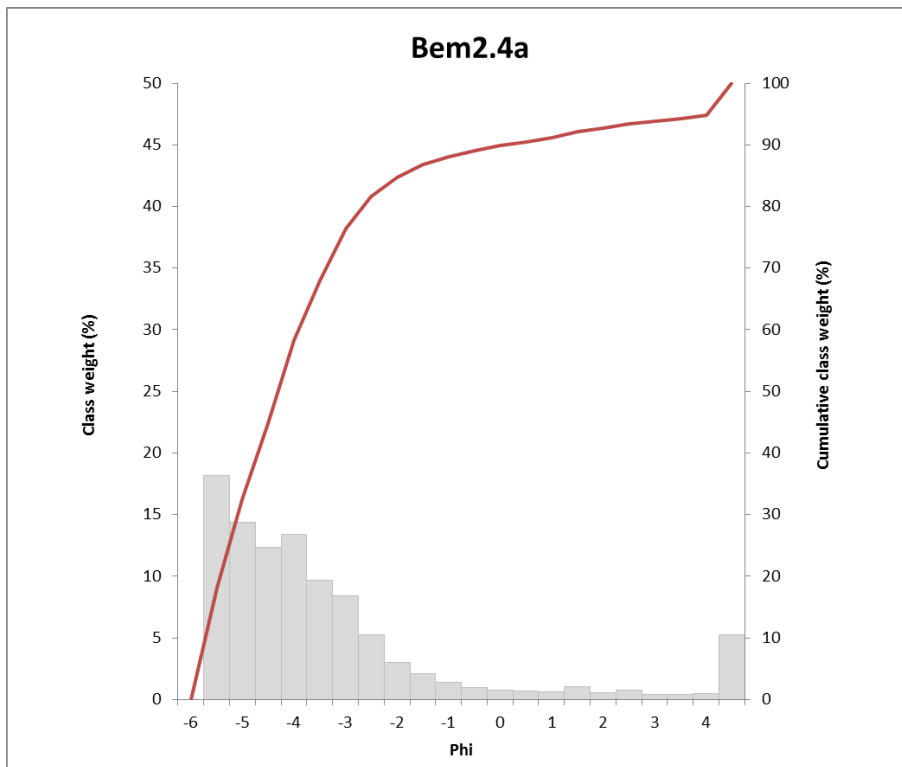


Figure A16.3 Percentage frequency and cumulative percentage frequency of sediment fractions present in sample BEM2.4a (top) and BEM2.4b (bottom).

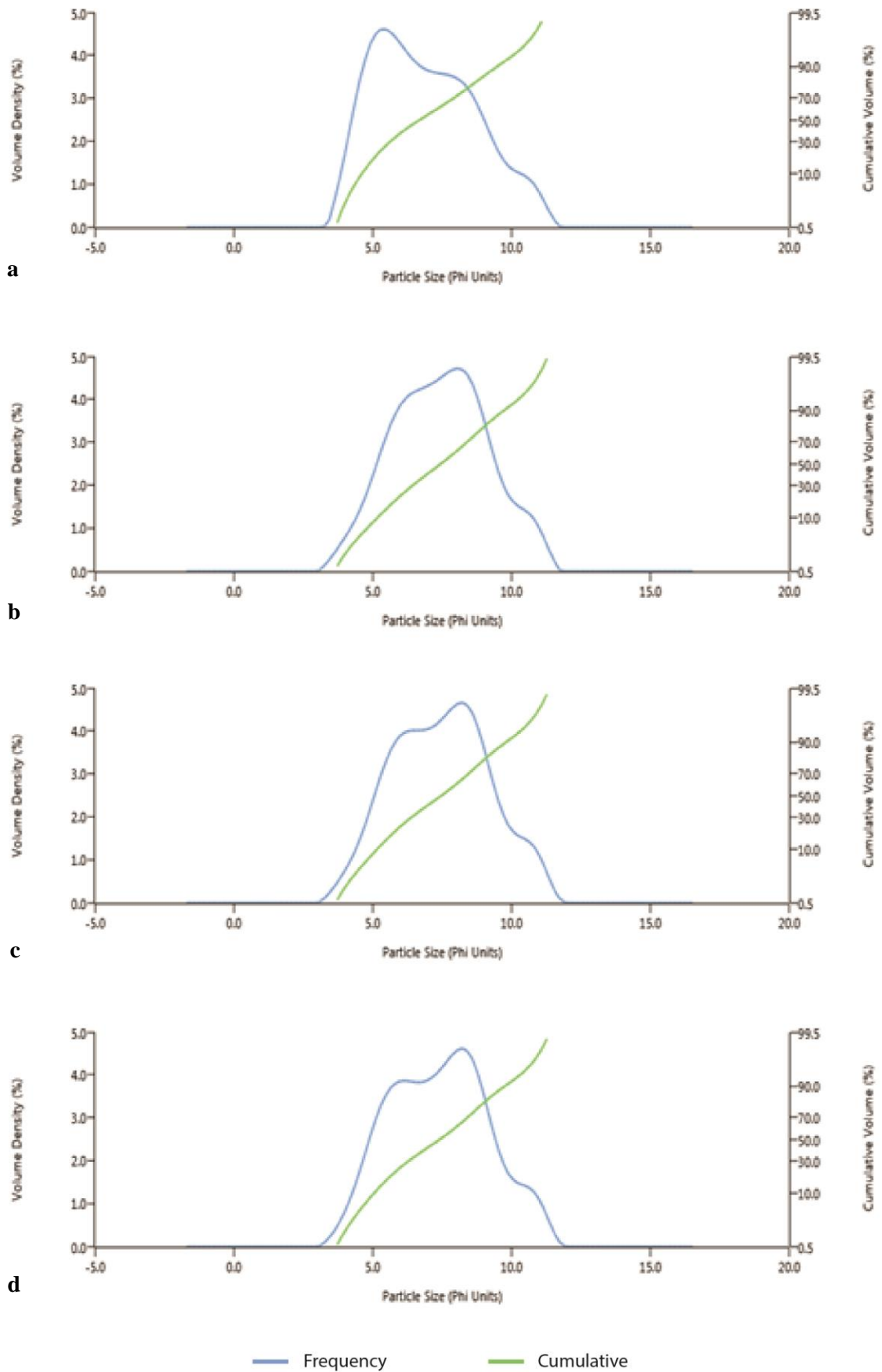


Figure A16.4. Particle size distribution of the <math><63\mu\text{m}</math> fraction of BEM2.2 (a), BEM2.3 (b), BEM2.4a (c) and BEM2.4b (d).

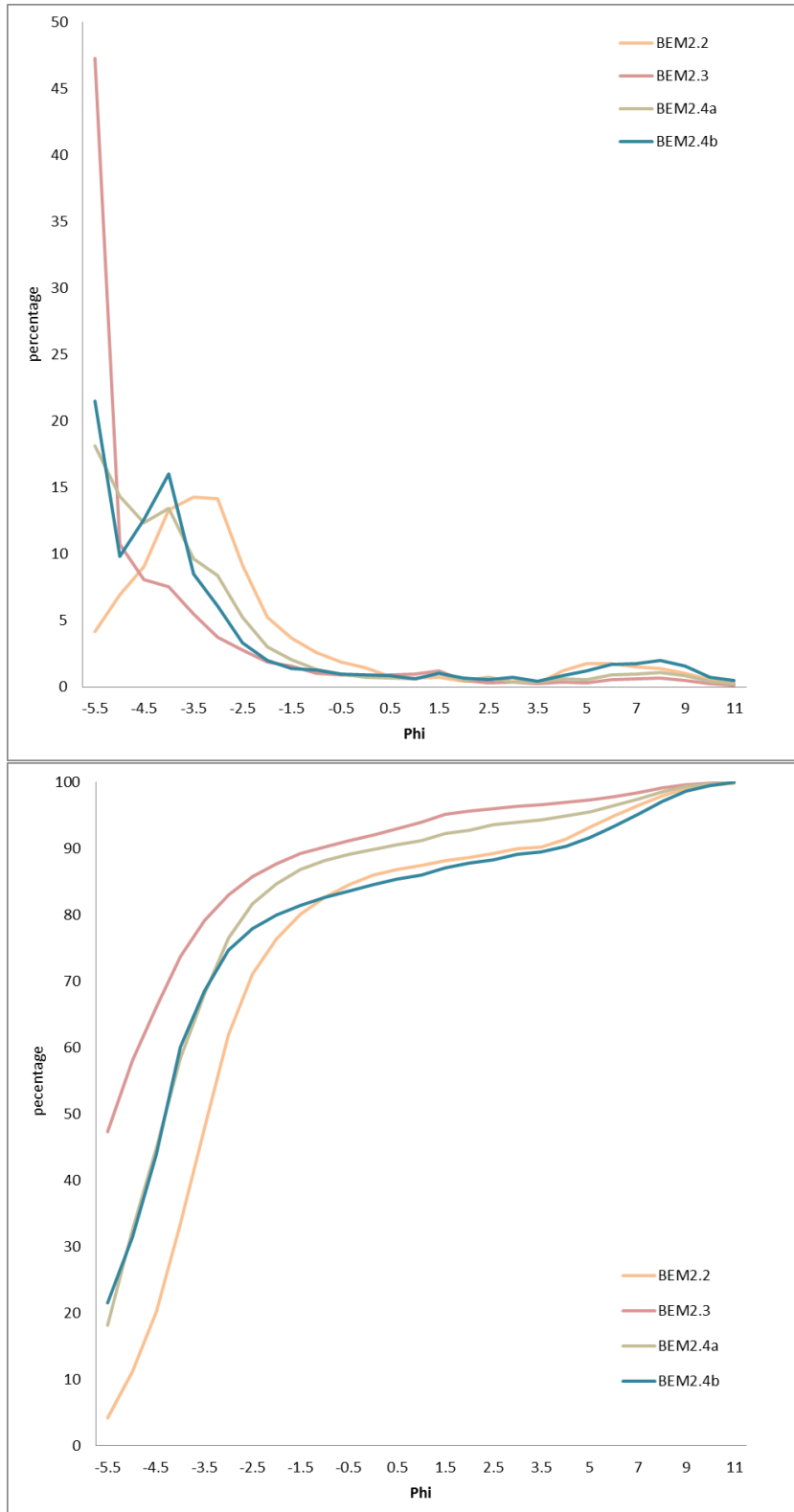


Figure A16.5 Comparison of the integrated particle size distribution curves of the four gravel samples from Bemerton showing weight in percentages of each size fraction (top) and the cumulative percentage of the weight in percentages (bottom).

Appendix 17 Bemerton clast size distribution statistics

		BEM2.2	BEM2.3	BEM2.4a	BEM2.4b
	SAMPLE TYPE:	Unimodal, Very Poorly Sorted	Unimodal, Poorly Sorted	Bimodal, Very Poorly Sorted	Bimodal, Very Poorly Sorted
	TEXTURAL GROUP:	Gravel	Gravel	Gravel	Gravel
	SEDIMENT NAME:	Medium Gravel	Very Coarse Gravel	Very Coarse Gravel	Very Coarse Gravel
METHOD OF MOMENTS Arithmetic (μm)	MEAN	14357.8	34789.4	23995.1	24081.1
	SORTING	13335.8	20692.0	18239.6	19156.6
	SKEWNESS	1.298	-0.452	0.427	0.405
	KURTOSIS	4.315	1.583	1.900	1.834
METHOD OF MOMENTS Geometric (μm)	MEAN	5293.2	18143.4	10608.7	7707.2
	SORTING	9.781	6.672	8.250	13.82
	SKEWNESS	-1.965	-2.735	-2.410	-1.915
	KURTOSIS	6.306	11.09	8.842	5.678
METHOD OF MOMENTS Logarithmic (ϕ)	MEAN	-2.404	-4.181	-3.407	-2.946
	SORTING	3.290	2.738	3.044	3.789
	SKEWNESS	1.965	2.735	2.410	1.915
	KURTOSIS	6.306	11.09	8.842	5.678
FOLK AND WARD METHOD (μm)	MEAN	7627.0	25254.5	15879.9	10673.9
	SORTING	6.641	3.724	5.128	9.534
	SKEWNESS	-0.500	-0.776	-0.481	-0.630
	KURTOSIS	2.140	1.675	1.874	2.211
FOLK AND WARD METHOD (ϕ)	MEAN	-2.931	-4.658	-3.989	-3.416
	SORTING	2.731	1.897	2.358	3.253
	SKEWNESS	0.500	0.776	0.481	0.630
	KURTOSIS	2.140	1.675	1.874	2.211

		BEM2.2	BEM2.3	BEM2.4a	BEM2.4b
FOLK AND WARD METHOD (Description)	MEAN:	Fine Gravel	Coarse Gravel	Medium Gravel	Medium Gravel
	SORTING:	Very Poorly Sorted	Poorly Sorted	Very Poorly Sorted	Very Poorly Sorted
	SKEWNESS:	Very Fine Skewed	Very Fine Skewed	Very Fine Skewed	Very Fine Skewed
	KURTOSIS:	Very Leptokurtic	Very Leptokurtic	Very Leptokurtic	Very Leptokurtic
	MODE 1 (μm):	9600.0	54000.0	54000.0	54000.0
	MODE 2 (μm):			19200.0	19200.0
	MODE 3 (μm):				
	MODE 1 (ϕ):	-3.243	-5.735	-5.735	-5.735
	MODE 2 (ϕ):			-4.243	-4.243
	MODE 3 (ϕ):				
	D ₁₀ (μm):	129.1	2147.4	949.9	75.54
	D ₅₀ (μm):	10638.2	41143.2	19721.2	19760.7
	D ₉₀ (μm):	33362.9	58674.7	52343.5	53887.5
	(D ₉₀ / D ₁₀) (μm):	258.5	27.32	55.10	713.3
	(D ₉₀ - D ₁₀) (μm):	33233.9	56527.4	51393.6	53812.0
	(D ₇₅ / D ₂₅) (μm):	4.516	3.595	4.484	5.142
	(D ₇₅ - D ₂₅) (μm):	15448.3	38068.2	29507.3	31985.5
	D ₁₀ (ϕ):	-5.060	-5.875	-5.710	-5.752
	D ₅₀ (ϕ):	-3.411	-5.363	-4.302	-4.305
	D ₉₀ (ϕ):	2.954	-1.103	0.074	3.727
	(D ₉₀ / D ₁₀) (ϕ):	-0.584	0.188	-0.013	-0.648
	(D ₉₀ - D ₁₀) (ϕ):	8.014	4.772	5.784	9.478
	(D ₇₅ / D ₂₅) (ϕ):	0.495	0.677	0.587	0.555
	(D ₇₅ - D ₂₅) (ϕ):	2.175	1.846	2.165	2.362

		BEM2.2	BEM2.3	BEM2.4a	BEM2.4b
COMPOSITION	% GRAVEL:	82.8%	90.2%	88.2%	82.7%
	% SAND:	8.8%	6.7%	6.8%	7.7%
	% MUD:	8.5%	3.1%	5.0%	9.6%
	% V COARSE GRAVEL:	10.8%	57.6%	31.9%	31.0%
	% COARSE GRAVEL:	22.7%	16.1%	26.4%	29.1%
	% MEDIUM GRAVEL:	28.5%	9.2%	18.1%	14.6%
	% FINE GRAVEL:	14.5%	4.7%	8.3%	5.4%
	% V FINE GRAVEL:	6.3%	2.6%	3.5%	2.7%
	% V COARSE SAND:	3.4%	1.8%	1.7%	1.9%
	% COARSE SAND:	1.5%	1.9%	1.3%	1.5%
	% MEDIUM SAND:	1.0%	1.6%	1.3%	1.5%
	% FINE SAND:	1.5%	0.8%	1.4%	1.6%
	% V FINE SAND:	1.5%	0.7%	1.0%	1.3%
	% V COARSE SILT:	1.7%	0.3%	0.6%	1.2%
	% COARSE SILT:	1.9%	0.6%	0.9%	1.8%
	% MEDIUM SILT:	1.5%	0.6%	1.0%	1.8%
	% FINE SILT:	1.4%	0.7%	1.1%	2.0%
	% V FINE SILT:	1.0%	0.5%	0.8%	1.5%
	% CLAY:	0.9%	0.4%	0.7%	1.2%

Appendix 18 Hatchet Gate Farm clast size distribution

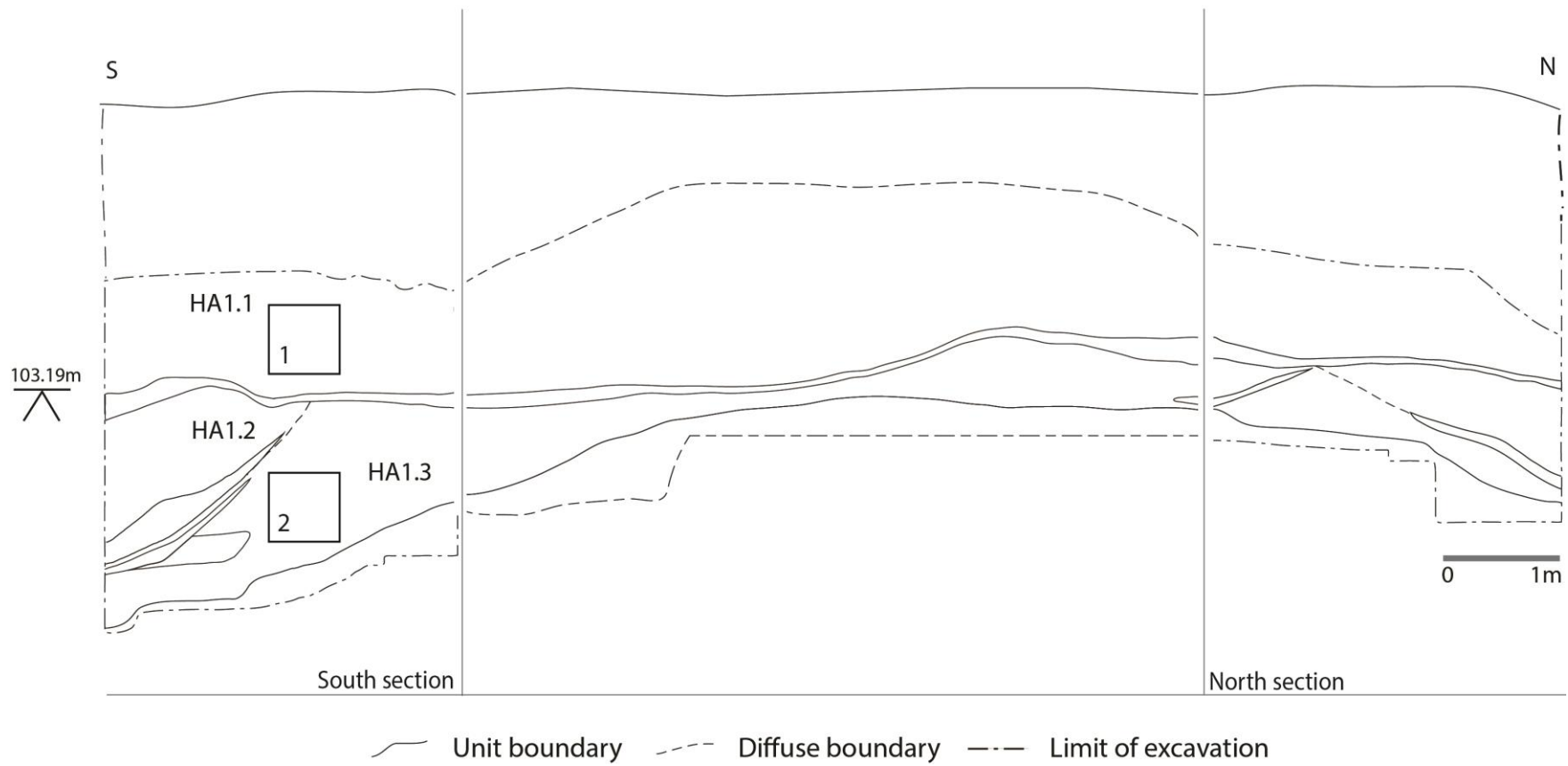


Figure A18.1 Section in terrace 10 at Hatchet Gate Farm showing gravel sample locations and the main stratigraphic units. 1= HA1.1; 2=HA1.3.

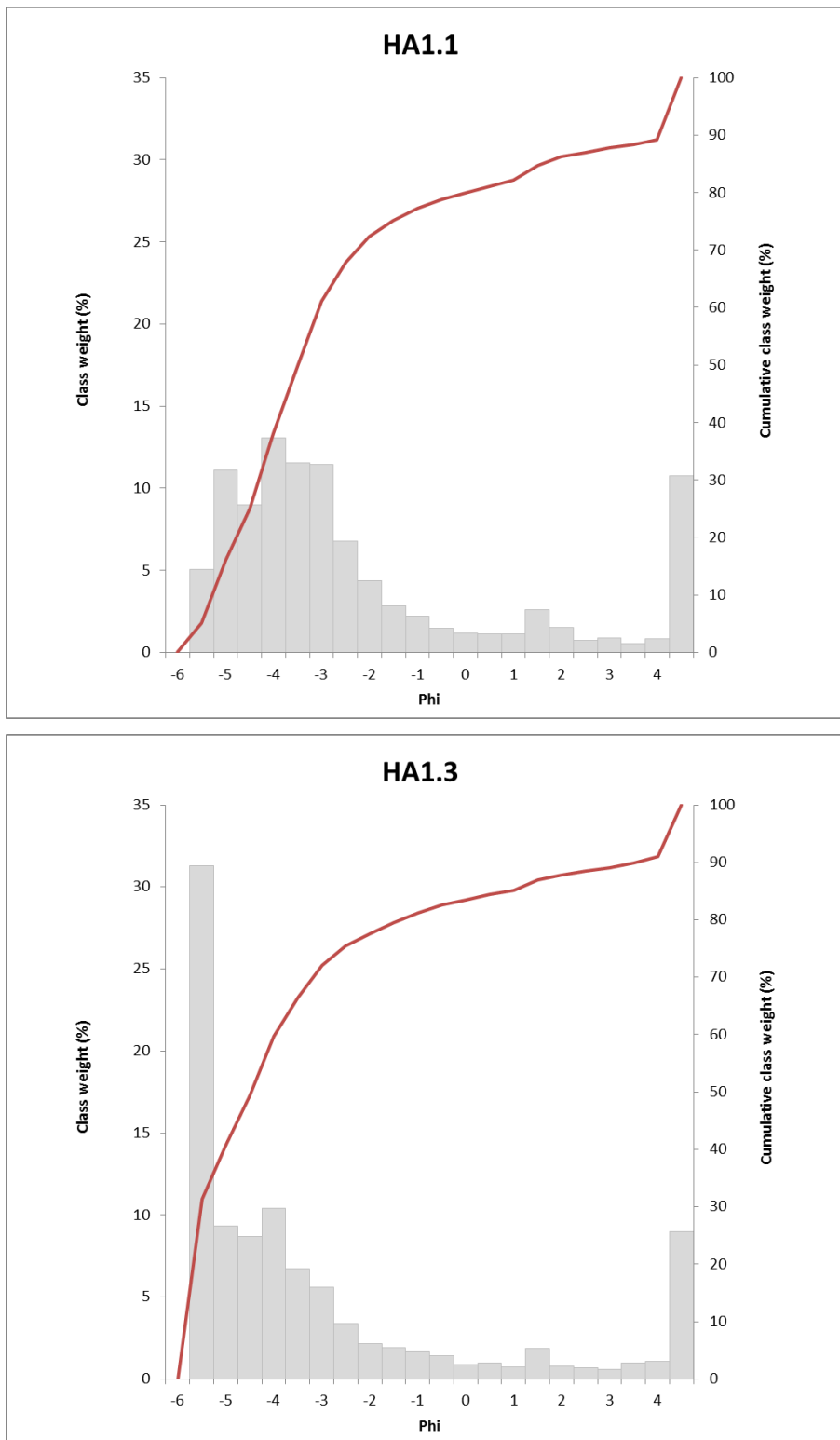


Figure A18.2 Percentage frequency and cumulative percentage frequency of sediment fractions present in sample HA1.1 (top) and HA1.3 (bottom).

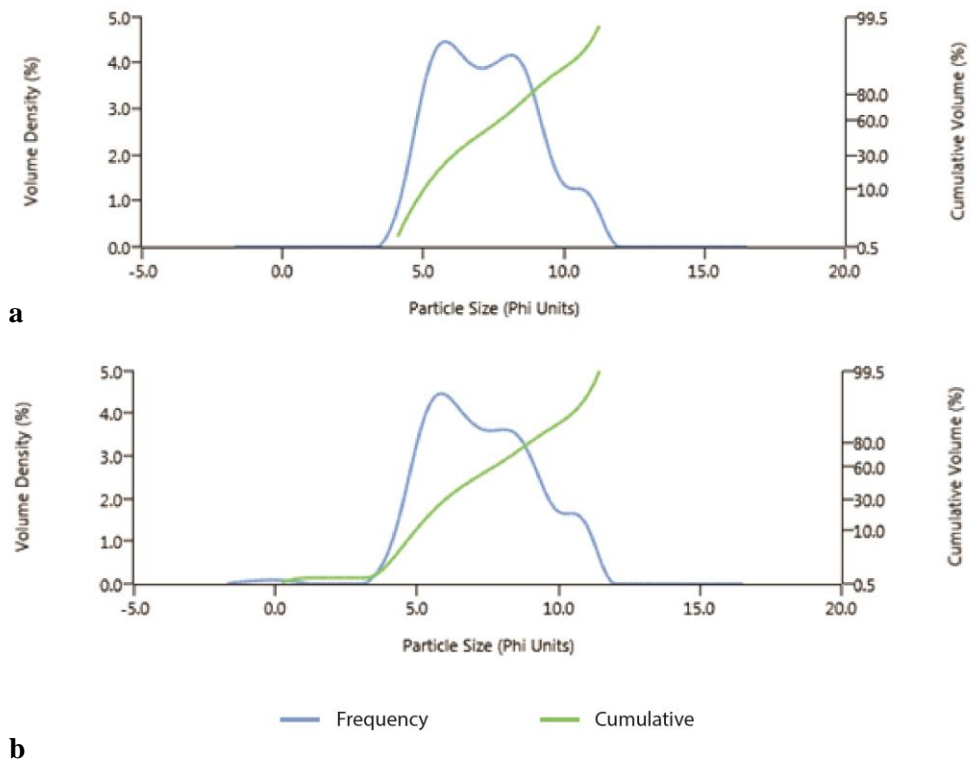


Figure A18.3 Particle size distribution of the <math><63\mu\text{m}</math> fraction of HA1.1 (a) and HA1.3 (b).

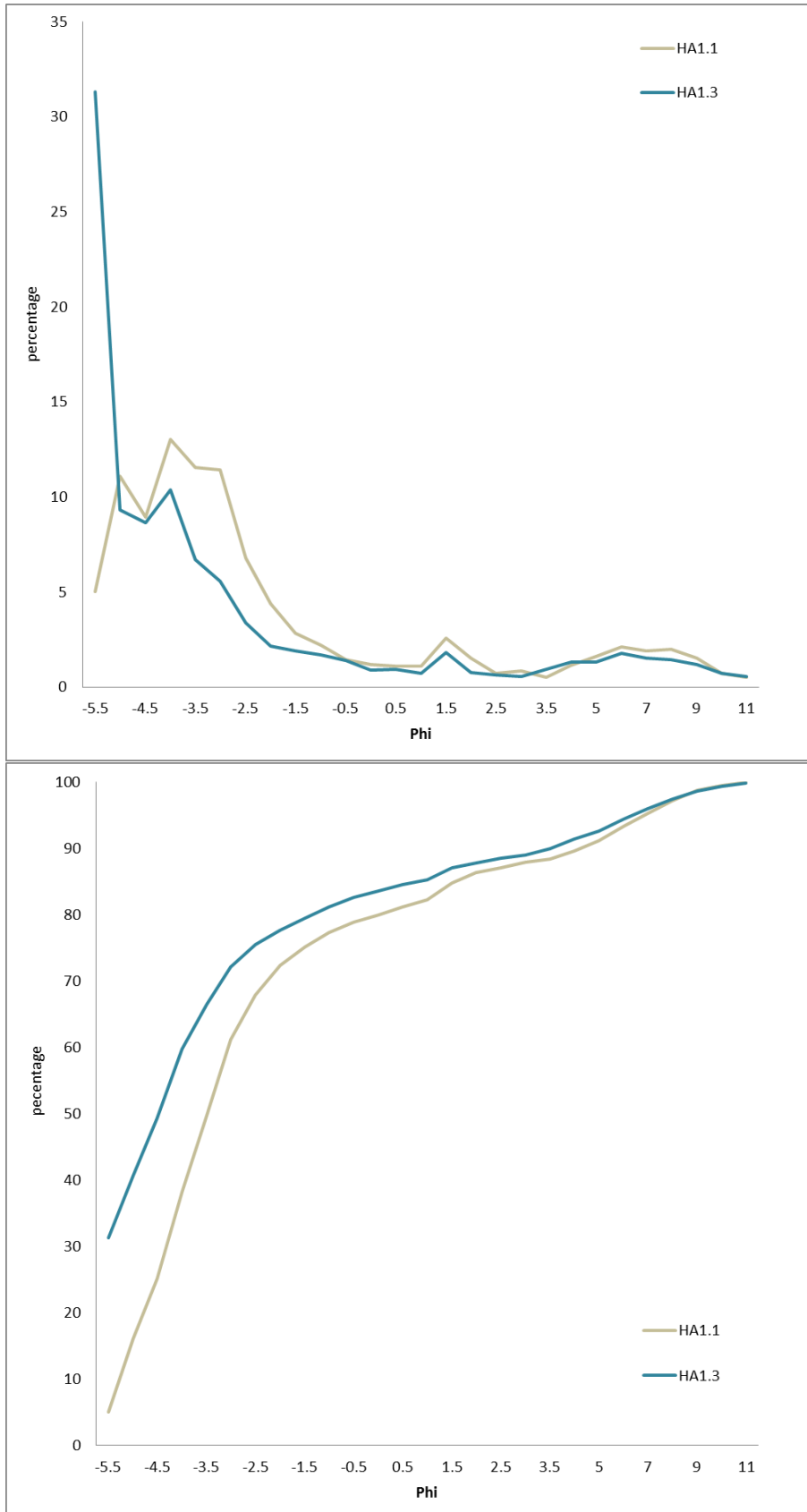


Figure A18.4 Comparison of the integrated particle size distribution curves of the two gravel samples from Hatchet Gate Farm showing weight in percentages of each size fraction (top) and the cumulative percentage of the weight in percentages (bottom).

Appendix 19 Hatchet Gate Farm clast size distribution statistics

		HA1.1	HA1.3
	SAMPLE TYPE:	Polymodal, Very Poorly Sorted	Bimodal, Very Poorly Sorted
	TEXTURAL GROUP:	Muddy Sandy Gravel	Gravel
	SEDIMENT NAME:	Coarse Silty Sandy Medium Gravel	Very Coarse Gravel
METHOD OF MOMENTS Arithmetic (μm)	MEAN	15459.3	26815.6
	SORTING	14841.5	21311.7
	SKEWNESS	1.021	0.154
	KURTOSIS	3.236	1.428
METHOD OF MOMENTS Geometric (μm)	MEAN	4405.5	8172.8
	SORTING	13.09	13.76
	SKEWNESS	-1.606	-1.794
	KURTOSIS	4.701	5.360
METHOD OF MOMENTS Logarithmic (ϕ)	MEAN	-2.139	-3.031
	SORTING	3.710	3.782
	SKEWNESS	1.606	1.794
	KURTOSIS	4.701	5.360
FOLK AND WARD METHOD (μm)	MEAN	5024.0	10065.3
	SORTING	11.17	10.02
	SKEWNESS	-0.602	-0.667
	KURTOSIS	1.698	1.651
FOLK AND WARD METHOD (ϕ)	MEAN	-2.329	-3.331
	SORTING	3.481	3.325
	SKEWNESS	0.602	0.667
	KURTOSIS	1.698	1.651

FOLK AND WARD METHOD (Description)		HA1.1	HA1.3
	MEAN:	Fine Gravel	Medium Gravel
	SORTING:	Very Poorly Sorted	Very Poorly Sorted
	SKEWNESS:	Very Fine Skewed	Very Fine Skewed
KURTOSIS:	Very Leptokurtic	Very Leptokurtic	
MODE 1 (μm):	19200.0	54000.0	
MODE 2 (μm):	9600.0	19200.0	
MODE 3 (μm):	38250.0		
MODE 1 (ϕ):	-4.243	-5.735	
MODE 2 (ϕ):	-3.243	-4.243	
MODE 3 (ϕ):	-5.235		
D ₁₀ (μm):	53.18	93.24	
D ₅₀ (μm):	11113.8	21984.1	
D ₉₀ (μm):	38368.6	56592.5	
(D ₉₀ / D ₁₀) (μm):	721.5	606.9	
(D ₉₀ - D ₁₀) (μm):	38315.4	56499.2	
(D ₇₅ / D ₂₅) (μm):	7.860	8.120	
(D ₇₅ - D ₂₅) (μm):	19631.6	42248.5	
D ₁₀ (ϕ):	-5.262	-5.823	
D ₅₀ (ϕ):	-3.474	-4.458	
D ₉₀ (ϕ):	4.233	3.423	
(D ₉₀ / D ₁₀) (ϕ):	-0.804	-0.588	
(D ₉₀ - D ₁₀) (ϕ):	9.495	9.245	
(D ₇₅ / D ₂₅) (ϕ):	0.338	0.460	
(D ₇₅ - D ₂₅) (ϕ):	2.975	3.022	

		HA1.1	HA1.3
COMPOSITION	% GRAVEL:	77.4%	81.3%
	% SAND:	12.3%	10.2%
	% MUD:	10.4%	8.5%
	% V COARSE GRAVEL:	15.6%	40.3%
	% COARSE GRAVEL:	22.5%	19.5%
	% MEDIUM GRAVEL:	23.0%	12.3%
	% FINE GRAVEL:	11.2%	5.6%
	% V FINE GRAVEL:	5.0%	3.6%
	% V COARSE SAND:	2.6%	2.3%
	% COARSE SAND:	2.2%	1.7%
	% MEDIUM SAND:	3.7%	2.2%
	% FINE SAND:	2.0%	1.6%
	% V FINE SAND:	1.7%	2.3%
	% V COARSE SILT:	1.6%	1.3%
	% COARSE SILT:	2.2%	1.8%
	% MEDIUM SILT:	1.9%	1.5%
	% FINE SILT:	2.0%	1.5%
	% V FINE SILT:	1.5%	1.2%
	% CLAY:	1.2%	1.2%

Appendix 20 Image-based automated grain-sizing at Hatchet Gate Farm

For each sedimentary layer identified at Hatchet Gate Farm a representative location was selected for image collection for image-based automated grainsizing (Figure A20.1). The photographs used for the IBAG analysis and the resulting grain size distributions are presented in Figure A20.2. The IBAG results of the three photographs show similar grain size distributions with the majority of the grains falling between 8-0.5mm (-3 and 0.5ϕ) and below 0.35mm. The latter is a result of the detection limit constrained by the number of pixels per millimetre. A comparison of the results from each photograph is presented in Figure A20.3. This again shows the similarity between the obtained grain size distributions with the exception of HA1.2 that a slightly larger proportion of medium to fine gravel (3ϕ).

The IBAG results are compared with the sieving data in Figure A20.4. The IBAG data shows an offset compared to the sieving results, underrepresenting the larger size fractions (medium to coarse gravel) and over representing the fine gravel to coarse sand fraction.

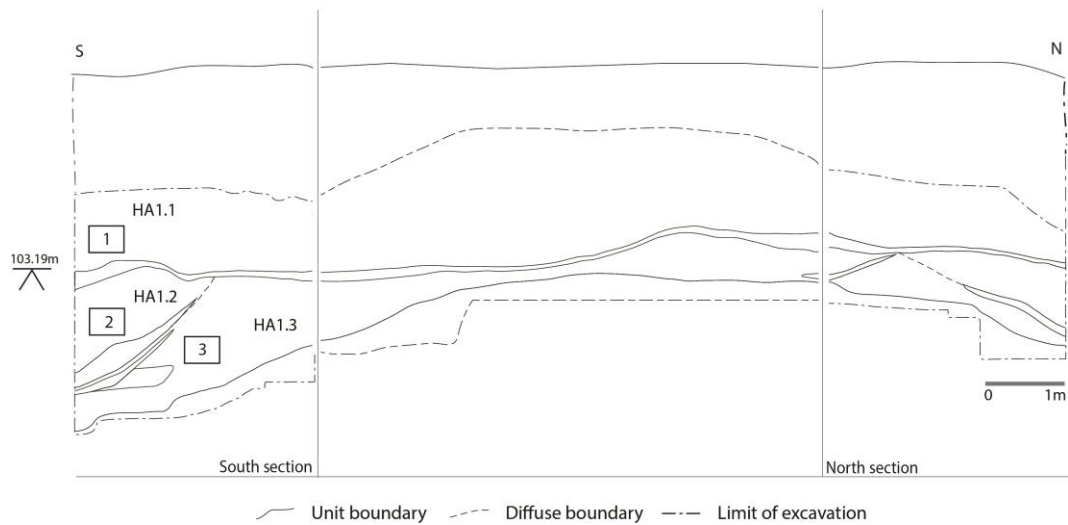


Figure A20.1 Section in terrace 10 at Hatchet Gate Farm showing image locations and the main stratigraphic units. 1= HA1.1; 2=HA1.2; 3=HA1.3.

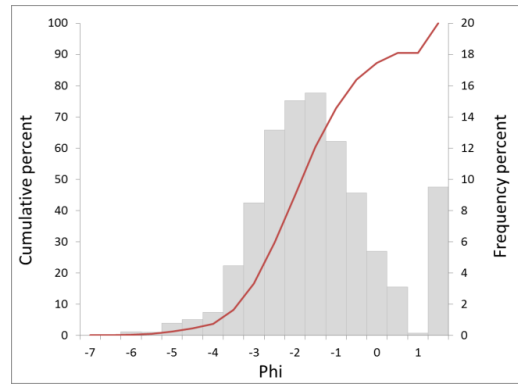
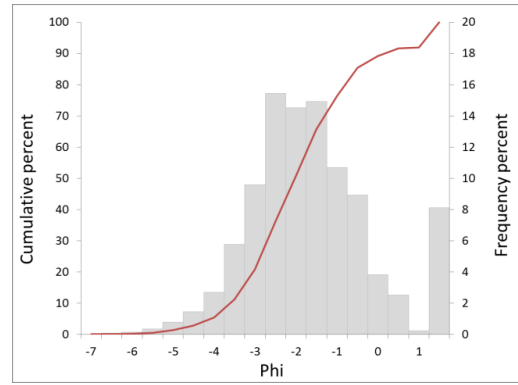
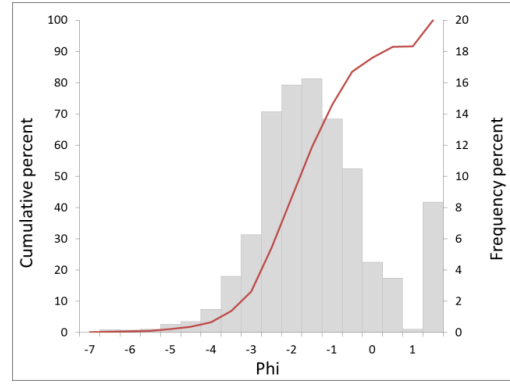


Figure A20.2 Photographs used for image-based automated grainsizing of HA1.1 (a), HA1.2 (b), and HA1.3 (c) and the resulting grain size distributions.

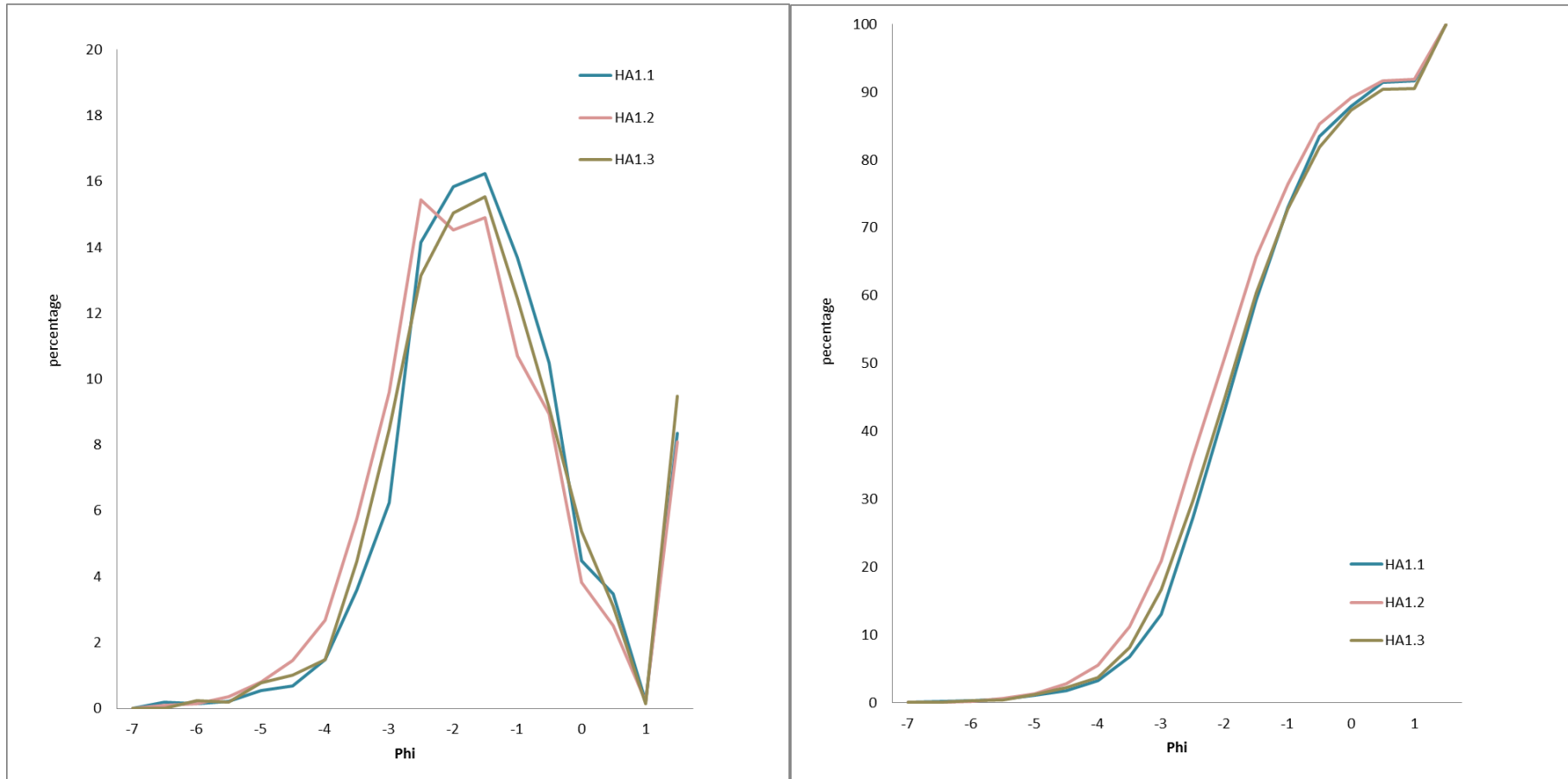


Figure A20.3 Comparison of percentage frequency (left) and cumulative percentage frequency (right) of the grain size distributions of HA1.1, HA1.2 and HA1.3 obtained from image-based automated grainsizing.

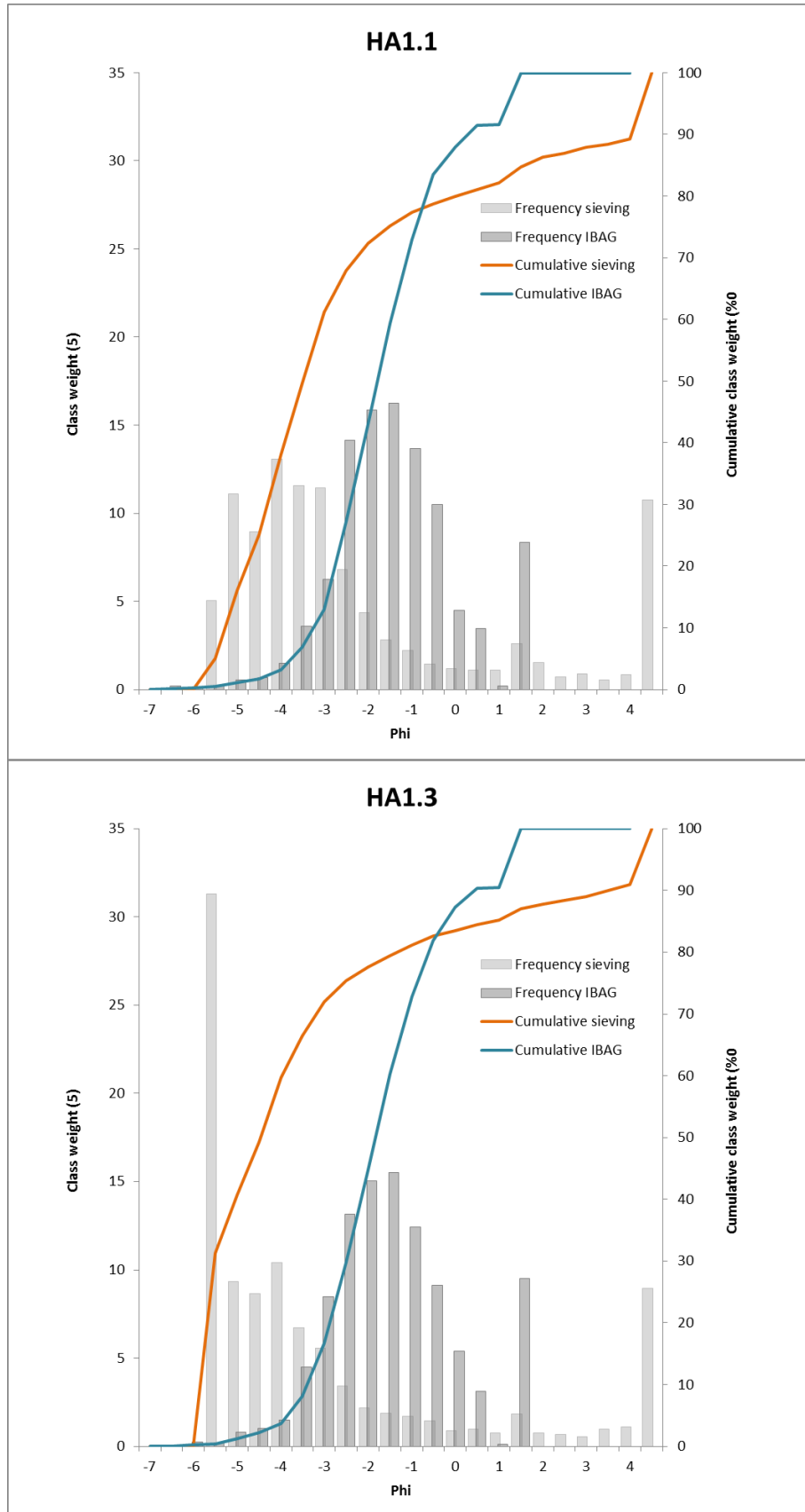


Figure A20.4 Comparison of sieving and IBAG results from HA1.1 and HA1.3.

Appendix 21 Woodriding clast size distributions

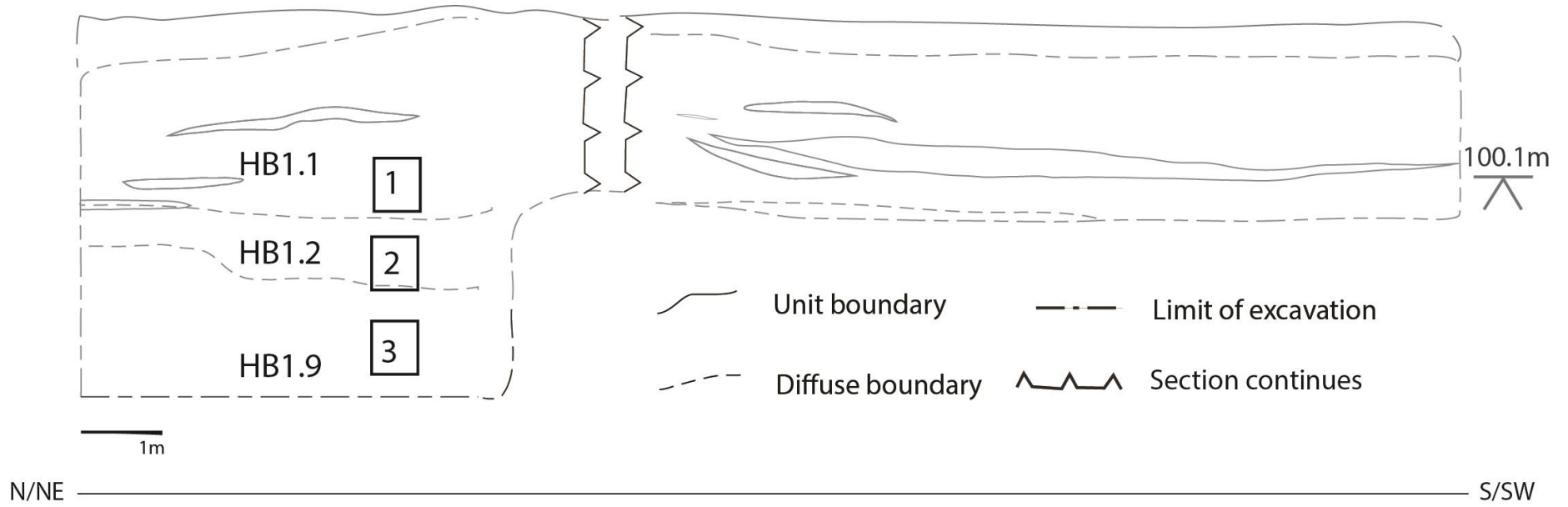


Figure A21.1 Section in terrace 10 at Woodriding showing gravel sample locations and the main stratigraphic units. 1= HB1.1; 2=HB1.2; 3=HB1.9.

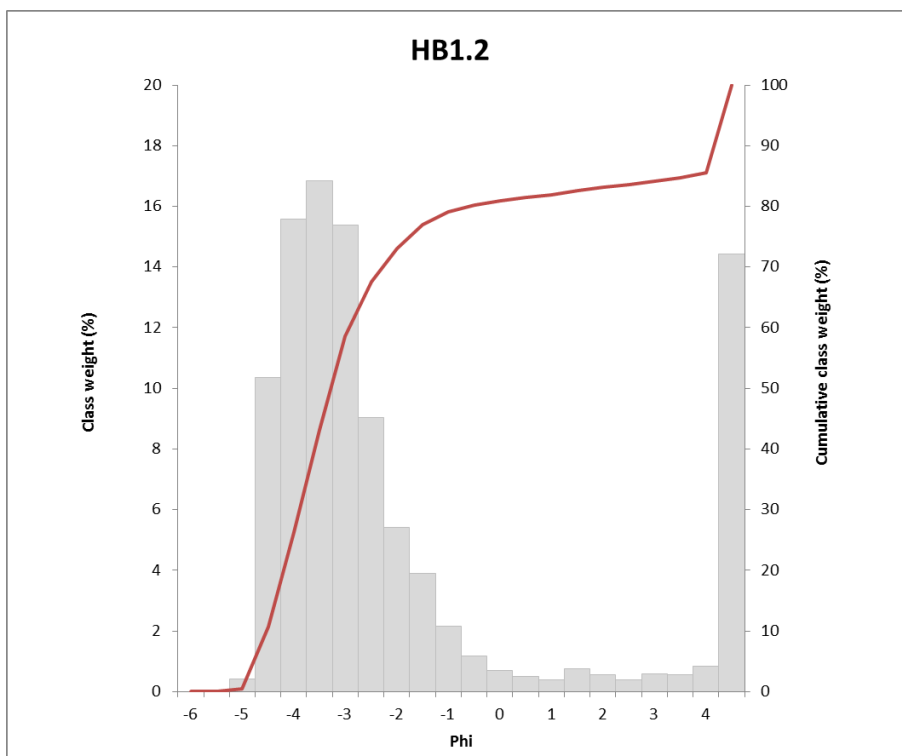
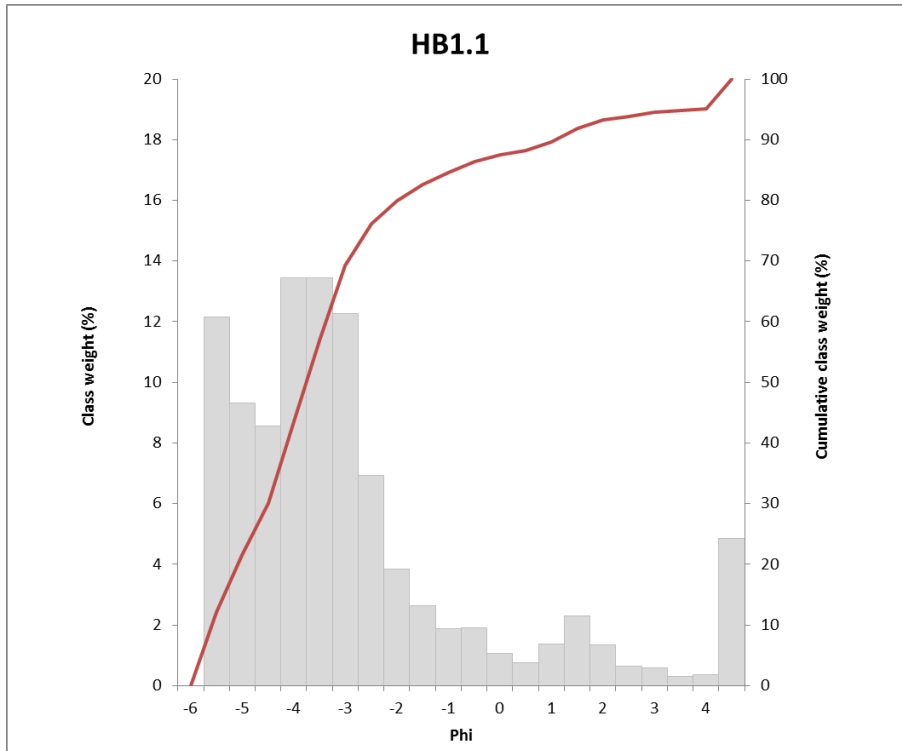


Figure A21.2 Percentage frequency and cumulative percentage frequency of sediment fractions present in sample HB1.1 (top) and HB1.2 (bottom).

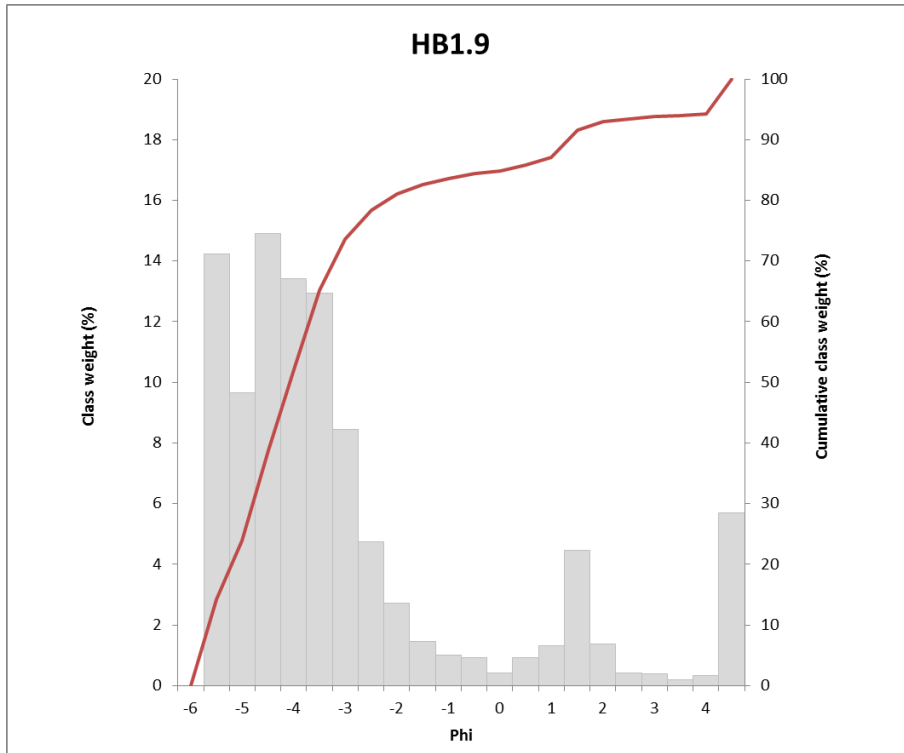


Figure A21.3 Percentage frequency and cumulative percentage frequency of sediment fractions present in sample HB1.9.

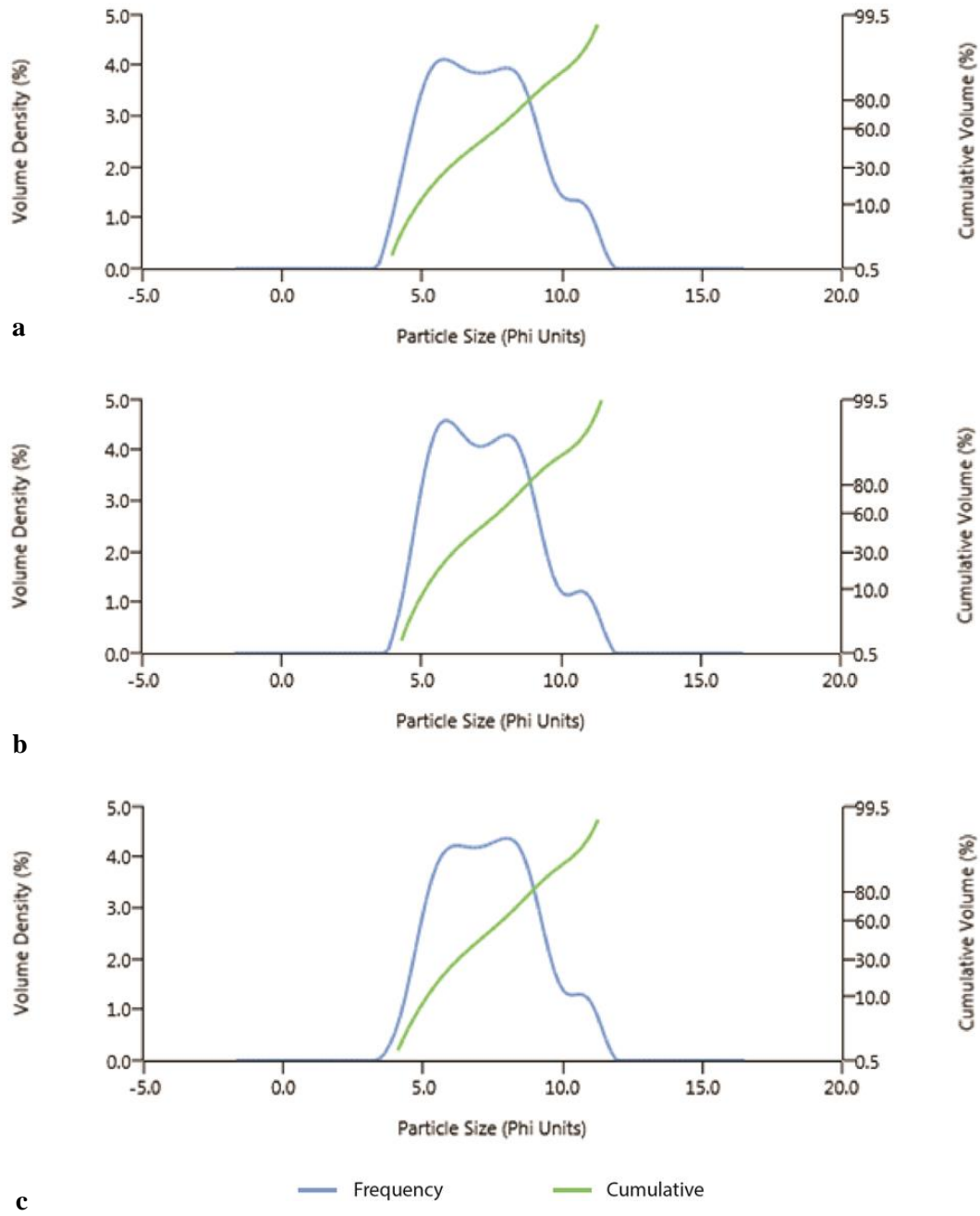


Figure A21.4 Particle size distribution of the <63 μ m fraction of HB1.1 (a), HB1.2 (b) and HB1.9 (c).

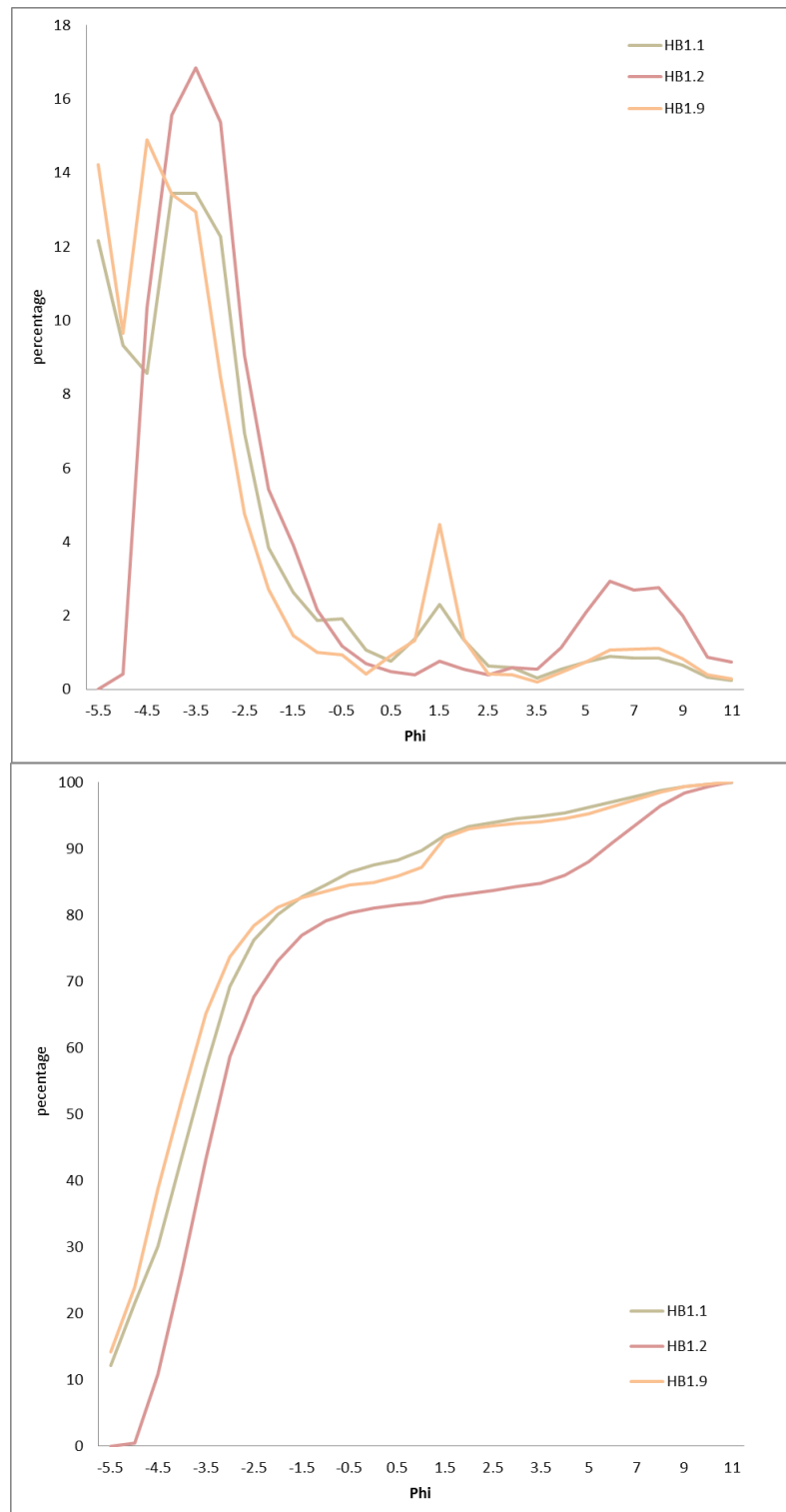


Figure A21.5 Comparison of the integrated particle size distribution curves of the three gravel samples from Woodriding showing weight in percentages of each size fraction (top) and the cumulative percentage of the weight in percentages (bottom).

Appendix 22 Woodriding clast size distribution statistics

		HB1.1	HB1.2	HB1.9
	SAMPLE TYPE:	Bimodal, Very Poorly Sorted	Unimodal, Very Poorly Sorted	Trimodal, Very Poorly Sorted
	TEXTURAL GROUP:	Gravel	Muddy Gravel	Gravel
	SEDIMENT NAME:	Medium Gravel	Coarse Silty Medium Gravel	Coarse Gravel
METHOD OF MOMENTS Arithmetic (μm)	MEAN	18913.1	10815.7	21132.2
	SORTING	16923.2	8559.4	17382.1
	SKEWNESS	0.923	0.513	0.666
	KURTOSIS	2.715	2.461	2.340
METHOD OF MOMENTS Geometric (μm)	MEAN	7904.9	3249.3	8357.5
	SORTING	7.625	14.34	9.018
	SKEWNESS	-2.094	-1.667	-2.065
	KURTOSIS	7.706	4.471	7.050
METHOD OF MOMENTS Logarithmic (ϕ)	MEAN	-2.983	-1.700	-3.063
	SORTING	2.931	3.842	3.173
	SKEWNESS	2.094	1.667	2.065
	KURTOSIS	7.706	4.471	7.050
FOLK AND WARD METHOD (μm)	MEAN	10510.1	3020.4	10643.7
	SORTING	5.475	12.43	6.755
	SKEWNESS	-0.414	-0.731	-0.552
	KURTOSIS	1.745	2.179	2.067
FOLK AND WARD METHOD (ϕ)	MEAN	-3.394	-1.595	-3.412
	SORTING	2.453	3.635	2.756
	SKEWNESS	0.414	0.731	0.552
	KURTOSIS	1.745	2.179	2.067

		HB1.1	HB1.2	HB1.9
FOLK AND WARD METHOD (Description)	MEAN:	Medium Gravel	Very Fine Gravel	Medium Gravel
	SORTING:	Very Poorly Sorted	Very Poorly Sorted	Very Poorly Sorted
	SKEWNESS:	Very Fine Skewed	Very Fine Skewed	Very Fine Skewed
	KURTOSIS:	Very Leptokurtic	Very Leptokurtic	Very Leptokurtic
	MODE 1 (μm):	19200.0	13600.0	26950.0
	MODE 2 (μm):	54000.0		54000.0
	MODE 3 (μm):			327.5
	MODE 1 (ϕ):	-4.243	-3.743	-4.731
	MODE 2 (ϕ):	-5.735		-5.735
	MODE 3 (ϕ):			1.616
	D ₁₀ (μm):	467.5	19.71	353.0
	D ₅₀ (μm):	13481.1	9650.9	16913.3
	D ₉₀ (μm):	47781.9	22980.5	49731.2
	(D ₉₀ / D ₁₀) (μm):	102.2	1165.8	140.9
	(D ₉₀ - D ₁₀) (μm):	47314.4	22960.7	49378.2
	(D ₇₅ / D ₂₅) (μm):	4.597	4.923	4.253
	(D ₇₅ - D ₂₅) (μm):	21446.3	13128.4	23484.8
	D ₁₀ (ϕ):	-5.578	-4.522	-5.636
	D ₅₀ (ϕ):	-3.753	-3.271	-4.080
	D ₉₀ (ϕ):	1.097	5.665	1.502
	(D ₉₀ / D ₁₀) (ϕ):	-0.197	-1.253	-0.267
	(D ₉₀ - D ₁₀) (ϕ):	6.675	10.19	7.138
	(D ₇₅ / D ₂₅) (ϕ):	0.539	0.431	0.577
	(D ₇₅ - D ₂₅) (ϕ):	2.201	2.300	2.089

		HB1.1	HB1.2	HB1.3
COMPOSITION	% GRAVEL:	84.6%	79.1%	83.6%
	% SAND:	10.9%	6.8%	10.9%
	% MUD:	4.6%	14.1%	5.5%
	% V COARSE GRAVEL:	21.1%	0.4%	23.5%
	% COARSE GRAVEL:	22.4%	25.9%	28.8%
	% MEDIUM GRAVEL:	25.7%	32.2%	21.4%
	% FINE GRAVEL:	10.8%	14.5%	7.5%
	% V FINE GRAVEL:	4.5%	6.1%	2.5%
	% V COARSE SAND:	3.0%	1.9%	1.3%
	% COARSE SAND:	2.1%	0.9%	2.2%
	% MEDIUM SAND:	3.2%	1.1%	5.4%
	% FINE SAND:	1.7%	1.2%	1.3%
	% V FINE SAND:	0.9%	1.7%	0.7%
	% V COARSE SILT:	0.7%	2.0%	0.7%
	% COARSE SILT:	0.9%	3.0%	1.1%
	% MEDIUM SILT:	0.8%	2.7%	1.1%
	% FINE SILT:	0.8%	2.7%	1.1%
	% V FINE SILT:	0.6%	2.0%	0.8%
	% CLAY:	0.6%	1.6%	0.7%

Appendix 23 Woodgreen clast size distributions

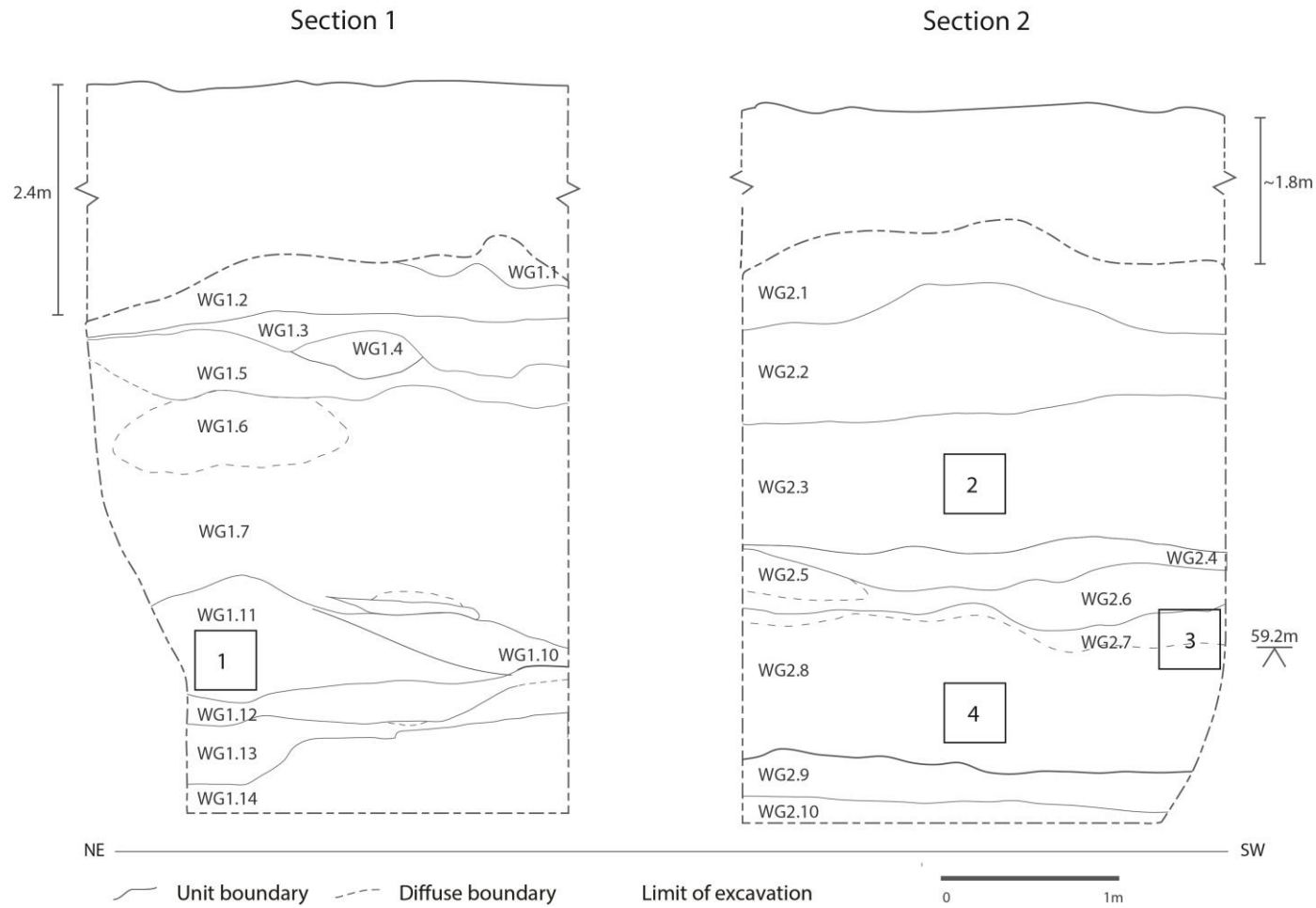


Figure A23.1 Two sections in terrace 7 at Woodgreen showing gravel sample locations and the main stratigraphic units. 1= WG1.11; 2=WG2.3; 3=WG2.7.4a; 4=WG2.8.

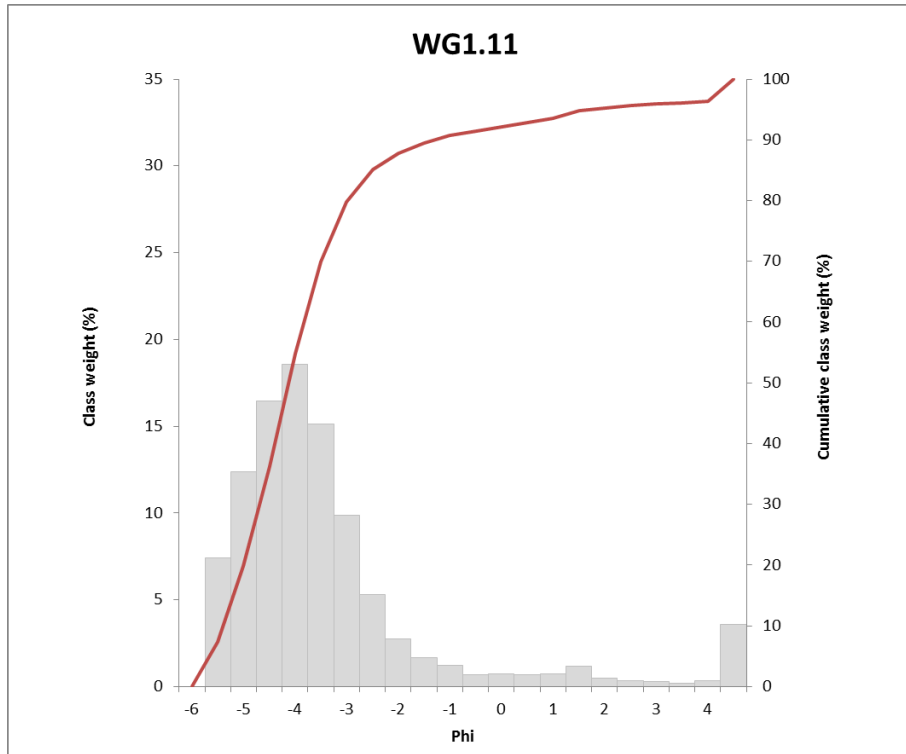


Figure A23.2 Percentage frequency and cumulative percentage frequency of sediment fractions present in sample WG1.11.

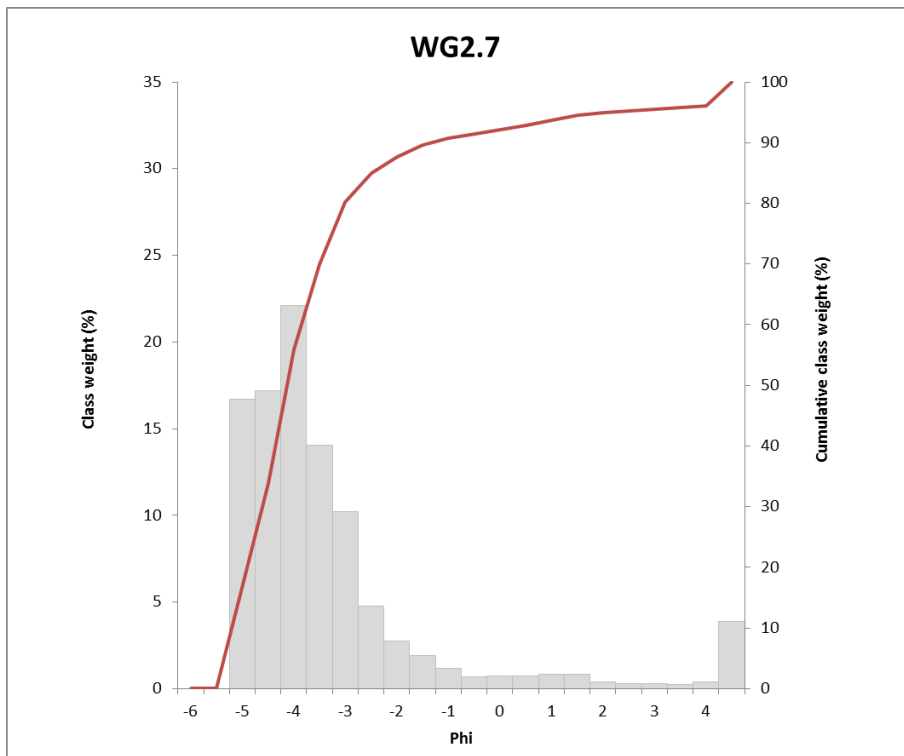
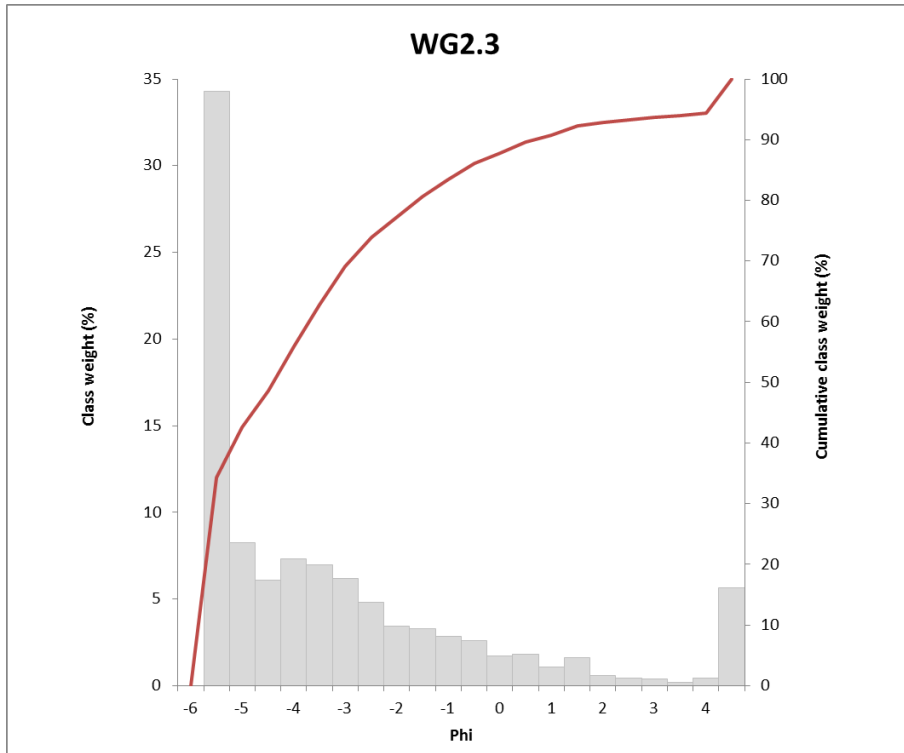


Figure A23.3 Percentage frequency and cumulative percentage frequency of sediment fractions present in sample WG2.3 (top) and WG2.7 (bottom).

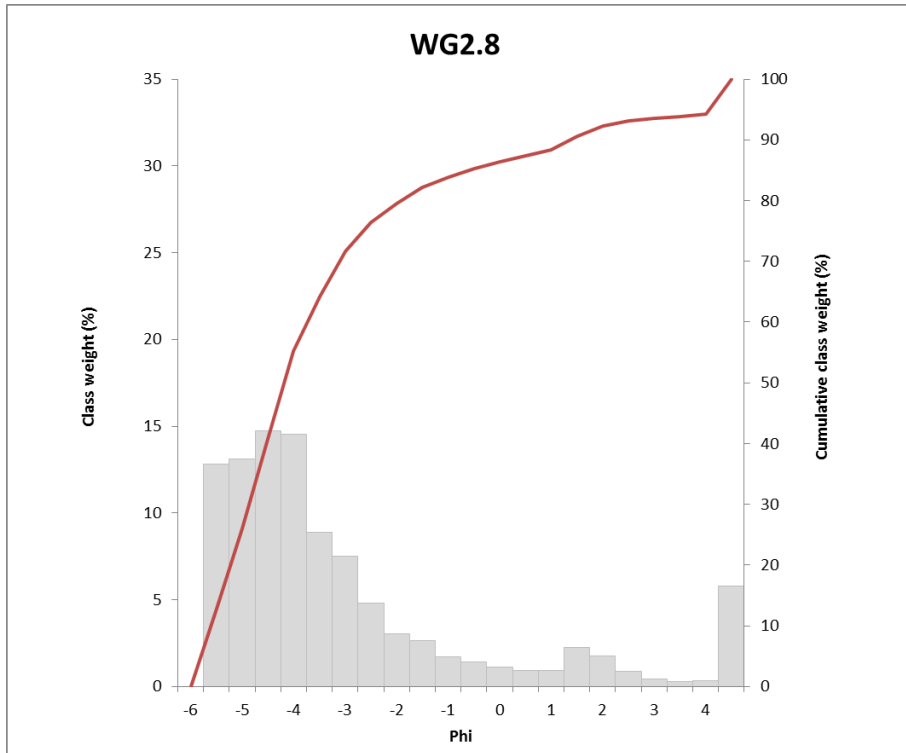


Figure A23.4 Percentage frequency and cumulative percentage frequency of sediment fractions present in sample WG2.8.

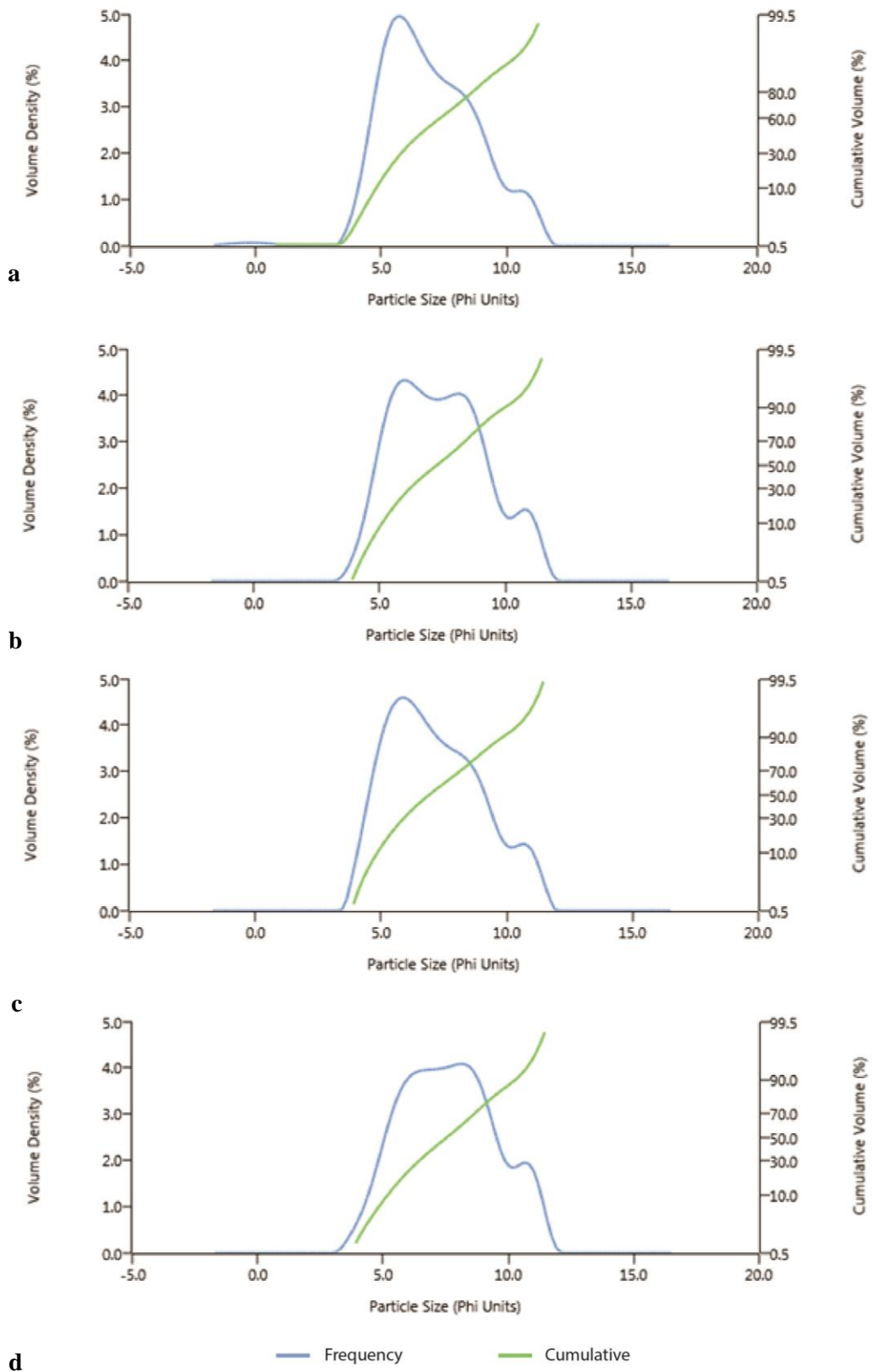


Figure A23.5 Particle size distribution of the <63 μ m fraction of WG1.11 (a), WG2.3 (b), WG2.7 (c) and WG2.8 (d).

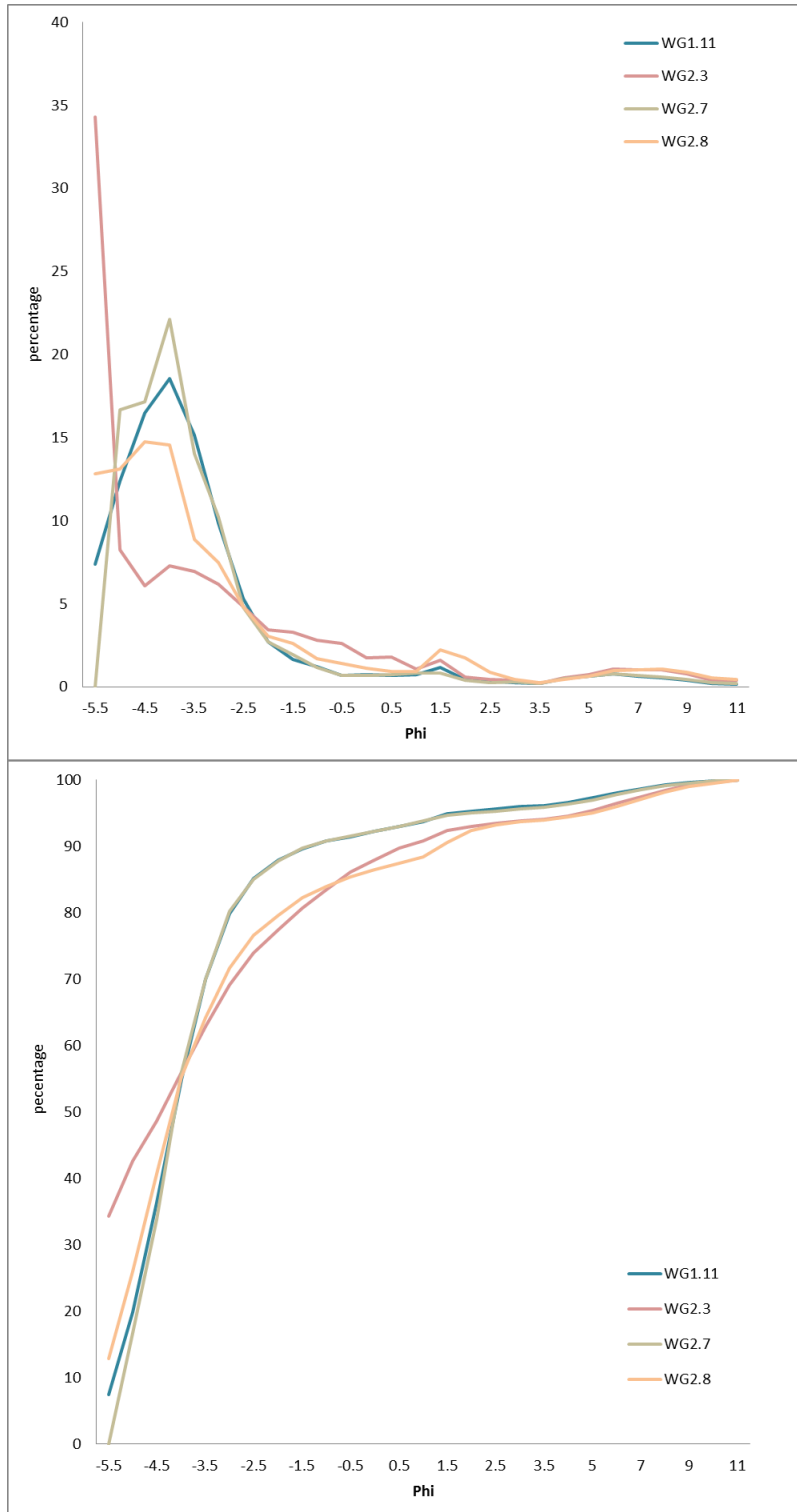


Figure A23.6 Comparison of the integrated particle size distribution curves of the four gravel samples from Woodgreen showing weight in percentages of each size fraction (top) and the cumulative percentage of the weight in percentages (bottom).

Appendix 24 Woodgreen clast size distribution statistics

		WG1.11	WG2.3	WG2.7	WG2.8
	SAMPLE TYPE:	Unimodal, Poorly Sorted	Bimodal, Very Poorly Sorted	Unimodal, Poorly Sorted	Bimodal, Very Poorly Sorted
	TEXTURAL GROUP:	Gravel	Gravel	Gravel	Gravel
	SEDIMENT NAME:	Coarse Gravel	Very Coarse Gravel	Coarse Gravel	Coarse Gravel
METHOD OF MOMENTS Arithmetic (μm)	MEAN	20373.9	27033.2	18733.2	21337.0
	SORTING	14524.3	21989.5	11747.0	17292.4
	SKEWNESS	0.744	0.152	0.246	0.570
	KURTOSIS	2.922	1.322	2.105	2.225
METHOD OF MOMENTS Geometric (μm)	MEAN	11228.6	9908.1	10632.4	8346.2
	SORTING	5.636	9.575	5.741	9.365
	SKEWNESS	-2.825	-1.974	-2.983	-2.120
	KURTOSIS	12.04	6.925	12.69	7.348
METHOD OF MOMENTS Logarithmic (ϕ)	MEAN	-3.489	-3.309	-3.410	-3.061
	SORTING	2.495	3.259	2.521	3.227
	SKEWNESS	2.825	1.974	2.983	2.120
	KURTOSIS	12.04	6.925	12.69	7.348
FOLK AND WARD METHOD (μm)	MEAN	15495.8	12834.3	15007.1	11364.2
	SORTING	3.420	6.980	3.351	6.627
	SKEWNESS	-0.400	-0.576	-0.480	-0.579
	KURTOSIS	1.949	1.308	2.074	1.862
FOLK AND WARD METHOD (ϕ)	MEAN	-3.954	-3.682	-3.908	-3.506
	SORTING	1.774	2.803	1.745	2.728
	SKEWNESS	0.400	0.576	0.480	0.579
	KURTOSIS	1.949	1.308	2.074	1.862

		WG1.11	WG2.3	WG2.7	WG2.8
FOLK AND WARD METHOD (Description)	MEAN:	Medium Gravel	Medium Gravel	Medium Gravel	Medium Gravel
	SORTING:	Poorly Sorted	Very Poorly Sorted	Poorly Sorted	Very Poorly Sorted
	SKEWNESS:	Very Fine Skewed	Very Fine Skewed	Very Fine Skewed	Very Fine Skewed
	KURTOSIS:	Very Leptokurtic	Leptokurtic	Very Leptokurtic	Very Leptokurtic
	MODE 1 (μm):	19200.0	54000.0	19200.0	19200.0
	MODE 2 (μm):		19200.0		54000.0
	MODE 3 (μm):				
	MODE 1 (ϕ):	-4.243	-5.735	-4.243	-4.243
	MODE 2 (ϕ):		-4.243		-5.735
	MODE 3 (ϕ):				
	D ₁₀ (μm):	2481.4	635.2	2534.1	341.2
	D ₅₀ (μm):	17474.7	21037.2	17522.3	18085.3
	D ₉₀ (μm):	41765.7	57113.4	36339.6	48475.2
	(D ₉₀ / D ₁₀) (μm):	16.83	89.92	14.34	142.1
	(D ₉₀ - D ₁₀) (μm):	39284.3	56478.3	33805.5	48134.0
	(D ₇₅ / D ₂₅) (μm):	2.994	9.782	2.811	5.160
	(D ₇₅ - D ₂₅) (μm):	18840.9	44258.9	17207.3	26080.7
	D ₁₀ (ϕ):	-5.384	-5.836	-5.183	-5.599
	D ₅₀ (ϕ):	-4.127	-4.395	-4.131	-4.177
	D ₉₀ (ϕ):	-1.311	0.655	-1.341	1.551
	(D ₉₀ / D ₁₀) (ϕ):	0.244	-0.112	0.259	-0.277
	(D ₉₀ - D ₁₀) (ϕ):	4.073	6.491	3.842	7.150
	(D ₇₅ / D ₂₅) (ϕ):	0.672	0.415	0.685	0.528
	(D ₇₅ - D ₂₅) (ϕ):	1.582	3.290	1.491	2.367

		WG1.11	WG2.3	WG2.7	WG2.8
COMPOSITION	% GRAVEL:	90.8%	83.5%	90.8%	83.9%
	% SAND:	5.9%	11.1%	5.5%	10.5%
	% MUD:	3.4%	5.4%	3.7%	5.6%
	% V COARSE GRAVEL:	19.3%	42.2%	15.9%	25.4%
	% COARSE GRAVEL:	35.6%	13.7%	40.0%	29.9%
	% MEDIUM GRAVEL:	25.0%	13.2%	24.3%	16.4%
	% FINE GRAVEL:	8.0%	8.3%	7.5%	7.9%
	% V FINE GRAVEL:	2.9%	6.1%	3.1%	4.3%
	% V COARSE SAND:	1.4%	4.4%	1.4%	2.5%
	% COARSE SAND:	1.5%	2.9%	1.6%	1.9%
	% MEDIUM SAND:	1.5%	1.9%	1.0%	3.3%
	% FINE SAND:	0.8%	1.2%	0.8%	2.0%
	% V FINE SAND:	0.7%	0.8%	0.7%	0.7%
	% V COARSE SILT:	0.6%	0.7%	0.6%	0.6%
	% COARSE SILT:	0.8%	1.1%	0.8%	1.0%
	% MEDIUM SILT:	0.6%	1.0%	0.7%	1.0%
	% FINE SILT:	0.5%	1.0%	0.6%	1.1%
	% V FINE SILT:	0.4%	0.8%	0.5%	0.9%
% CLAY:	0.4%	0.8%	0.5%	1.0%	

Appendix 25 Image-based automated grain-sizing at Woodgreen

Photographs for image-based automated grainsizing were collected across the entire section (Figure A25.1). The photographs used for the IBAG analysis and the resulting grain size distributions are presented in Figure A25.2 and Figure A25.3. The IBAG results of the eight photographs show similar grain size distributions with the majority of the grains falling between 8-0.5mm (-3 and -0.5ϕ) and below 0.35mm resulting from the detection limit. The data obtained from frame 1 does not record a 1.5ϕ and smaller fraction but a high percentage of medium sand (1ϕ). A comparison of the results from each photograph is presented in Figure A25.4 and Figure A25.5. This shows the similarity between the obtained grain size distributions with the exception of frame 1 that shows a large percentage of medium sand.

The IBAG results are compared with the sieving data in Figure A25.6 and Figure A25.7. The IBAG data shows an offset compared to the sieving results, underrepresenting the larger size fractions (medium to coarse gravel) and over representing the fine gravel to medium sand fraction and the $>0.35\text{mm}$ sediment.

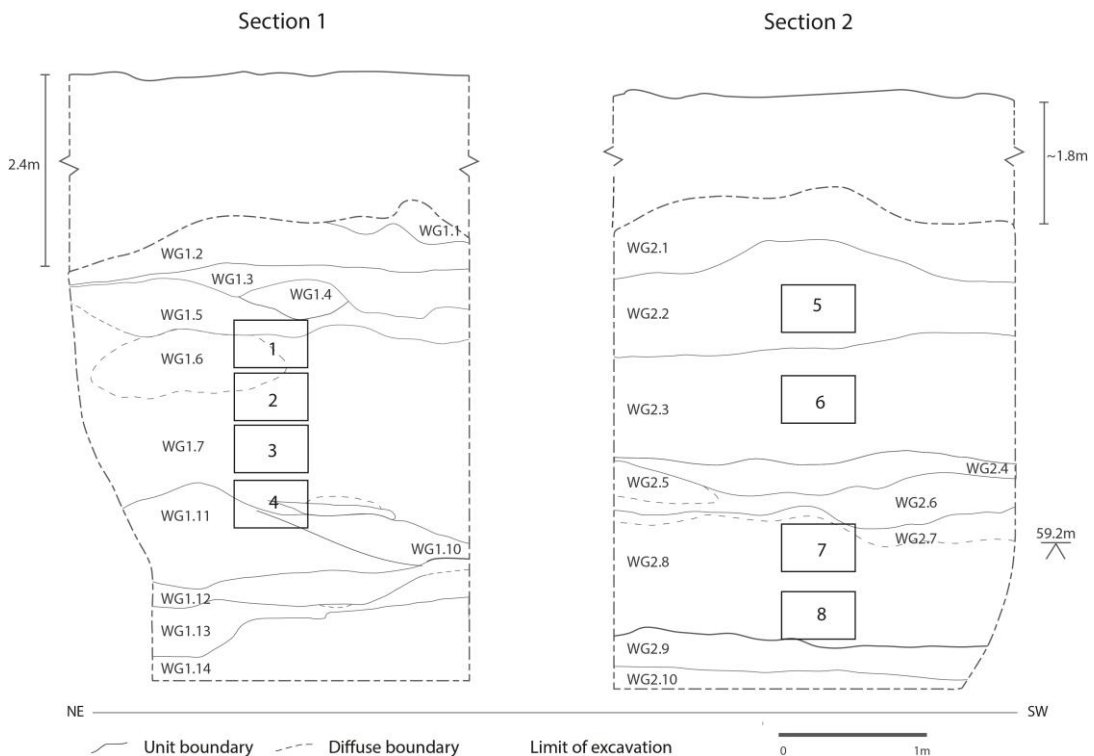


Figure A25.1 Two sections in terrace 7 at Woodgreen showing image locations and the main stratigraphic units.

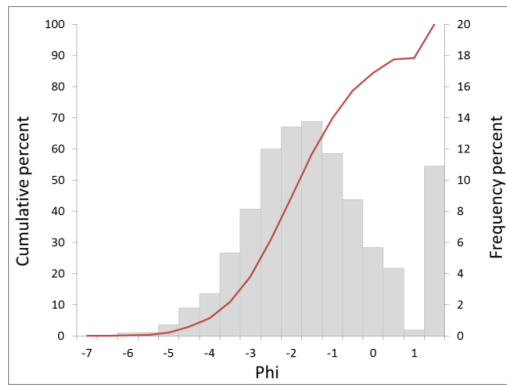
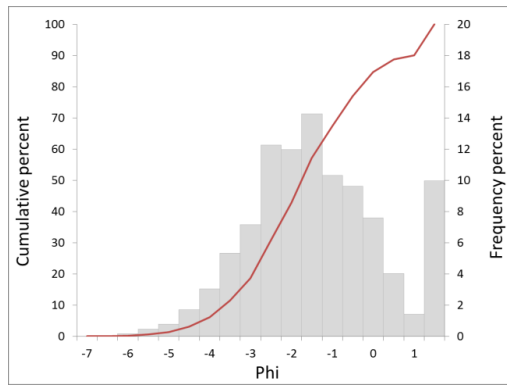
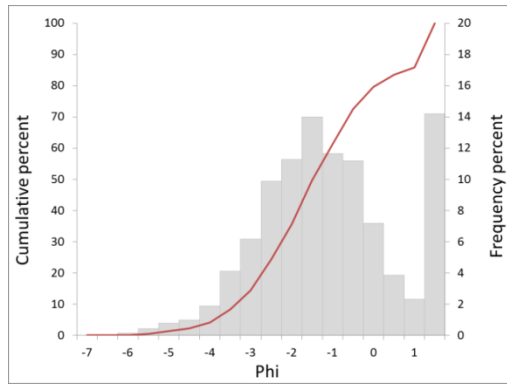
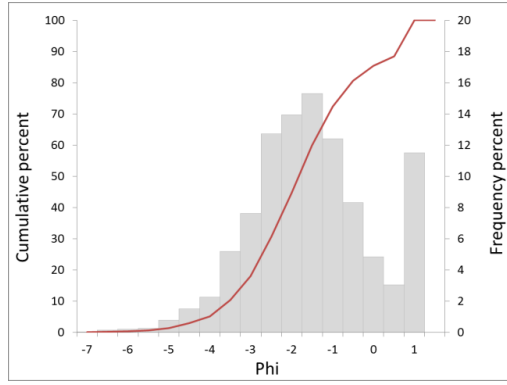


Figure A25.2 Woodgreen frame 1-4.

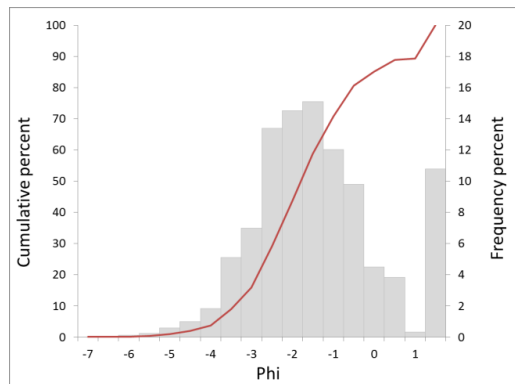
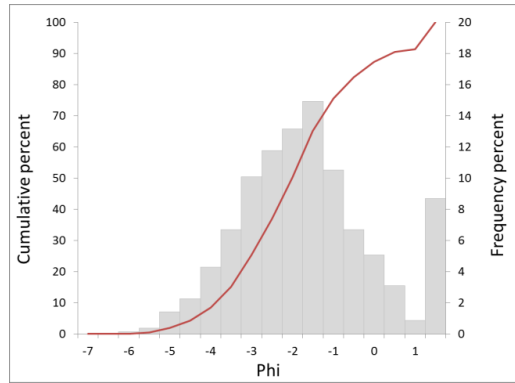
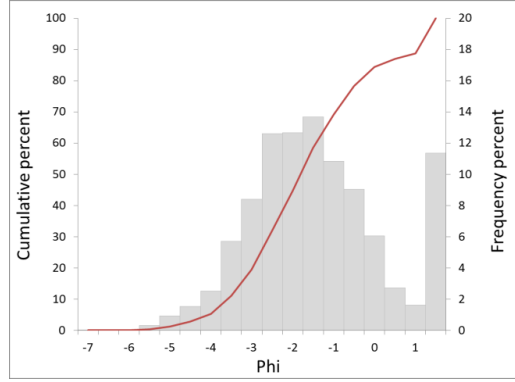
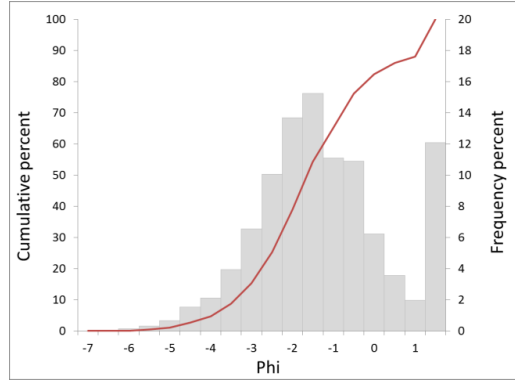


Figure A25.3 Woodgreen frame 5-8.

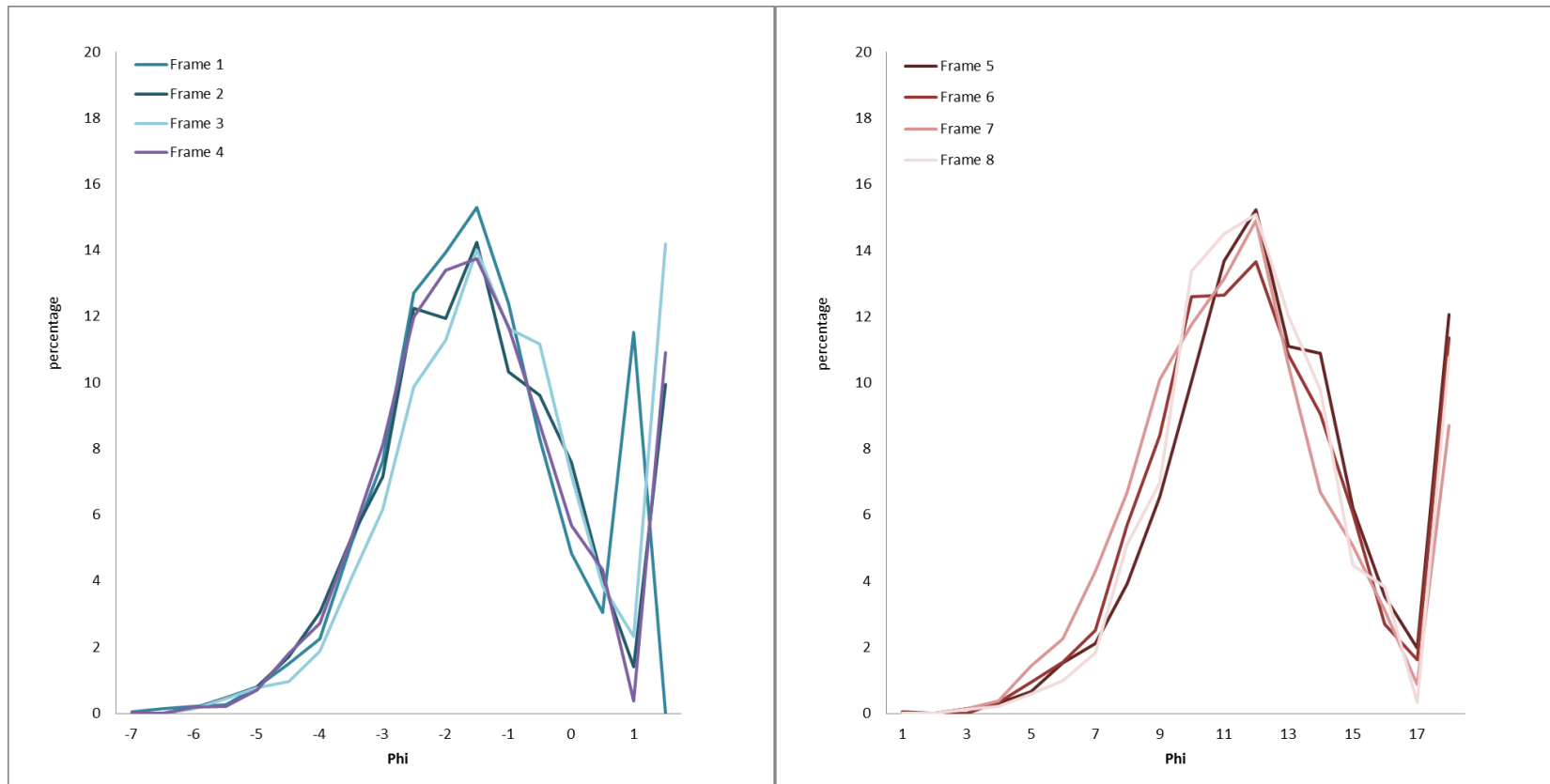


Figure A25.4 Comparison of percentage frequencies obtained from IBAG in Woodgreen section 1 (left) and section 2 (right).

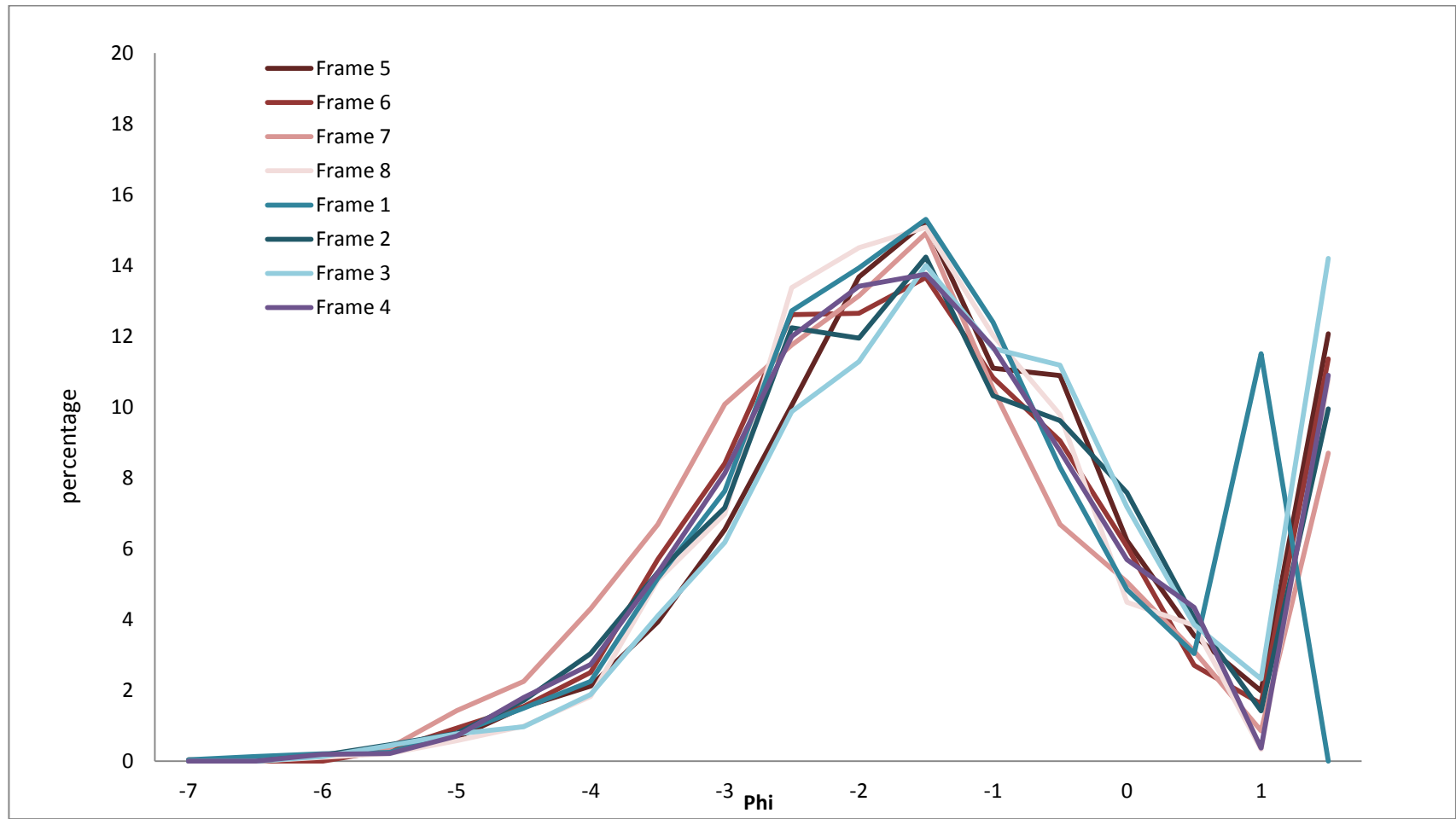


Figure A25.5 Comparison of percentage frequencies obtained from IBAG from both sections at Woodgreen.

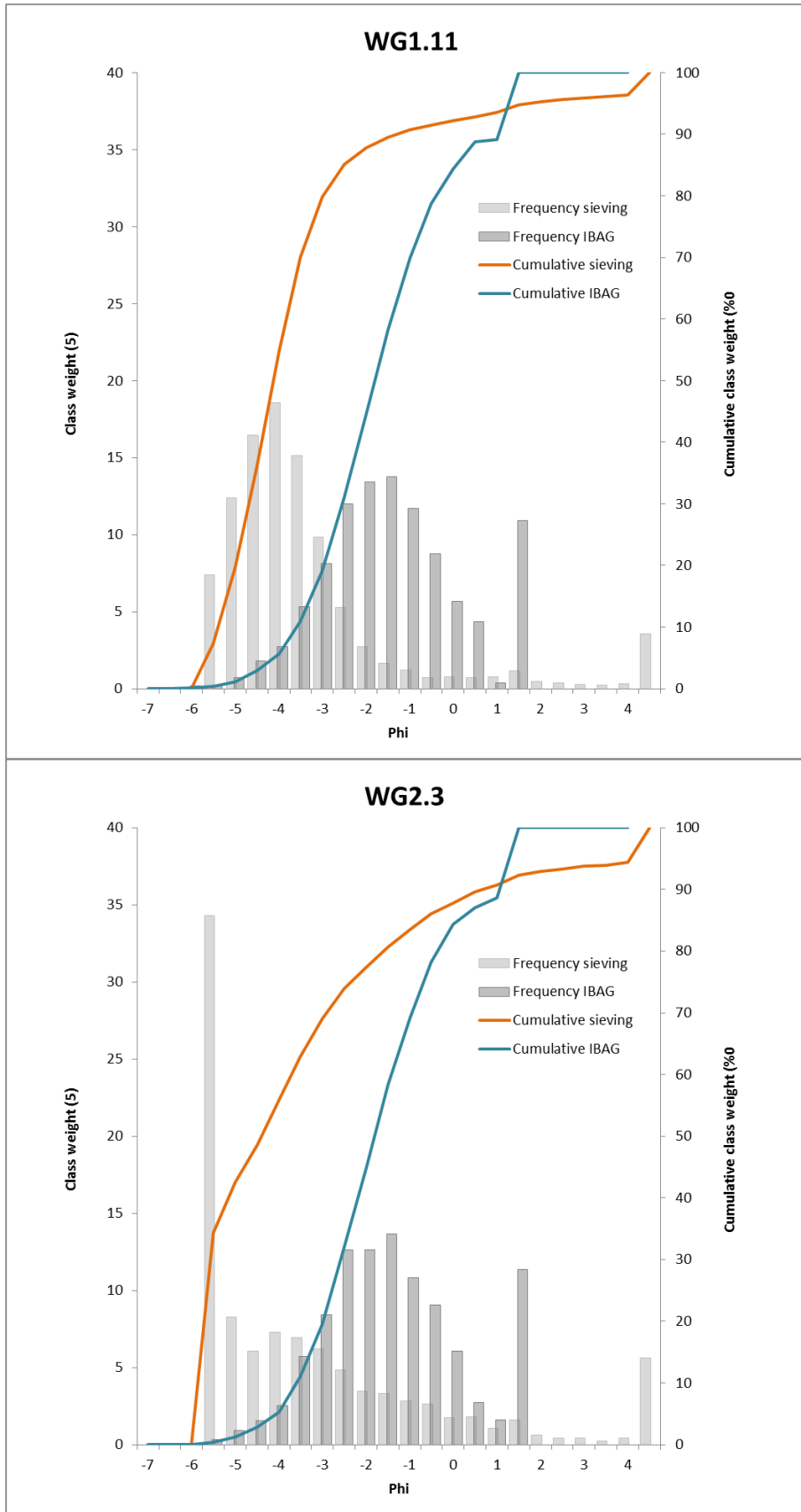


Figure A25.6 Comparison of sieving and IBAG results from WG1.11 and frame 4 and WG2.3 and frame 6.

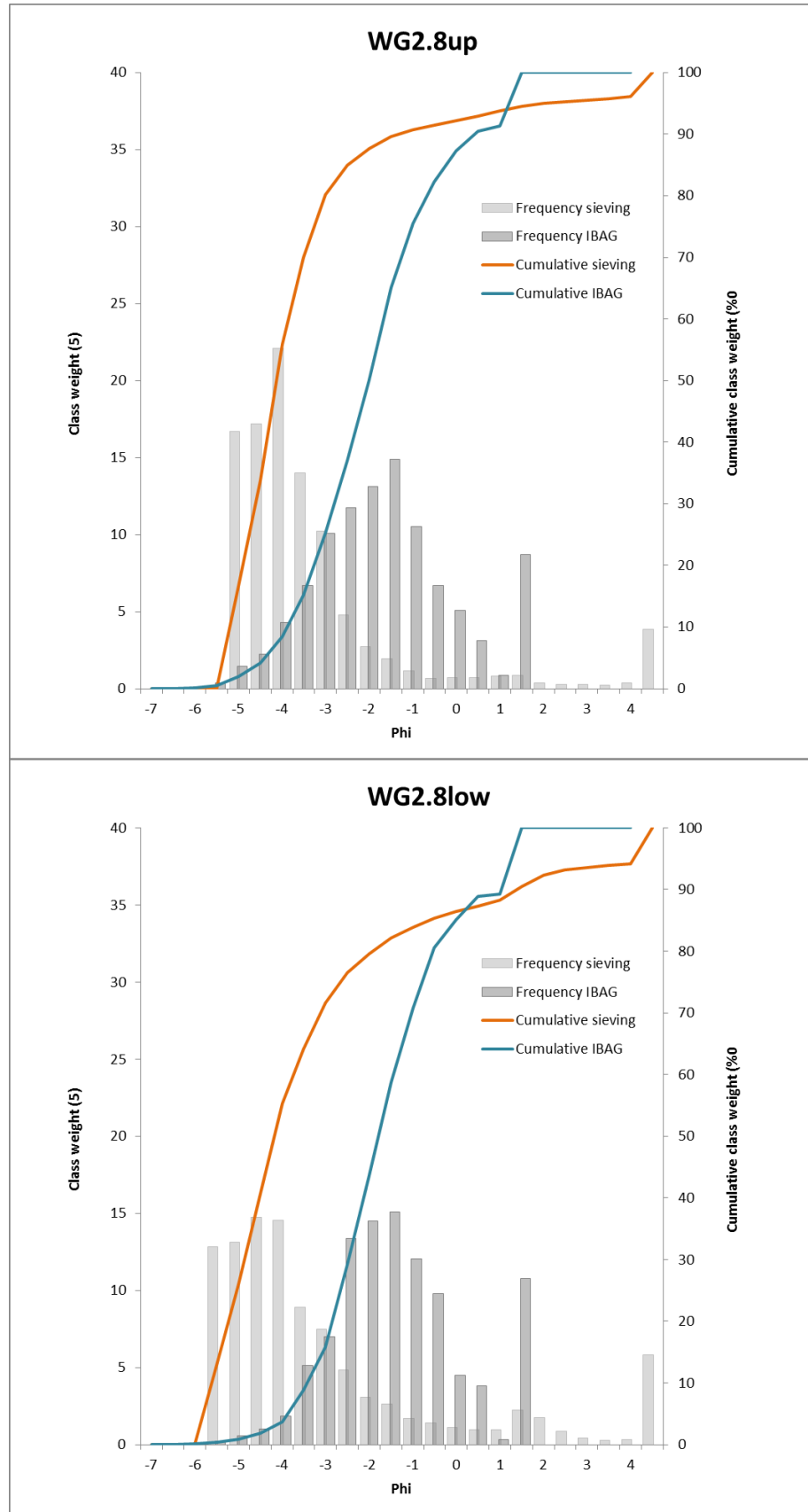


Figure A25.7 Comparison of sieving and IBAG results from WG2.8up and frame 7 and WG28low and frame 8.

Appendix 26 Somerley clast size distributions

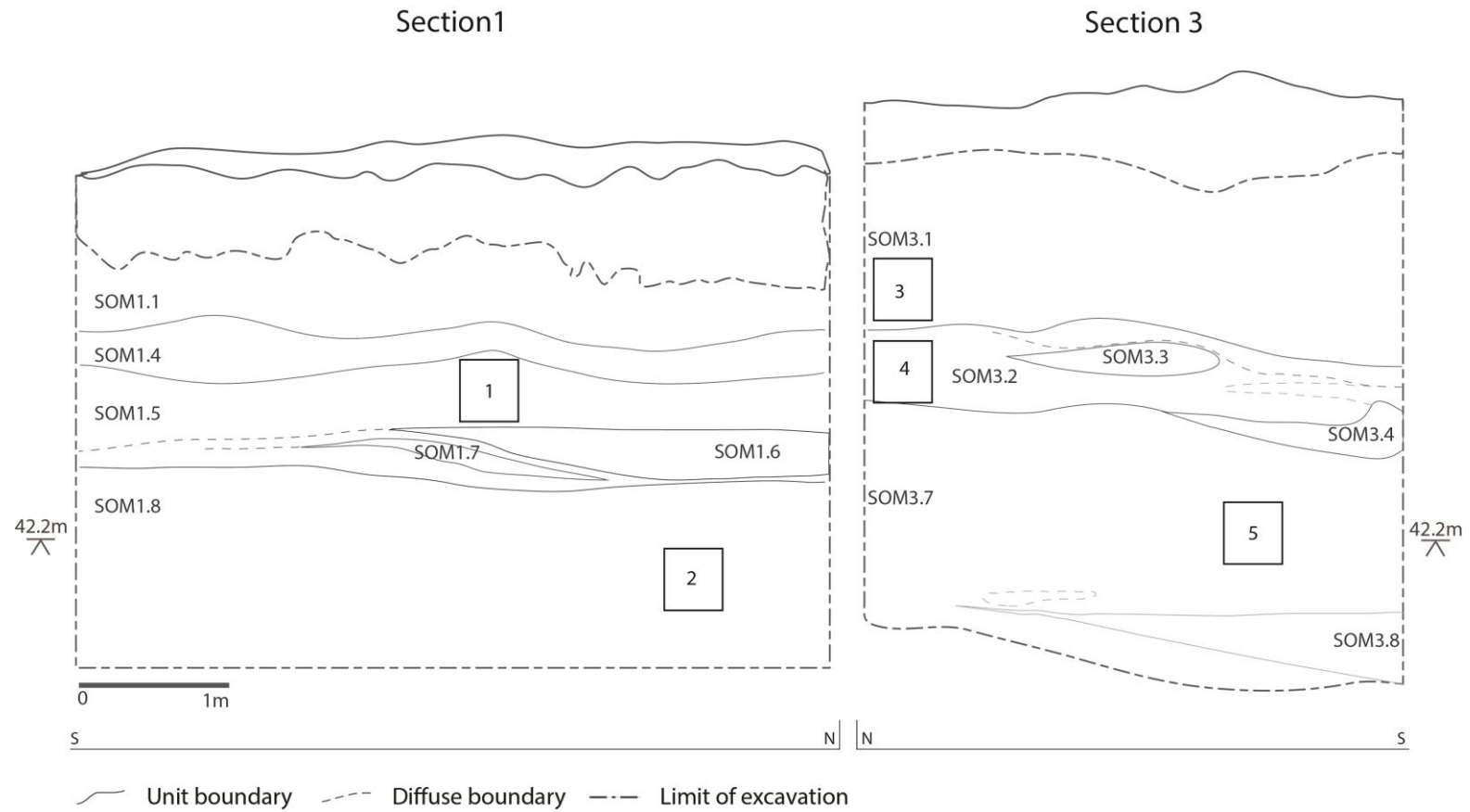


Figure A26.1 Two sections in terrace 6 in Somerley pit showing gravel sample locations and the main stratigraphic units. 1= SOM1.5; 2=SOM1.8; 3=SOM3.1; 4=SOM3.2; 5=SOM3.7.

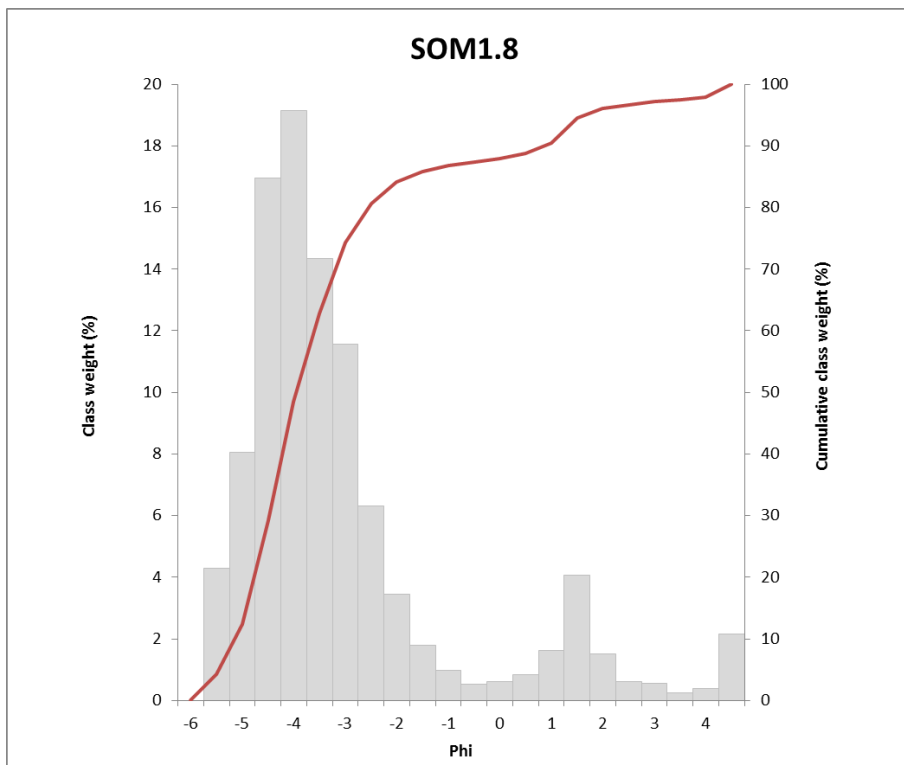
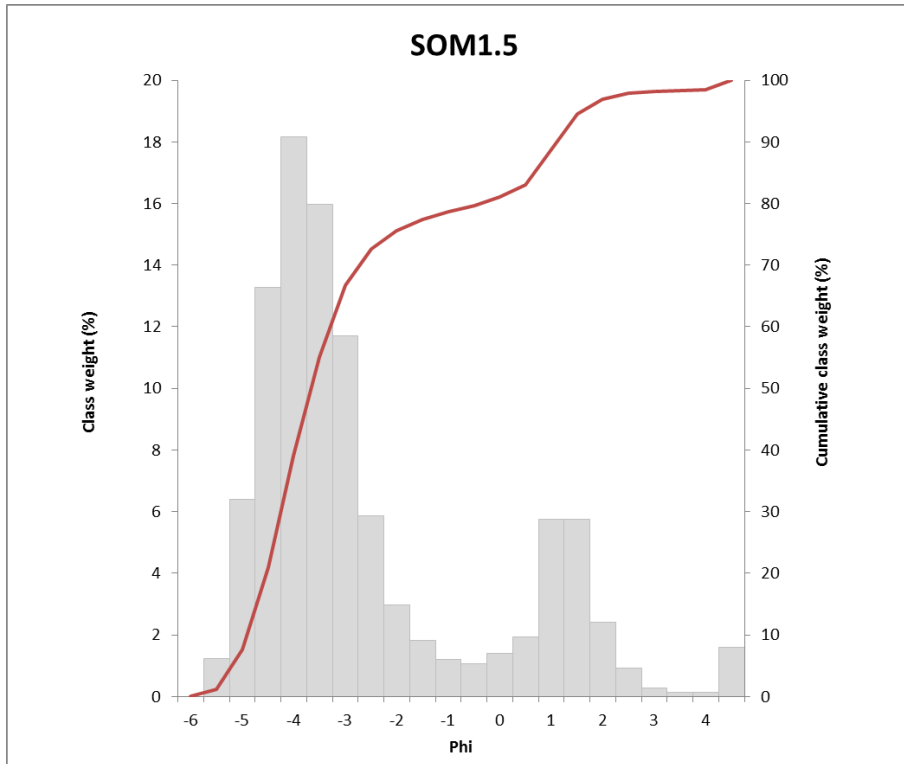


Figure A26.2 Percentage frequency and cumulative percentage frequency of sediment fractions present in sample SOM1.5 (top) and SOM1.8 (bottom).

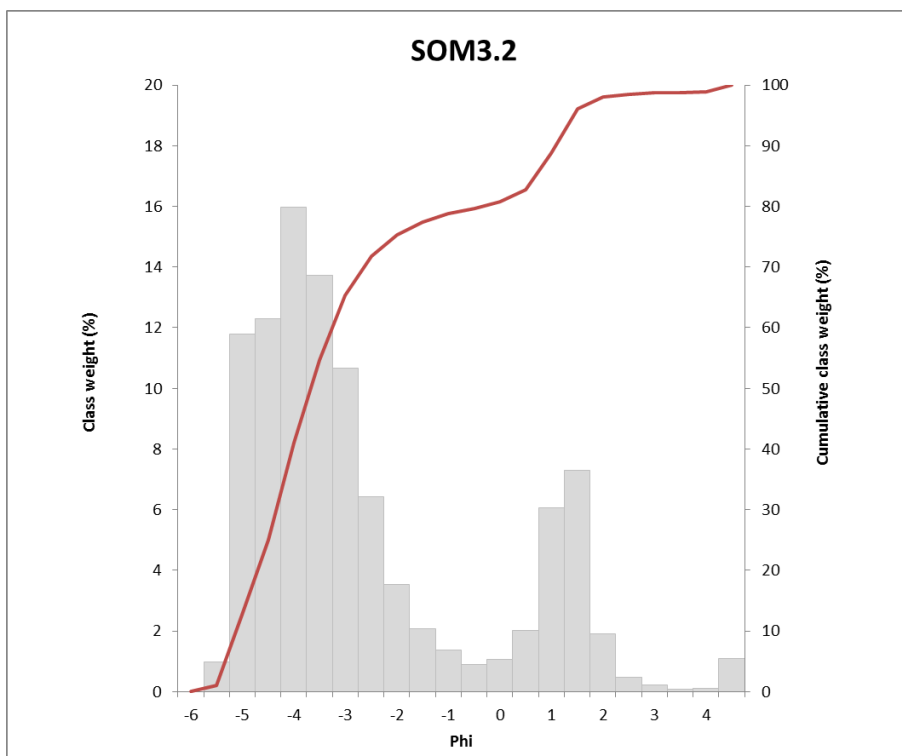
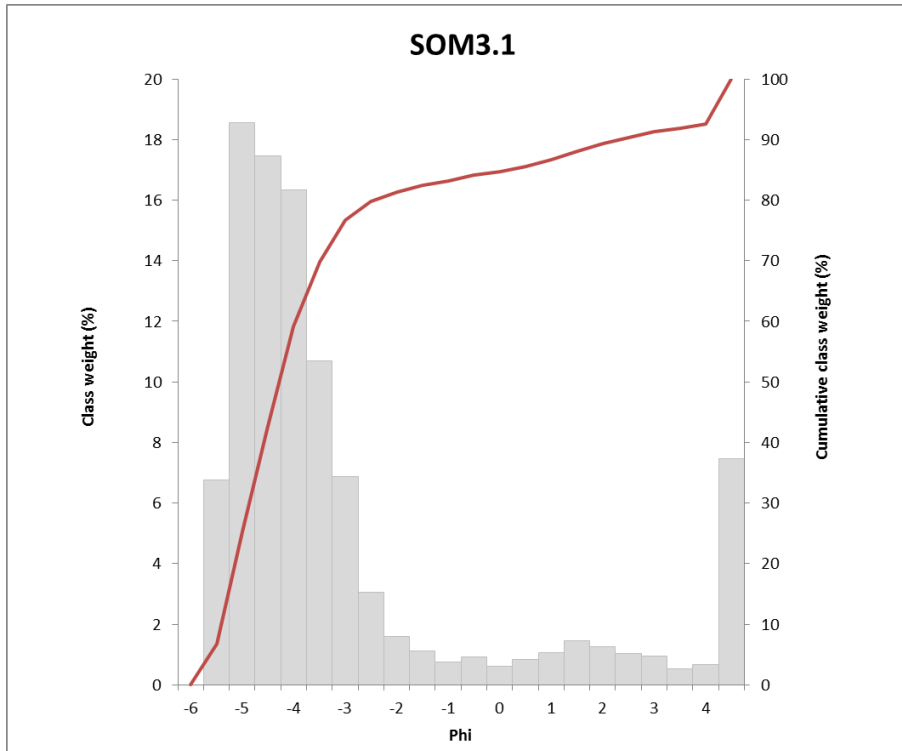


Figure A26.3 Percentage frequency and cumulative percentage frequency of sediment fractions present in sample SOM3.1 (top) and SOM3.2 (bottom).

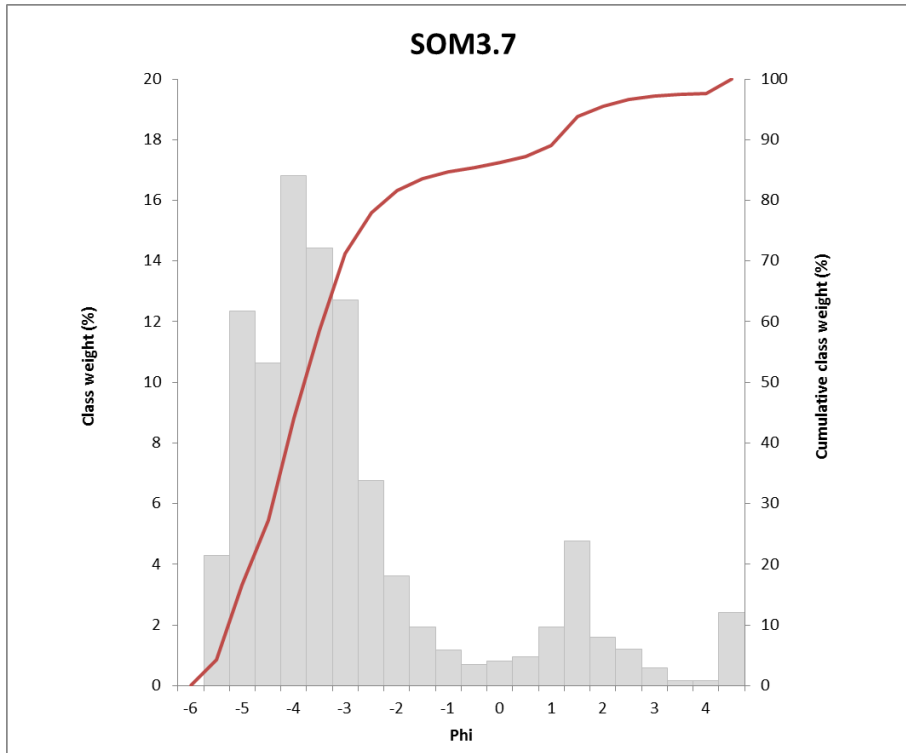


Figure A26.4 Percentage frequency and cumulative percentage frequency of sediment fractions present in sample SOM3.7.

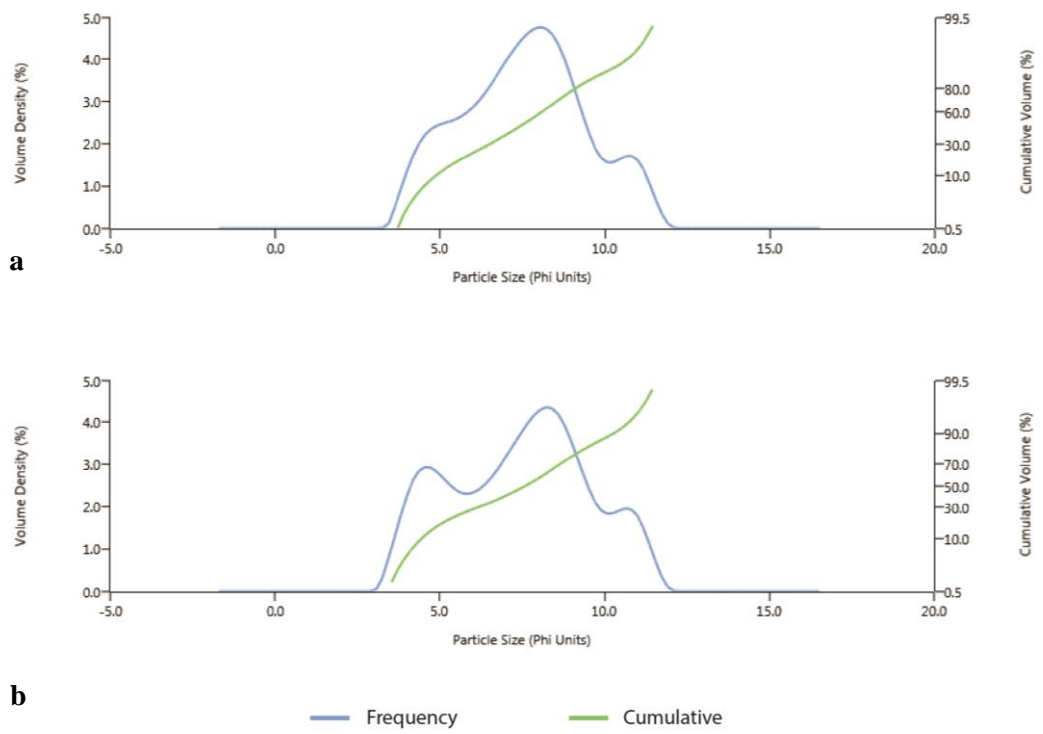


Figure A26.5 Particle size distribution of the <63 μ m fraction of SOM1.5 (a) and SOM1.8 (b).

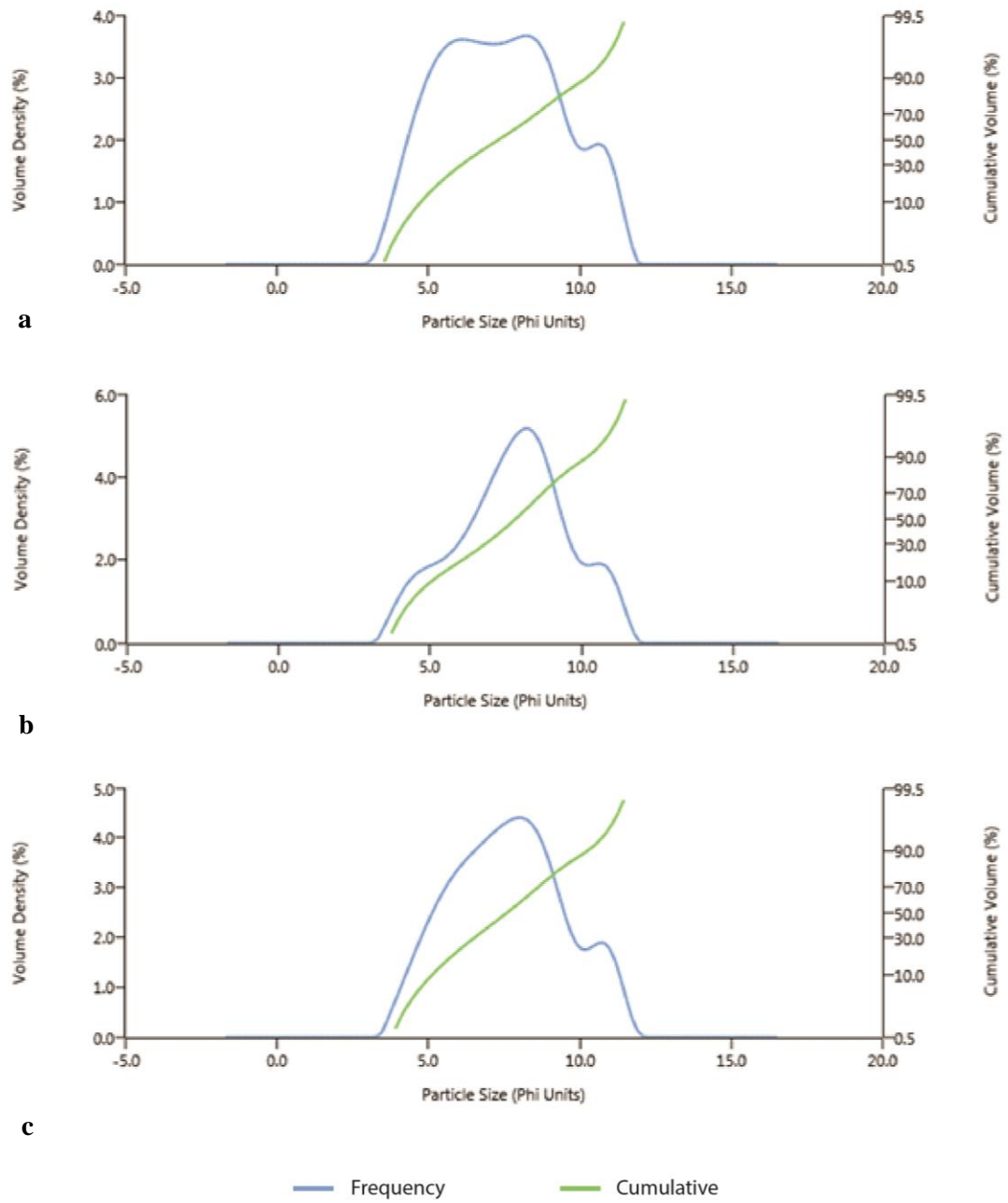


Figure A26.6 Particle size distribution of the <63 μ m fraction of SOM3.1 (a), SOM3.2 (b) and SOM3.7 (c).

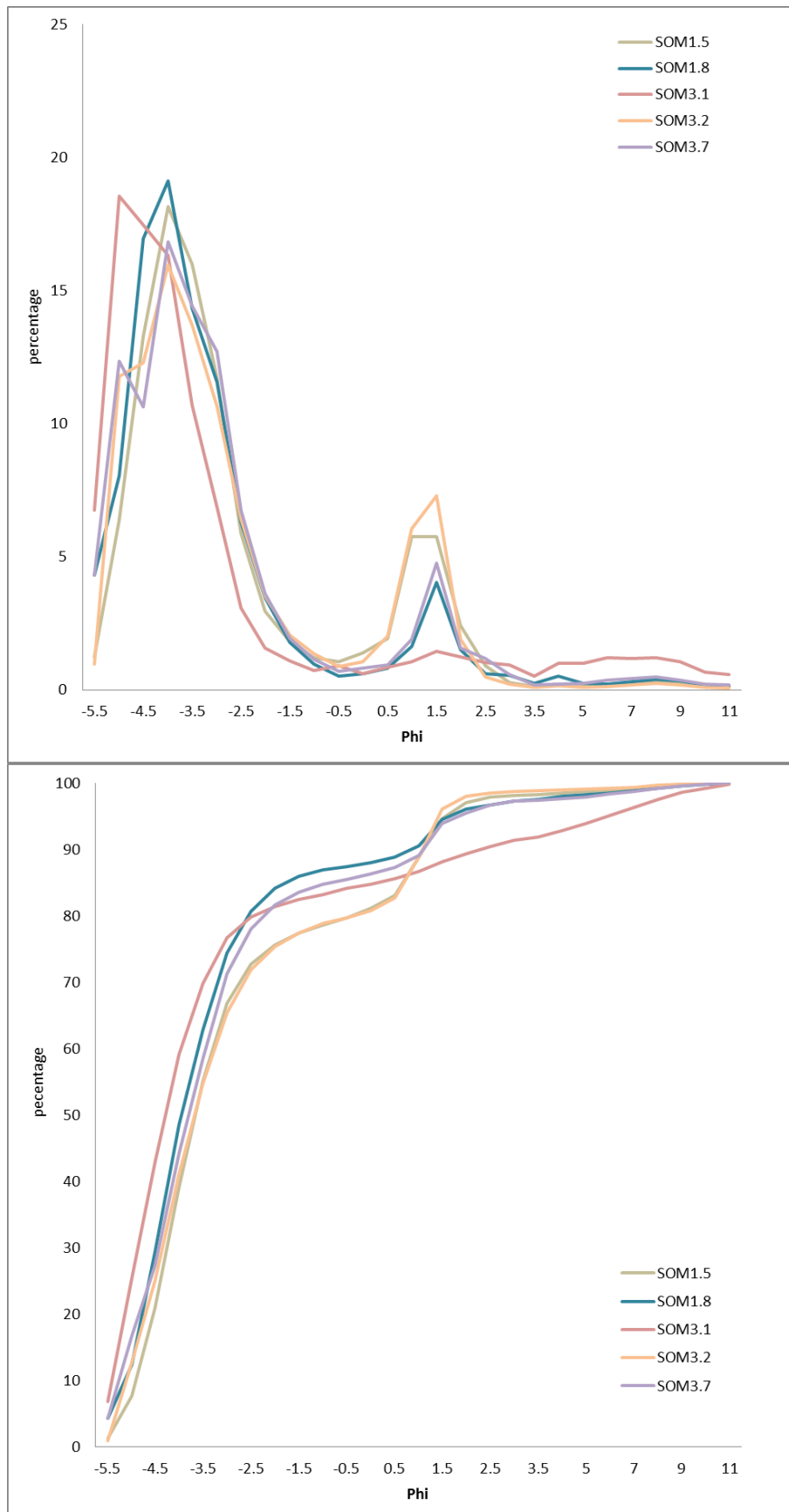


Figure A26.7 Comparison of the integrated particle size distribution curves of the five gravel samples from Somerley Pit showing weight in percentages of each size fraction (top) and the cumulative percentage of the weight in percentages (bottom).

Appendix 27 Somerley clast size distribution statistics

		SOM1.5	SOM1.8	SOM3.1	SOM3.2	SOM3.7
	SAMPLE TYPE:	Trimodal, Very Poorly Sorted	Bimodal, Poorly Sorted	Unimodal, Very Poorly Sorted	Trimodal, Very Poorly Sorted	Trimodal, Very Poorly Sorted
	TEXTURAL GROUP:	Sandy Gravel	Gravel	Gravel	Sandy Gravel	Gravel
	SEDIMENT NAME:	Sandy Coarse Gravel	Coarse Gravel	Coarse Gravel	Sandy Coarse Gravel	Coarse Gravel
METHOD OF MOMENTS Arithmetic (μm)	MEAN	14234.3	17453.5	21139.1	15124.0	17123.0
	SORTING	11605.2	13182.4	15440.0	12623.9	13960.8
	SKEWNESS	0.838	0.888	0.391	0.710	0.892
	KURTOSIS	3.545	3.563	2.334	2.734	3.166
METHOD OF MOMENTS Geometric (μm)	MEAN	6725.7	9192.7	8053.6	7080.3	8246.3
	SORTING	5.580	5.444	10.89	5.378	6.008
	SKEWNESS	-1.659	-2.346	-2.110	-1.481	-2.114
	KURTOSIS	6.189	9.624	6.752	5.511	8.278
METHOD OF MOMENTS Logarithmic (ϕ)	MEAN	-2.750	-3.200	-3.010	-2.824	-3.044
	SORTING	2.480	2.445	3.445	2.427	2.587
	SKEWNESS	1.659	2.346	2.110	1.481	2.114
	KURTOSIS	6.189	9.624	6.752	5.511	8.278
FOLK AND WARD METHOD (μm)	MEAN	5980.1	12241.5	10418.5	6220.1	10341.5
	SORTING	5.174	3.509	7.337	5.254	4.186
	SKEWNESS	-0.586	-0.468	-0.673	-0.540	-0.449
	KURTOSIS	1.261	1.791	2.508	1.145	1.650
FOLK AND WARD METHOD (ϕ)	MEAN	-2.580	-3.614	-3.381	-2.637	-3.370
	SORTING	2.371	1.811	2.875	2.393	2.066
	SKEWNESS	0.586	0.468	0.673	0.540	0.449
	KURTOSIS	1.261	1.791	2.508	1.145	1.650

		SOM1.5	SOM1.8	SOM3.1	SOM3.2	SOM3.7
FOLK AND WARD METHOD (Description)	MEAN:	Fine Gravel	Medium Gravel	Medium Gravel	Fine Gravel	Medium Gravel
	SORTING:	Very Poorly Sorted	Poorly Sorted	Very Poorly Sorted	Very Poorly Sorted	Very Poorly Sorted
	SKEWNESS:	Very Fine Skewed	Very Fine Skewed	Very Fine Skewed	Very Fine Skewed	Very Fine Skewed
	KURTOSIS:	Leptokurtic	Very Leptokurtic	Very Leptokurtic	Leptokurtic	Very Leptokurtic
	MODE 1 (μm):	19200.0	19200.0	38250.0	19200.0	19200.0
	MODE 2 (μm):	605.0	427.5		427.5	38250.0
	MODE 3 (μm):	275.0			275.0	327.5
	MODE 1 (φ):	-4.243	-4.243	-5.235	-4.243	-4.243
	MODE 2 (φ):	0.747	1.247		1.247	-5.235
	MODE 3 (φ):	1.868			1.868	1.616
	D ₁₀ (μm):	459.0	563.6	196.6	468.1	449.8
	D ₅₀ (μm):	12543.5	15404.7	19345.0	12661.7	13834.3
	D ₉₀ (μm):	29641.4	34965.8	42302.4	34233.6	38169.6
	(D ₉₀ / D ₁₀) (μm):	64.58	62.04	215.2	73.13	84.85
	(D ₉₀ - D ₁₀) (μm):	29182.4	34402.2	42105.8	33765.5	37719.7
	(D ₇₅ / D ₂₅) (μm):	4.837	3.161	3.628	5.417	3.667
	(D ₇₅ - D ₂₅) (μm):	16475.8	16702.9	22983.7	18281.3	17528.8
	D ₁₀ (φ):	-4.890	-5.128	-5.403	-5.097	-5.254
	D ₅₀ (φ):	-3.649	-3.945	-4.274	-3.662	-3.790
	D ₉₀ (φ):	1.123	0.827	2.347	1.095	1.153
	(D ₉₀ / D ₁₀) (φ):	-0.230	-0.161	-0.434	-0.215	-0.219
	(D ₉₀ - D ₁₀) (φ):	6.013	5.955	7.750	6.192	6.407
	(D ₇₅ / D ₂₅) (φ):	0.480	0.640	0.627	0.457	0.592
	(D ₇₅ - D ₂₅) (φ):	2.274	1.660	1.859	2.437	1.875

		SOM1.5	SOM1.8	SOM3.1	SOM3.2	SOM3.7
COMPOSITION	% GRAVEL:	78.7%	87.0%	83.3%	78.8%	84.8%
	% SAND:	19.8%	11.1%	9.7%	20.2%	12.9%
	% MUD:	1.5%	1.9%	7.0%	1.0%	2.3%
	% V COARSE GRAVEL:	7.3%	12.0%	24.6%	12.2%	16.1%
	% COARSE GRAVEL:	31.7%	36.5%	34.7%	28.8%	28.0%
	% MEDIUM GRAVEL:	27.7%	25.9%	17.6%	24.4%	27.2%
	% FINE GRAVEL:	8.8%	9.8%	4.7%	10.0%	10.4%
	% V FINE GRAVEL:	3.0%	2.8%	1.9%	3.4%	3.1%
	% V COARSE SAND:	2.5%	1.1%	1.6%	1.9%	1.5%
	% COARSE SAND:	7.7%	2.5%	1.9%	8.1%	2.9%
	% MEDIUM SAND:	7.3%	5.5%	2.1%	9.0%	5.6%
	% FINE SAND:	2.0%	1.3%	2.6%	0.9%	2.5%
	% V FINE SAND:	0.3%	0.8%	1.5%	0.2%	0.4%
	% V COARSE SILT:	0.2%	0.3%	1.0%	0.1%	0.2%
	% COARSE SILT:	0.2%	0.2%	1.3%	0.1%	0.4%
	% MEDIUM SILT:	0.3%	0.3%	1.2%	0.2%	0.4%
	% FINE SILT:	0.3%	0.4%	1.2%	0.2%	0.5%
	% V FINE SILT:	0.2%	0.3%	1.0%	0.2%	0.4%
% CLAY:	0.2%	0.4%	1.2%	0.2%	0.4%	

Appendix 28 Image-based automated grain-sizing at Somerley

For each sedimentary layer identified at Somerley several locations were selected to photograph for image-based automated grainsizing (Figure A28.1). The images used for the IBAG analysis and the resulting grain size distributions are presented in Figure A28.2 and Figure A28.3. The IBAG results of the three photographs show similar grain size distributions with the majority of the grains falling between 8-0.5mm (-3 and 0.5ϕ) and below 0.35mm. The latter is a result of the detection limit constrained by the number of pixels per millimetre. A comparison of the results from each photograph is presented in Figure A28.4. This again shows the similarity between the obtained grain size distributions.

The IBAG results are compared with the sieving data in Figure A28.5-1.62.. The IBAG data shows an offset compared to the sieving results, underrepresenting the larger size fractions (medium to coarse gravel) and over representing the fine gravel to coarse sand fraction

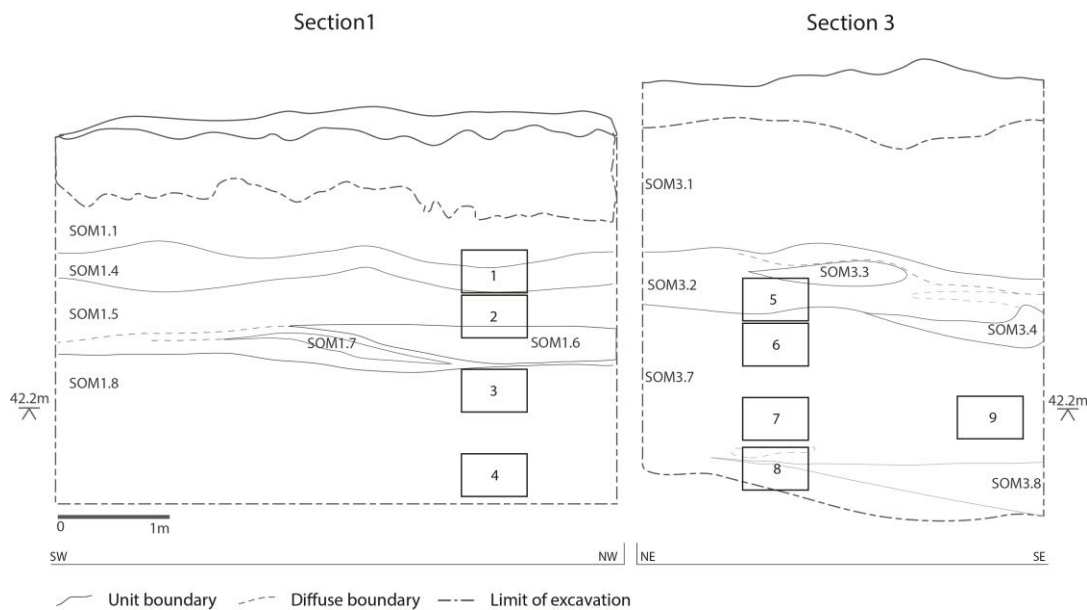
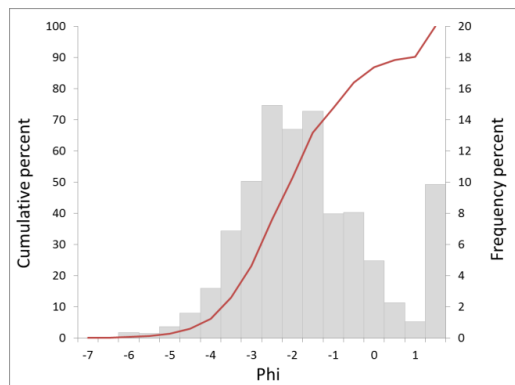
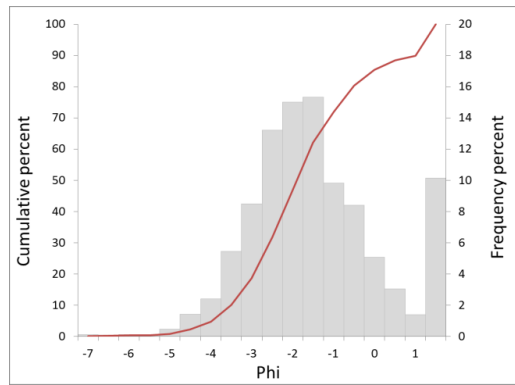
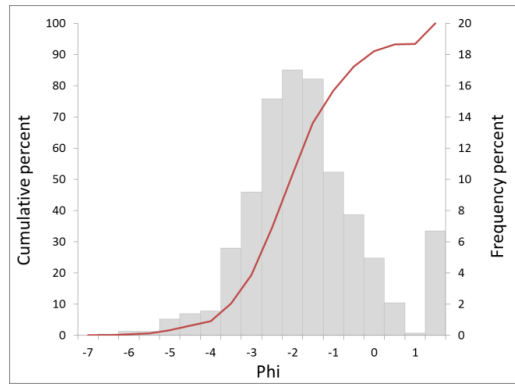
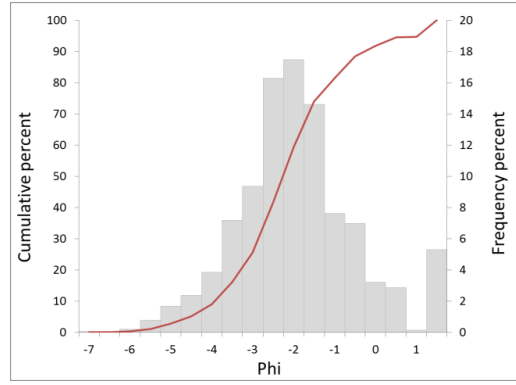


Figure A28.1 Two sections in terrace 6 in Somerley pit showing photograph locations for image-based automated grainsizing and the main stratigraphic units.



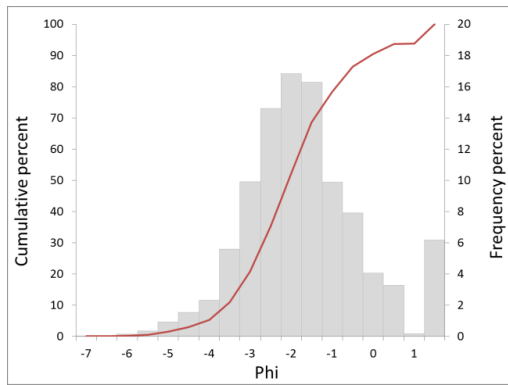
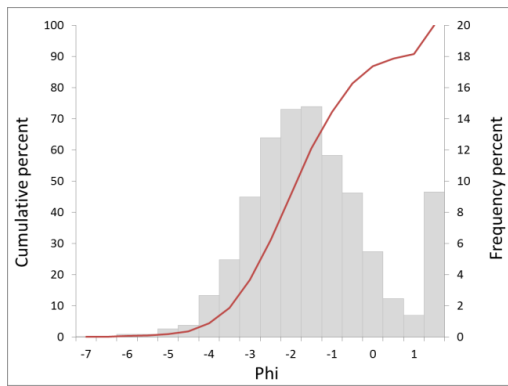
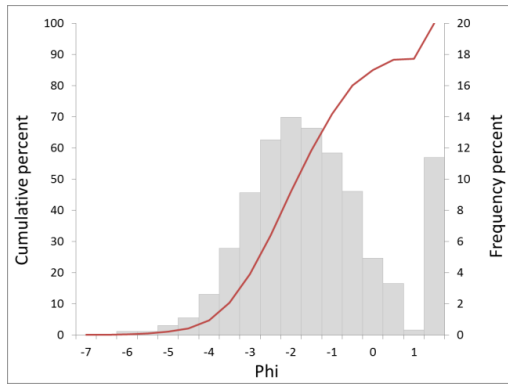


Figure A28.2 Photographs and the resulting grain size distributions of frames 1-4 (previous page) and 3-7 (this page) at Somerley pit.

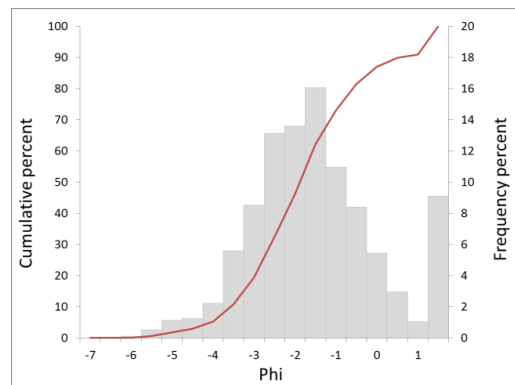
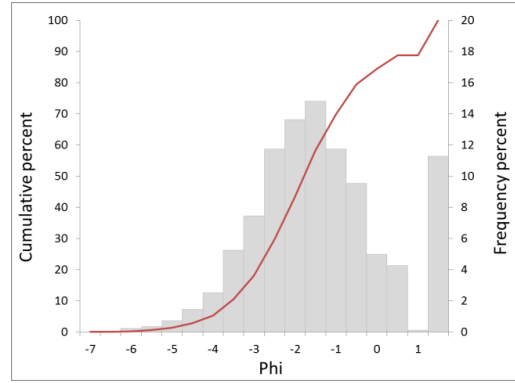


Figure A28.3 Photographs and the resulting grain size distributions of frame 8 and 9 at Somerley pit.

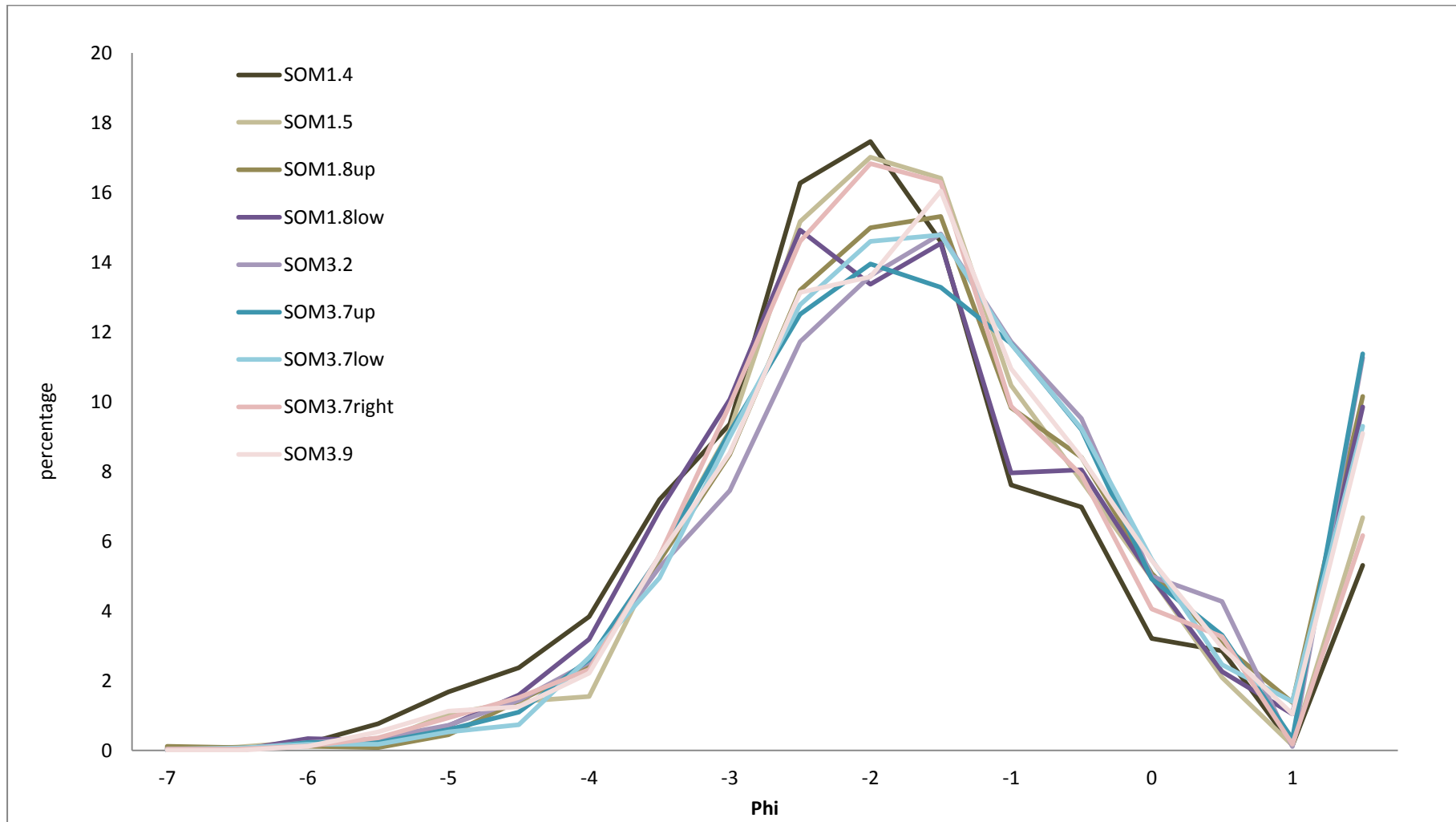


Figure A28.4 Comparison of percentage frequencies obtained from IBAG from both sections at Somerley pit.

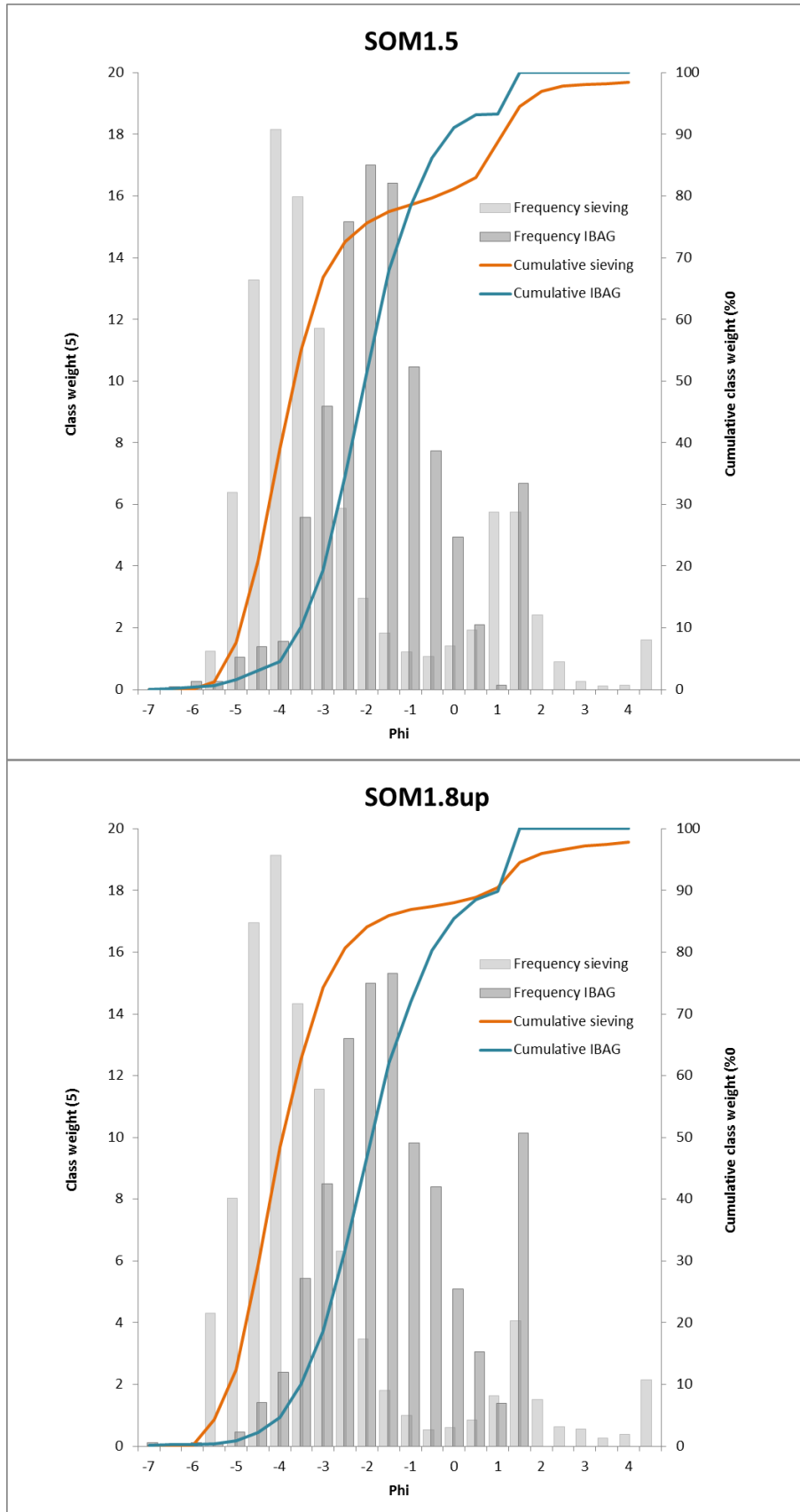


Figure A28.5 Comparison of sieving and IBAG results from SOM1.5 and frame 2 and SOM1.8up and frame 3.

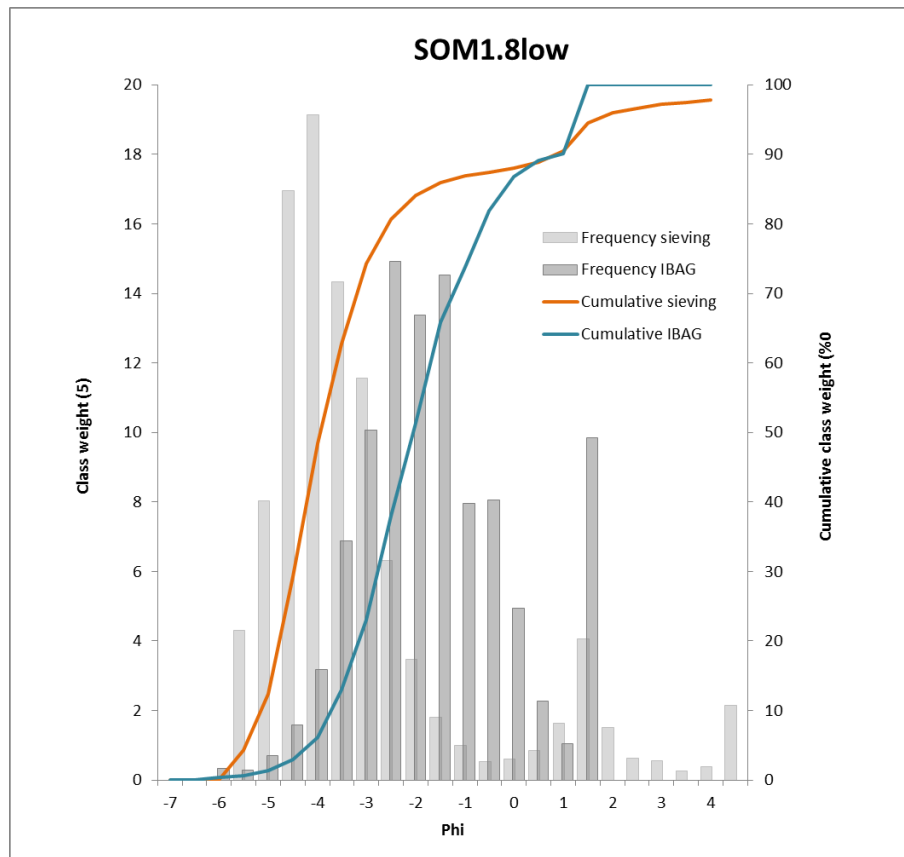


Figure A28.6 Comparison of sieving and IBAG results from SOM1.8low and frame 4.

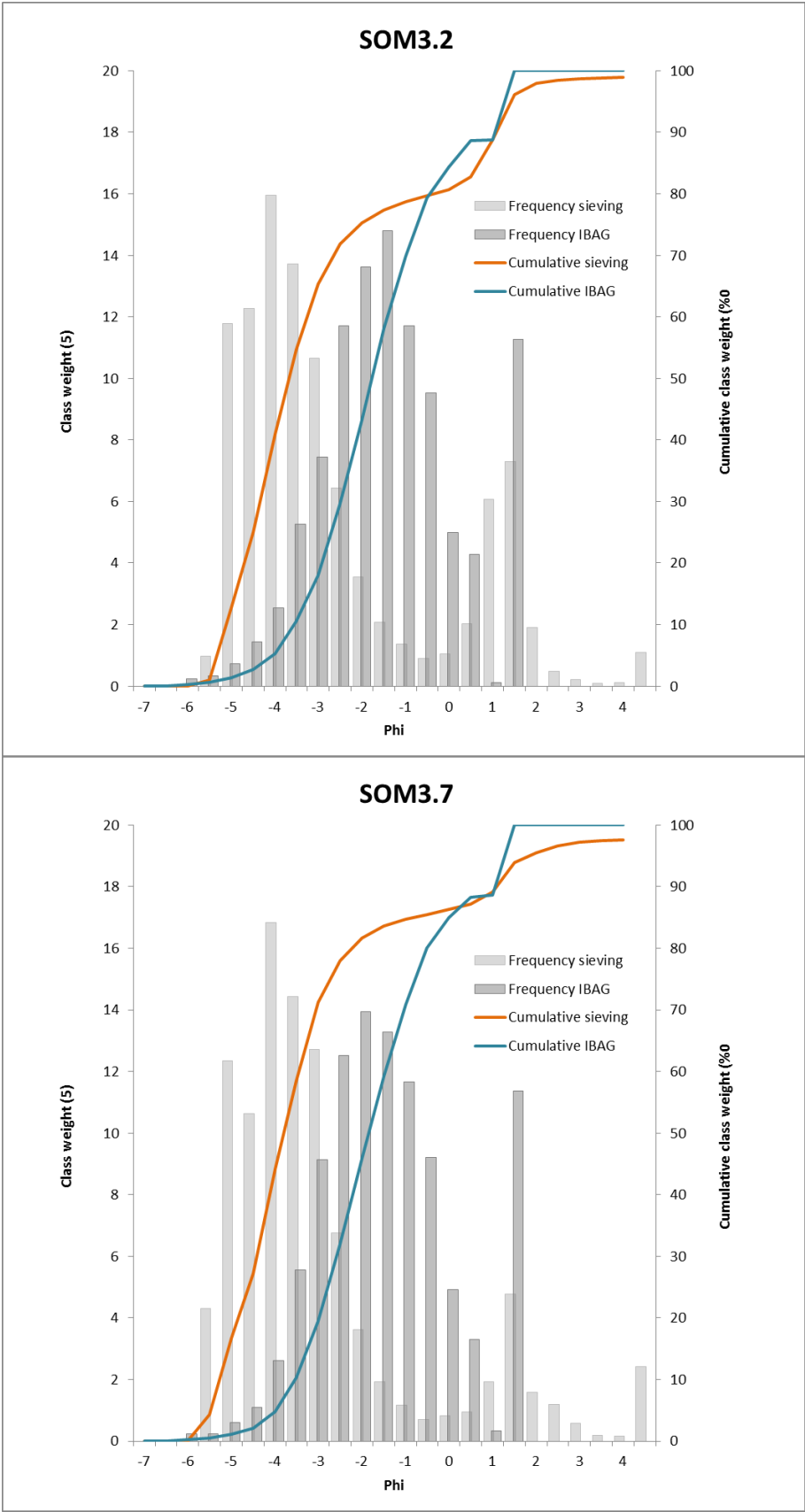


Figure A28.7 Comparison of sieving and IBAG results from SOM3.2 and frame 5 and SOM3.7 and frame 9.

Appendix 29 Ashely clast size distributions

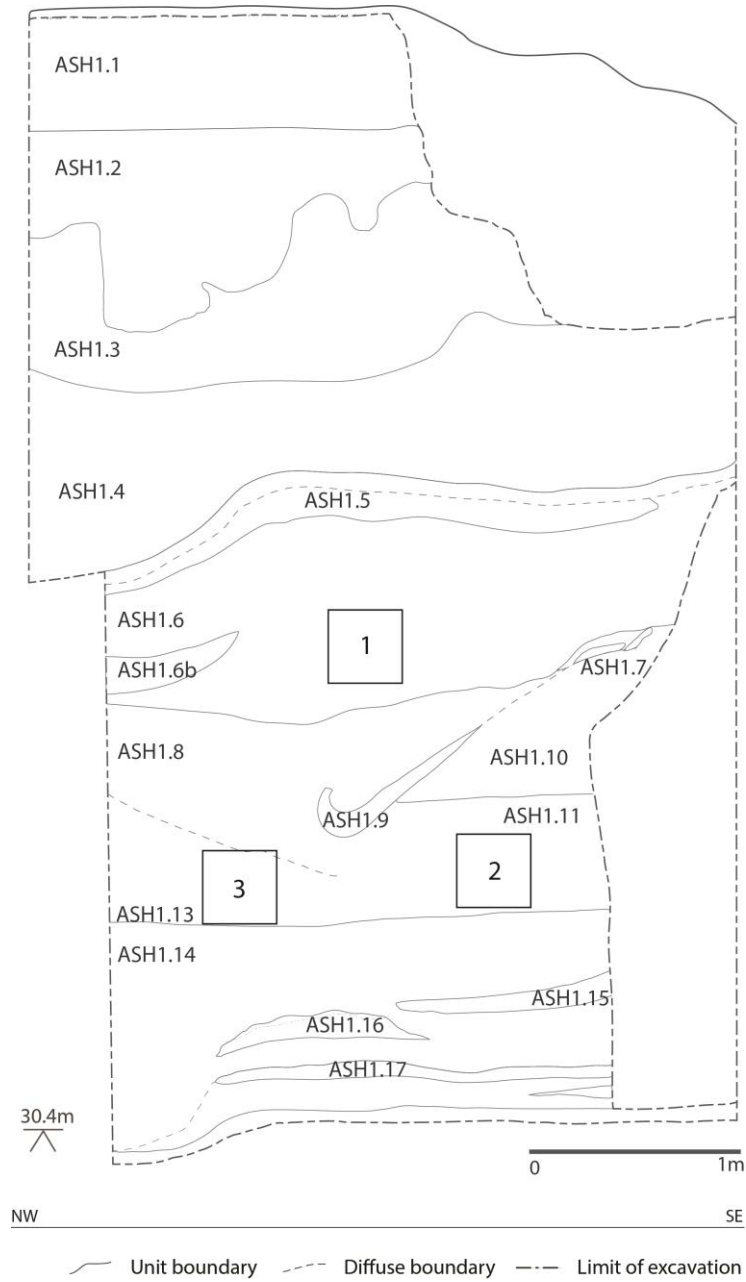


Figure A29.1 Section in terrace 5 at Ashley Pit showing gravel sample locations and the main stratigraphic units. 1= ASH1.6; 2=ASH1.11; 3=ASH1.13.

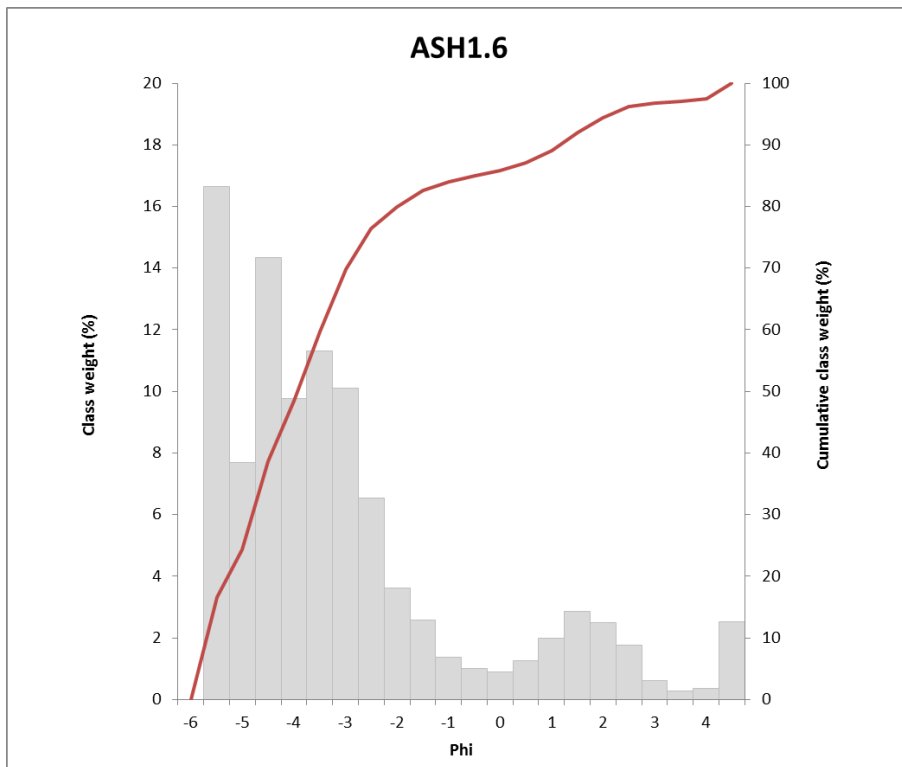


Figure A29.2 Percentage frequency and cumulative percentage frequency of sediment fractions present in sample ASH1.6.

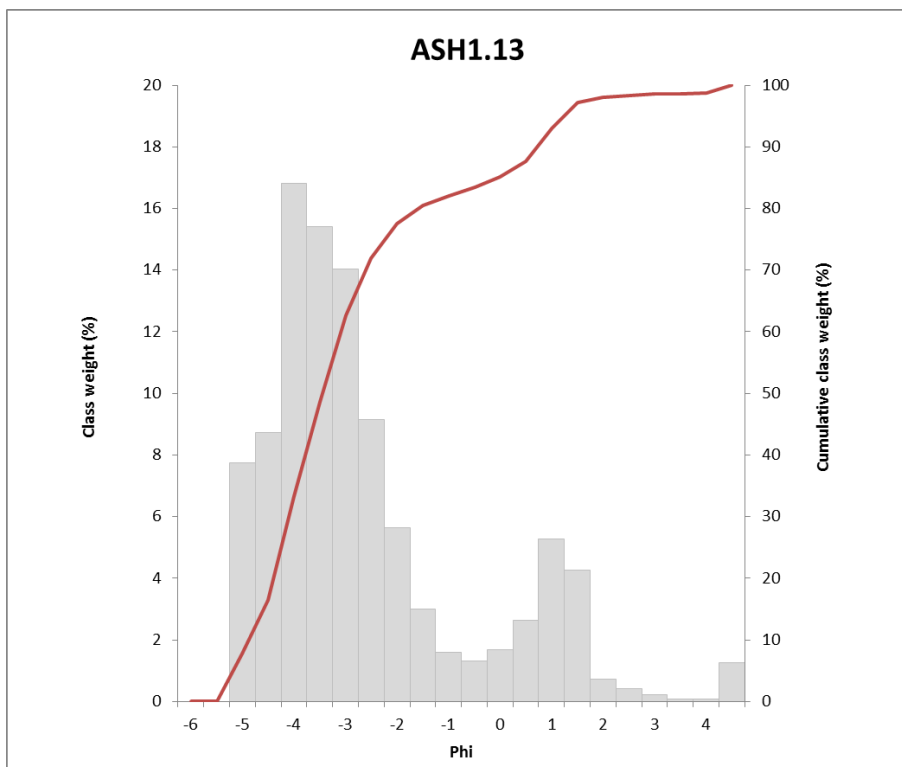
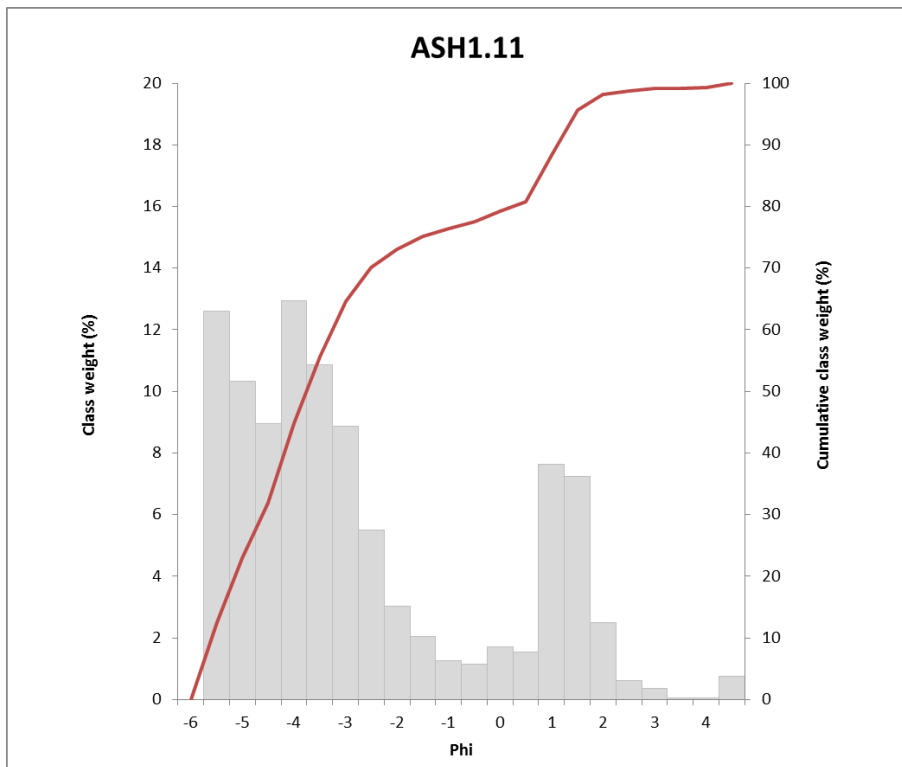


Figure A29.3 Percentage frequency and cumulative percentage frequency of sediment fractions present in sample ASH1.11 (top) and ASH1.13 (bottom).

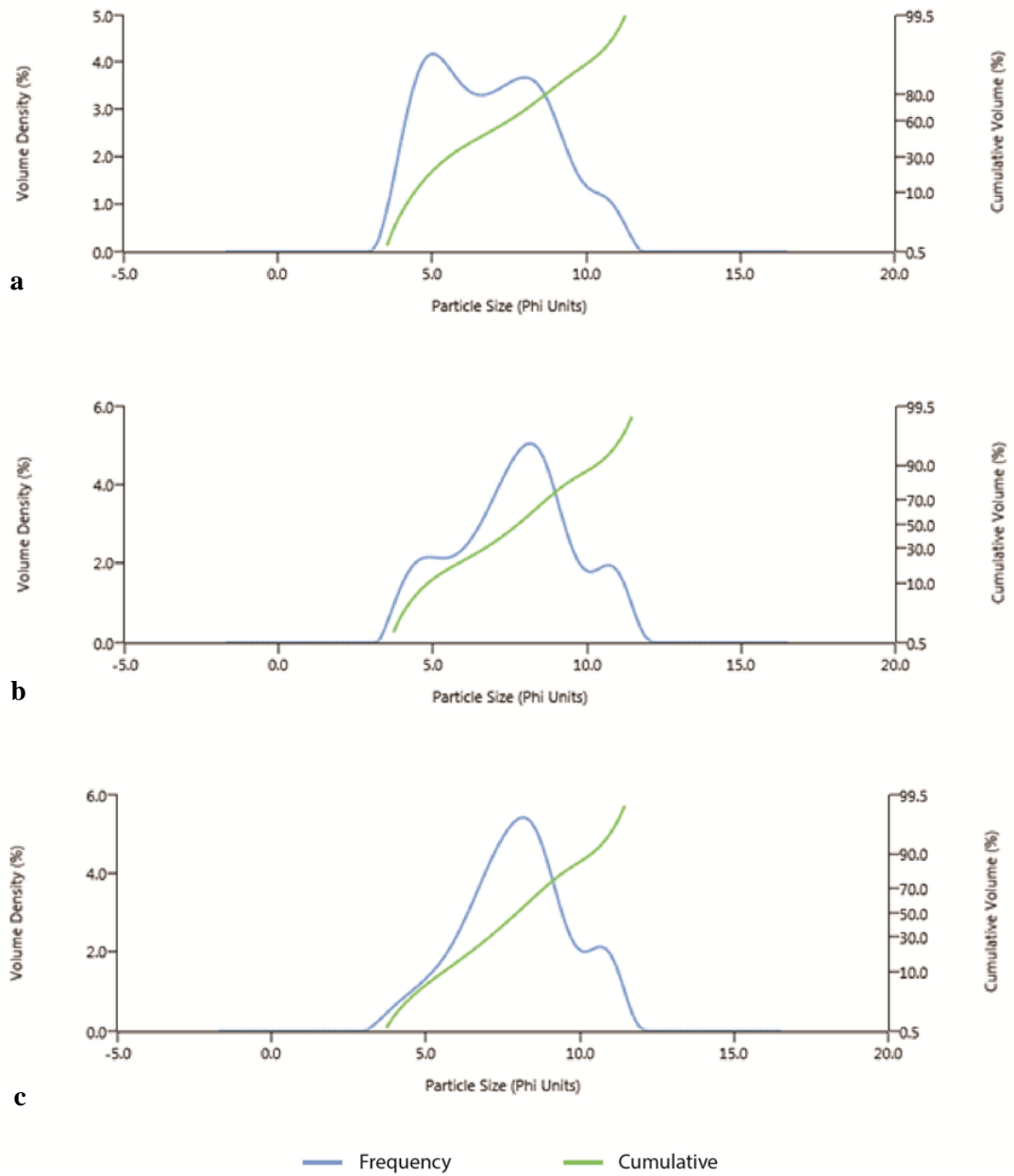


Figure A29.4 Particle size distribution of the <math><63\mu\text{m}</math> fraction of ASH1.6 (a), ASH1.11 (b) and ASH1.13 (c).

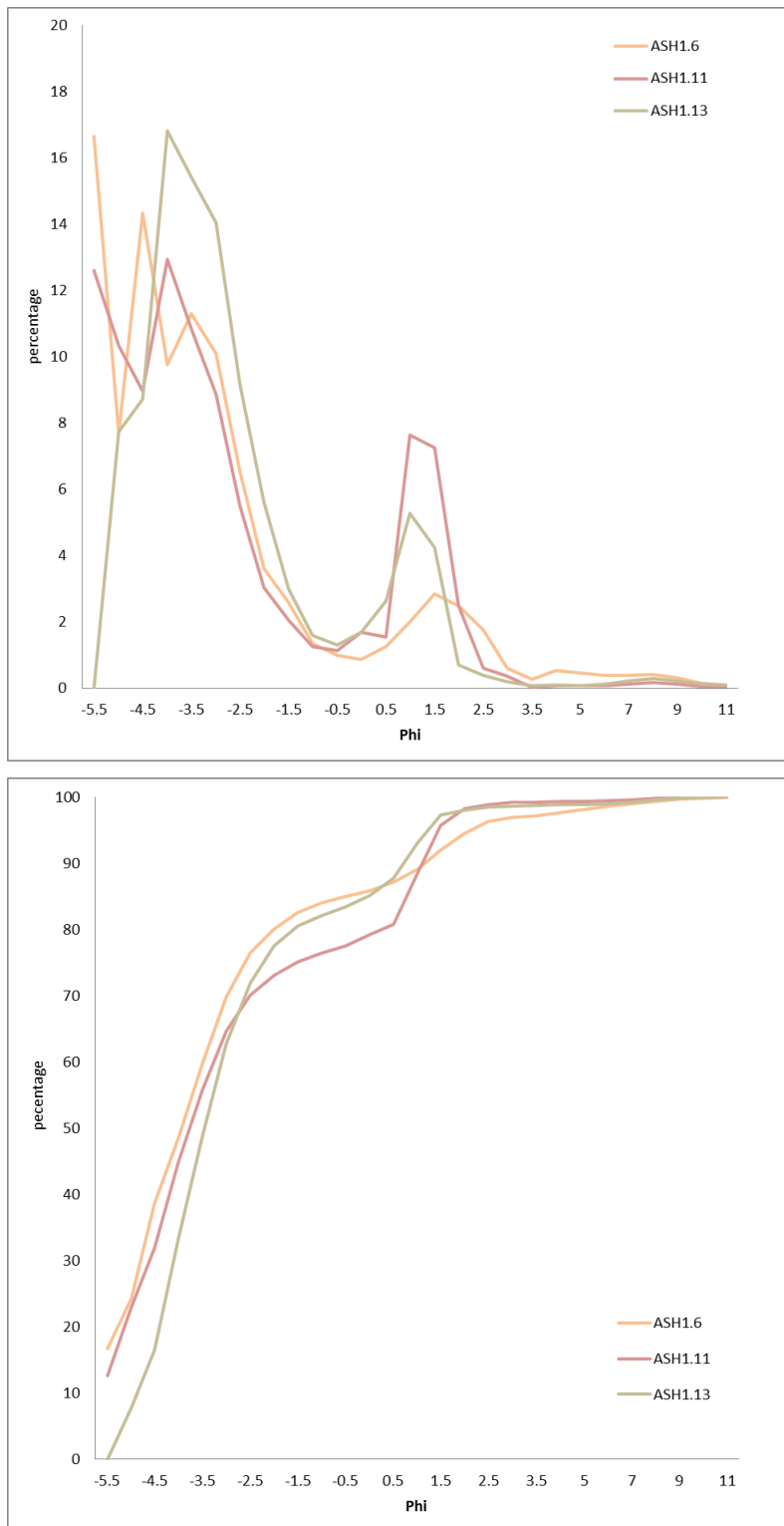


Figure A29.5 Comparison of the integrated particle size distribution curves of the three gravel samples from Ashley Pit showing weight in percentages of each size fraction (top) and the cumulative percentage of the weight in percentages (bottom).

Appendix 30 Ashley clast size distribution statistics

		ASH1.6	ASH1.11	ASH1.13
SAMPLE TYPE:		Polymodal, Very Poorly Sorted	Polymodal, Very Poorly Sorted	Bimodal, Very Poorly Sorted
TEXTURAL GROUP:		Gravel	Sandy Gravel	Gravel
SEDIMENT NAME:		Coarse Gravel	Sandy Very Coarse Gravel	Medium Gravel
METHOD OF MOMENTS Arithmetic (μm)	MEAN	21009.2	18740.0	13133.0
	SORTING	18219.8	17662.2	10656.6
	SKEWNESS	0.703	0.823	0.856
	KURTOSIS	2.217	2.473	3.061
METHOD OF MOMENTS Geometric (μm)	MEAN	9125.2	7607.7	6952.4
	SORTING	6.519	5.934	4.654
	SKEWNESS	-1.785	-1.101	-1.897
	KURTOSIS	6.524	3.924	8.241
METHOD OF MOMENTS Logarithmic (ϕ)	MEAN	-3.190	-2.927	-2.798
	SORTING	2.705	2.569	2.218
	SKEWNESS	1.785	1.101	1.897
	KURTOSIS	6.524	3.924	8.241
FOLK AND WARD METHOD (μm)	MEAN	11196.7	6919.5	6762.0
	SORTING	5.121	6.185	4.067
	SKEWNESS	-0.415	-0.466	-0.477
	KURTOSIS	1.415	0.909	1.307
FOLK AND WARD METHOD (ϕ)	MEAN	-3.485	-2.791	-2.757
	SORTING	2.356	2.629	2.024
	SKEWNESS	0.415	0.466	0.477
	KURTOSIS	1.415	0.909	1.307

		ASH1.6	ASH1.11	ASH1.13
FOLK AND WARD METHOD (Description)	MEAN:	Medium Gravel	Fine Gravel	Fine Gravel
	SORTING:	Very Poorly Sorted	Very Poorly Sorted	Very Poorly Sorted
	SKEWNESS:	Very Fine Skewed	Very Fine Skewed	Very Fine Skewed
	KURTOSIS:	Leptokurtic	Mesokurtic	Leptokurtic
	MODE 1 (μm):	54000.0	19200.0	19200.0
	MODE 2 (μm):	26950.0	54000.0	605.0
	MODE 3 (μm):	13600.0	605.0	
	MODE 1 (ϕ):	-5.735	-4.243	-4.243
	MODE 2 (ϕ):	-4.731	-5.735	0.747
	MODE 3 (ϕ):	-3.743	0.747	
	D ₁₀ (μm):	433.6	456.2	611.1
	D ₅₀ (μm):	15249.1	13505.6	10852.4
	D ₉₀ (μm):	51484.7	48227.6	28833.3
	(D ₉₀ / D ₁₀) (μm):	118.7	105.7	47.18
	(D ₉₀ - D ₁₀) (μm):	51051.1	47771.5	28222.2
	(D ₇₅ / D ₂₅) (μm):	5.115	10.12	4.060
	(D ₇₅ - D ₂₅) (μm):	24956.6	26233.4	14228.3
	D ₁₀ (ϕ):	-5.686	-5.592	-4.850
	D ₅₀ (ϕ):	-3.931	-3.755	-3.440
	D ₉₀ (ϕ):	1.206	1.132	0.710
	(D ₉₀ / D ₁₀) (ϕ):	-0.212	-0.203	-0.147
	(D ₉₀ - D ₁₀) (ϕ):	6.892	6.724	5.560
	(D ₇₅ / D ₂₅) (ϕ):	0.525	0.313	0.523
	(D ₇₅ - D ₂₅) (ϕ):	2.355	3.339	2.021

		ASH1.6	ASH1.11	ASH1.13
COMPOSITION	% GRAVEL:	84.0%	76.4%	82.1%
	% SAND:	13.7%	22.9%	16.7%
	% MUD:	2.2%	0.7%	1.2%
	% V COARSE GRAVEL:	24.0%	22.5%	7.4%
	% COARSE GRAVEL:	24.5%	22.4%	25.9%
	% MEDIUM GRAVEL:	21.4%	19.7%	29.5%
	% FINE GRAVEL:	10.2%	8.5%	14.8%
	% V FINE GRAVEL:	4.0%	3.3%	4.6%
	% V COARSE SAND:	1.9%	2.8%	3.0%
	% COARSE SAND:	3.3%	9.2%	7.9%
	% MEDIUM SAND:	4.0%	9.1%	4.7%
	% FINE SAND:	3.7%	1.6%	0.9%
	% V FINE SAND:	0.8%	0.1%	0.2%
	% V COARSE SILT:	0.5%	0.1%	0.1%
	% COARSE SILT:	0.4%	0.1%	0.1%
	% MEDIUM SILT:	0.4%	0.1%	0.2%
	% FINE SILT:	0.4%	0.2%	0.3%
	% V FINE SILT:	0.3%	0.1%	0.2%
% CLAY:	0.3%	0.1%	0.2%	

Appendix 31 Image-based automated grain-sizing at Ashley

At Ashley pit four locations were selected for to photograph for image-based automated grainsizing (Figure A31.1). The images used for the IBAG analysis and the resulting grain size distributions are presented in Figure A31.2. The IBAG results of the four photographs show similar grain size distributions with the majority of the grains falling between 8-0.5mm (-3 and 0.5ϕ) and below 0.35mm. The latter fraction is largest in frame 4 (ASH1.14) this could reflect the detection of the sand layer in the photograph. A comparison of the results from each photograph is presented in Figure A31.3. This again shows the similarity between the obtained grain size distributions. ASH1.6 shows a higher percentage of 0.5mm grains and no >0.35 mm sediments have been detected.

The IBAG results are compared with the sieving data in Figure A31.4 and Figure A31.5. The IBAG data shows an offset compared to the sieving results, underrepresenting the larger size fractions (medium to coarse gravel) and over representing the fine gravel to coarse sand fraction. The medium sand fraction retained from the sieving data coincides with higher percentages of medium sand detected by using the IBAG method. As this is a bin category for all the particles below the detection limit, this similarity should be used with caution.

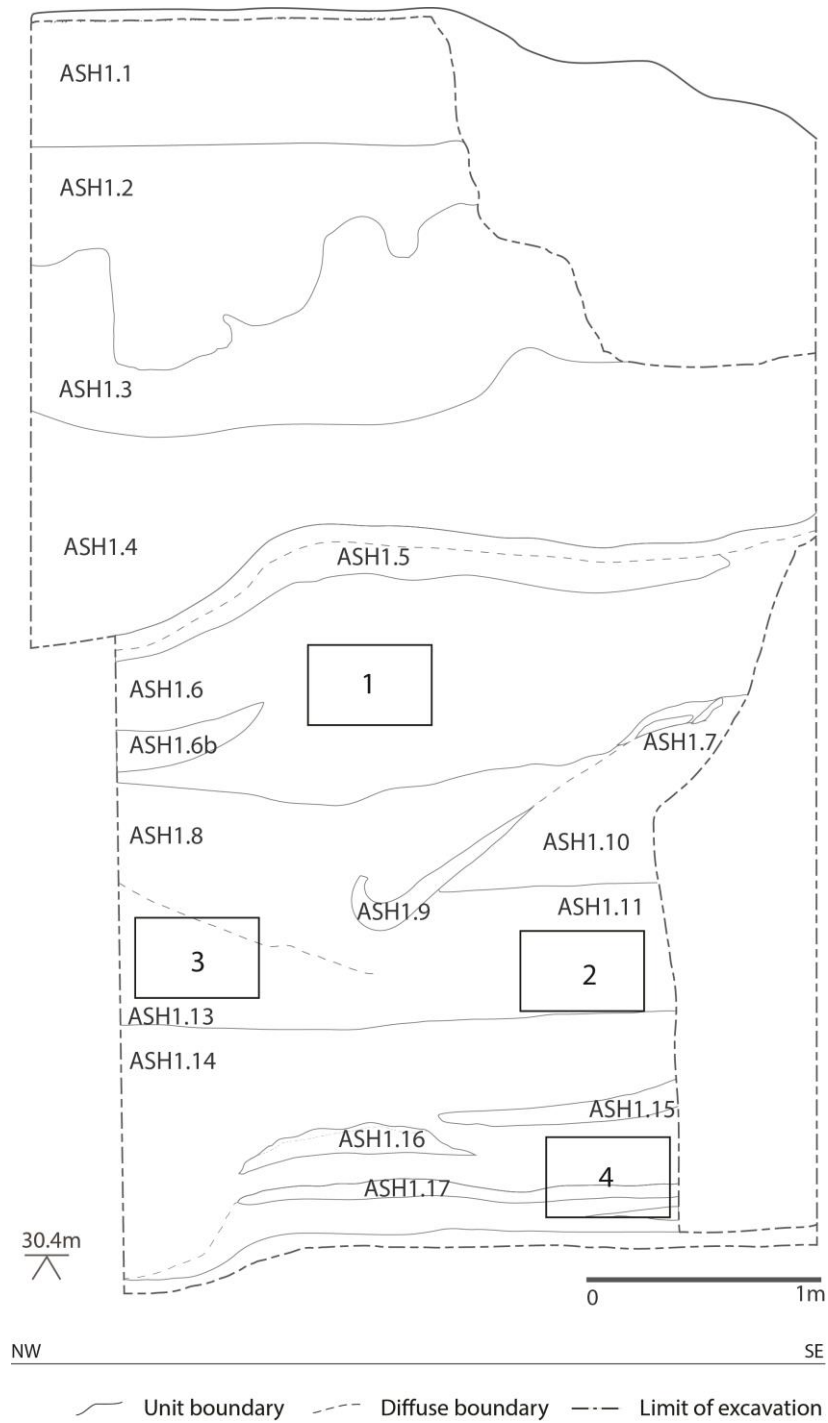


Figure A31.1 Section drawing of terrace 5 at Ashley Pit showing photograph locations for image-based automated grainsizing and the main stratigraphic units.

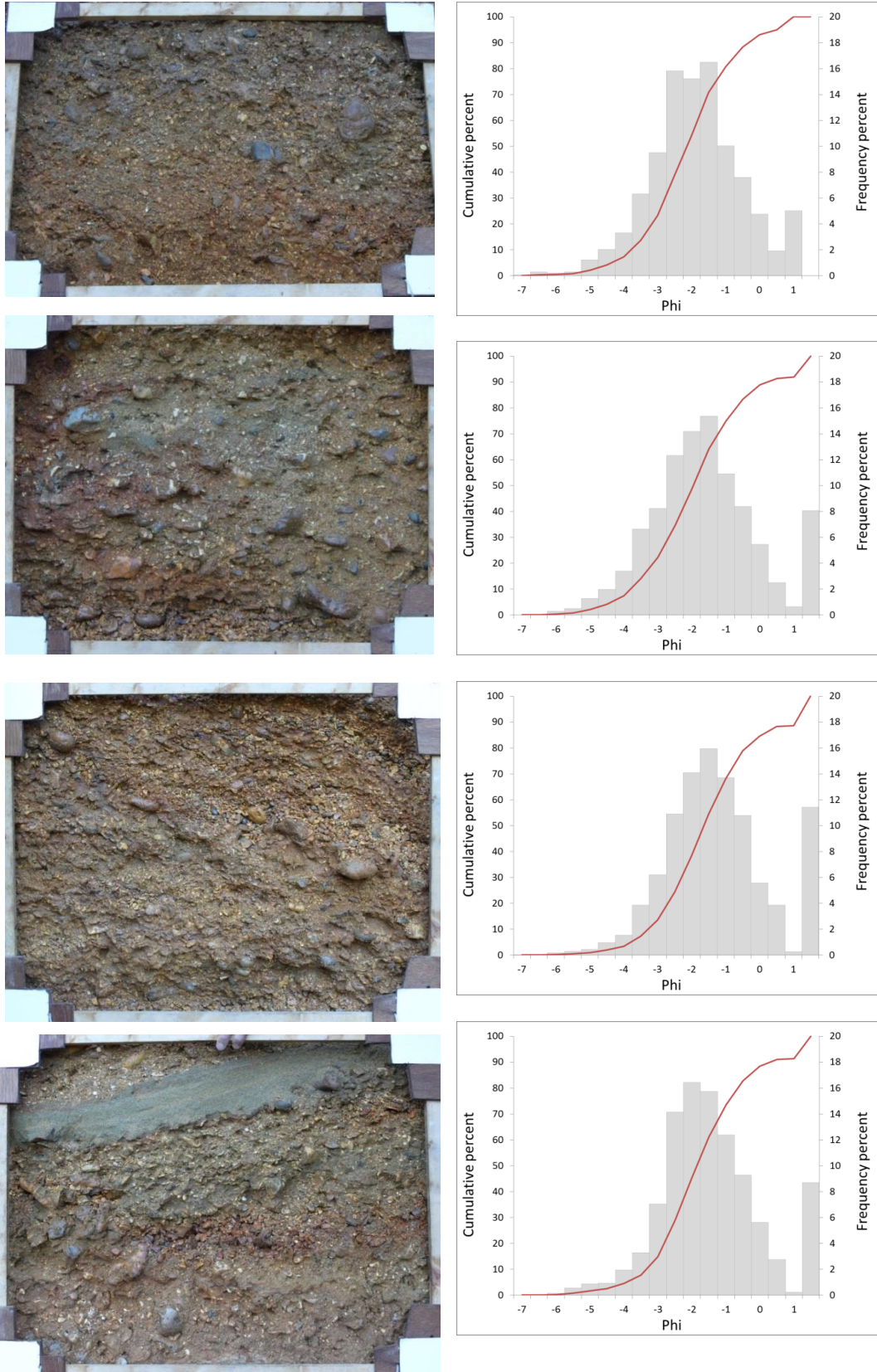


Figure A31.2 Photographs and the resulting grain size distributions of frames 1-3 at Ashley pit.

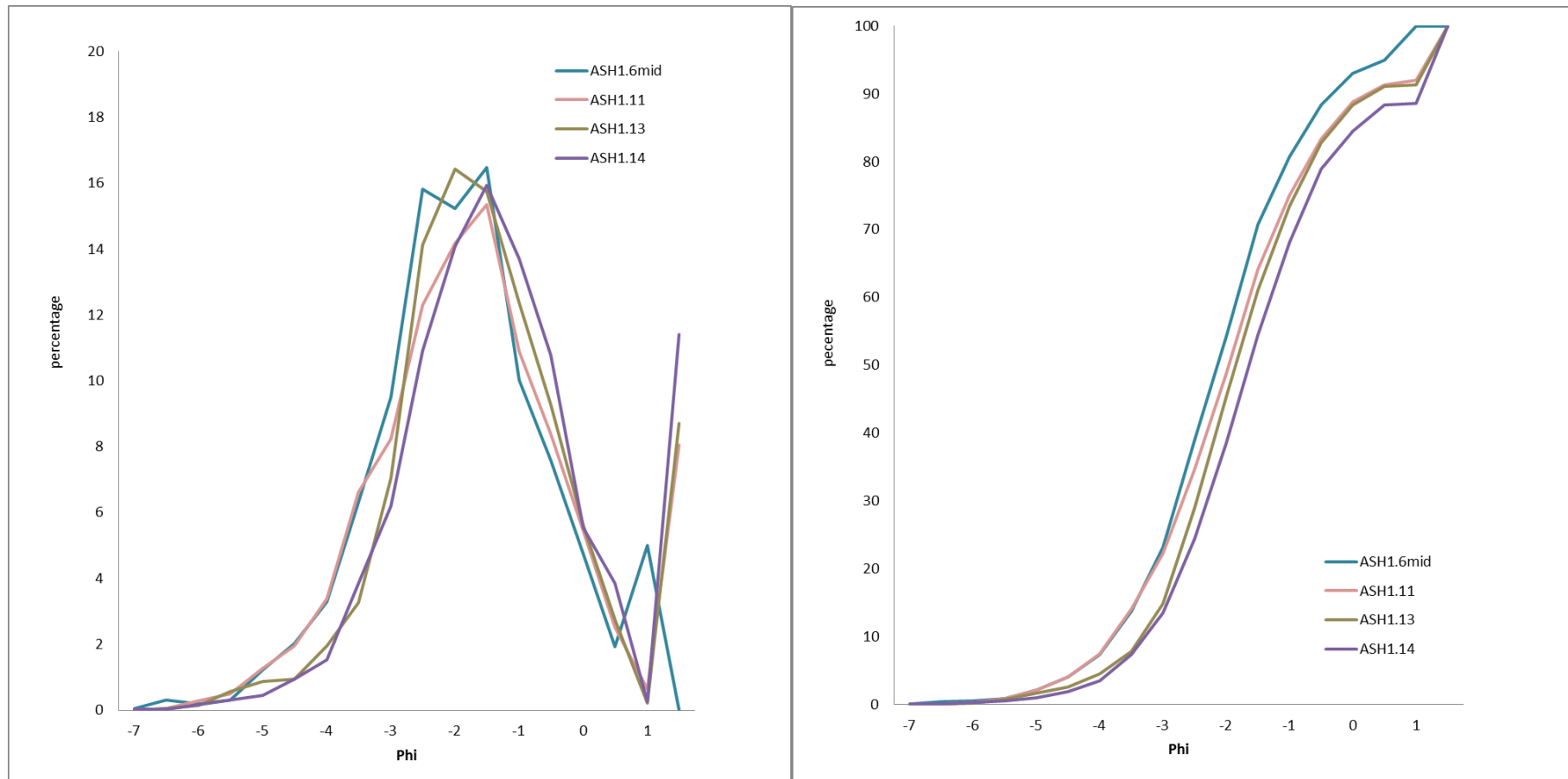


Figure A31.3 Comparison of percentage frequency (left) and cumulative percentage frequency (right) of the grain size distributions of ASH1.6, ASH1.11 and ASH1.13 obtained from image-based automated grainsizing.

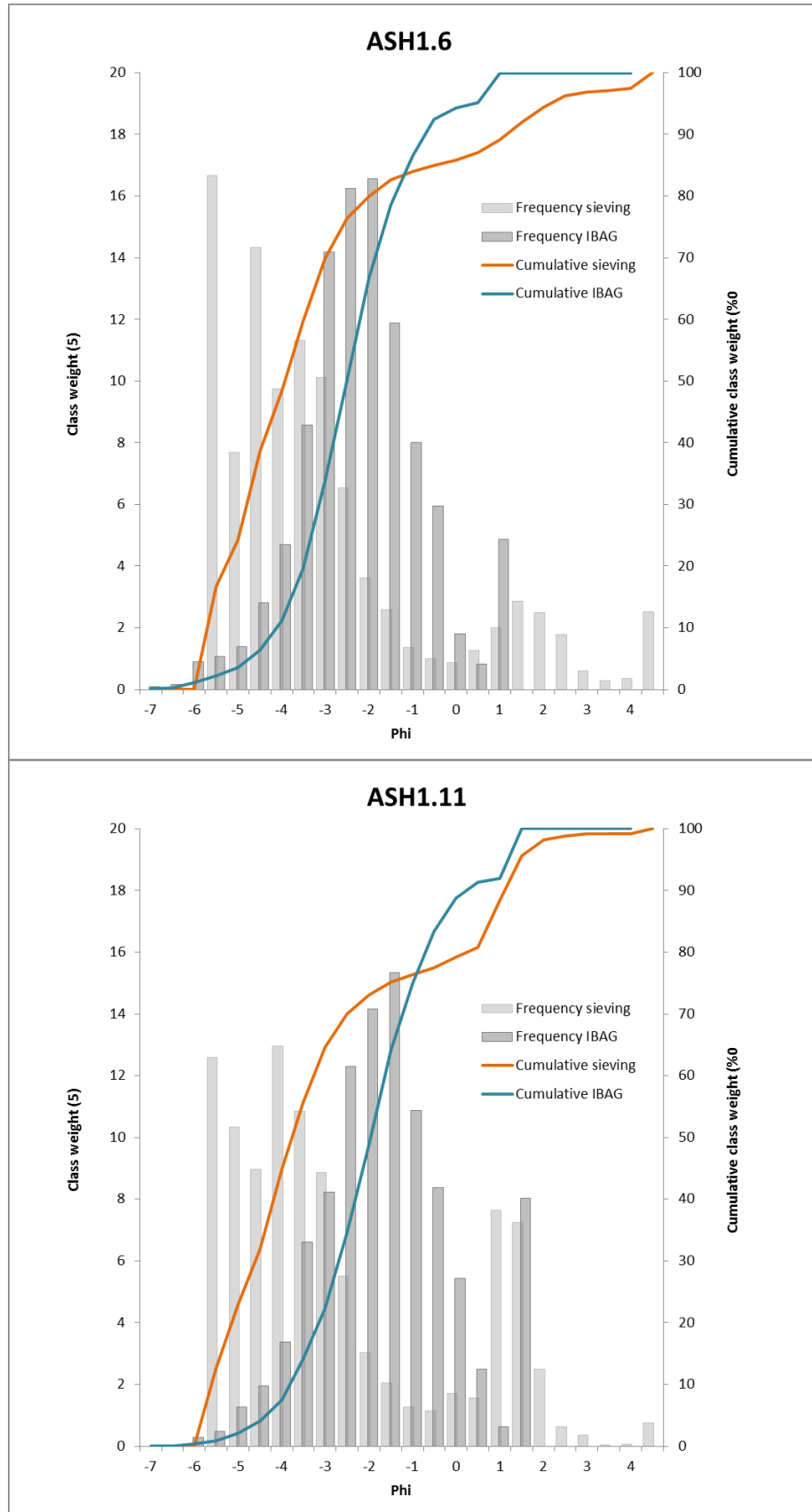


Figure A31.4 Comparison of sieving and IBAG results from ASH1.6 and frame 1 and ASH1.11 and frame 2.

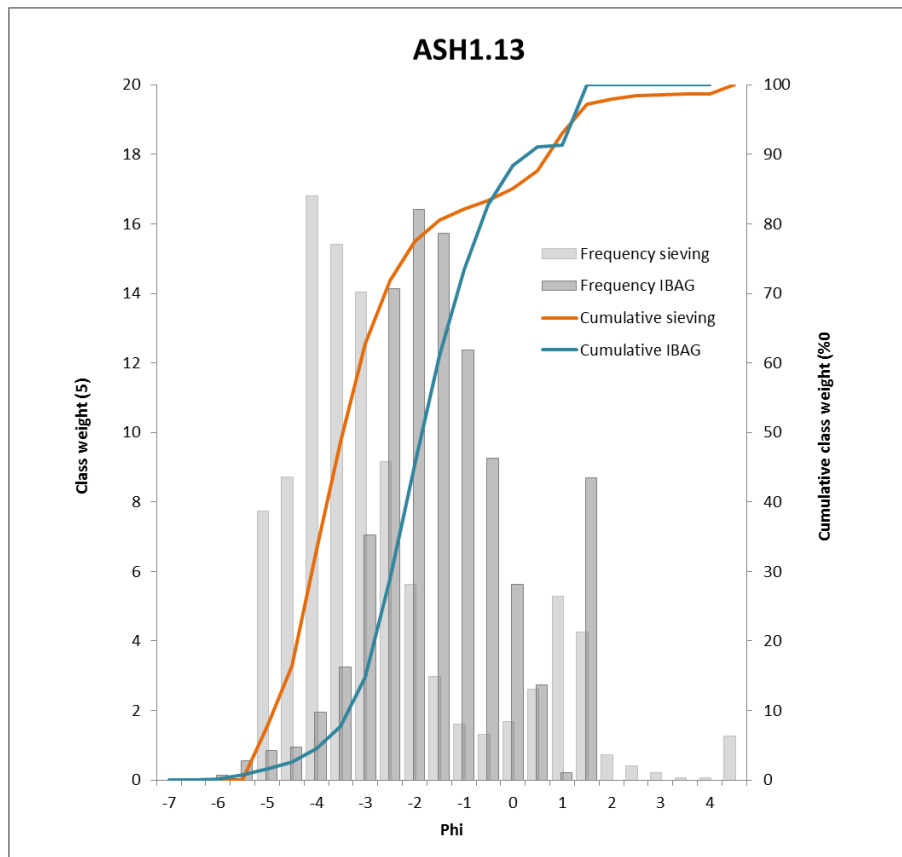


Figure A31.5 Comparison of sieving and IBAG results from ASH1.13 and frame 3.

Appendix 32 Clast lithology of all size fractions

Sample	Size fraction	Nodular flint	Broken flint	Weathered flint	Tertiary flint	Broken Tertiary flint	Sandstone	Chert	Quartz	Grey chert	Limestone	Ironstone	Count
BEM2.4a	>45mm	-	16.7	25.0	-	-	-	-	-	-	-	-	12
	31.5-45mm	27.6	44.8	24.1	-	-	3.4	-	-	-	-	-	29
	22.4-31.5mm	37.9	24.1	28.7	-	-	8.0	1.1	-	-	-	-	87
	16-22.4mm	21.0	24.0	42.7	-	-	10.3	1.9	-	-	-	-	262
	11.2-16mm	12.4	27.4	49.4	-	-	9.7	0.8	0.4	-	-	-	259
BEM2.4b	8-11.2mm	33.8	-	56.3	0.6	1.1	8.0	-	0.2	-	-	-	465
	>45mm	63.6	9.1	27.3	-	-	-	-	-	-	-	-	11
	31.5-45mm	52.2	8.7	30.4	-	-	8.7	-	-	-	-	-	23
	22.4-31.5mm	36.8	18.4	30.3	-	-	13.2	1.3	-	-	-	-	76
	16-22.4mm	7.9	12.6	68.8	-	-	8.7	2.0	-	-	-	-	253
HA1.1	11.2-16mm	18.9	21.9	48.4	-	-	9.8	-	-	-	0.8	-	366
	8-11.2mm	2.5	9.2	80.5	0.2	-	6.7	-	-	-	0.4	0.4	476
	>45mm	40.0	40.0	20.0	-	-	-	-	-	-	-	-	5
	31.5-45mm	42.3	34.6	19.2	-	3.8	-	-	-	-	-	-	26
	22.4-31.5mm	24.1	42.6	27.8	-	3.7	-	1.9	-	-	-	-	54
HA1.3	16-22.4mm	14.2	34.3	45.1	1.9	1.1	3.4	-	-	-	-	-	268
	11.2-16mm	13.3	22.0	58.8	1.2	2.0	2.0	0.6	-	-	-	-	490
	8-11.2mm	9.6	24.8	60.1	0.9	2.0	0.7	0.9	0.9	-	-	-	541
	>45mm	40.0	-	40.0	20.0	-	-	-	-	-	-	-	5
	31.5-45mm	8.7	26.1	60.9	-	-	-	4.3	-	-	-	-	23
HB1.2	22.4-31.5mm	6.2	6.2	72.3	-	3.1	9.2	3.1	-	-	-	-	65
	16-22.4mm	2.8	12.6	76.4	2.4	0.4	4.9	0.4	-	-	-	-	246
	11.2-16mm	2.8	14.8	76.0	1.4	1.4	2.5	1.1	-	-	-	-	283
	8-11.2mm	1.7	9.9	80.8	1.7	0.8	4.2	0.3	0.6	-	-	-	354
	>45mm	-	-	-	-	-	-	-	-	-	-	-	-
HB1.8	31.5-45mm	-	-	-	-	-	-	-	-	-	-	-	-
	22.4-31.5mm	34.8	13.6	42.4	-	3.0	4.5	1.5	-	-	-	-	66
	16-22.4mm	13.9	15.6	65.0	0.3	0.3	4.4	0.3	-	-	-	-	294
	11.2-16mm	1.5	10.5	83.9	0.6	0.3	2.9	0.3	-	-	-	-	342
	8-11.2mm	8.0	9.1	77.4	1.2	1.8	1.8	-	-	-	-	0.8	514
HB1.8	>45mm	33.3	-	66.7	-	-	-	-	-	-	-	-	6
	31.5-45mm	23.8	14.3	52.4	4.8	4.8	-	-	-	-	-	-	21
	22.4-31.5mm	12.4	11.2	66.3	2.2	3.4	3.4	1.1	-	-	-	-	89
	16-22.4mm	10.8	11.2	64.6	5.4	2.3	5.4	0.4	-	-	-	-	260
HB1.8	11.2-16mm	6.9	11.2	75.7	1.0	2.2	1.7	1.0	0.2	-	-	-	403
	8-11.2mm	5.8	10.2	75.9	2.0	1.7	3.8	0.3	0.3	-	-	-	344

Table A32.1 Clast size lithology of all size fractions (cont. below).

Sample	Size fraction	Nodular flint	Broken flint	Weathered flint	Tertiary flint	Broken Tertiary flint	Sandstone	Chert	Quartz	Grey chert	Limestone	Ironstone	Count
WG2.3b	>45mm	50.0	33.3	16.7	-	-	-	-	-	-	-	-	18
	31.5-45mm	45.5	36.4	4.5	-	-	9.1	4.5	-	-	-	-	22
	22.4-31.5mm	28.8	38.5	28.8	1.9	-	1.9	-	-	-	-	-	52
	16-22.4mm	16.2	36.5	43.1	1.2	1.2	1.2	0.6	-	-	-	-	167
	11.2-16mm	6.4	21.0	69.1	0.6	0.6	2.2	-	-	-	-	-	314
WG1.11	8-11.2mm	3.1	15.2	77.4	0.9	1.2	1.9	-	0.3	-	-	-	323
	>45mm	50.0	37.5	12.5	-	-	-	-	-	-	-	-	8
	31.5-45mm	32.6	51.2	16.3	-	-	-	-	-	-	-	-	43
	22.4-31.5mm	20.3	65.0	8.4	2.8	0.7	2.8	-	-	-	-	-	143
	16-22.4mm	11.5	80.3	4.0	1.0	1.0	2.2	-	-	-	-	-	401
SOM1.1	11.2-16mm	1.6	71.3	19.8	1.2	1.2	4.5	0.4	-	-	-	-	247
	8-11.2mm	3.3	88.5	3.7	1.6	1.2	1.6	-	-	-	-	-	485
	>45mm	100	-	-	-	-	-	-	-	-	-	-	1
	31.5-45mm	33.3	22.2	44.4	-	-	-	-	-	-	-	-	9
	22.4-31.5mm	22.6	22.6	41.5	5.7	3.8	1.9	1.9	-	-	-	-	53
SOM1.5	16-22.4mm	13.2	11.7	65.4	3.4	2.9	2.9	0.5	-	-	-	-	205
	11.2-16mm	5.8	10.5	76.4	-	2.0	1.4	3.4	0.4	0.2	-	-	504
	8-11.2mm	9.2	14.2	70.2	0.7	3.1	1.8	0.2	0.2	-	0.4	-	457
	>45mm	-	50.0	50.0	-	-	-	-	-	-	-	-	4
	31.5-45mm	31.3	31.3	31.3	-	6.3	-	-	-	-	-	-	16
SOM1.5	22.4-31.5mm	24.2	28.4	34.7	4.2	5.3	2.1	1.1	-	-	-	-	95
	16-22.4mm	28.0	41.3	22.0	3.5	1.4	1.7	0.7	-	0.3	1.0	-	286
	11.2-16mm	12.8	22.6	57.3	1.8	2.4	2.4	-	-	-	0.9	-	337
SOM1.5	8-11.2mm	16.6	16.4	60.1	2.2	2.7	1.7	0.2	-	-	-	-	409

Sample	Size fraction	Nodular flint	Broken flint	Weathered flint	Tertiary flint	Broken Tertiary flint	Sandstone	Chert	Quartz	Grey chert	Limestone	Ironstone	Count
ASH1.6	>45mm	16.7	-	83.3	-	-	-	-	-	-	-	-	6
	31.5-45mm	20.0	20.0	50.0	10.0	-	-	-	-	-	-	-	10
	22.4-31.5mm	17.6	35.3	33.8	4.4	2.9	4.4	1.5	-	-	-	-	68
	16-22.4mm	13.9	34.4	44.4	2.6	2.6	2.0	-	-	-	-	-	151
	11.2-16mm	15.1	19.5	60.1	2.2	1.1	1.1	0.4	0.2	-	0.2	-	456
ASH1.11	8-11.2mm	6.4	12.5	73.4	2.6	1.9	1.9	0.6	0.3	-	0.3	-	312
	>45mm	66.7	16.7	16.7	-	-	-	-	-	-	-	-	12
	31.5-45mm	36.8	15.8	44.7	-	-	2.6	-	-	-	-	-	38
	22.4-31.5mm	26.4	37.9	26.4	4.6	2.3	-	2.3	-	-	-	-	87
	16-22.4mm	26.5	11.6	54.5	5.6	-	1.6	-	0.3	-	-	-	378
ASH1.13	11.2-16mm	26.9	18.2	49.3	1.7	1.7	2.1	-	-	-	-	-	286
	8-11.2mm	10.1	32.0	52.6	1.1	1.8	2.2	0.2	-	-	-	-	447
	>45mm	-	-	-	-	-	-	-	-	-	-	-	-
	31.5-45mm	68.4	5.3	-	-	15.8	10.5	-	-	-	-	-	19
	22.4-31.5mm	71.2	13.5	9.6	5.8	-	-	-	-	-	-	-	52
ASH1.13	16-22.4mm	33.4	30.1	28.4	3.3	2.0	2.0	0.7	-	-	-	-	299
	11.2-16mm	20.5	42.7	29.5	2.4	2.7	1.9	0.3	-	-	-	-	745
	8-11.2mm	41.9	28.8	23.8	1.3	2.1	1.6	-	0.2	-	0.2	-	944

Appendix 33 Clast angularity-roundedness

Angularity-roundedness of flint presented per sample and per size fraction as percentages of the total flint clasts.

Sample	Size fraction	Angularity					
		VA	A	SA	SR	R	WR
BEM2.4a	22.4-31.5mm	1,9	7,4	84,5	4,9	1,3	0,0
	11.2-16mm	0,0	3,5	90,0	6,1	0,4	0,0
BEM2.4b	22.4-31.5mm	4,5	19,9	62,9	10,3	2,4	0,0
	11.2-16mm	11,3	56,6	26,6	4,6	0,9	0,0
HA1.1	22.4-31.5mm	4,8	15,4	63,8	11,2	4,5	0,3
	11.2-16mm	2,1	10,3	75,9	10,9	0,4	0,4
HA1.3	22.4-31.5mm	0,7	13,4	76,6	6,9	1,4	1,0
	11.2-16mm	3,7	6,2	79,1	8,1	2,2	0,7
HB1.2	22.4-31.5mm	0,6	28,1	57,6	12,0	1,8	0,0
	11.2-16mm	0,0	8,2	78,5	9,1	3,9	0,3
HB1.8	22.4-31.5mm	1,5	10,6	74,5	10,6	1,2	1,5
	11.2-16mm	1,3	12,5	80,1	5,4	0,8	0,0
WG2.3b	22.4-31.5mm	2,8	22,3	71,2	3,3	0,5	0,0
	11.2-16mm	3,3	25,7	66,4	3,9	0,7	0,0
WG1.11	22.4-31.5mm	0,6	17,5	69,5	10,0	1,7	0,8
	11.2-16mm	0,9	5,1	83,8	6,4	3,4	0,4
SOM1.1	22.4-31.5mm	0,8	10,0	79,9	5,6	3,2	0,4
	11.2-16mm	1,0	10,5	81,1	6,3	0,8	0,2
SOM1.5	22.4-31.5mm	0,3	6,5	76,3	13,9	2,5	0,5
	11.2-16mm	0,0	6,4	89,0	3,4	1,2	0,0
ASH1.6	22.4-31.5mm	0,0	10,4	80,2	8,5	0,9	0,0
	11.2-16mm	2,7	10,7	76,1	8,7	1,1	0,7
ASH1.11	22.4-31.5mm	1,5	14,0	66,7	10,7	5,3	1,8
	11.2-16mm	0,4	10,0	73,2	12,9	2,9	0,7
ASH1.13	22.4-31.5mm	0,0	9,6	54,8	27,7	6,4	1,5
	11.2-16mm	0,0	17,7	64,7	12,8	4,8	0,0

Table A33.1 Clast angularity-roundness of deposits from all sites.

Appendix 34 Details on equivalent dose and dose rate estimation for OSL dating

34.1 Introduction

The mechanisms and principles of OSL dating are discussed in chapter 5. This appendix provides additional information on D_e and D_r acquisition (section 34.2). The tests that were applied to assess their accuracy are explained in section 34.3. The results of these tests determine the influence of laboratory and environmental factors on the acquired OSL age estimates and are presented in Appendix 36.

34.2 Specifications of D_e acquisition

D_e values were quantified according to the SAR protocol using the Risø TL-DA-15 irradiation-stimulation-detection system (Botter-Jensen et al. 1999; Markey et al. 1997). *“Within this apparatus, optical signal stimulation of each sample was provided by one of two light sources: an assembly of blue diodes (five packs of six Nichia NSPB500S), filtered to $470\pm 80\text{nm}$, conveying $15\text{mW}\cdot\text{cm}^{-2}$ using a 3mm Schott GG420 positioned in front of each diode pack, or a 150W tungsten halogen lamp, filtered to a broad blue-green light, 420-560nm conveying $16\text{mW}\cdot\text{cm}^{-2}$, using three 2mm Schott GG420 and a broadband interference filter. Infrared (IR) stimulation, provided by 6 IR diodes (Telefunken TSHA 6203) stimulating at $875\pm 80\text{nm}$ delivering $\sim 5\text{mW}\cdot\text{cm}^{-2}$, was used to indicate the presence of contaminant feldspars (Hütt et al 1988). Stimulated photon emissions from quartz aliquots are in the ultraviolet (UV) range and were filtered from stimulating photons by 7.5mm HOYA U-340 glass and detected by an EMI 9235QA photomultiplier fitted with a blue-green sensitive bialkali photocathode. Aliquot irradiation was conducted using a 1.48GBq $^{90}\text{Sr}/^{90}\text{Y}$ β source calibrated for multi-grain aliquots of each isolated quartz fraction against the ‘Hotspot 800’ ^{60}Co γ source located at the National Physical Laboratory (NPL), UK.”* (Toms et al. 2008, p. 9).

34.3 Test procedures

34.3.1 Laboratory factors

The measurement of the regeneration doses is preceded by a preheat-treatment to a fixed temperature for a set duration to remove unstable electrons from shallow traps to ensure the OSL signal measured is only that of stably accumulated electrons during burial and to ensure comparability between natural and laboratory-induced signals. The optimal preheat temperature can be assessed through a dose recovery test.

The **dose recovery test** attempts to quantify the effect of thermal transfer and sample sensitisation. The dose recovery test measures a laboratory-induced signal as if it

were a natural signal. After measuring and removing the natural dose, a known dose is administered to the sample before applying the SAR protocol. The applied dose and recovered D_e value should be statistically concordant with unity. Six aliquots were assigned a 10s preheat between 180°C and 280°C. The measurement of D_e at a range of different temperatures facilitates the assessment of D_e dependence on preheat treatment. If higher preheat temperatures result in significantly higher D_e values thermal transfer (heat-sensitive electrons transferring into light-sensitive electrons) or sample sensitisation may have been occurring and lower pre-heating temperatures should be used. The preheat treatment that meets the required dose recovery accuracy was selected to generate the final D_e values from the further 12 aliquots.

The laboratory procedures of preheating aliquots between irradiation and optical stimulation may lead to signal sensitisation that is monitored and corrected for by the addition of the **test dose** procedure to the SAR protocol (Murray and Wintle 2003). A fixed radiation dose is applied and recovered from the aliquot in the second half of each SAR procedure cycle. Any change in sensitivity can be monitored and corrected for by plotting the obtained luminescence signal as a function of the sensitivity corrected luminescence. The test dose applied to the sediments analysed in this research was set to 5 Gy preheated to 220°C for 10s.

Inter aliquot D_e variability expresses the homogeneity of absorption of radiation during burial and/or the response to the SAR protocol. (cf. Galbraith 1990). This is illustrated in quasi-radial plots in which D_e values are shown relative to obtained natural D_e values or the applied regenerated signals. If >5% of the obtained D_e values exceed $\pm 2\sigma$ of the standardising value, D_e values are over-dispersed as a result of heterogeneous absorption of irradiation during burial or response to the SAR protocol. Multi grains aliquots showing over-dispersed D_e values are not necessarily inaccurate. However, when over-dispersed values are obtained from regenerated signals, the age estimation should be accepted tentatively. Repeat dose ratios can be used to measure SAR protocol success, whereby ratios between 0.9 and 1.1 are acceptable (Murray and Wintle 2003). However, variation of the repeat dose ratios in the high-dose region can have a significant impact on the D_e interpolation. The influence of this effect can be outlined by quantifying the ratio of interpolated to applied regenerative-dose ratios.

Luminescence signals in feldspar tend to fade anomalously, leading to an age underestimation and its presence must be limited and quantified. **Feldspar contamination** is limited through applying density separation in sodium polytungstate (SPT) and removal of

plagioclase feldspar within quartz by treatment with hydrofluoric acid 40% (HF) (Mauz and Lang 2004) (see laboratory preparation). The feldspar component that can be present within quartz is detected by applying infra-red stimulation (IRSL) to the aliquots. At room temperature feldspar responds to IR where quartz does not. The IR signal can be used to evaluate the presence of feldspar in the sample. When its contribution to OSL is insignificant the repeat dose ratio of OSL to post-IR OSL should be statistically consistent with unity (Duller 2003) (Figure 6 appendix 36).

34.3.2 Environmental factors

Apart for the above mentioned laboratory factors there are environmental factors influencing the accuracy of the D_e value. Residual luminescence signal acquired from pre-burial natural radiation can result in an over-estimation of age when sunlight exposure is limited in spectrum, intensity, and/or duration causing partial bleaching (Murray et al. 1995). This is especially of influence in fluvially deposited sediments (Olley et al. 1998; Wallinga 2002). The single-aliquot regenerative-dose method provides two diagnostics for partial resetting; signal analysis and inter-aliquot D_e distribution studies.

The **signal analysis test** relies on the principle that quartz grains inhibit different electron traps that bleach with different efficiency and electrons will be evicted at certain light wavelengths. In completely bleached samples the shine-down curve of the luminescence signal shows an exponential decay as stimulation progresses. Partially bleaching of a sample is indicated when statistically significant peaks occur in the D_e signal decay curve. To test the presence of partial bleaching the statistically significant increase in D_e must be observed when partial bleaching is simulated in the laboratory and a significant rise in D_e should be absent when full bleaching is simulated. No increase in D_e value should be observed when zero dose is simulated. The impact of partial bleaching in the estimated OSL age becomes proportionally less important in older samples.

Post-depositional processes can further affect the luminescence signal through pedo- and cryoturbation resulting in grain movements. Bioturbation and illuviation can introduce younger grains to older strata and vice versa. In stratigraphic sections such processes can be identified and taken into account when choosing sample locations (see section 4.5.4).

Appendix 35 Details of OSL dating results

35.1 Explanation of diagnostic diagrams

The influence of laboratory and environmental factors on the acquisition of D_e and D_r values are assessed for each sample and the diagnostics are illustrated per sample in eight diagrams. These diagrams illustrate the analytical acceptability of the presented OSL results.

1. Signal calibration. The Natural blue and laboratory-induced infrared (IR) OSL signals. Detectable IR signal decays are diagnostic of feldspar contamination. The inset: the natural blue OSL signal (open triangle) of each aliquot is calibrated against known laboratory doses (blue diamonds) to yield equivalent dose (D_e) values. Repeats of low and high doses (open diamonds) illustrate the success of sensitivity correction.

2. Age range. The mean age range (red) provides an estimate of burial period based on mean D_e and D_r values with analytical uncertainties. The probability distribution (blue) indicates inter-aliquot distribution. The maximum influence of temporal variations in D_r values resulting from minima-maxima variation in moisture content and overburden thickness are presented by the grey dashed lines.

3. Dose recovery. Presents the combined effects of thermal transfer and sensitisation on the natural signal using a precise laboratory dose to simulate the natural dose. Based on this an appropriate thermal treatment is selected to generate the final D_e value.

4. Inter-aliquot D_e distribution. Provides the variation in D_e values from natural irradiation. Distribution beyond ± 2 standardised $\ln D_e$ suggests heterogeneous dose absorption and/or inaccuracies in calibration.

5. Repeat regenerative-doses. Measures the accordance of D_e from low (red) and high (green) repeat regenerative-doses with applied regenerative doses. Discordance (those points lying beyond $\pm 2 \ln D_e$ standardised against the applied regenerative-dose) of low and high applied regenerative-dose rates with repeat regenerative-dose rates indicate the impact of uncorrected sensitisation upon dose response and D_e interpolation.

6. OSL to Post-IR OSL. Measures the concordance of the post-IR OSL D_e with the applied regenerative-doses. Discordant, underestimating data (those points lying below $-2 \ln D_e$ standardised against the applied regenerative-dose) coupled with an IRSL signal (Fig.1) highlight the presence of significant feldspar contamination.

7. Signal Analysis. Presents D_e per signal stimulation period. A significant increase in D_e with signal stimulation period indicates partial bleaching.

8. U-activity. Equilibrium (green) in the activities of the daughter radioisotope ^{226}Ra with its parent ^{238}U may signify the temporal stability of D_r emissions from these chains. Significant difference ($>50\%$ =red) in activity indicate addition or removal of isotopes creating time-dependent variations in D_r values and increased uncertainty in the accuracy of age estimates. A 20% (blue) disequilibrium marker is also shown.

Field Code	Lab Code	Overburden (m)	Grain size (µm)	Moisture content (%)	NaI γ-spectrometry (in situ) γ D _r (Gy.ka ⁻¹)	Ge γ-spectrometry (ex situ)			α D _r (Gy.ka ⁻¹)	β D _r (Gy.ka ⁻¹)	Cosmic D _r (Gy.ka ⁻¹)	Preheat (°C for 10s)	Low Dose Repeat Ratio	Interpolated:Applied Low Regenerative-dose D _r	High Dose Repeat Ratio	Interpolated:Applied High Regenerative-dose D _r	Post-IR OSL Ratio
						K (%)	Th (ppm)	U (ppm)									
BP02	GL14038	1.45	5-15	14 ± 3	0.55 ± 0.04*	0.63 ± 0.04	7.31 ± 0.48	1.35 ± 0.10	0.30 ± 0.03	0.74 ± 0.06	0.17 ± 0.02	270	1.00 ± 0.04	1.00 ± 0.04	1.04 ± 0.03	1.16 ± 0.10	1.01 ± 0.04
BP04	GL14039	1.45	125-180	14 ± 3	0.80 ± 0.08*	1.09 ± 0.06	9.89 ± 0.61	1.82 ± 0.12	-	1.05 ± 0.10	0.17 ± 0.02	260	1.04 ± 0.01	1.08 ± 0.01	1.05 ± 0.01	1.31 ± 0.05	1.04 ± 0.01
BP01	GL14040	0.85	5-15	16 ± 4	0.88 ± 0.05*	0.80 ± 0.05	8.96 ± 0.54	1.80 ± 0.11	0.37 ± 0.04	0.92 ± 0.08	0.18 ± 0.02	260	1.01 ± 0.01	1.03 ± 0.02	1.06 ± 0.01	1.24 ± 0.04	1.10 ± 0.02
BP03	GL14041	0.90	125-180	6 ± 1	0.92 ± 0.08*	1.22 ± 0.06	10.37 ± 0.60	1.72 ± 0.11	-	1.26 ± 0.10	0.18 ± 0.02	260	1.05 ± 0.01	1.11 ± 0.02	1.02 ± 0.01	1.17 ± 0.04	1.05 ± 0.01
WGREG01	GL14042	4.50	125-180	6 ± 1	0.22 ± 0.01	0.33 ± 0.03	2.41 ± 0.30	0.37 ± 0.07	-	0.32 ± 0.04	0.10 ± 0.01	260	1.02 ± 0.01	1.04 ± 0.02	1.01 ± 0.01	1.20 ± 0.05	1.01 ± 0.01
WGREG02	GL14043	4.50	125-180	6 ± 1	0.19 ± 0.04	0.34 ± 0.03	1.87 ± 0.29	0.35 ± 0.07	-	0.31 ± 0.04	0.10 ± 0.01	260	1.05 ± 0.01	1.11 ± 0.01	1.04 ± 0.01	1.27 ± 0.04	1.05 ± 0.01
WGREG03	GL14044	4.60	125-180	7 ± 2	0.23 ± 0.04	0.32 ± 0.03	2.48 ± 0.33	0.51 ± 0.07	-	0.33 ± 0.04	0.10 ± 0.01	260	1.15 ± 0.01	1.28 ± 0.01	1.04 ± 0.01	1.21 ± 0.02	1.20 ± 0.01
HALE02	GL14045	2.60	5-15	18 ± 4	0.90 ± 0.08	1.21 ± 0.06	12.67 ± 0.68	1.99 ± 0.12	0.46 ± 0.05	1.25 ± 0.11	0.14 ± 0.01	240	1.03 ± 0.04	1.04 ± 0.04	1.03 ± 0.04	1.08 ± 0.09	1.01 ± 0.04
HALE01	GL14046	2.40	5-15	16 ± 4	0.57 ± 0.05	0.71 ± 0.04	7.13 ± 0.48	1.63 ± 0.10	0.31 ± 0.03	0.80 ± 0.07	0.14 ± 0.01	240	1.02 ± 0.02	1.04 ± 0.02	1.03 ± 0.02	1.13 ± 0.05	1.08 ± 0.02
HALE03	GL14047	1.80	125-180	12 ± 3	0.40 ± 0.05	0.59 ± 0.04	5.70 ± 0.41	0.46 ± 0.07	-	0.53 ± 0.06	0.16 ± 0.02	260	1.03 ± 0.01	1.07 ± 0.01	1.01 ± 0.01	1.13 ± 0.04	1.04 ± 0.01
HALE04	GL14048	1.90	125-180	12 ± 3	0.34 ± 0.05	0.43 ± 0.04	5.16 ± 0.38	0.39 ± 0.07	-	0.41 ± 0.05	0.15 ± 0.01	240	1.06 ± 0.01	1.14 ± 0.02	1.03 ± 0.01	1.28 ± 0.04	1.04 ± 0.01
ASH01	GL15033	2.00	125-180	5 ± 1	0.72 ± 0.07	0.97 ± 0.05	7.57 ± 0.51	1.50 ± 0.10	-	1.01 ± 0.08	0.15 ± 0.01	260	1.04 ± 0.01	1.09 ± 0.02	1.03 ± 0.01	1.22 ± 0.04	1.01 ± 0.01
ASH02	GL15034	3.10	180-250	7 ± 2	0.09 ± 0.03	0.11 ± 0.03	1.07 ± 0.22	0.21 ± 0.07	-	0.12 ± 0.03	0.13 ± 0.01	260	1.05 ± 0.01	1.09 ± 0.02	1.01 ± 0.01	1.06 ± 0.04	1.01 ± 0.01
ASH03	GL15035	4.10	125-180	11 ± 3	0.16 ± 0.05	0.47 ± 0.04	1.15 ± 0.30	0.12 ± 0.13	-	0.34 ± 0.05	0.11 ± 0.01	260	1.02 ± 0.02	1.04 ± 0.02	1.02 ± 0.02	1.12 ± 0.04	1.00 ± 0.02
ASH05	GL15036	1.80	180-250	10 ± 2	0.23 ± 0.04	0.31 ± 0.03	2.49 ± 0.32	0.54 ± 0.08	-	0.30 ± 0.04	0.16 ± 0.01	260	1.00 ± 0.02	1.00 ± 0.02	1.05 ± 0.02	1.09 ± 0.03	1.01 ± 0.02
ASH04	GL15037	4.40	125-180	11 ± 3	0.10 ± 0.03	0.16 ± 0.03	1.05 ± 0.25	0.20 ± 0.08	-	0.15 ± 0.03	0.10 ± 0.01	260	1.05 ± 0.01	1.09 ± 0.01	1.02 ± 0.01	1.12 ± 0.03	1.04 ± 0.01
SOM01	GL15038	1.50	125-180	13 ± 3	0.20 ± 0.05	0.58 ± 0.04	1.09 ± 0.61	0.33 ± 0.09	-	0.42 ± 0.06	0.16 ± 0.02	260	0.99 ± 0.02	1.06 ± 0.02	0.99 ± 0.02	1.13 ± 0.04	0.99 ± 0.02
SOM02	GL15039	2.00	180-250	12 ± 3	0.18 ± 0.04	0.53 ± 0.04	1.31 ± 0.27	0.18 ± 0.08	-	0.37 ± 0.05	0.15 ± 0.01	260	1.04 ± 0.01	1.07 ± 0.02	1.04 ± 0.01	1.14 ± 0.04	1.01 ± 0.01
SOM03	GL15040	2.10	180-250	8 ± 2	0.23 ± 0.05	0.72 ± 0.05	1.20 ± 0.33	0.17 ± 0.14	-	0.51 ± 0.07	0.15 ± 0.01	260	1.04 ± 0.02	1.08 ± 0.02	1.04 ± 0.02	1.12 ± 0.04	1.02 ± 0.02
SOM04	GL15041	2.20	180-250	11 ± 3	0.21 ± 0.04	0.57 ± 0.04	1.72 ± 0.28	0.19 ± 0.07	-	0.41 ± 0.05	0.15 ± 0.01	260	1.02 ± 0.01	1.03 ± 0.02	1.02 ± 0.01	1.22 ± 0.06	0.99 ± 0.01
SOM05	GL15042	3.50	180-250	9 ± 2	0.20 ± 0.04	0.43 ± 0.04	1.38 ± 0.35	0.45 ± 0.07	-	0.35 ± 0.05	0.12 ± 0.01	260	1.01 ± 0.02	1.05 ± 0.01	1.02 ± 0.02	1.13 ± 0.03	0.99 ± 0.02
BICK01	GL15075	1.20	125-180	11 ± 3	0.17 ± 0.05*	0.36 ± 0.03	0.75 ± 0.67	0.61 ± 0.08	-	0.31 ± 0.06	0.17 ± 0.02	260	0.99 ± 0.03	1.00 ± 0.04	0.98 ± 0.03	1.00 ± 0.04	0.98 ± 0.03
BICK02	GL15076	1.80	125-180	19 ± 5	0.43 ± 0.06*	0.96 ± 0.05	3.59 ± 0.47	1.24 ± 0.10	-	0.73 ± 0.09	0.16 ± 0.02	240	0.98 ± 0.02	0.98 ± 0.01	0.98 ± 0.02	1.02 ± 0.01	0.98 ± 0.02
BICK03	GL15077	1.30	180-250	8 ± 2	0.20 ± 0.04*	0.33 ± 0.03	1.13 ± 0.25	0.77 ± 0.08	-	0.32 ± 0.04	0.17 ± 0.02	240	1.03 ± 0.01	0.99 ± 0.02	1.02 ± 0.01	1.00 ± 0.02	1.00 ± 0.01
BICK04	GL15078	1.20	180-250	13 ± 3	0.27 ± 0.05*	0.58 ± 0.04	2.11 ± 0.32	0.68 ± 0.08	-	0.47 ± 0.06	0.17 ± 0.02	260	1.02 ± 0.04	1.03 ± 0.03	1.00 ± 0.03	1.01 ± 0.04	1.00 ± 0.04

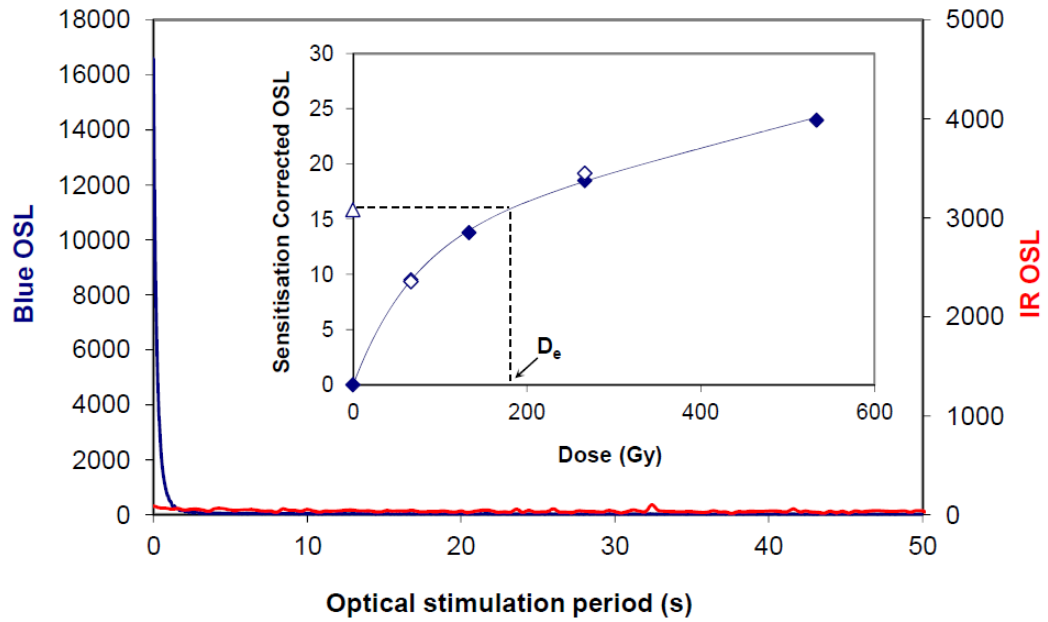
*Gamma dose rate derived ex situ by laboratory-based Ge gamma spectrometry

Table A35.1 Summary laboratory procedures, applied Dr values and the results of the analytical tests per sample.

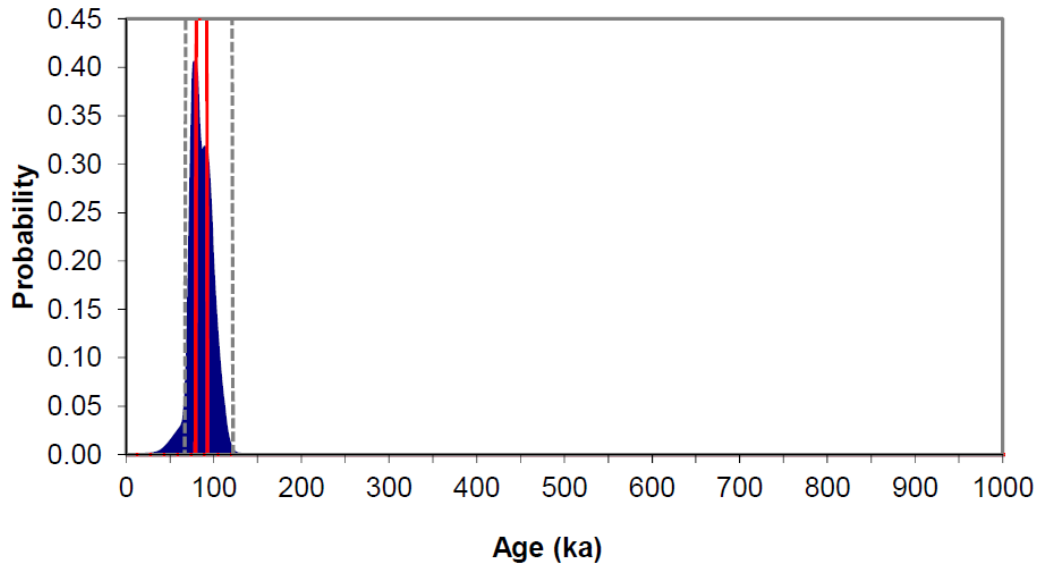
Appendix 36 Diagnostics of OSL results presented per site

Bemerton GL14038

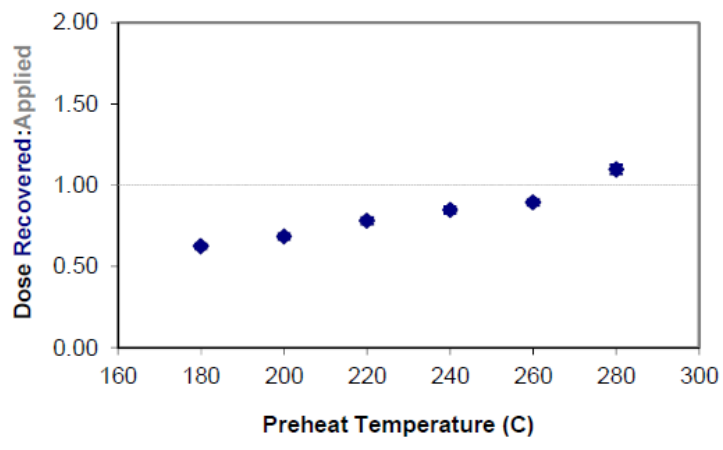
1



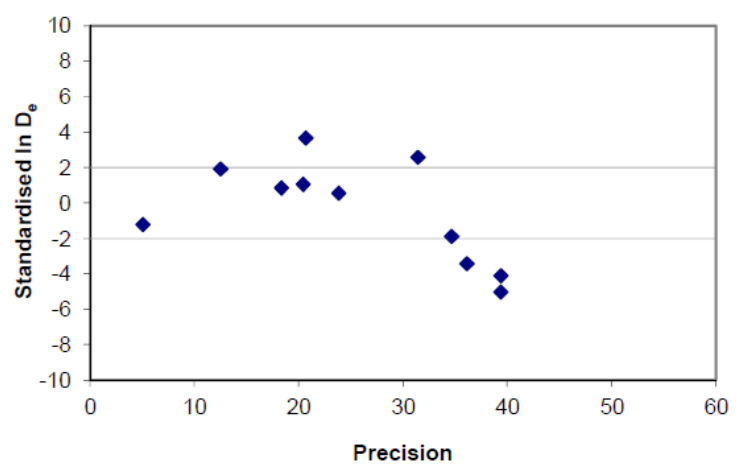
2



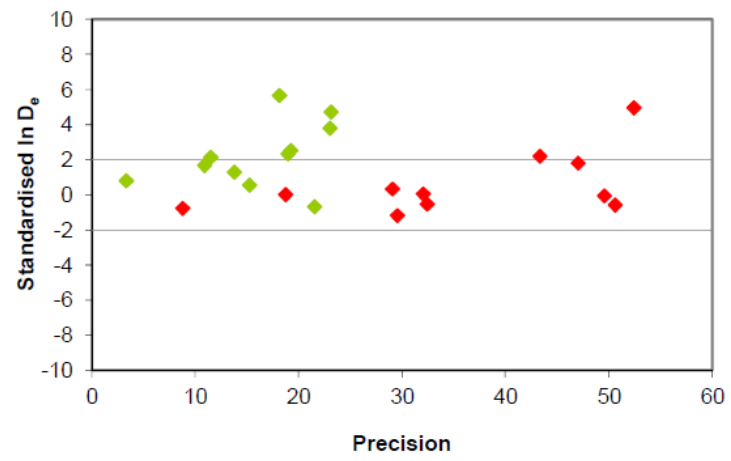
3



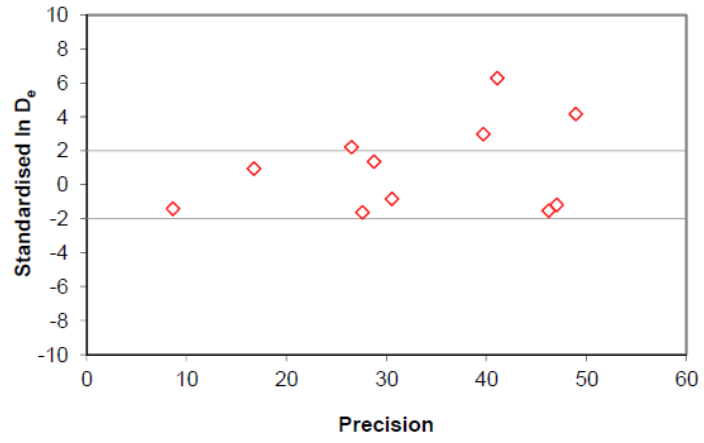
4



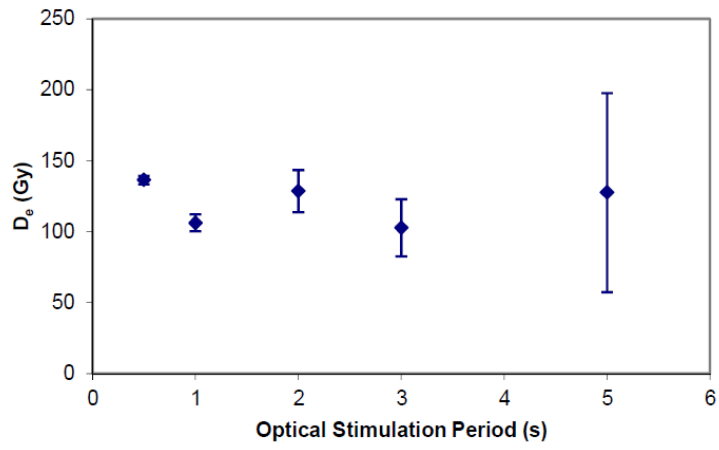
5



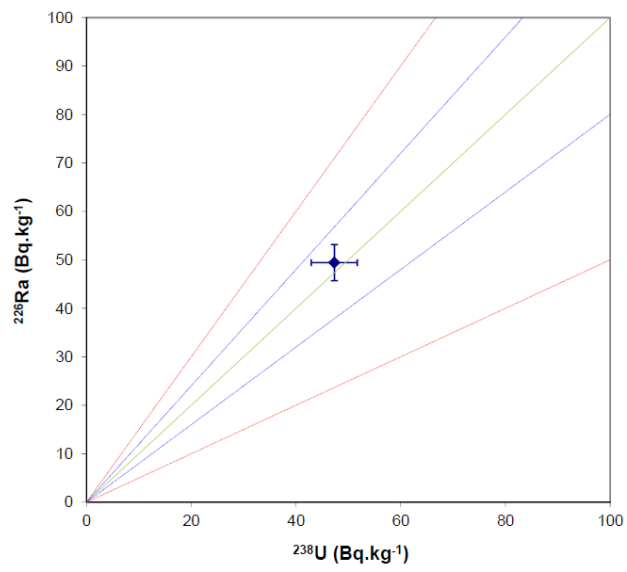
6



7

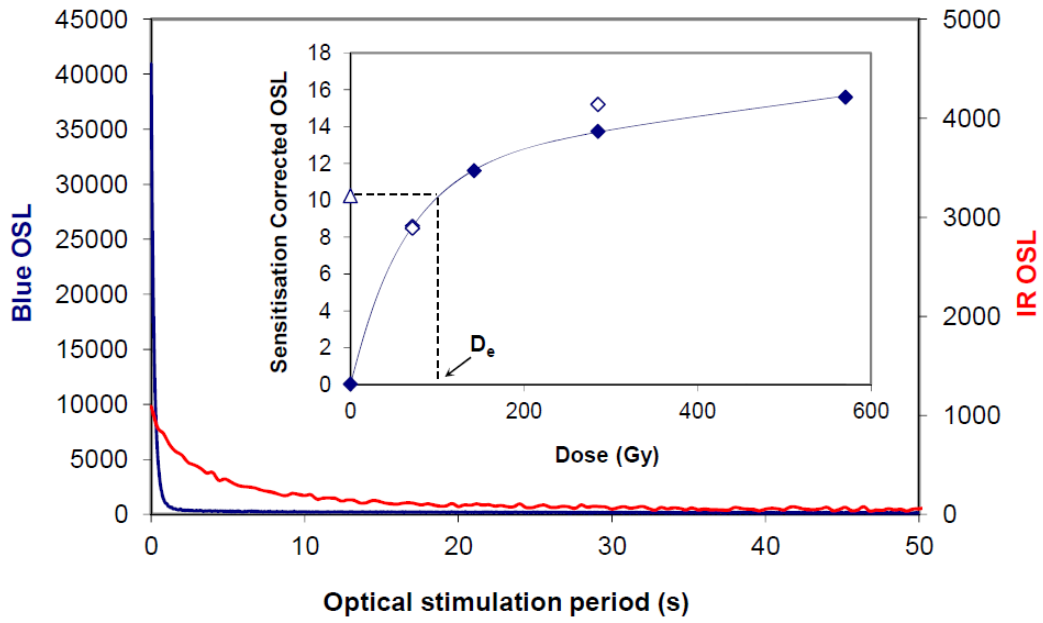


8

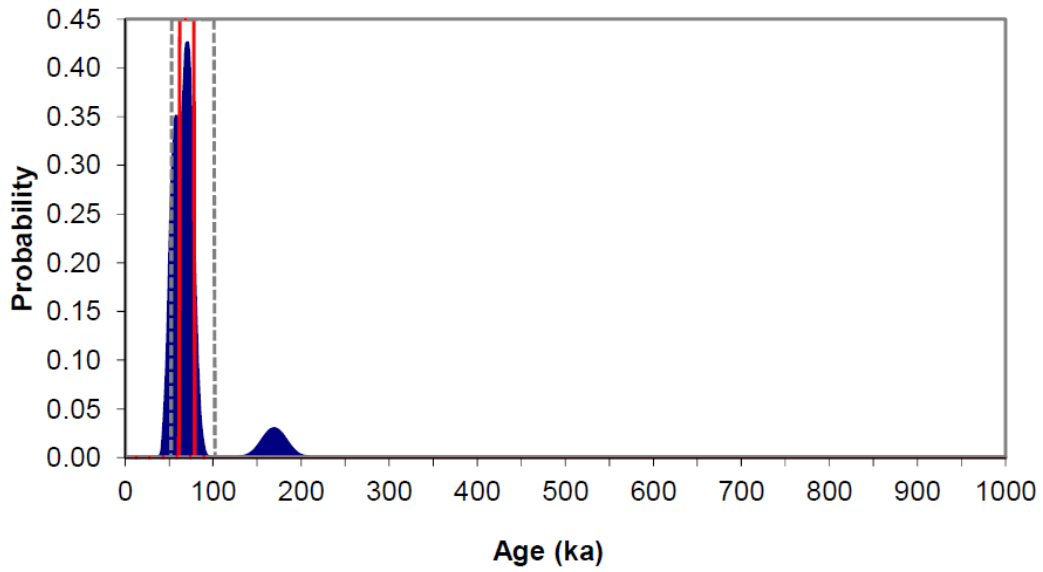


Bemerton GL14039

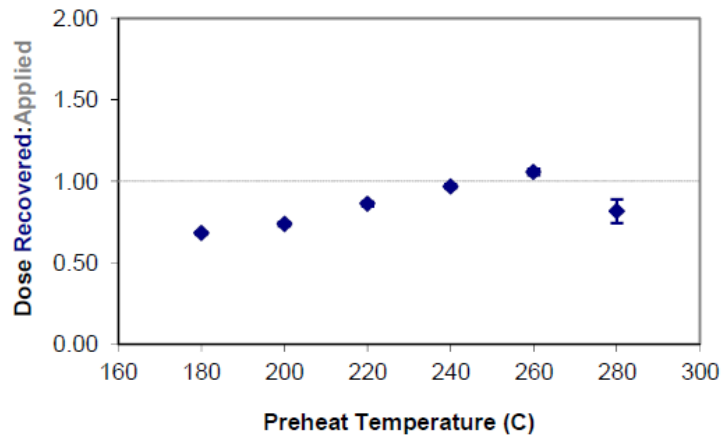
1



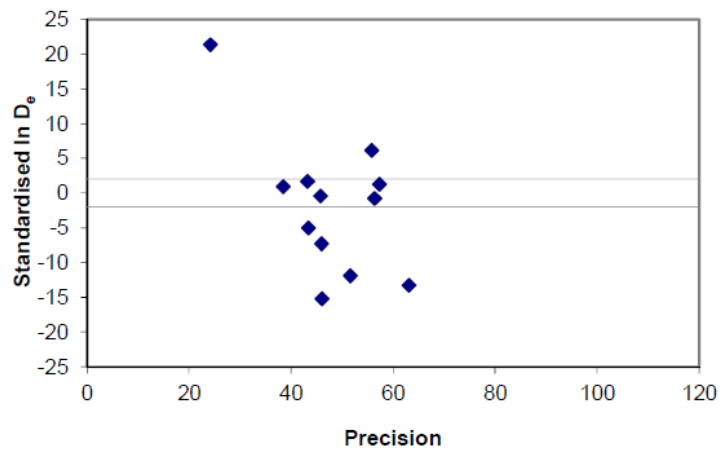
2



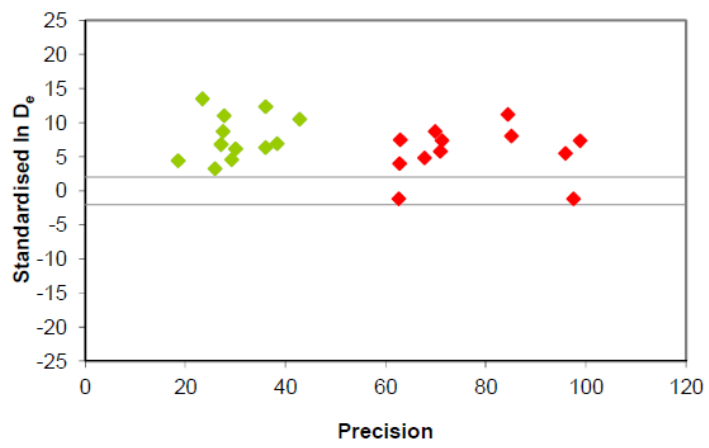
3



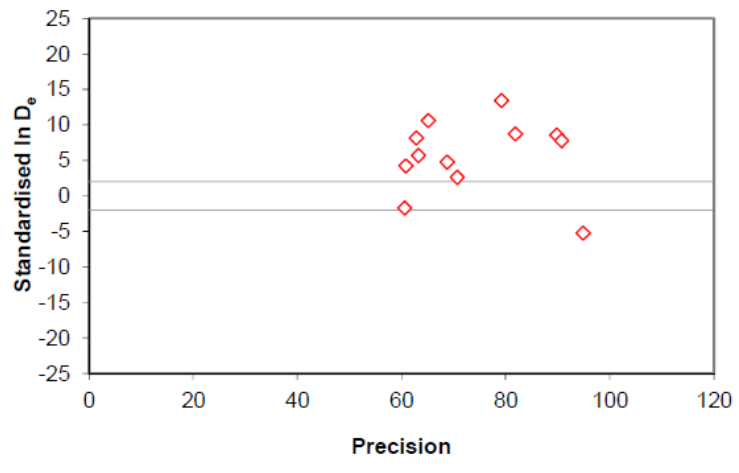
4



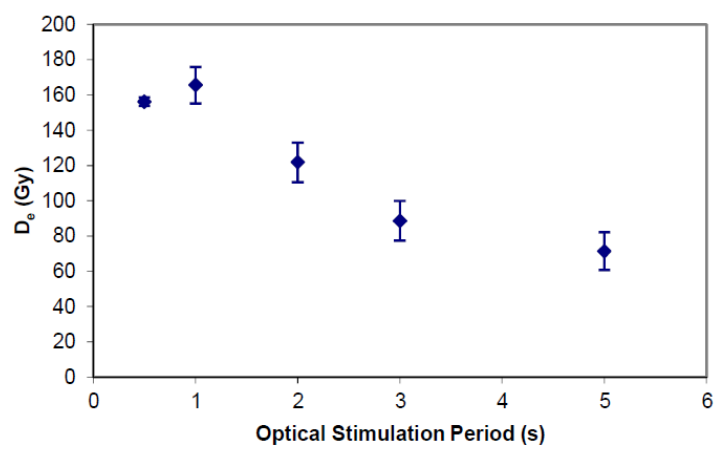
5



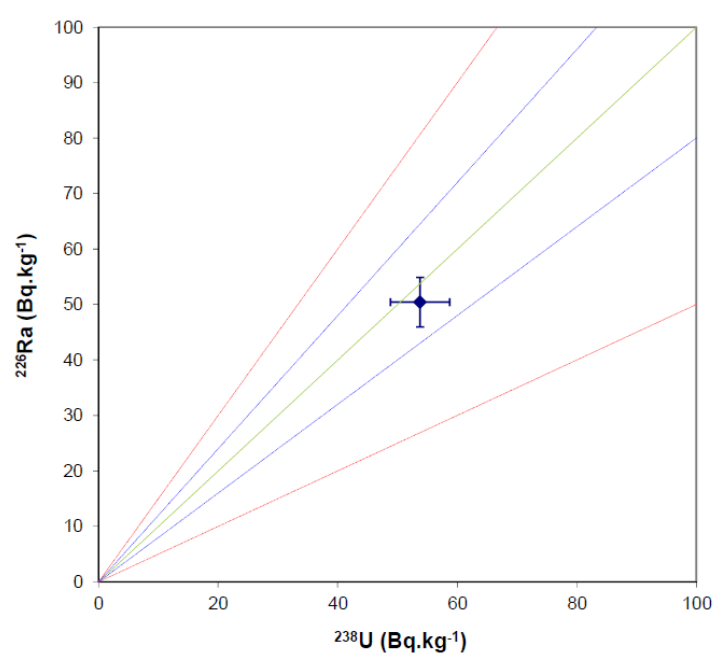
6



7

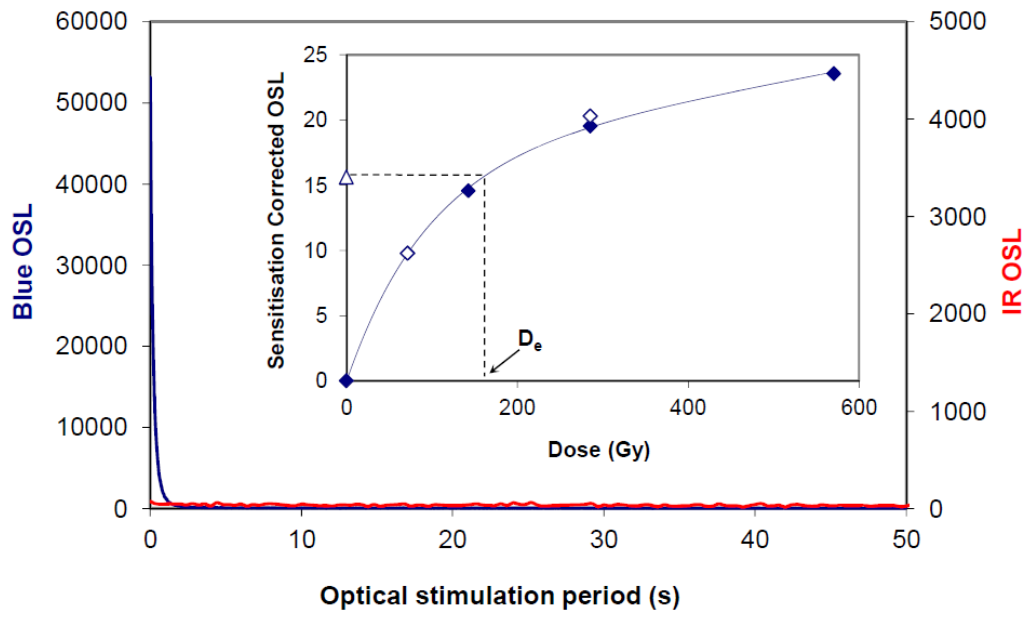


8

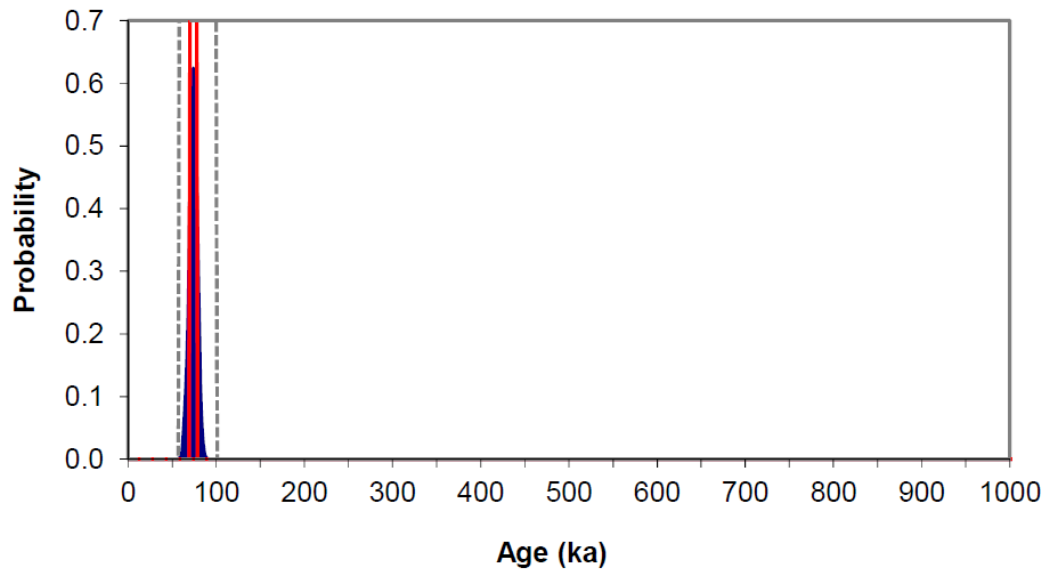


Bemerton GL14040

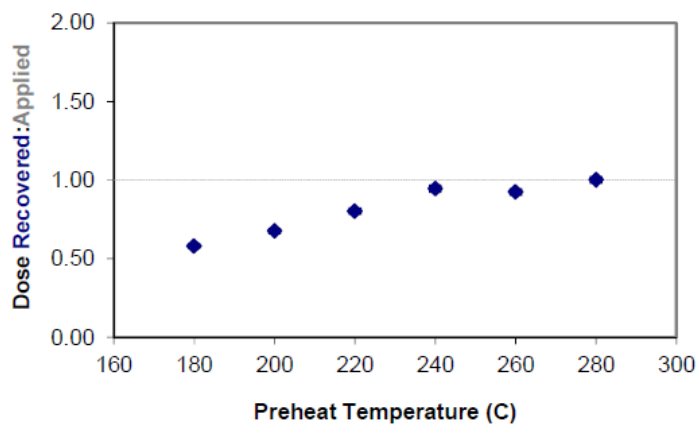
1



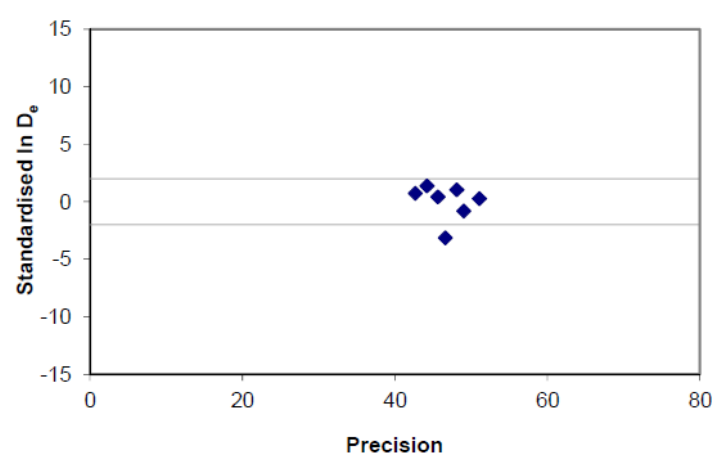
2



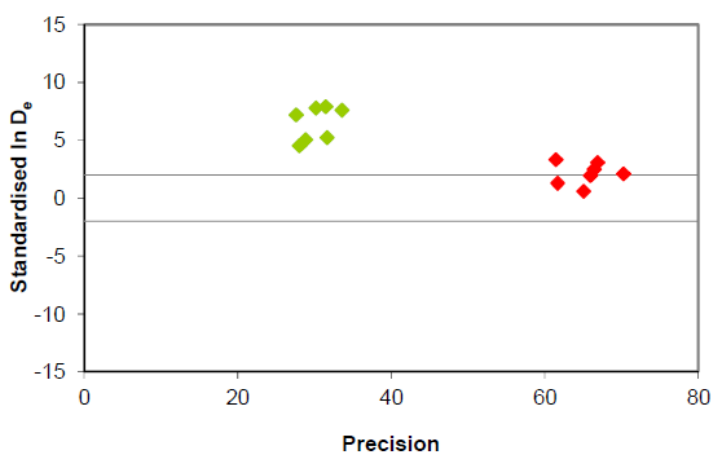
3



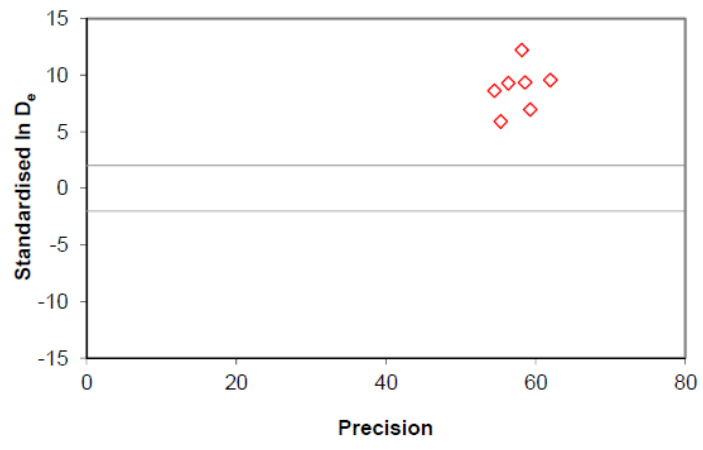
4



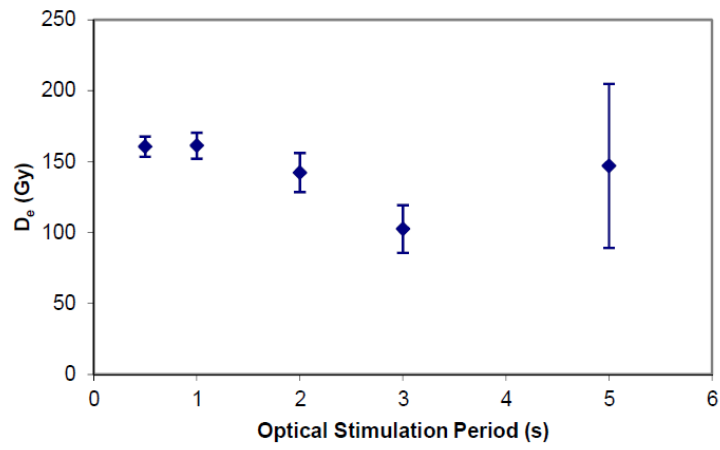
5



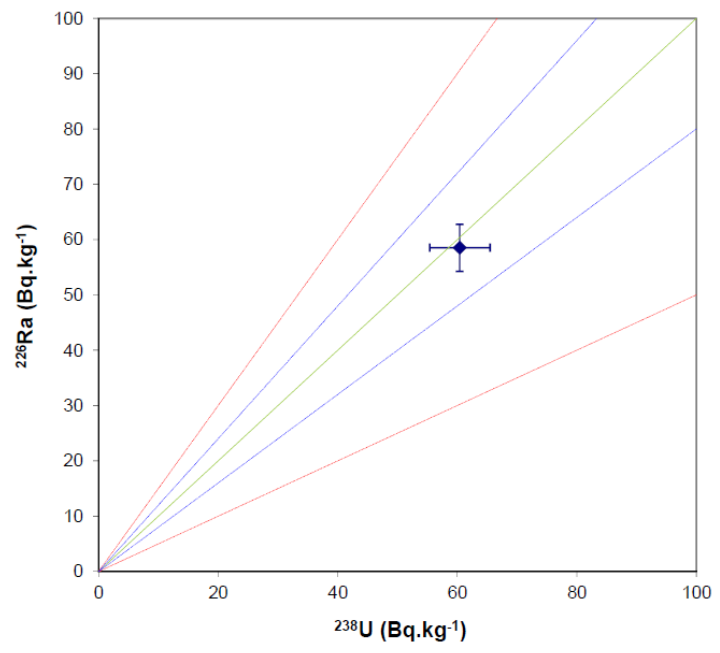
6



7

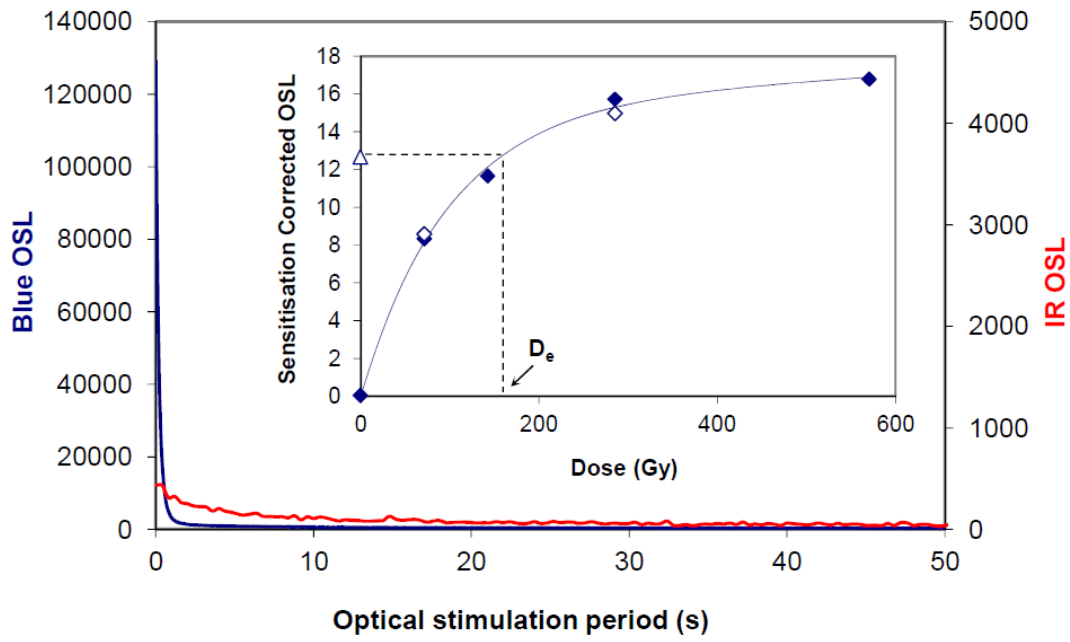


8

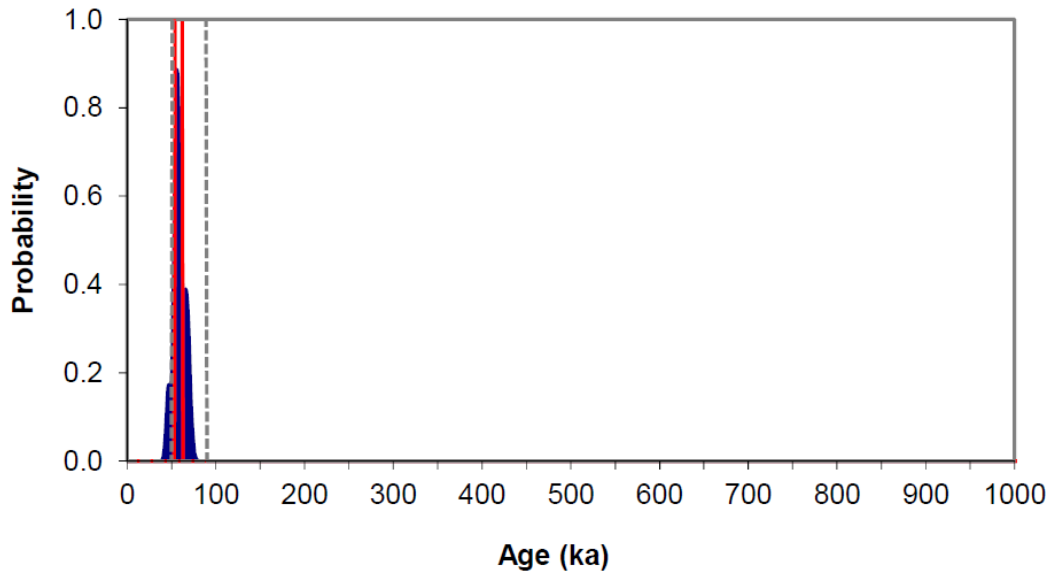


Bemerton GL14041

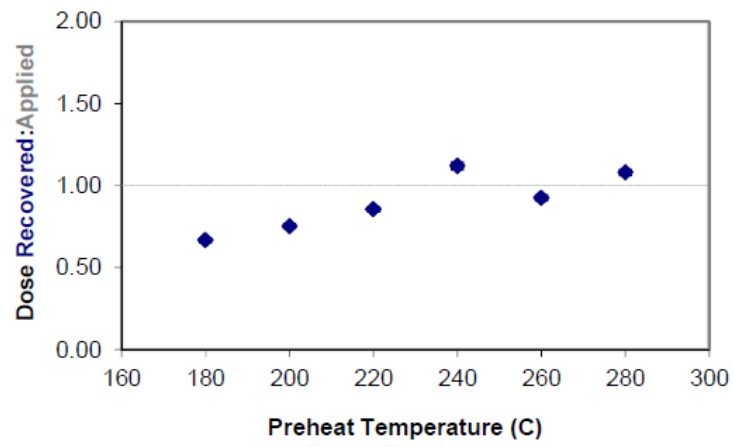
1



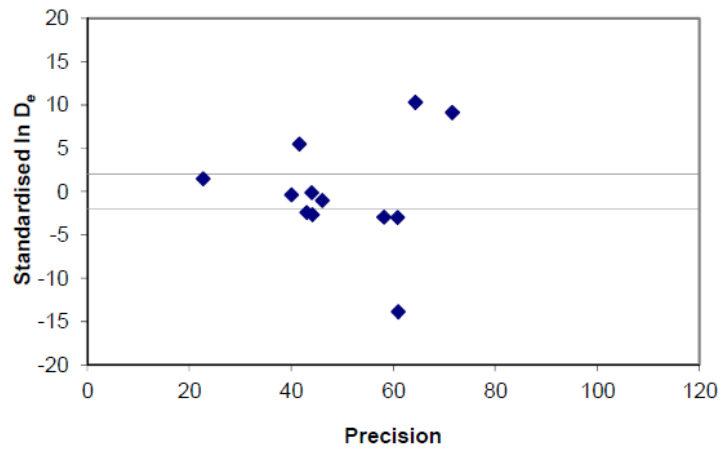
2



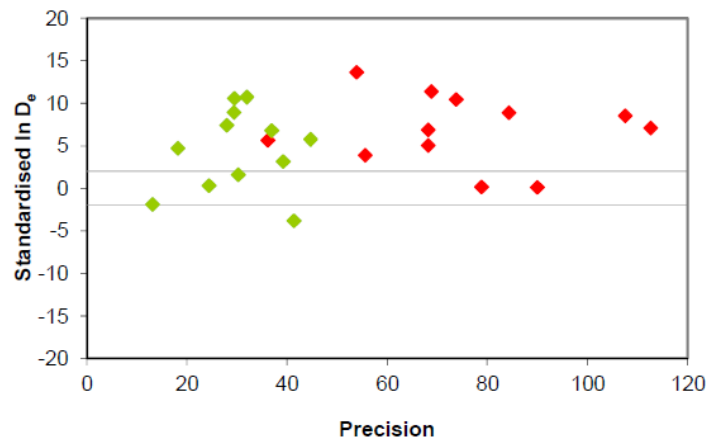
3



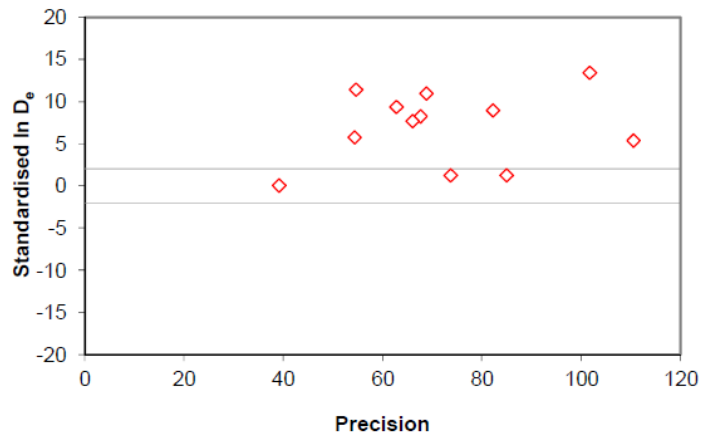
4



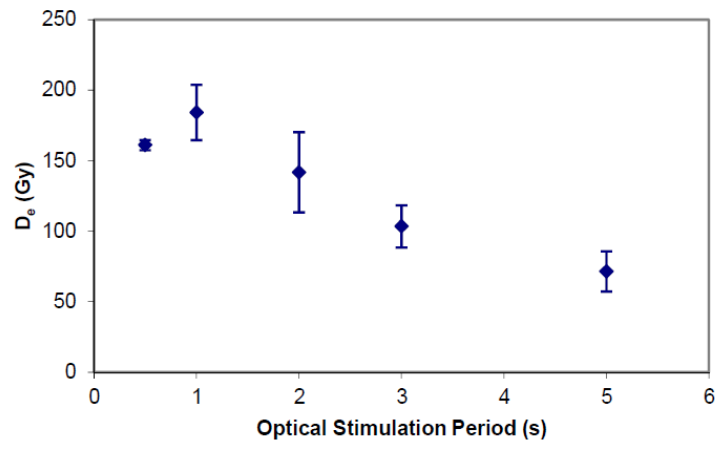
5



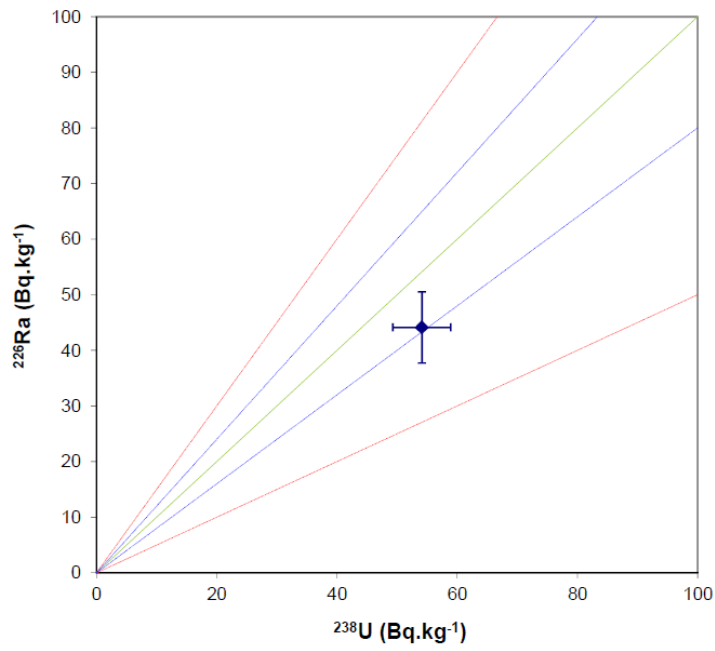
6



7

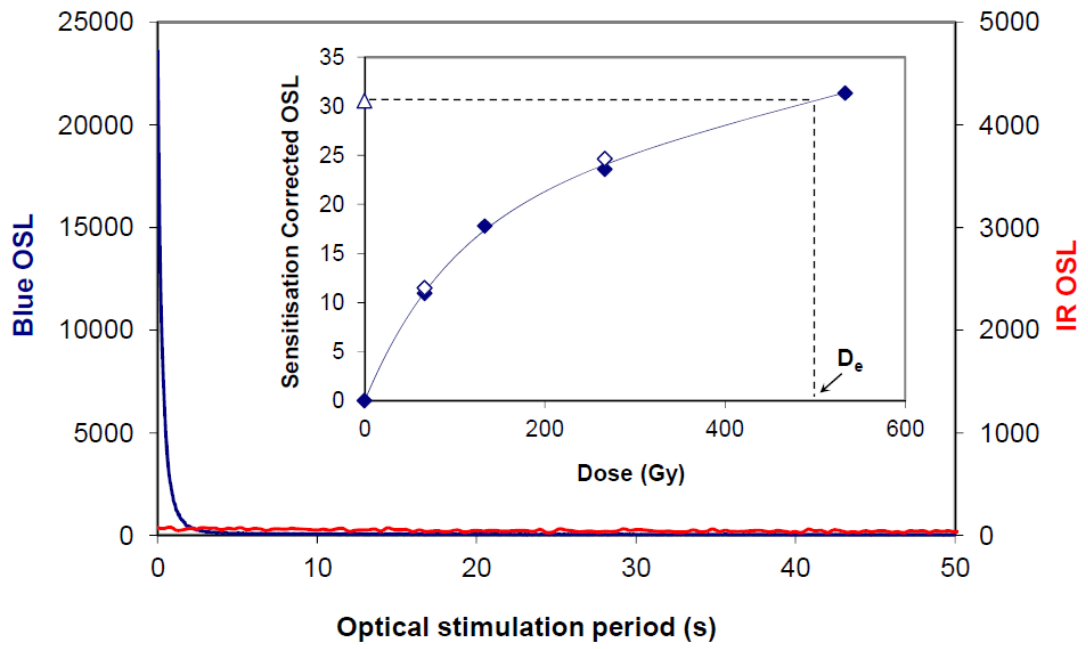


8

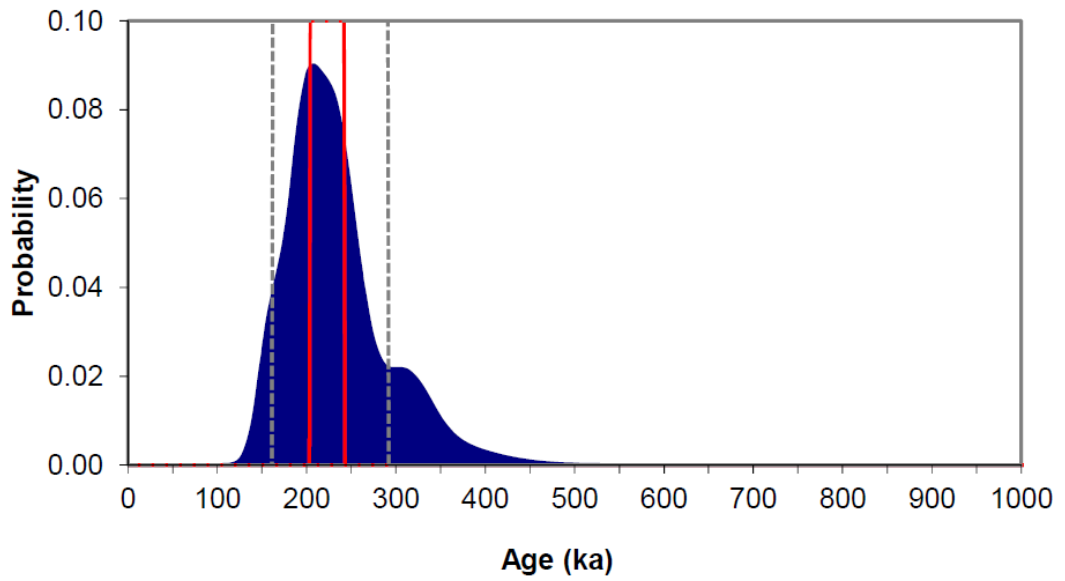


Hatchet Gate Farm GL14045

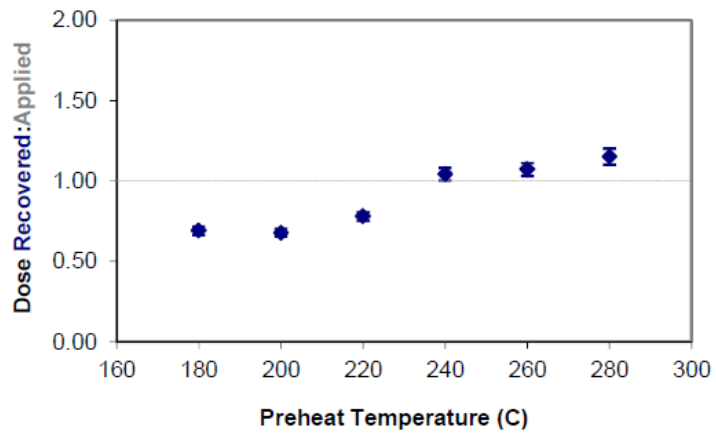
1



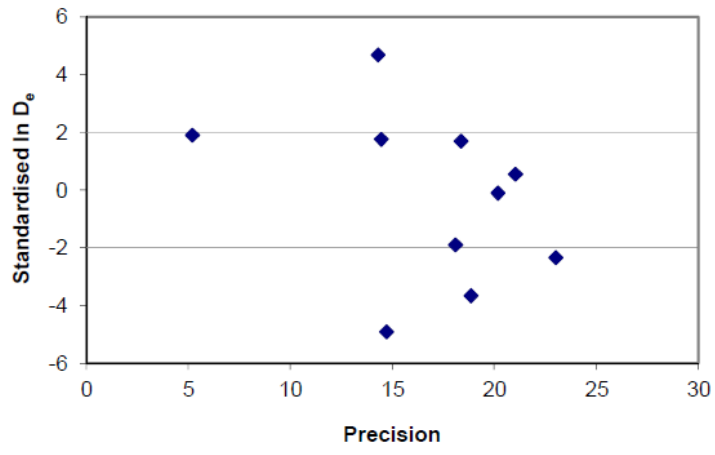
2



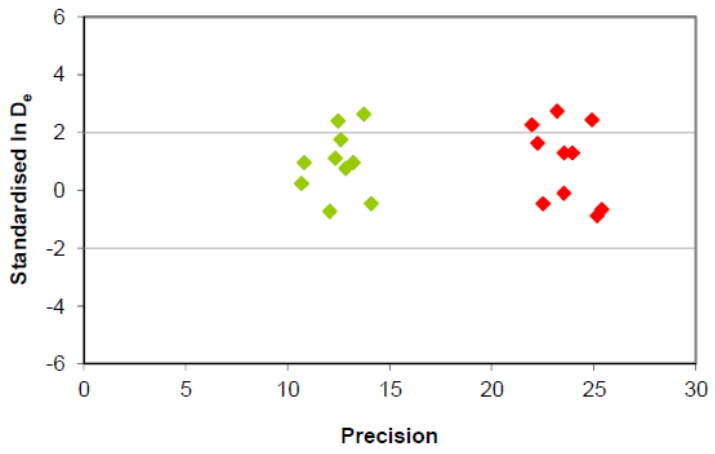
3



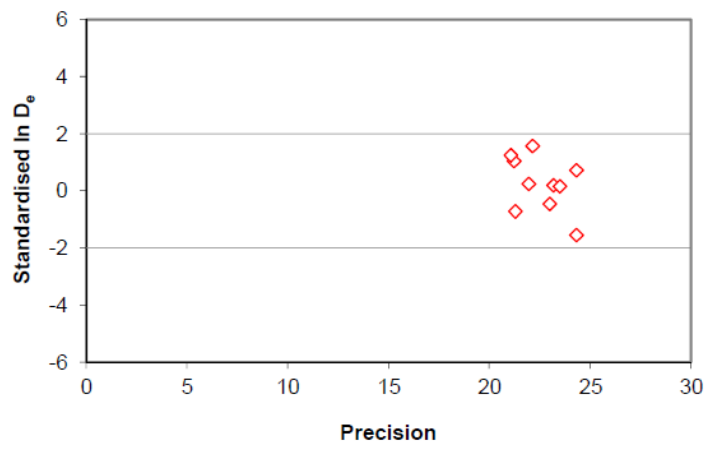
4



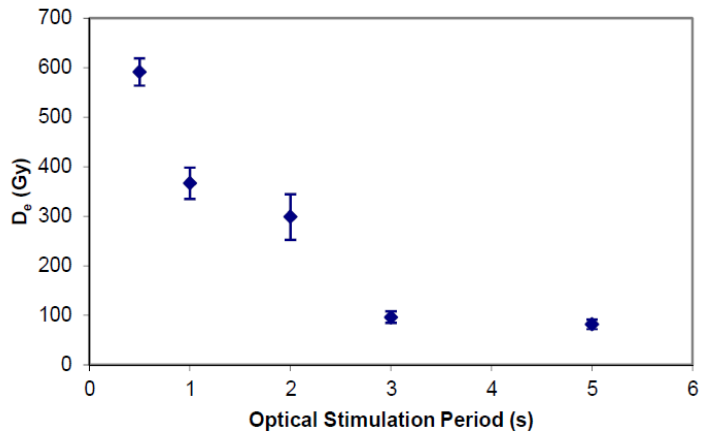
5



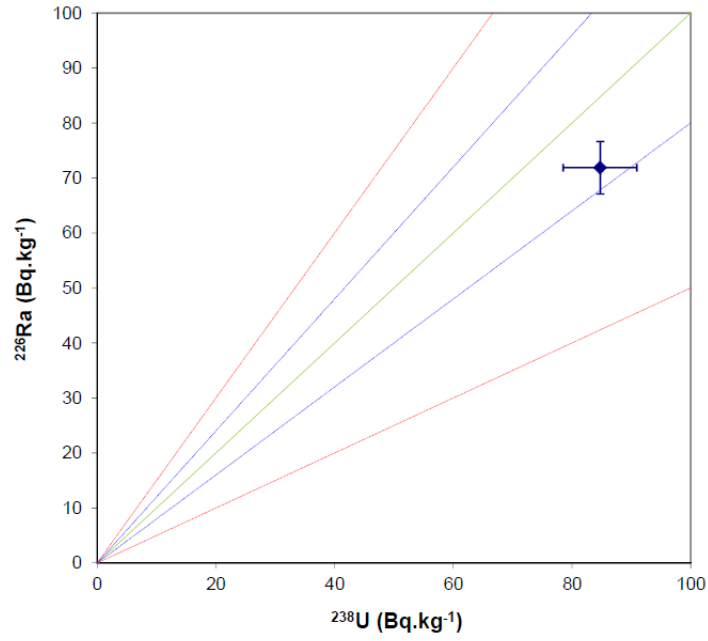
6



7

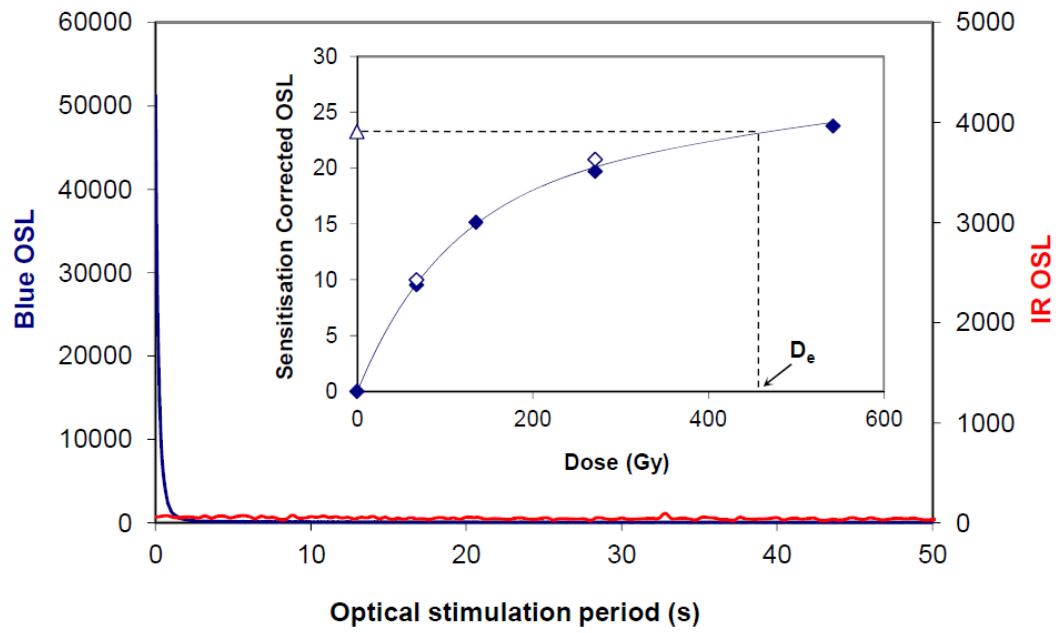


8

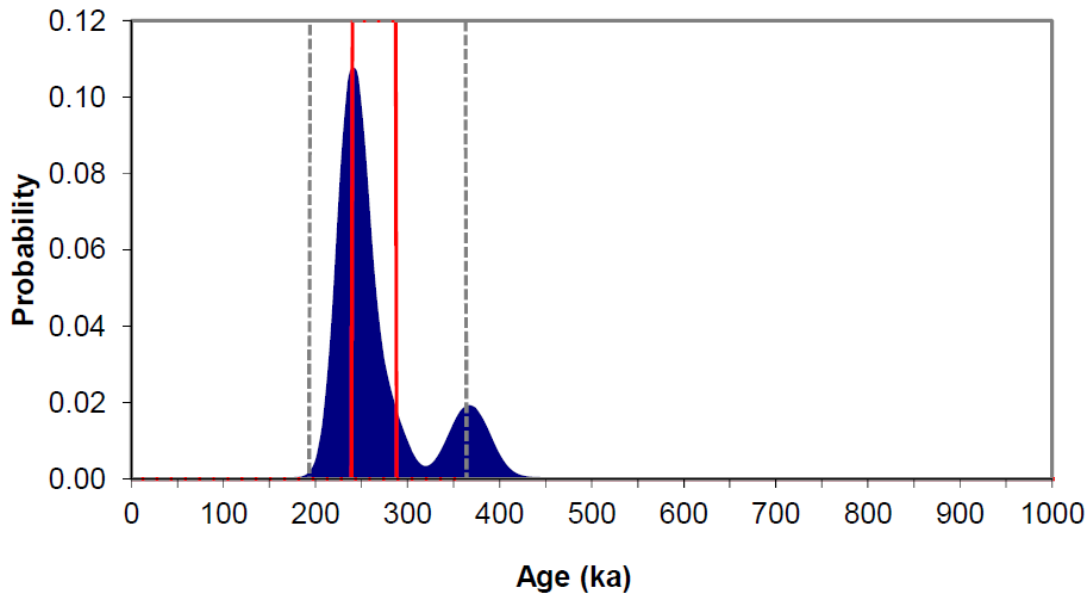


Hatchet Gate Farm GL14046

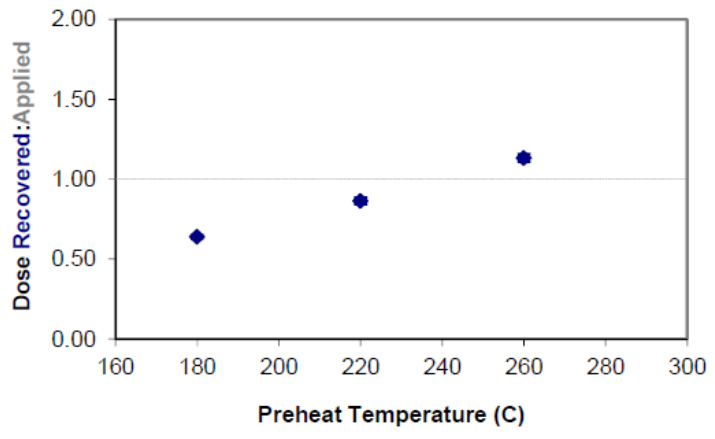
1



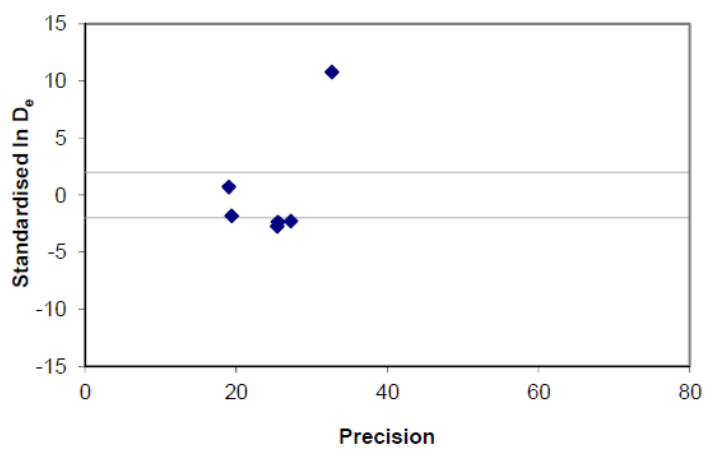
2



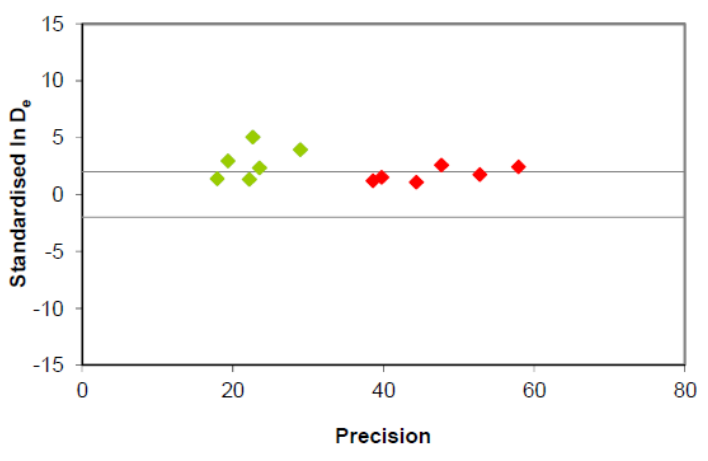
3



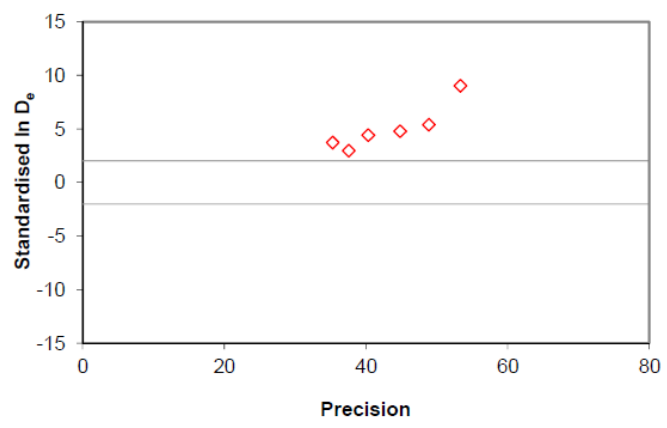
4



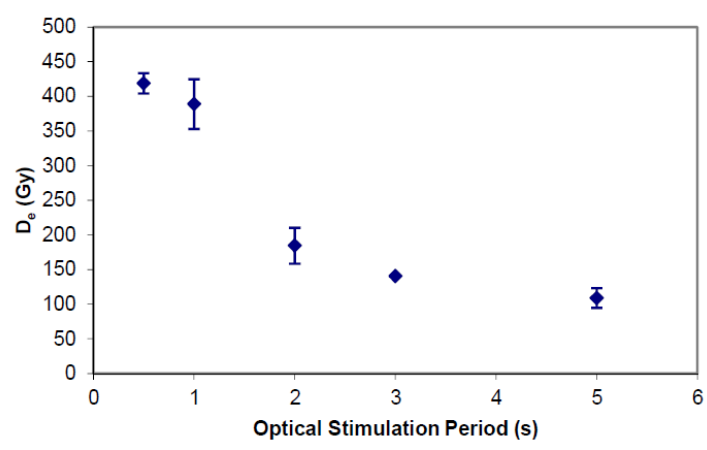
5



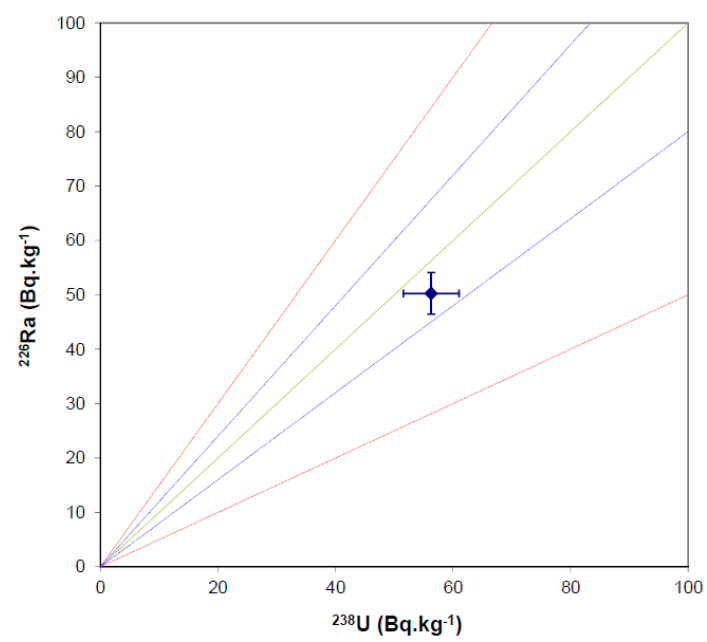
6



7

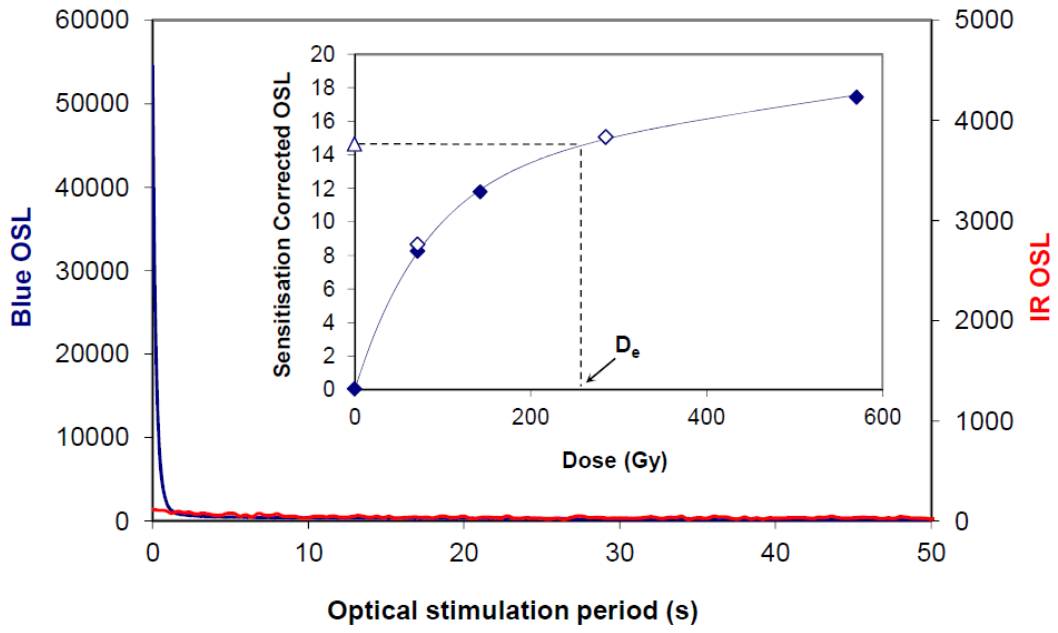


8

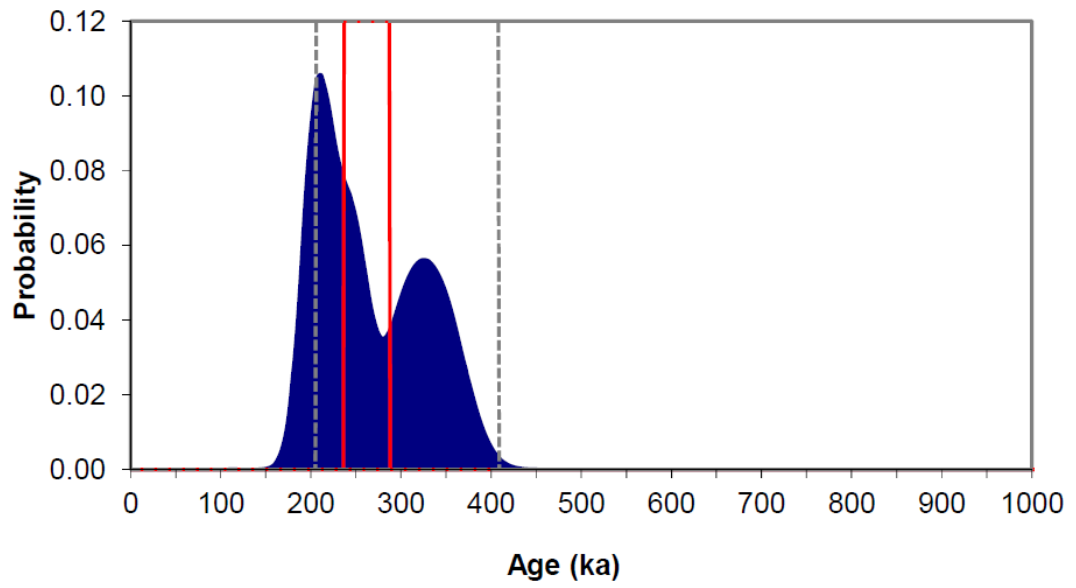


Woodriding GL14047

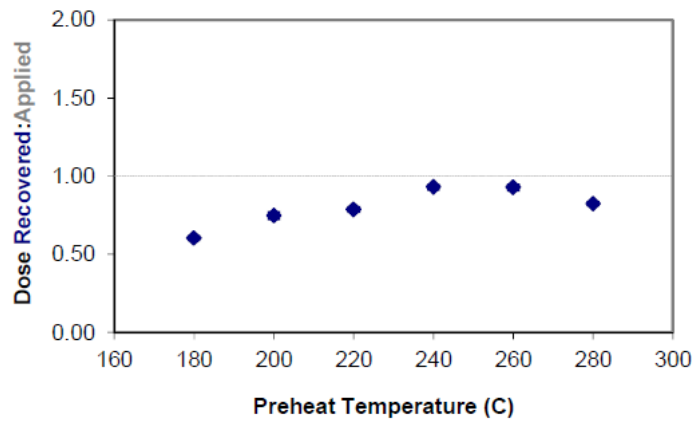
1



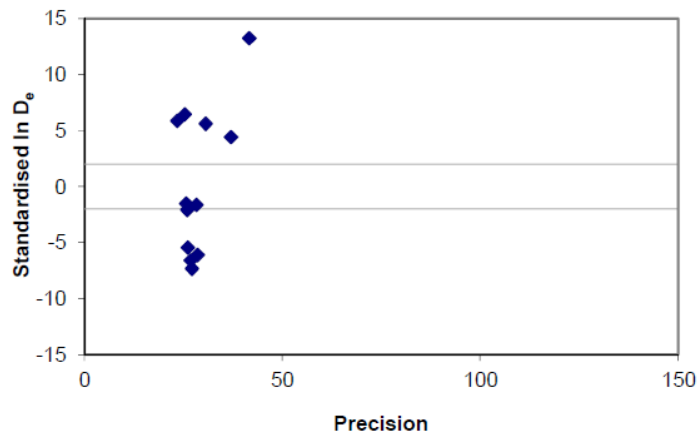
2



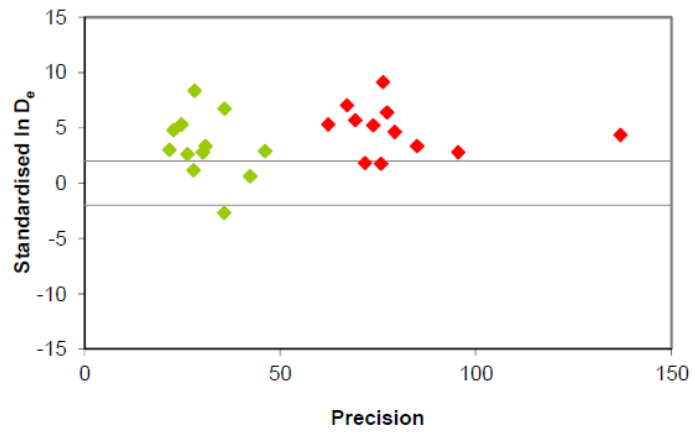
3



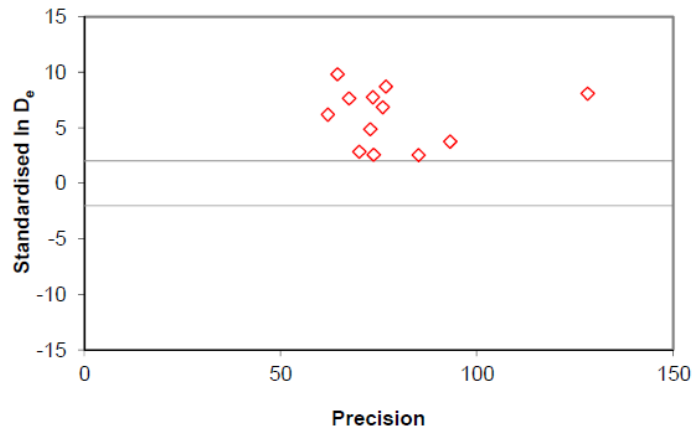
4



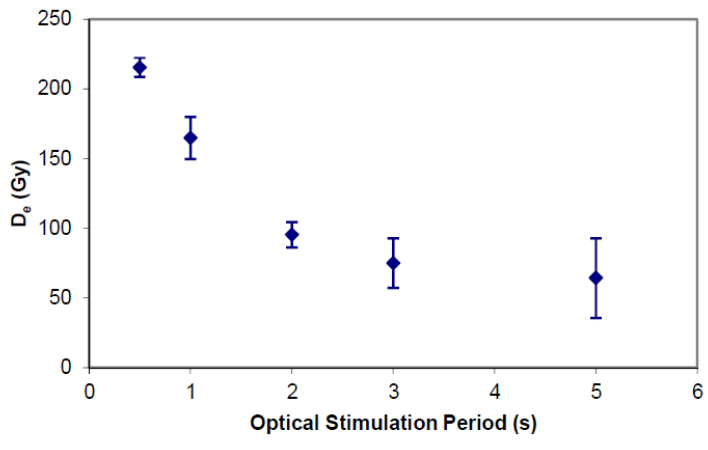
5



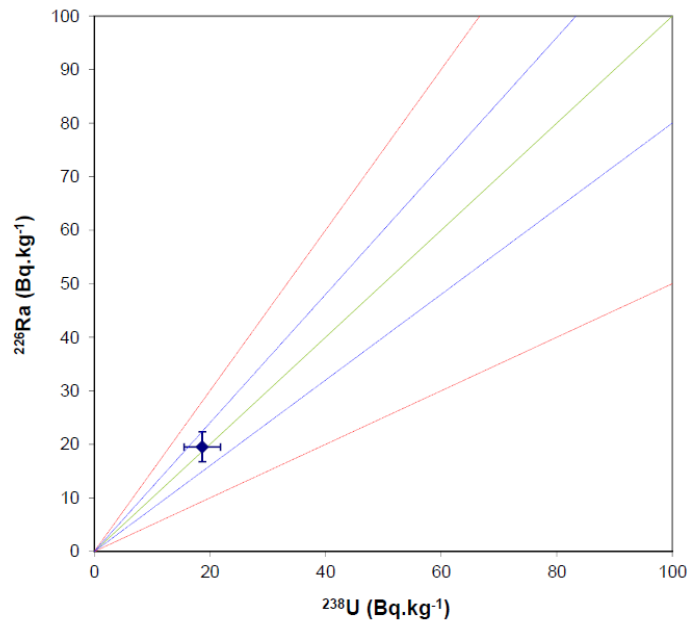
6



7

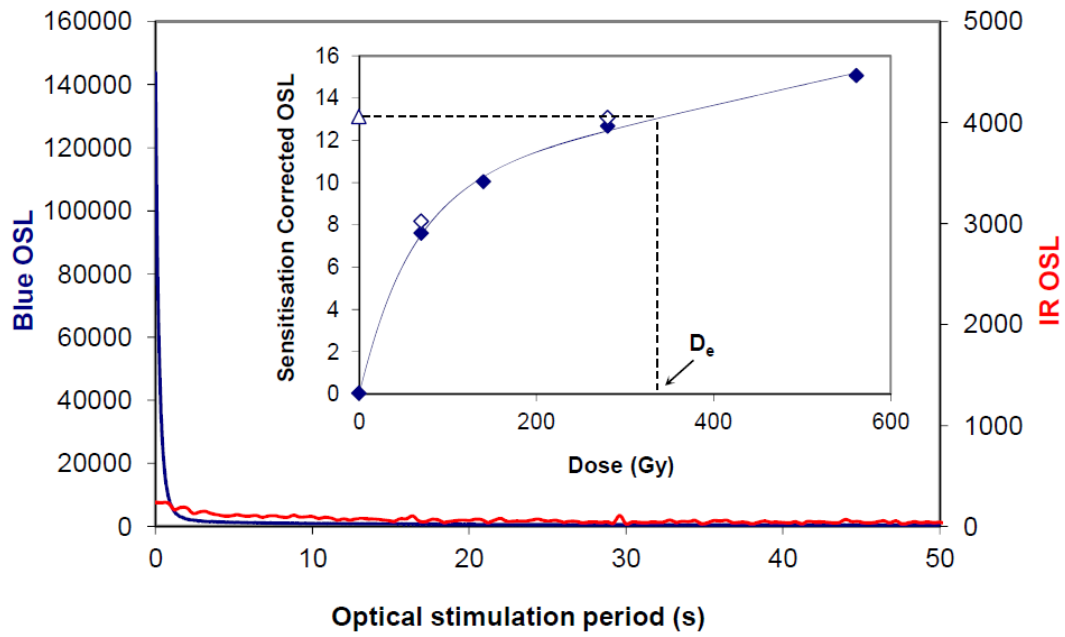


8

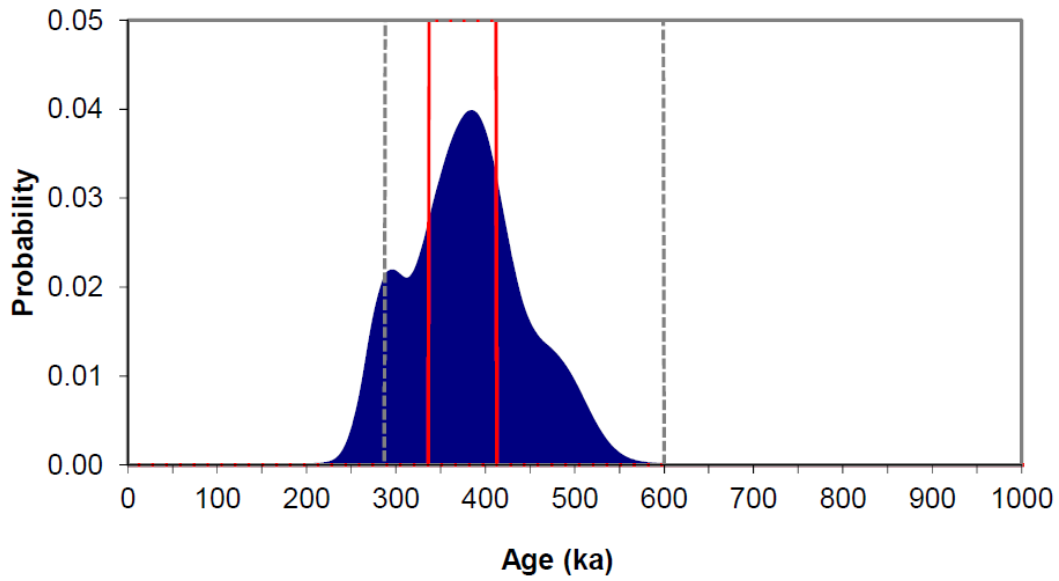


Woodriding GL14048

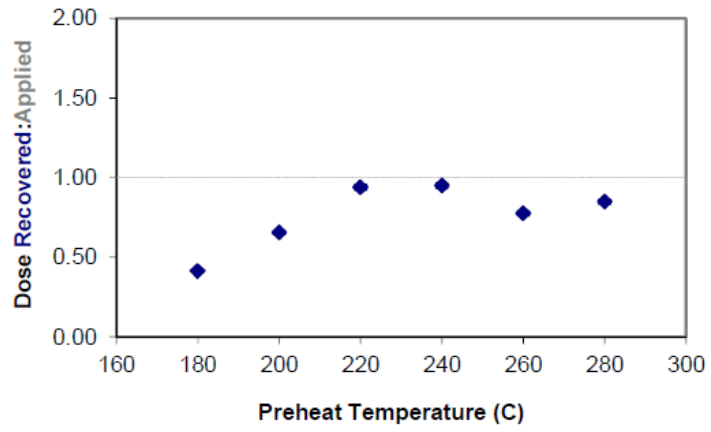
1



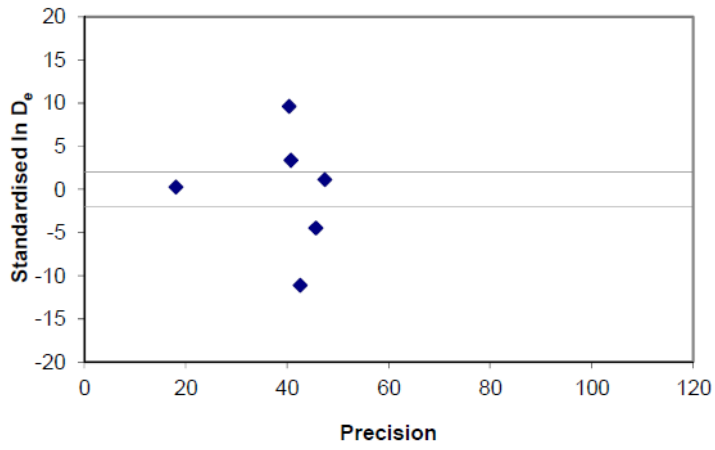
2



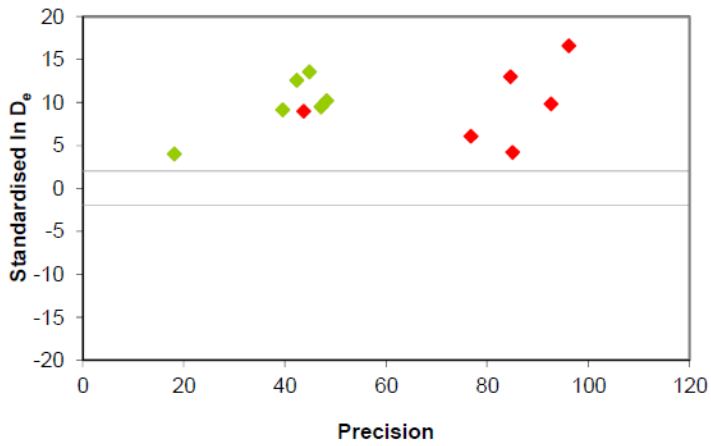
3



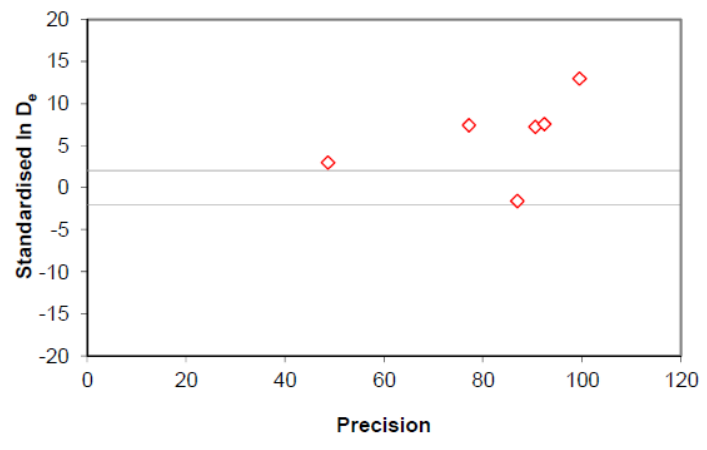
4



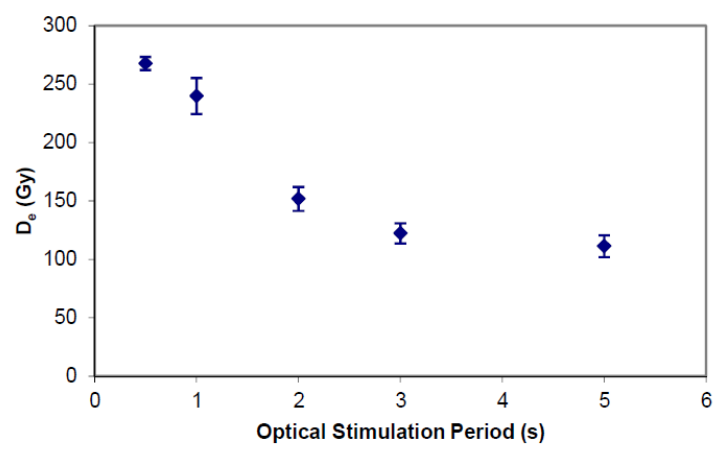
5



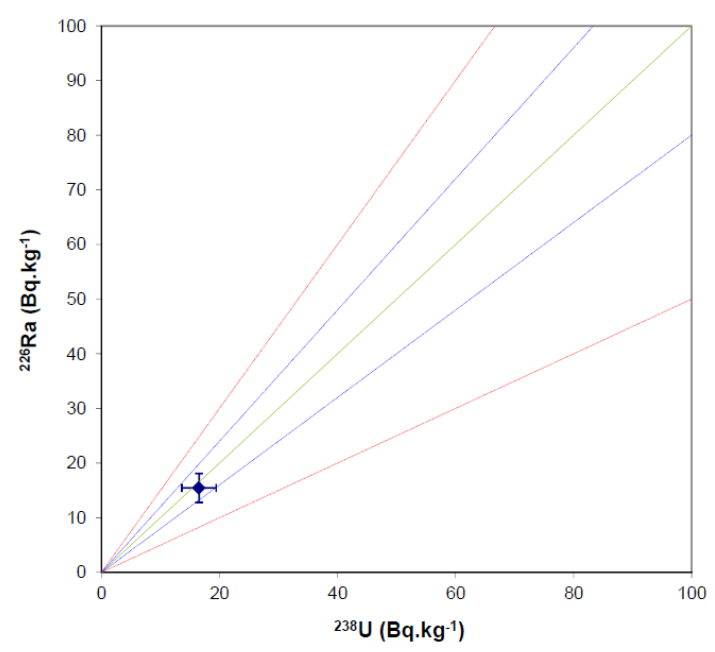
6



7

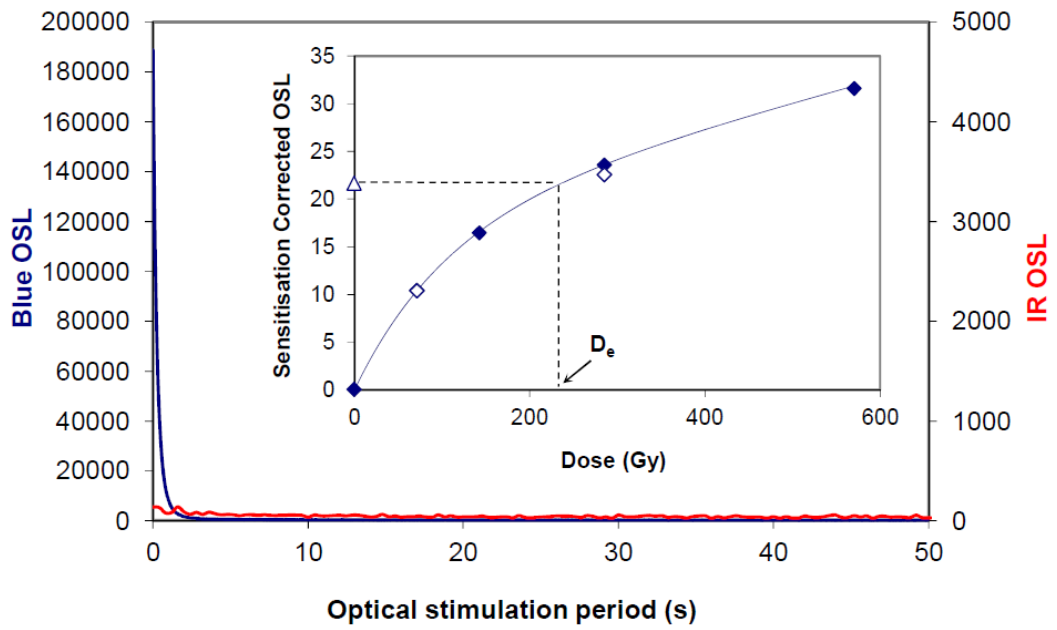


8

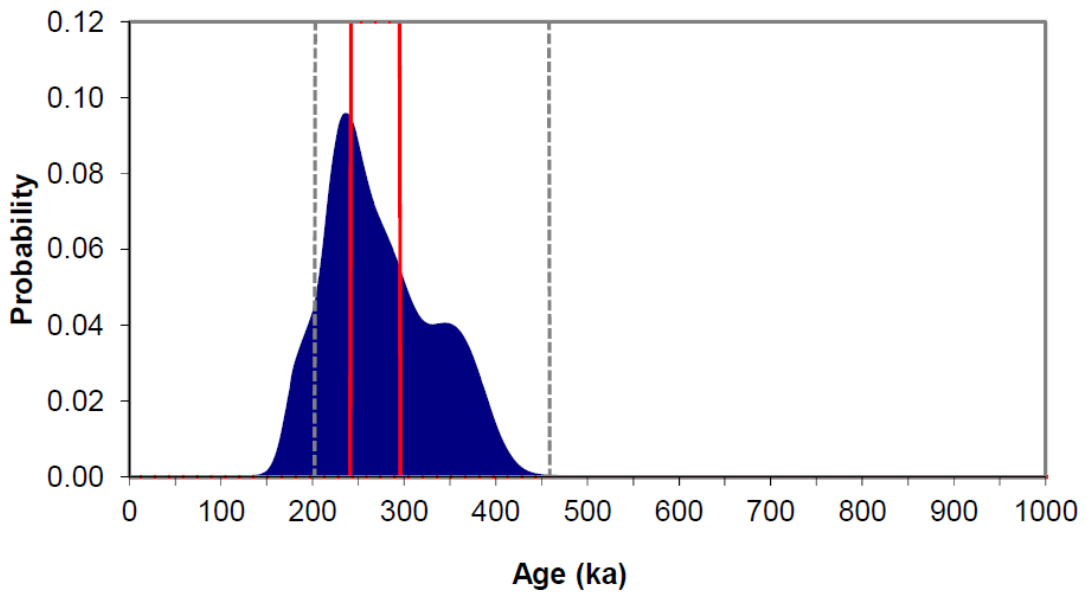


Woodgreen GL14042

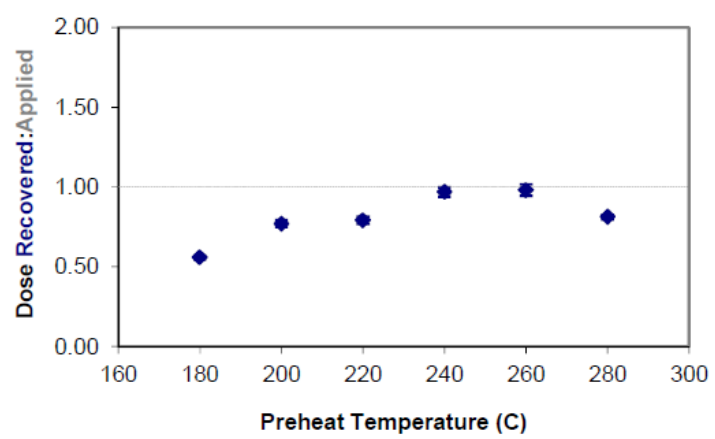
1



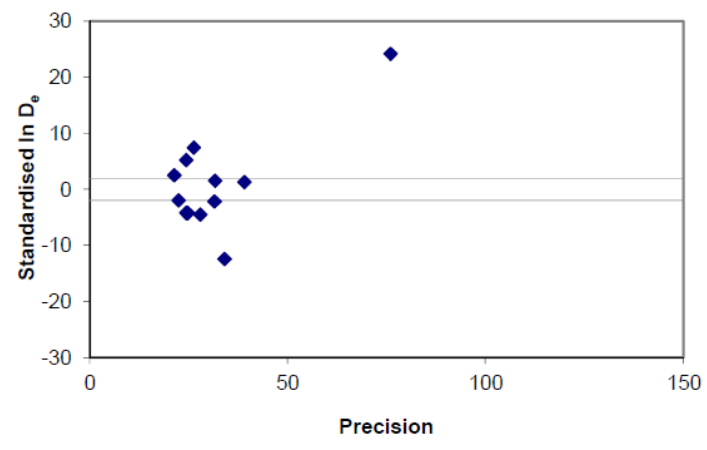
2



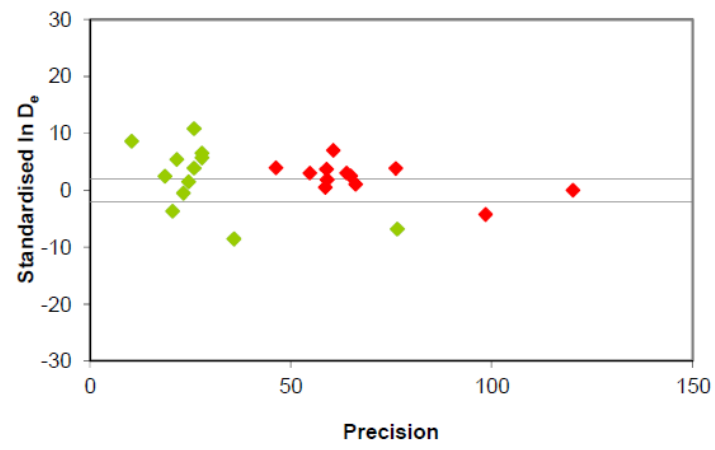
3



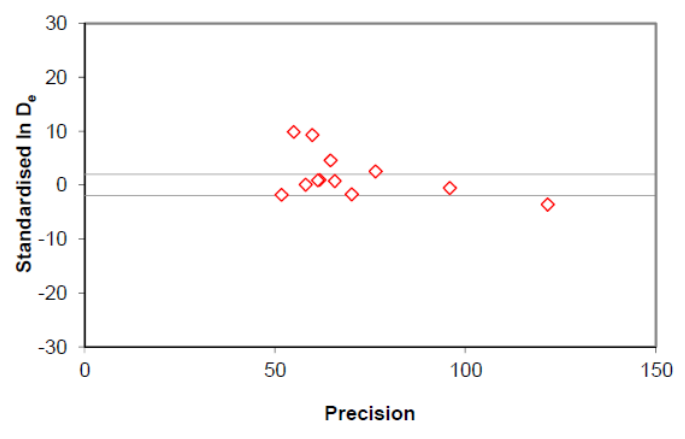
4



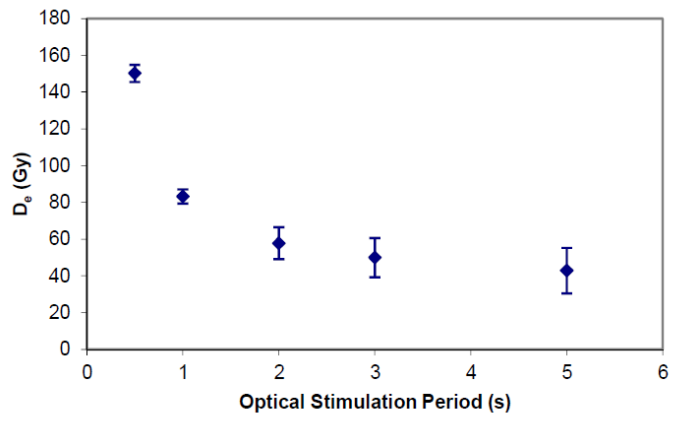
5



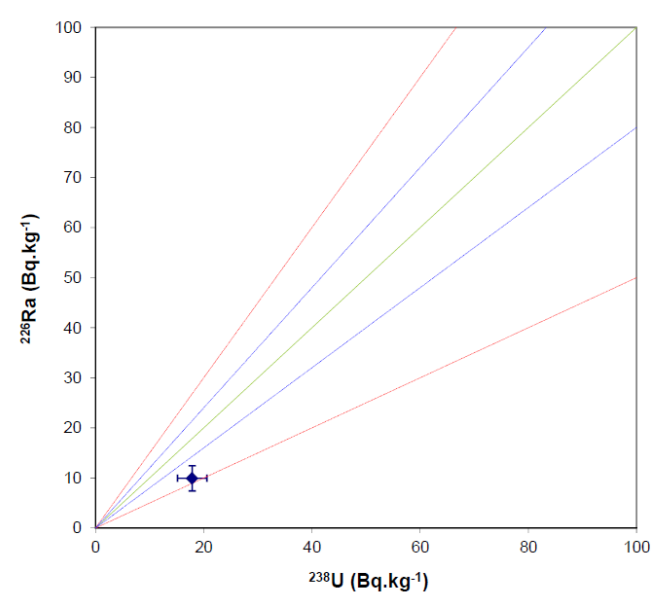
6



7

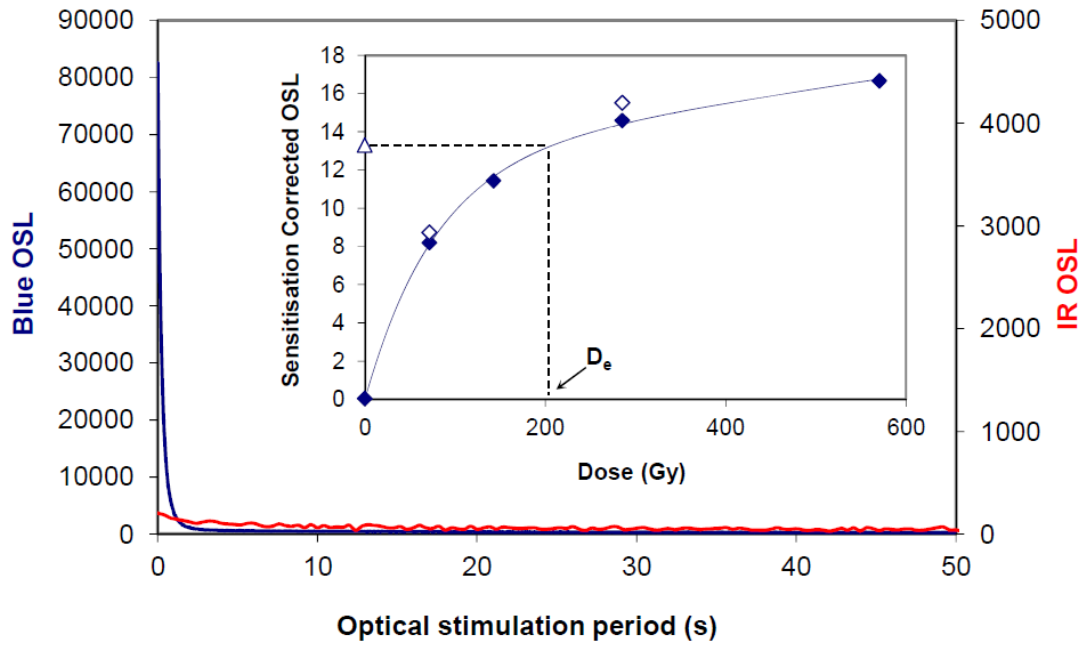


8

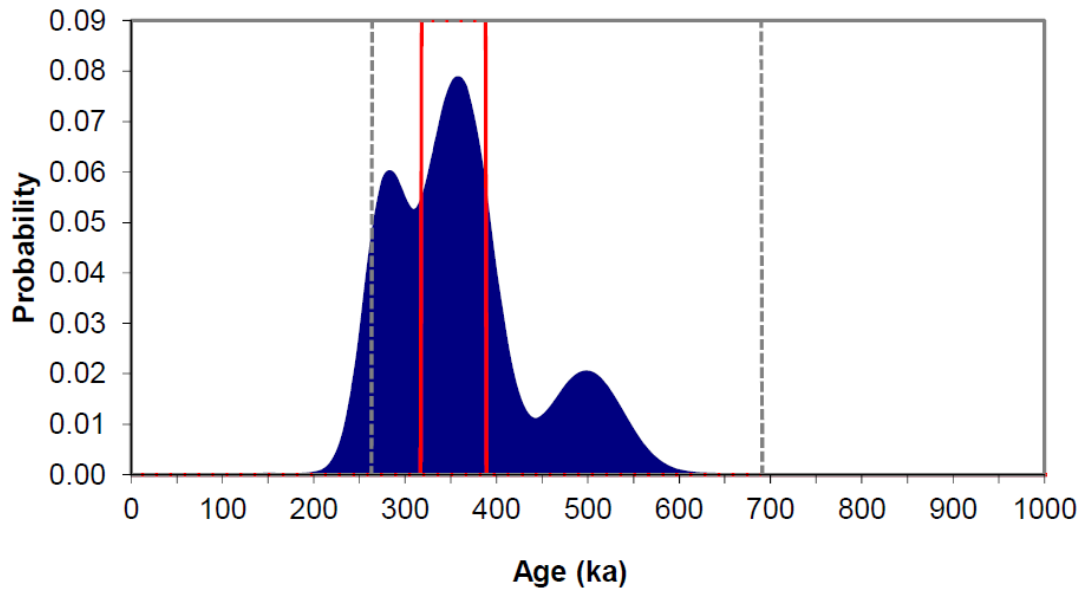


Woodgreen GL14043

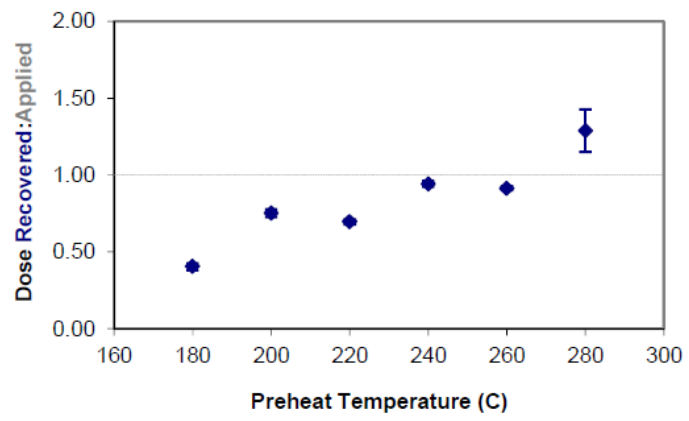
1



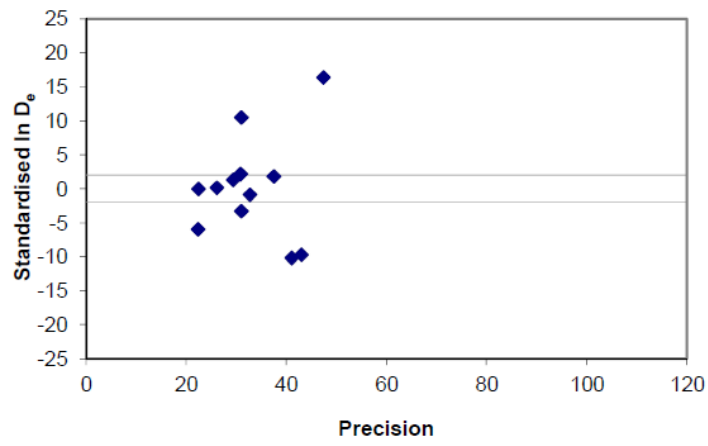
2



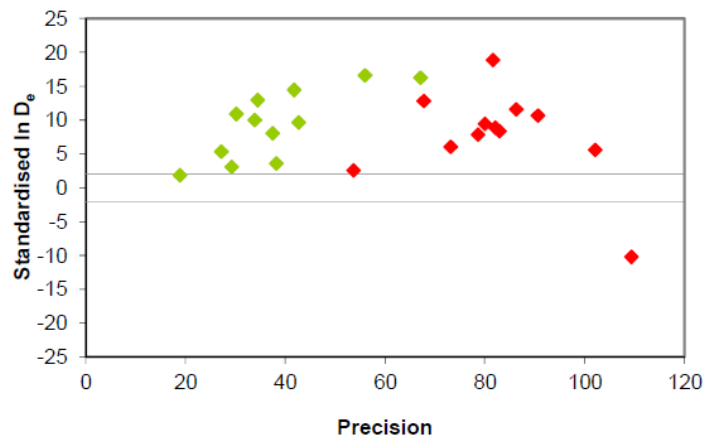
3



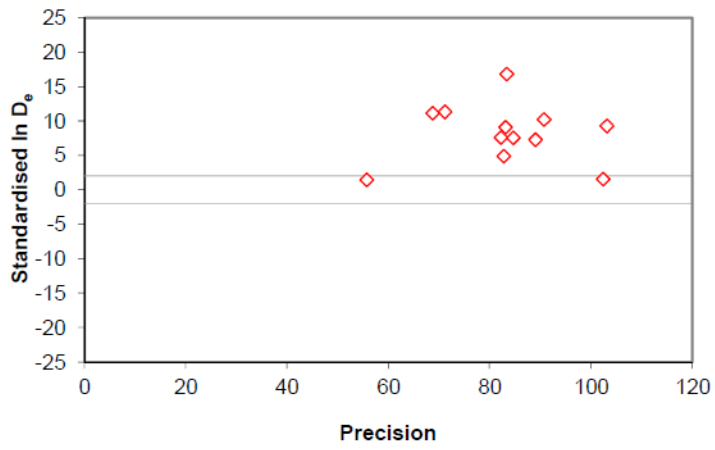
4



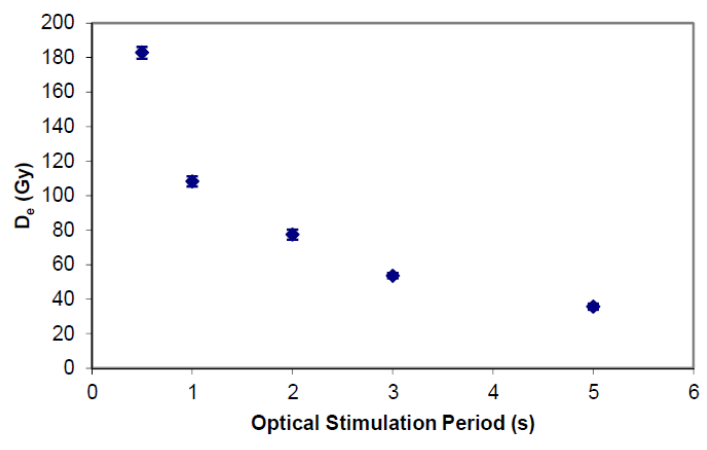
5



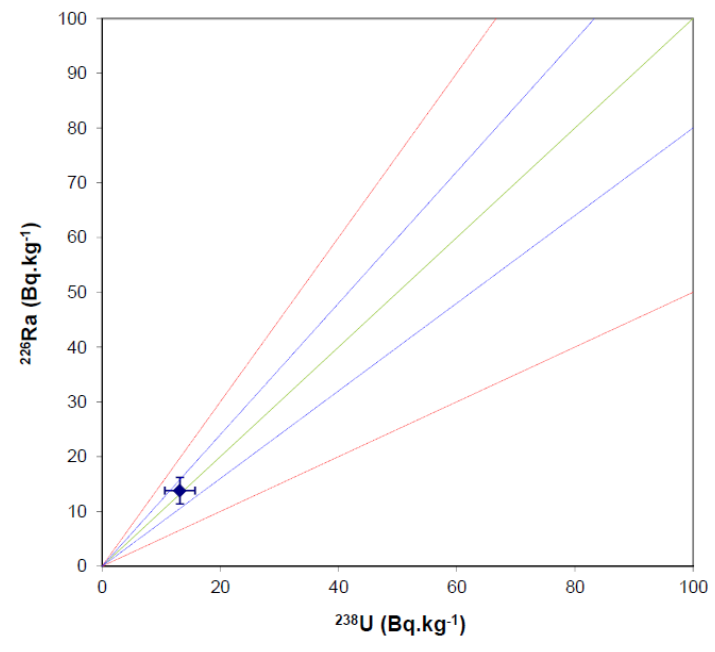
6



7

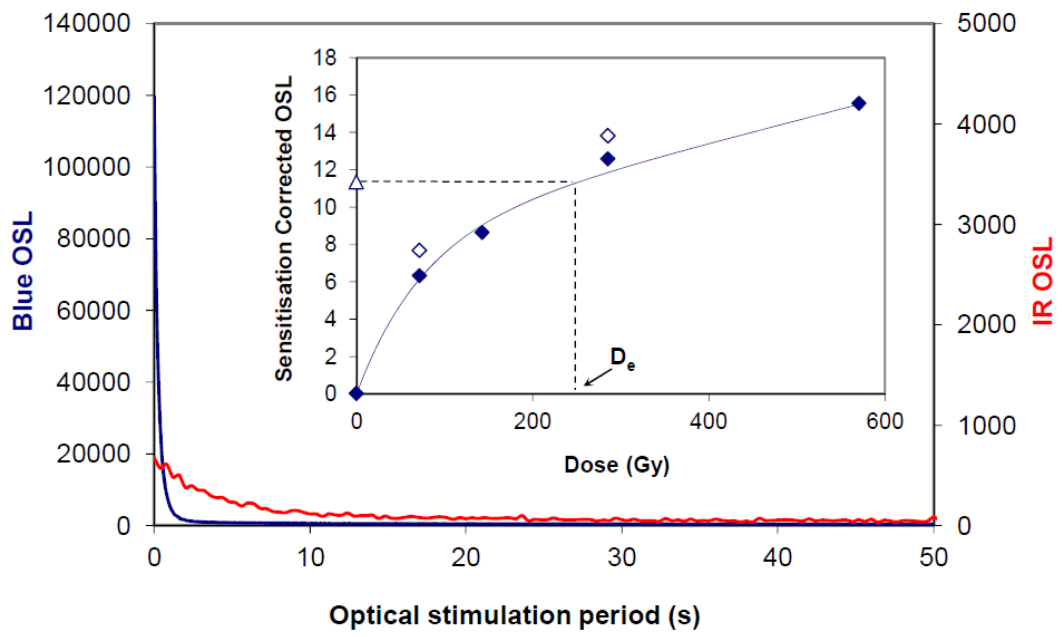


8

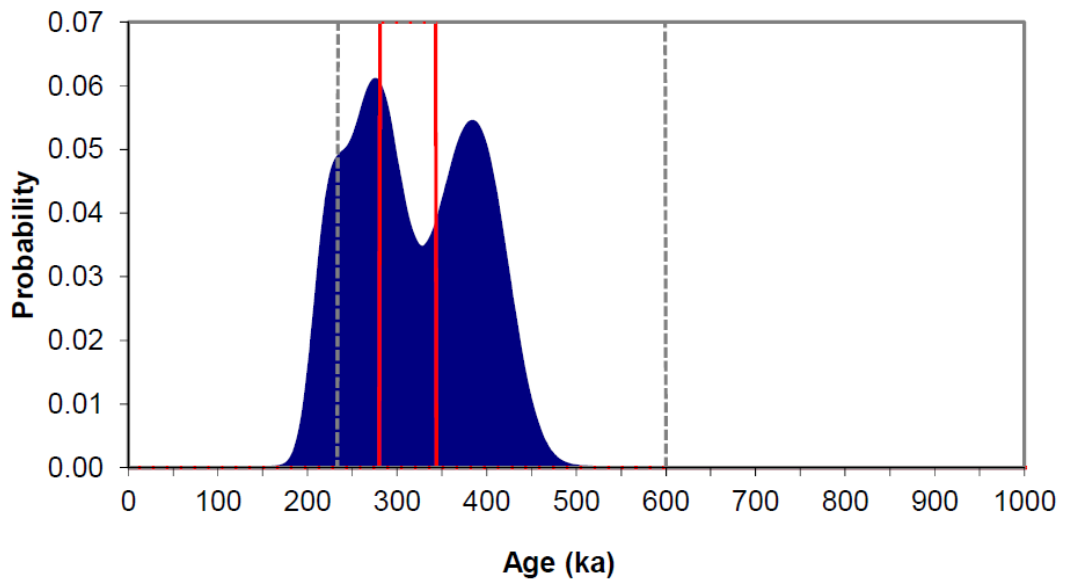


Woodgreen GL14044

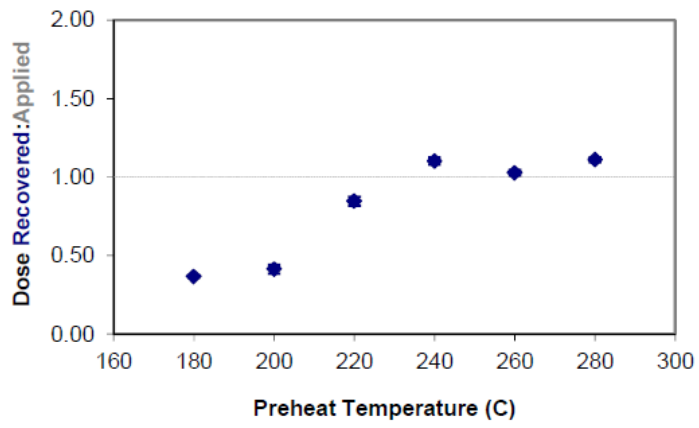
1



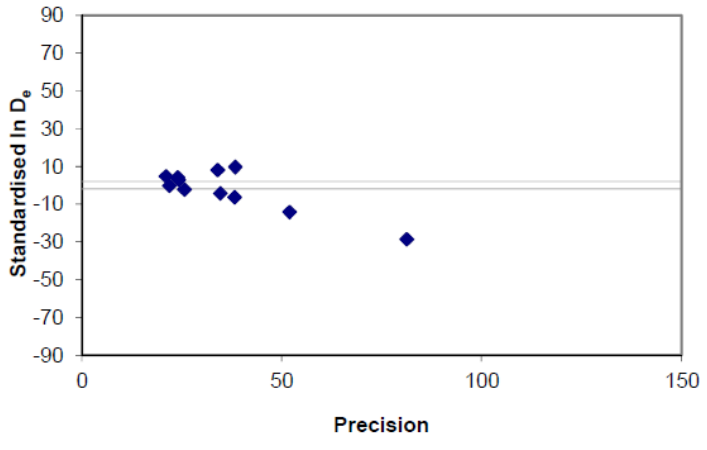
2



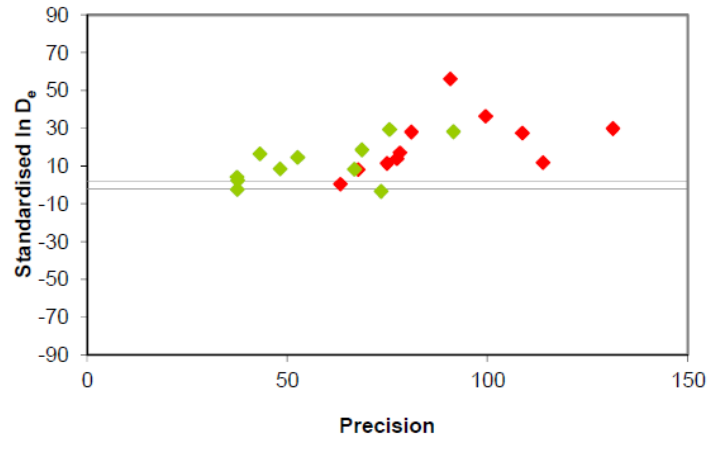
3



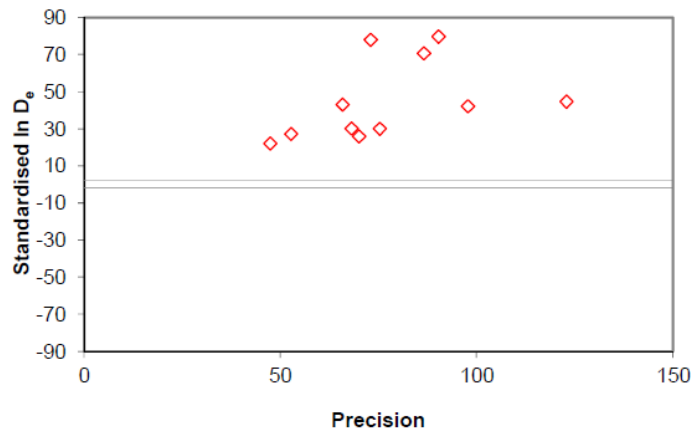
4



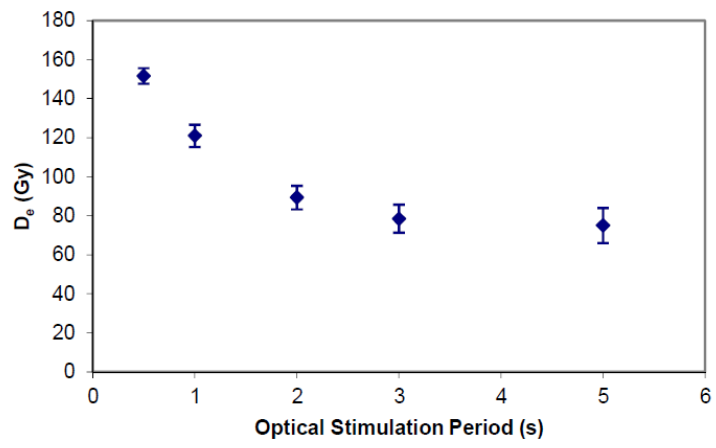
5



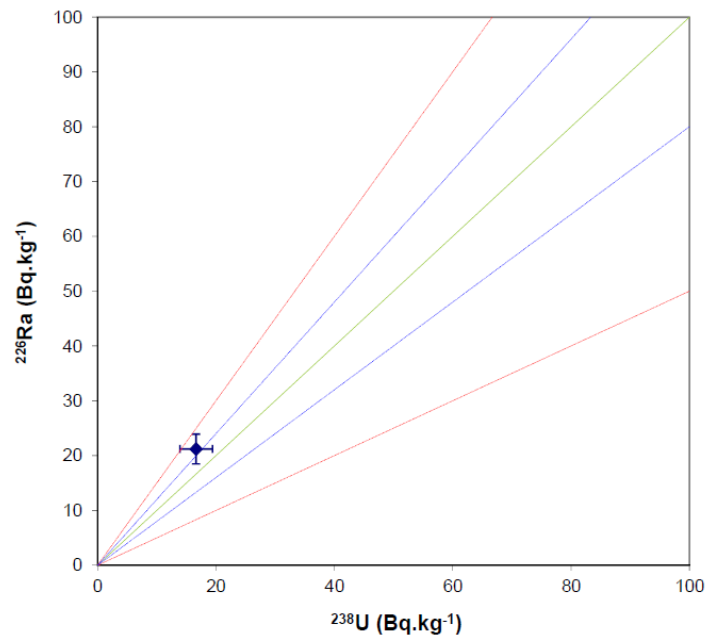
6



7

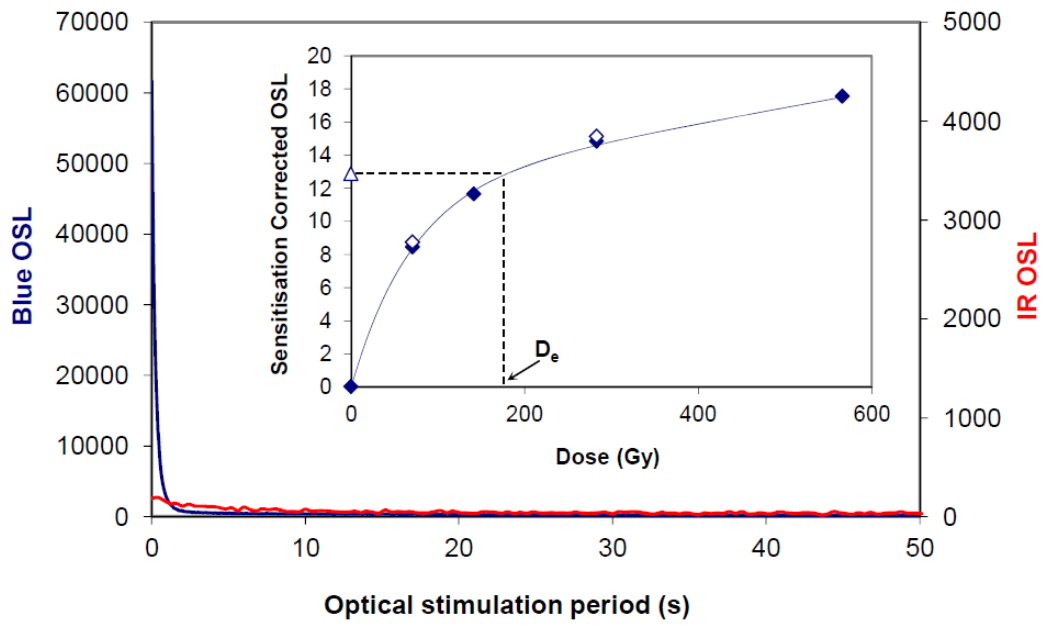


8

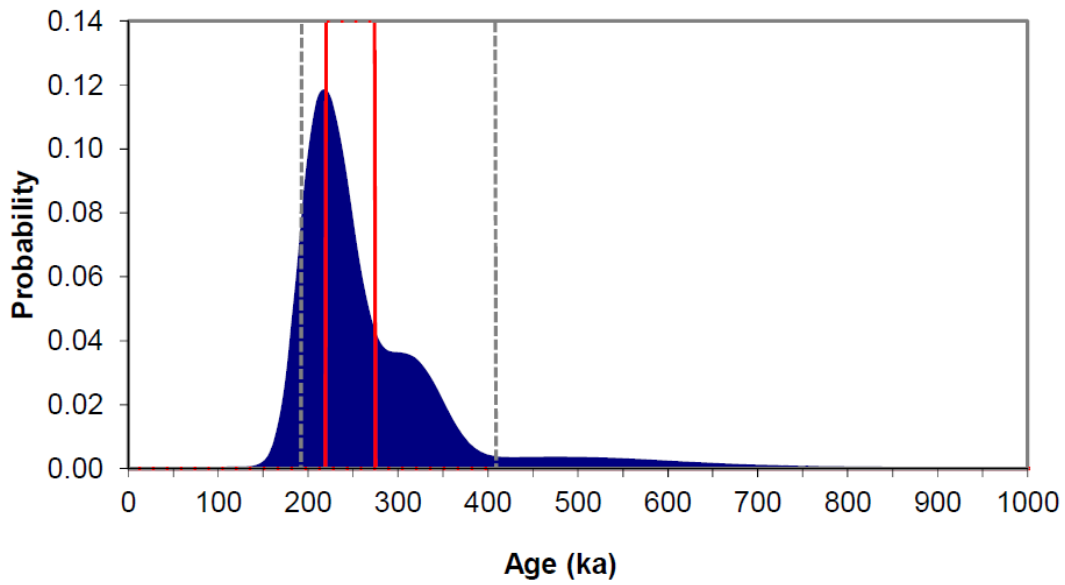


Somerley GL15038

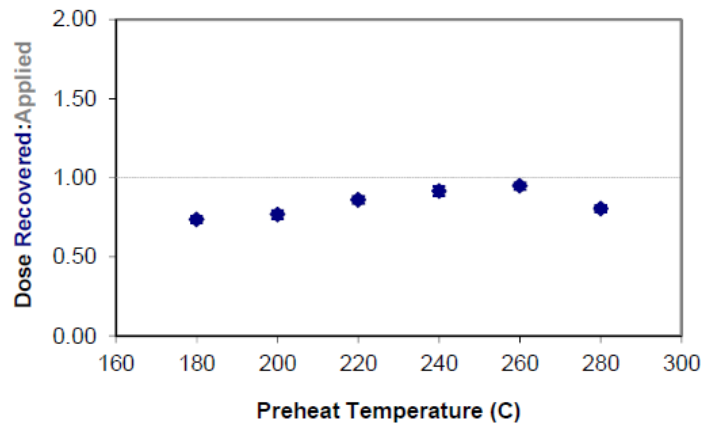
1



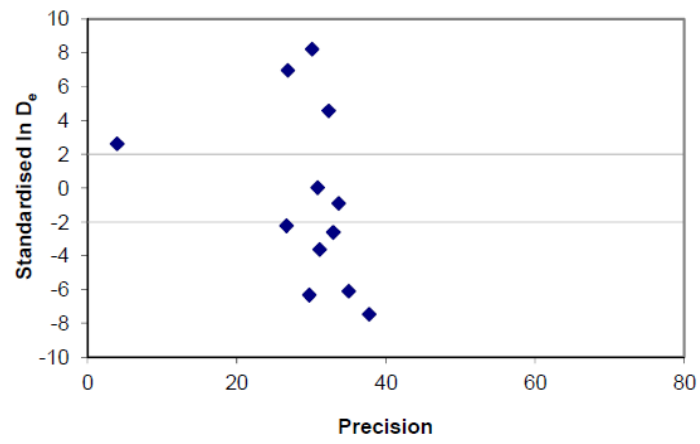
2



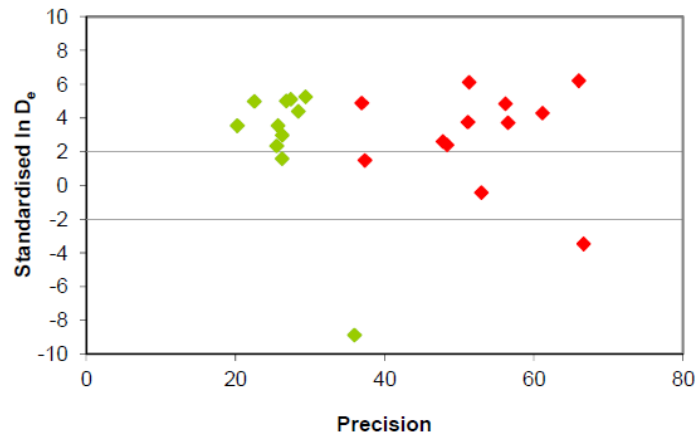
3



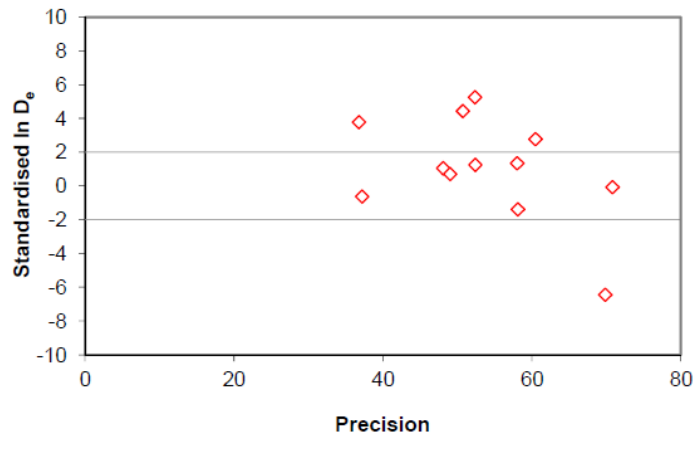
4



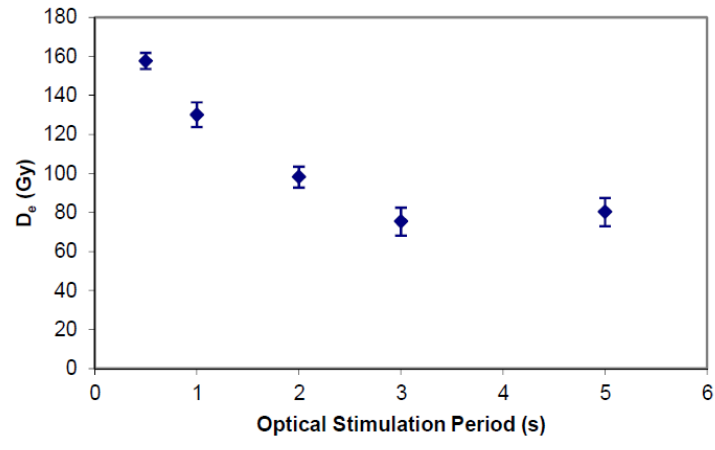
5



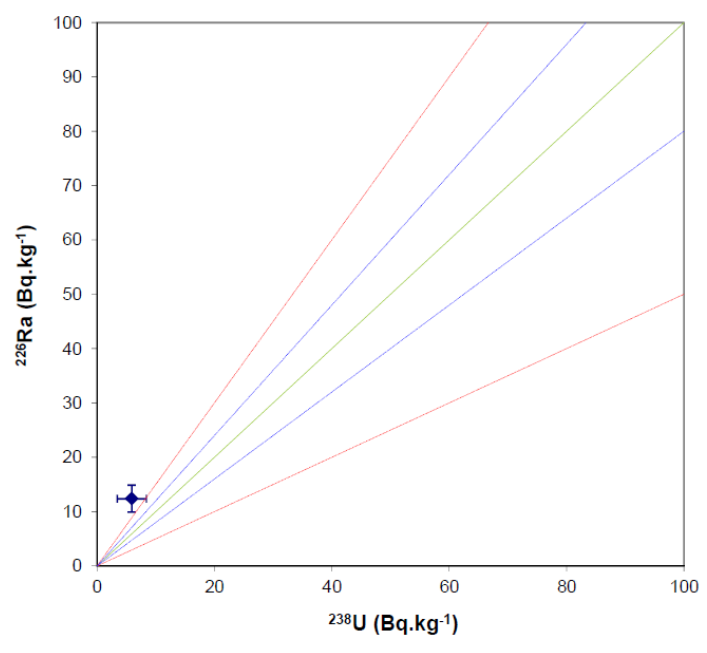
6



7

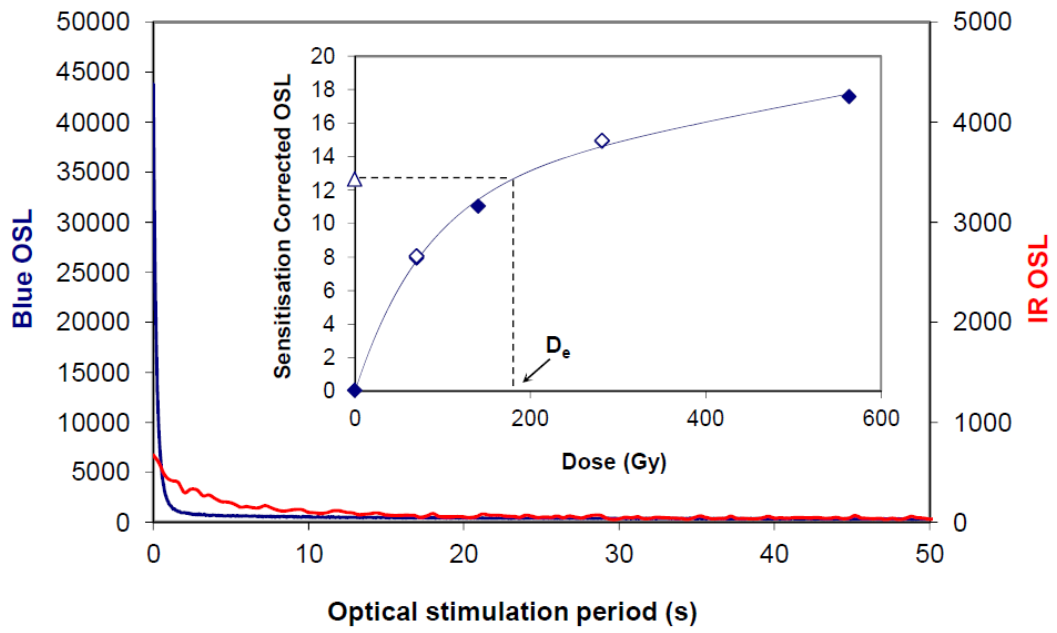


8

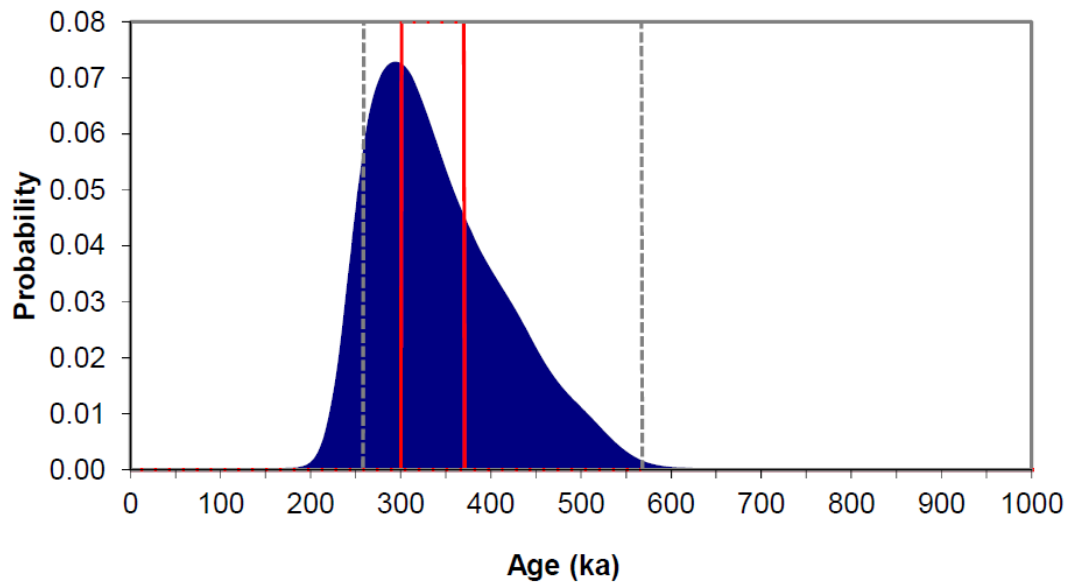


Somerley GL15039

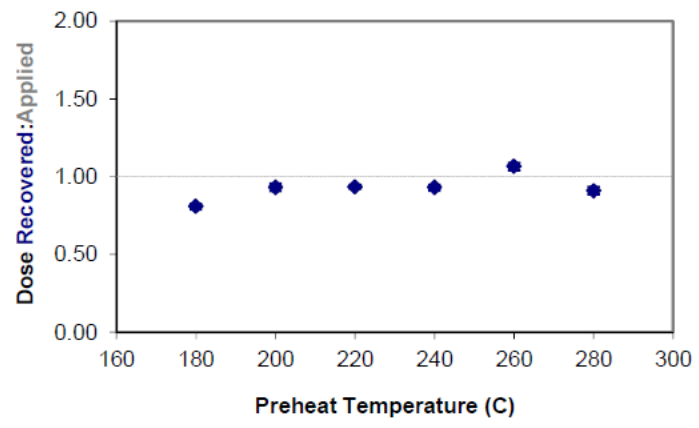
1



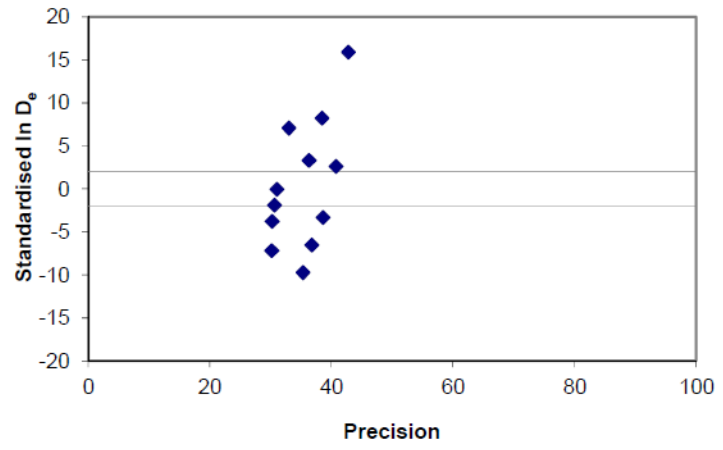
2



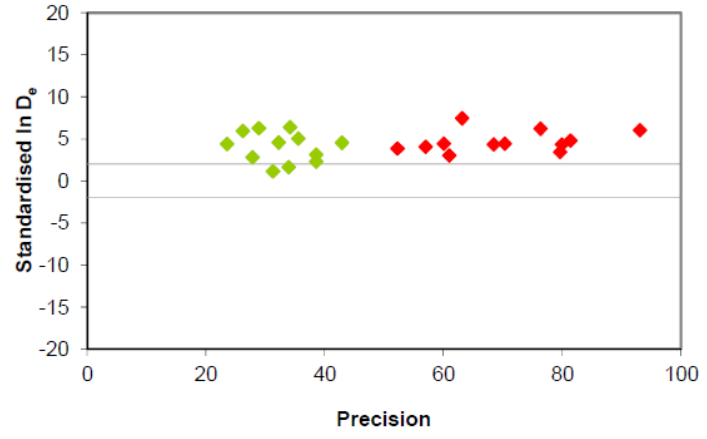
3



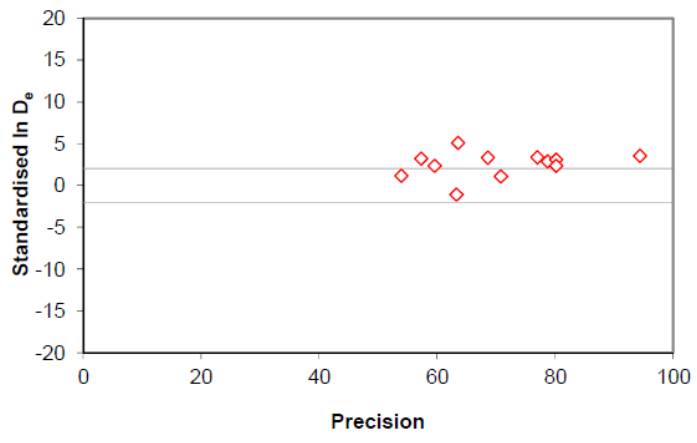
4



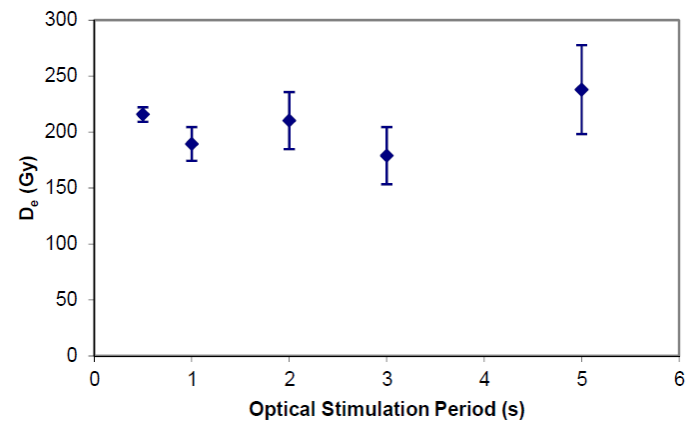
5



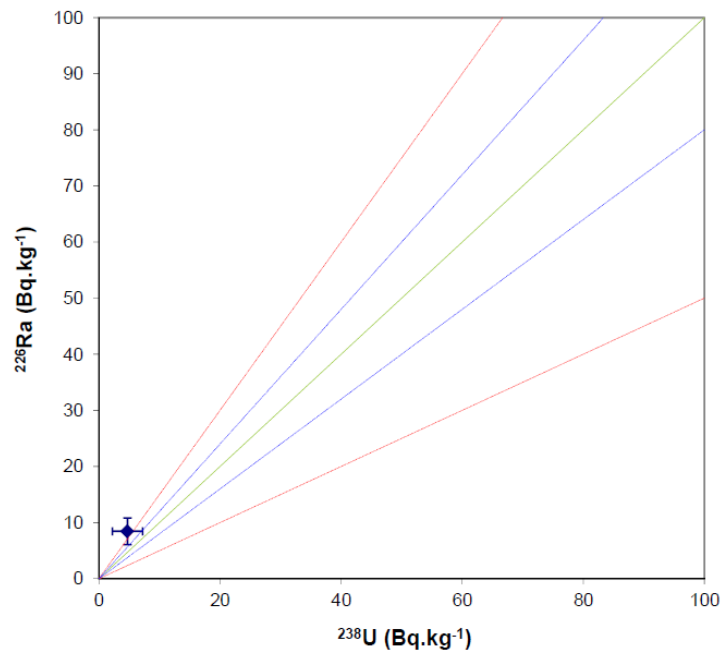
6



7

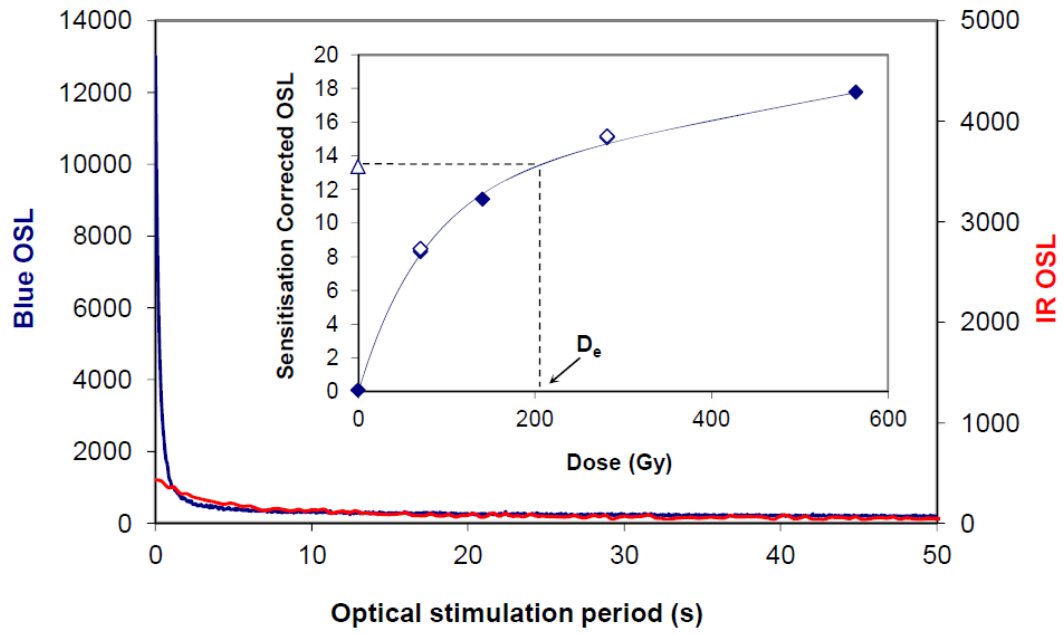


8

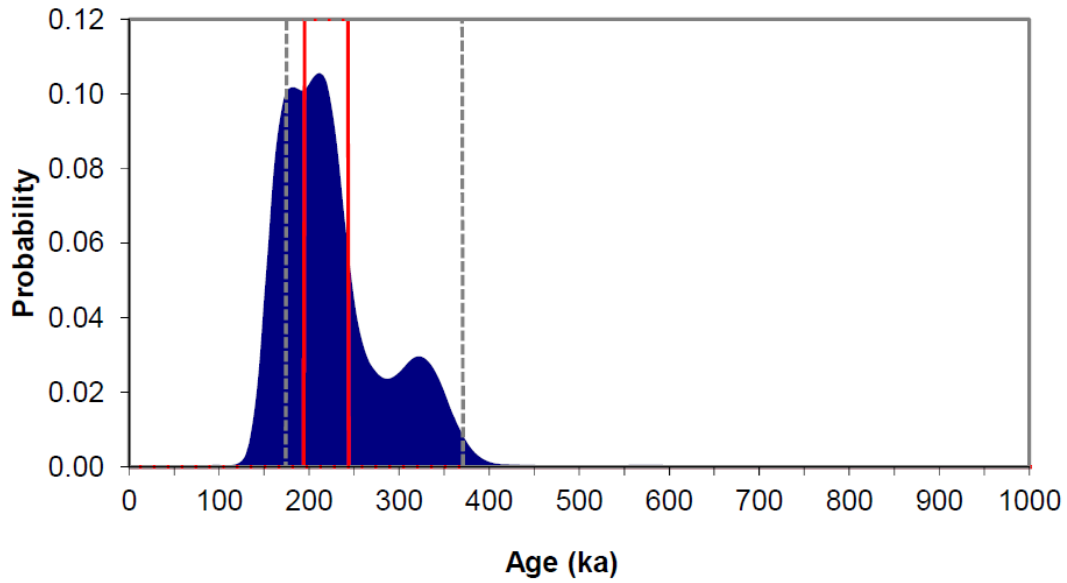


Somerley GL15040

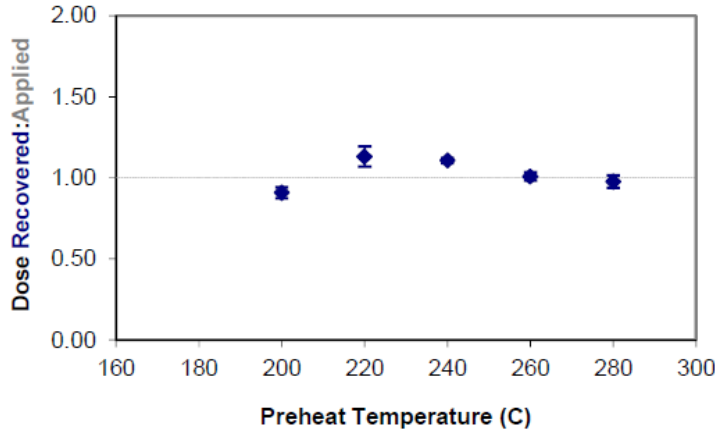
1



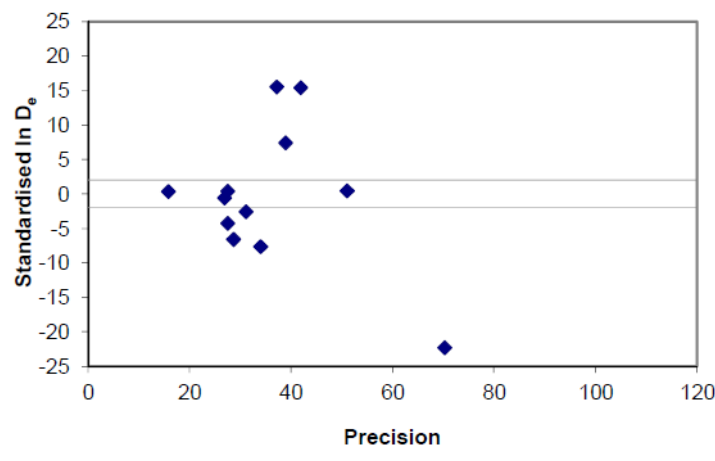
2



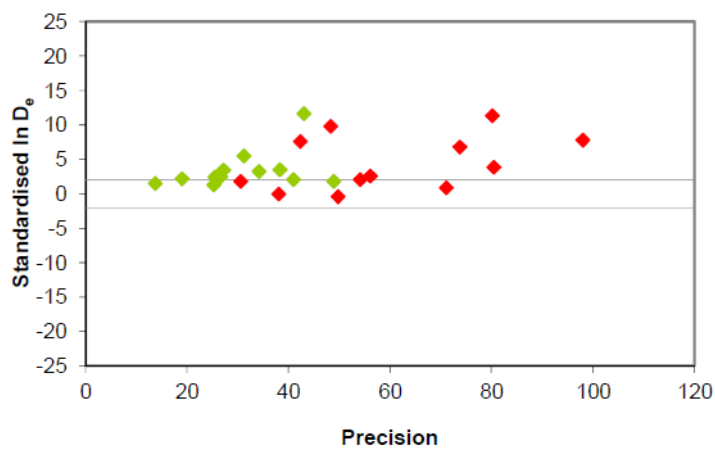
3



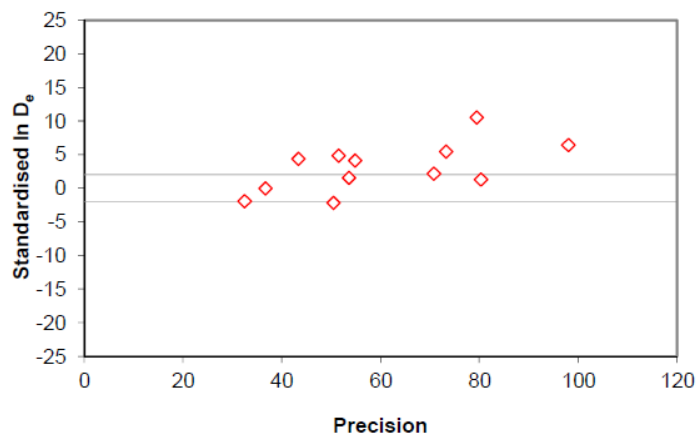
4



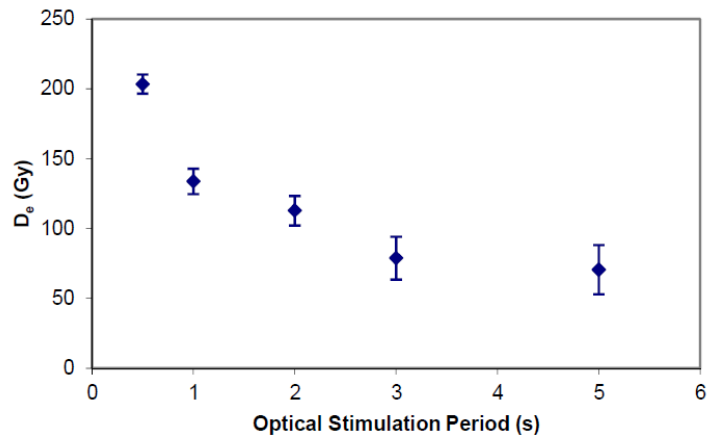
5



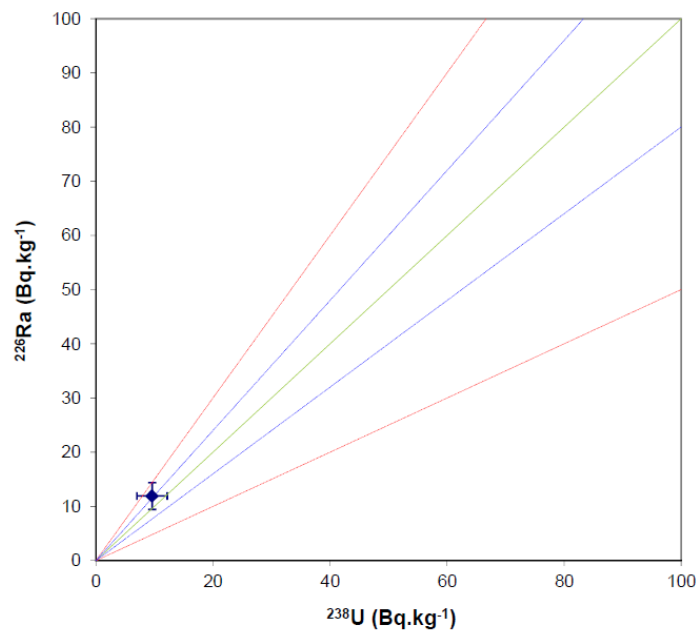
6



7

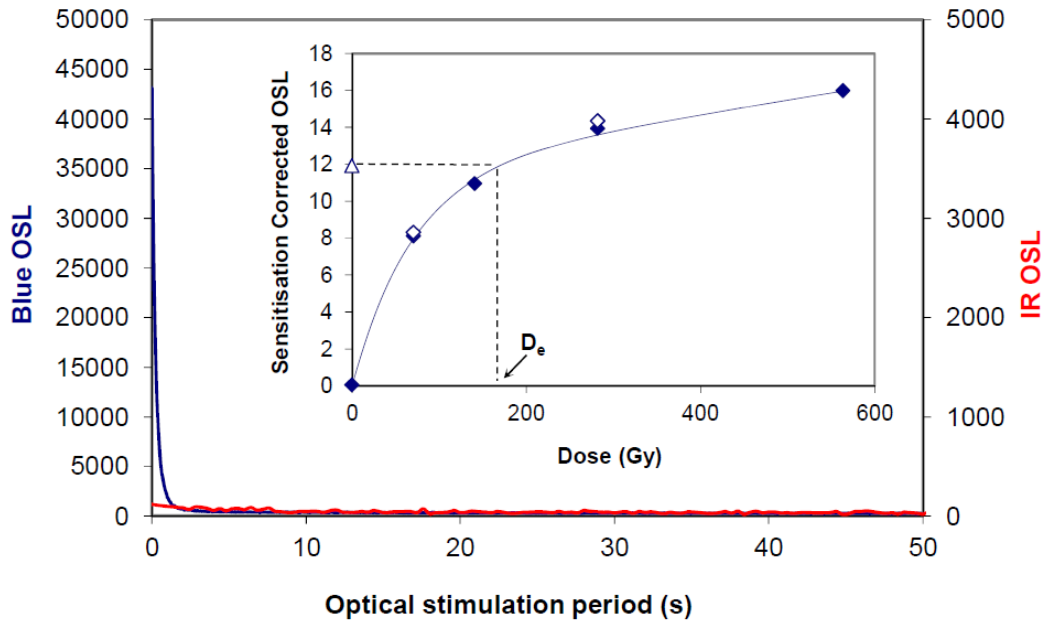


8

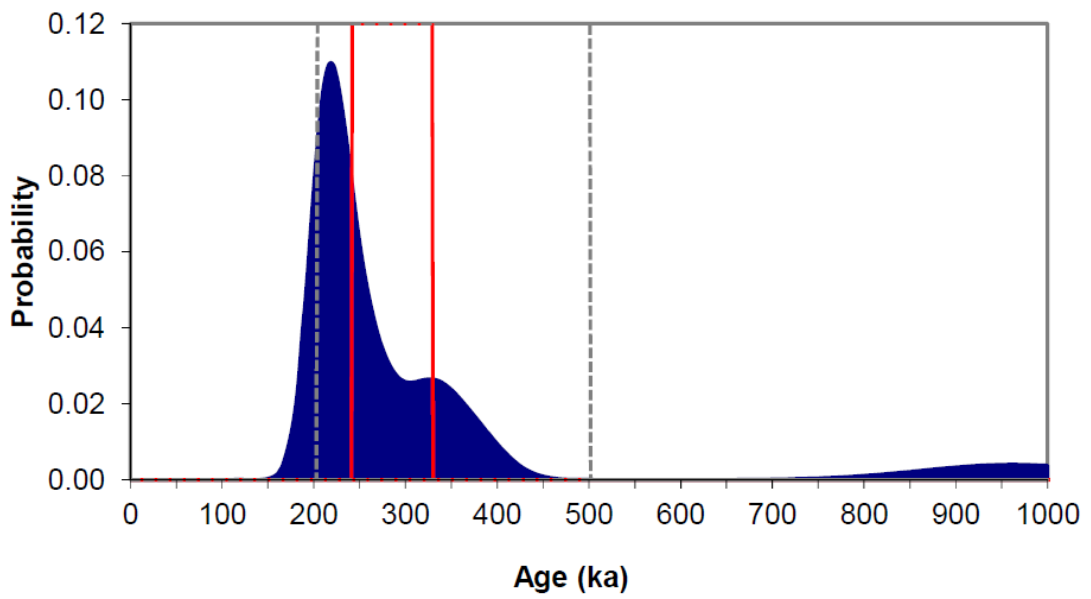


Somerley GL15041

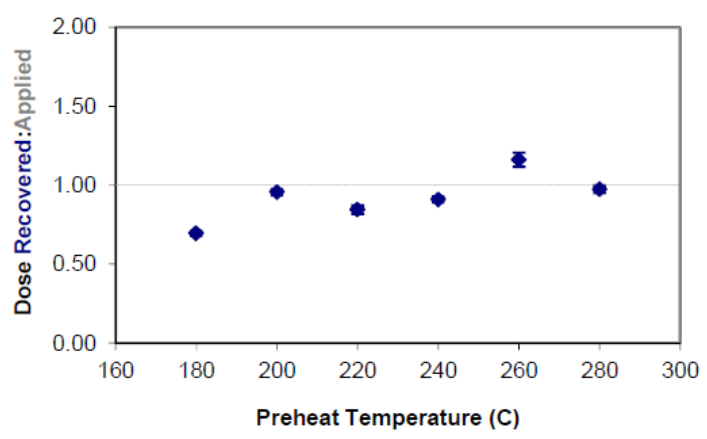
1



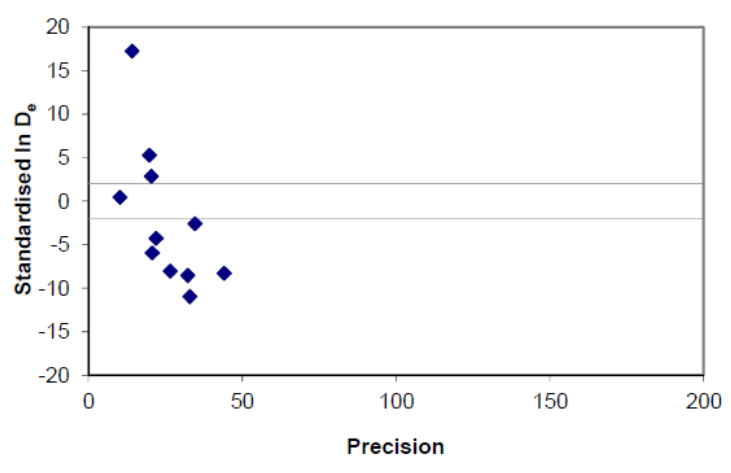
2



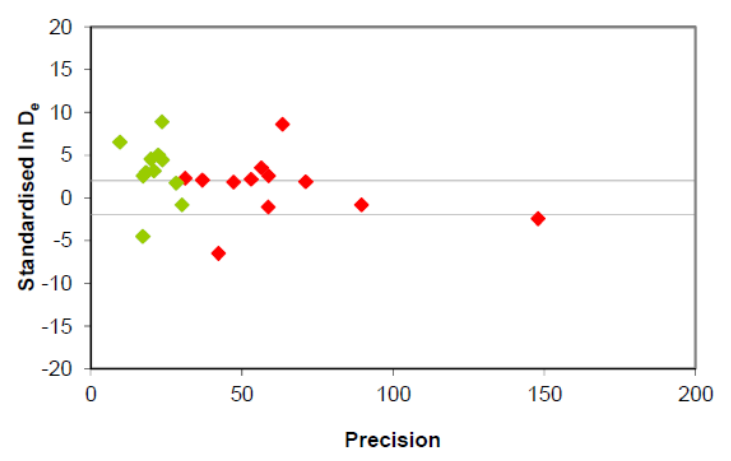
3



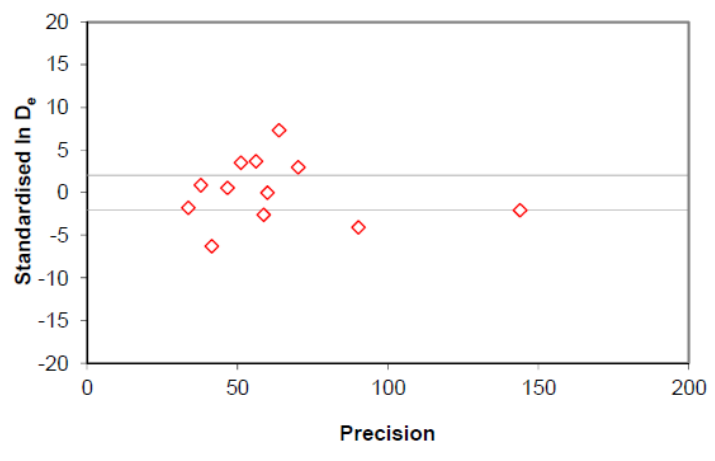
4



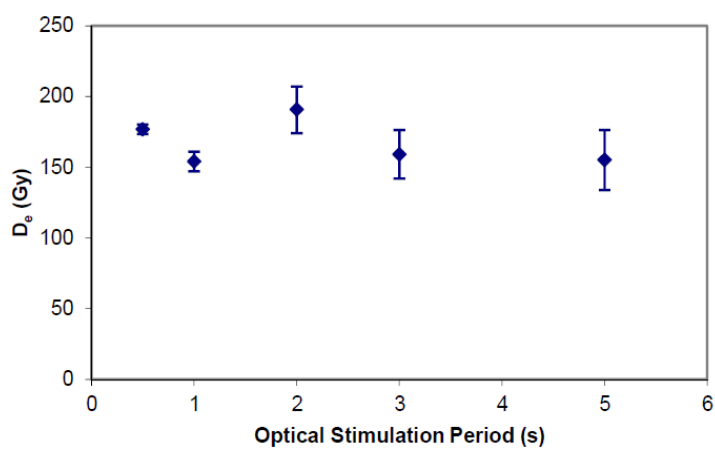
5



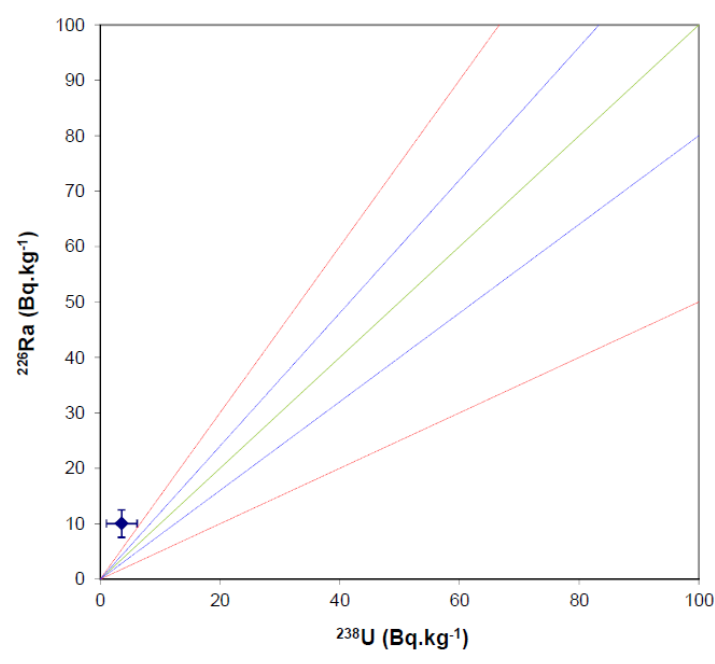
6



7

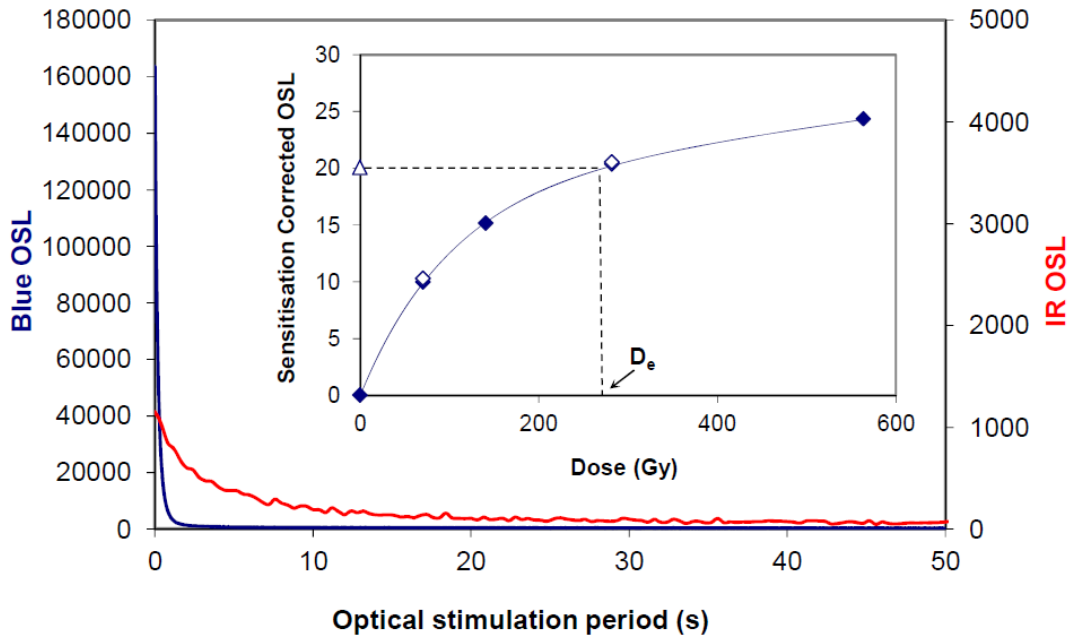


8

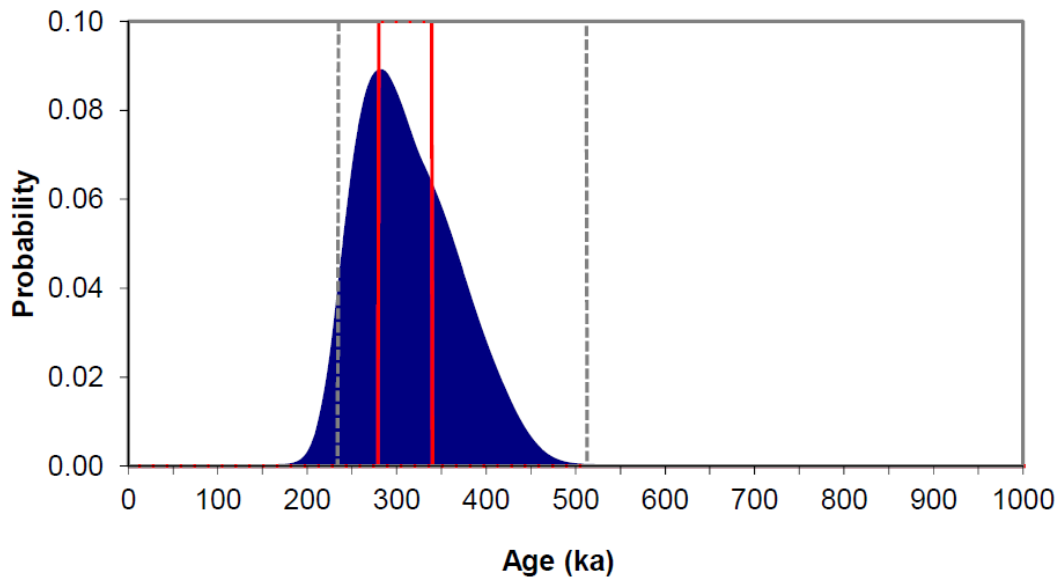


Somerley GL15042

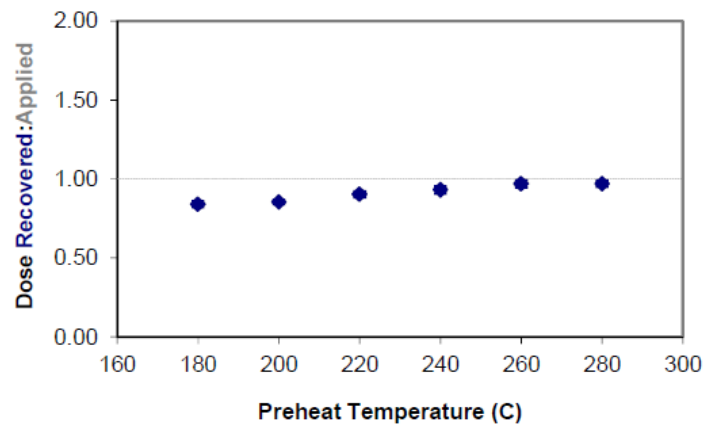
1



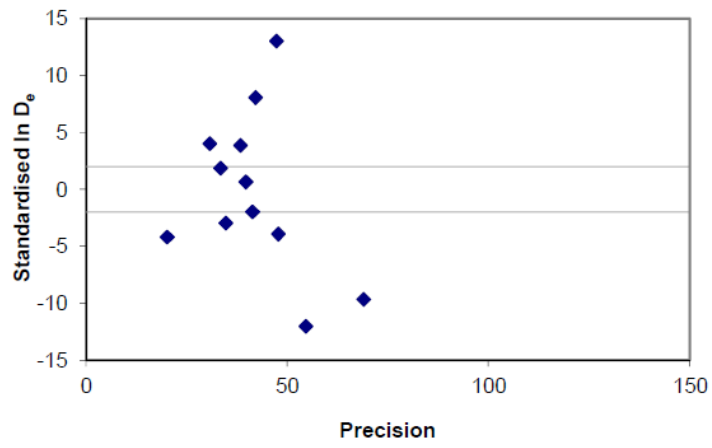
2



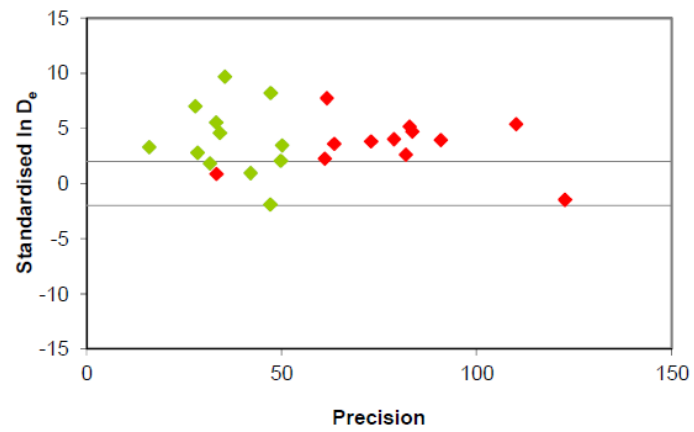
3



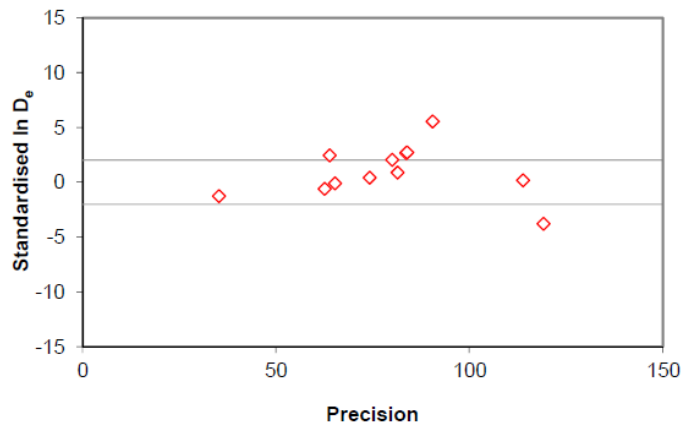
4



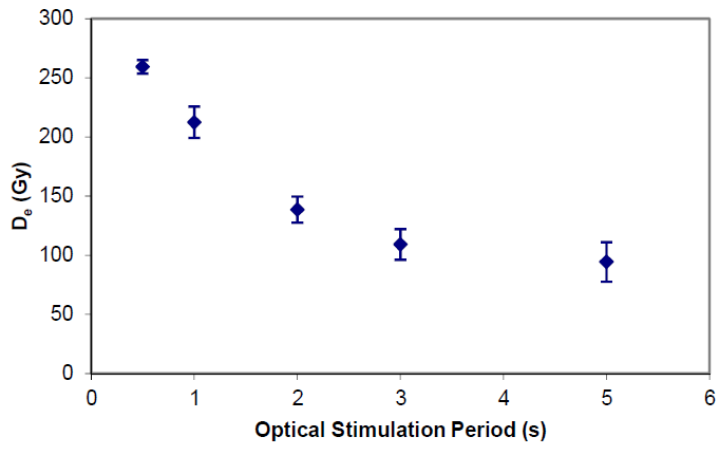
5



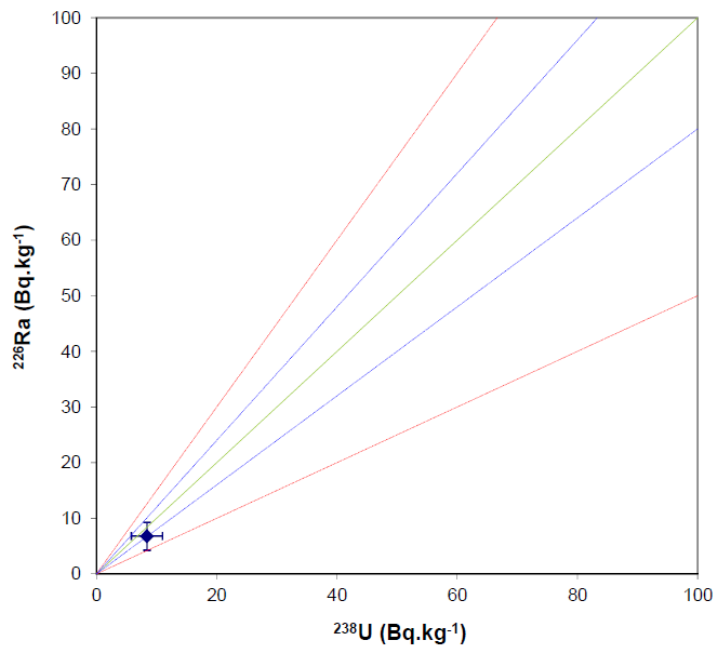
6



7

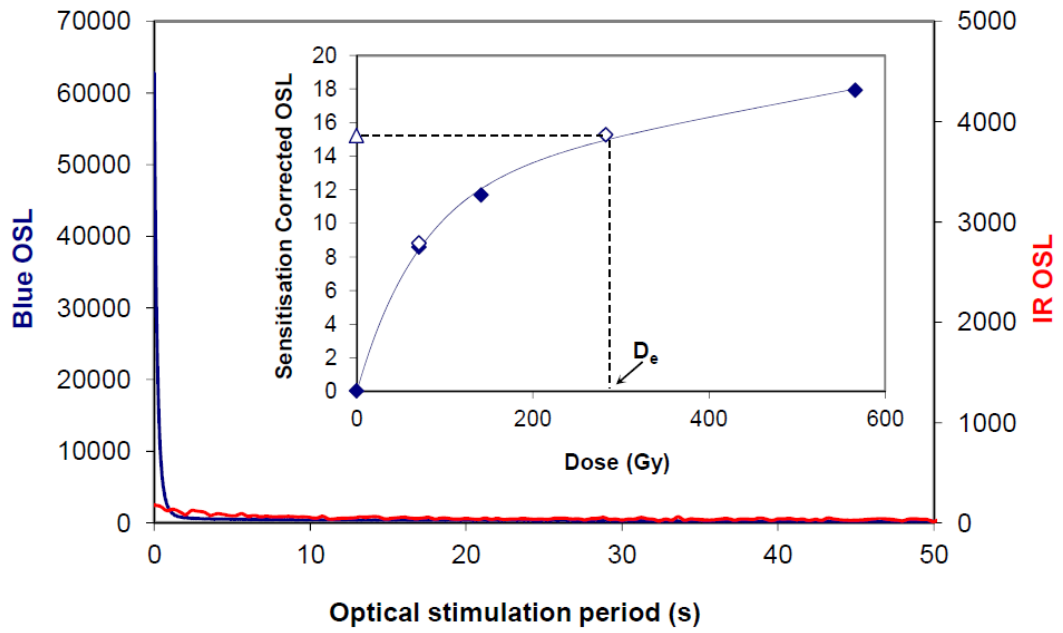


8

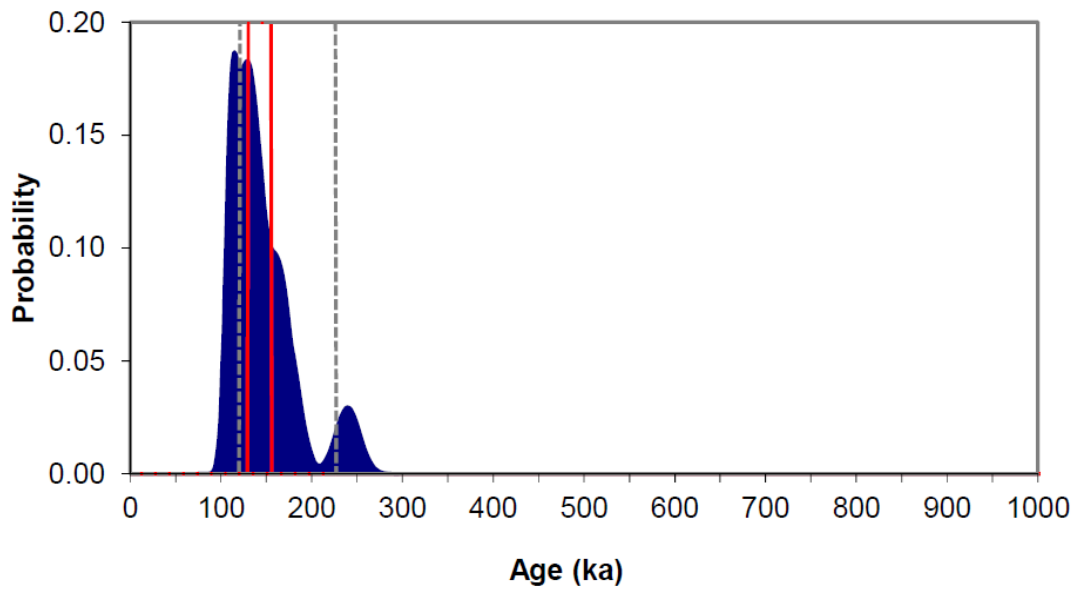


Ashley GL15033

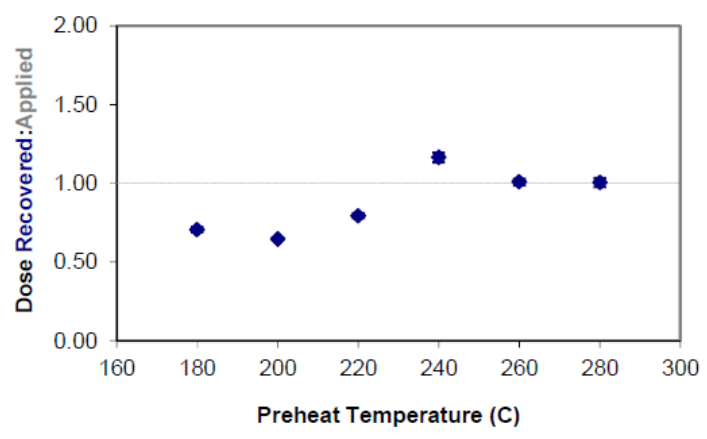
1



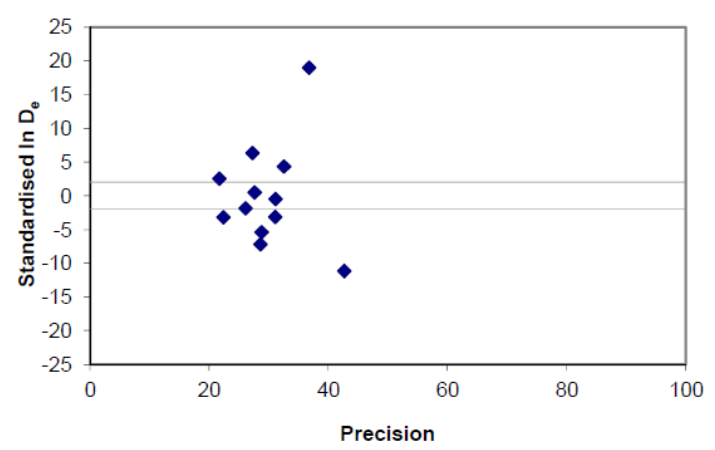
2



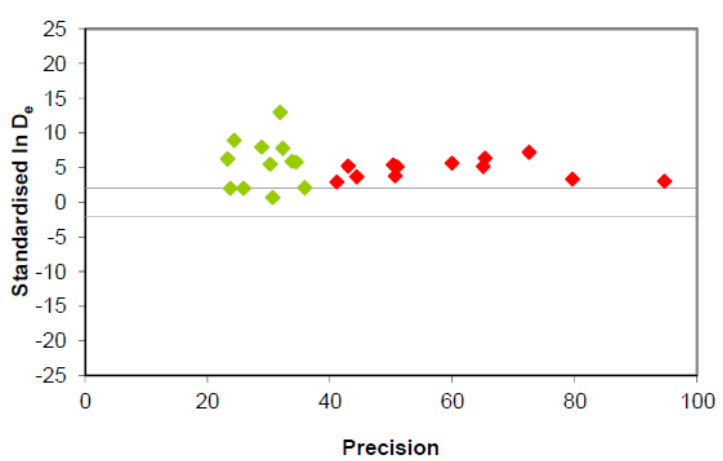
3



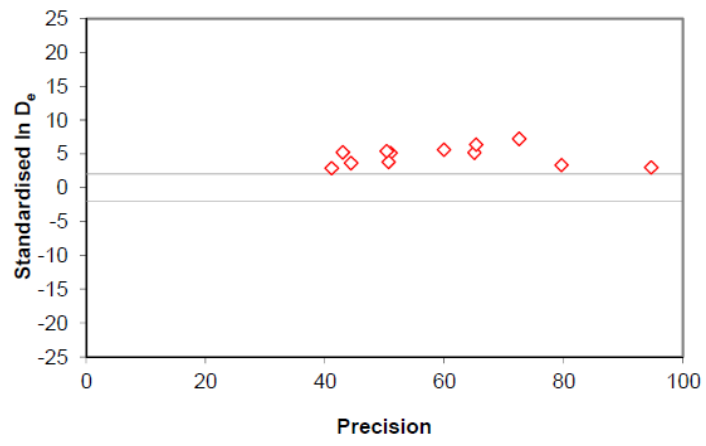
4



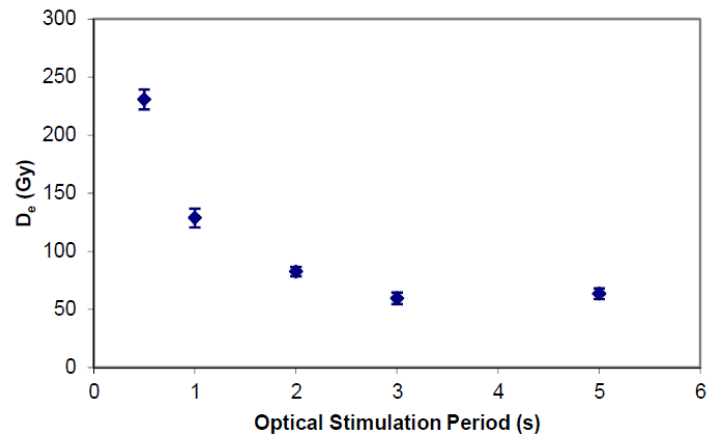
5



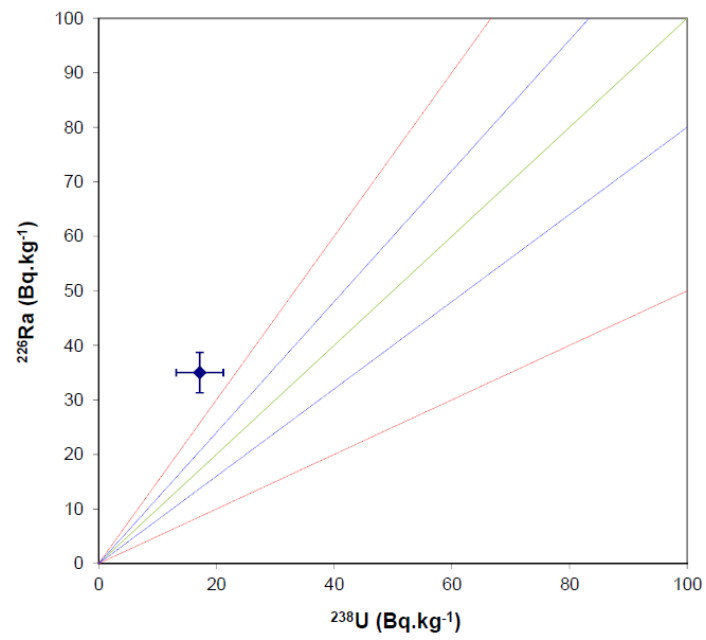
6



7

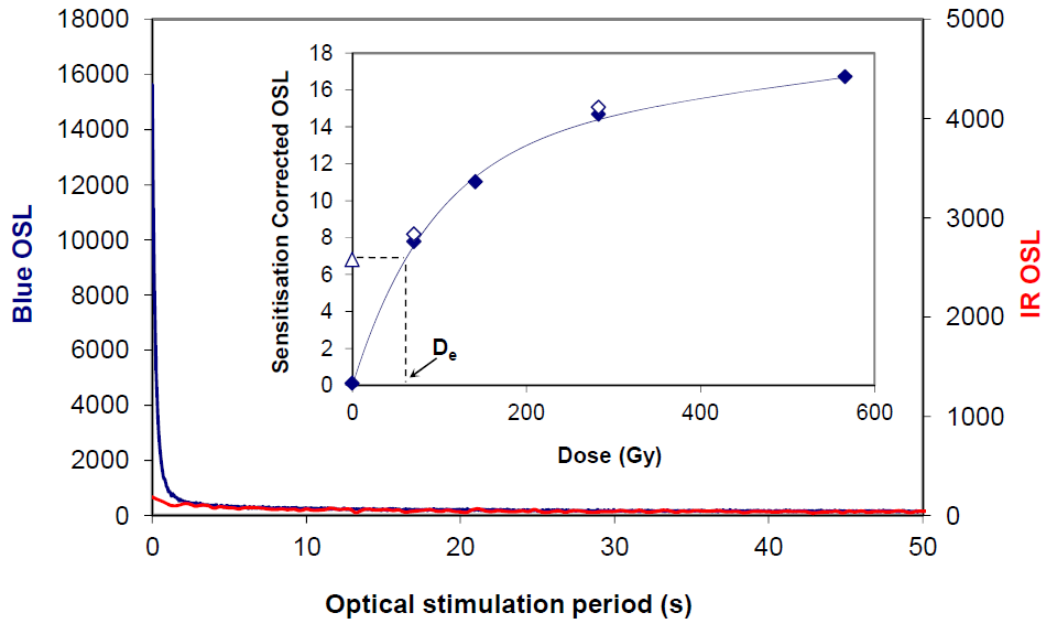


8

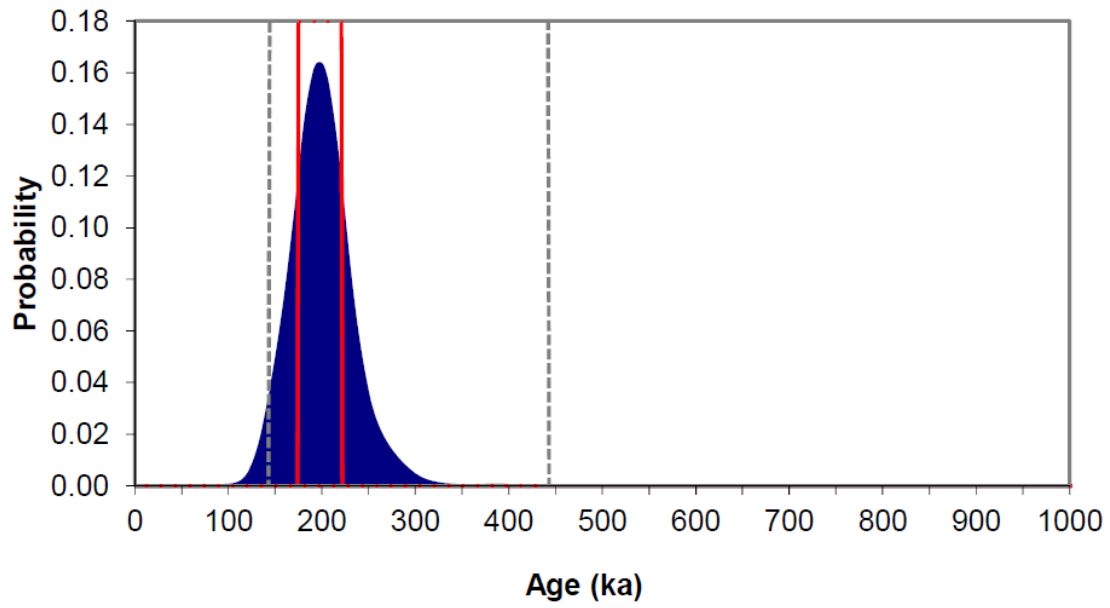


Ashley GL15034

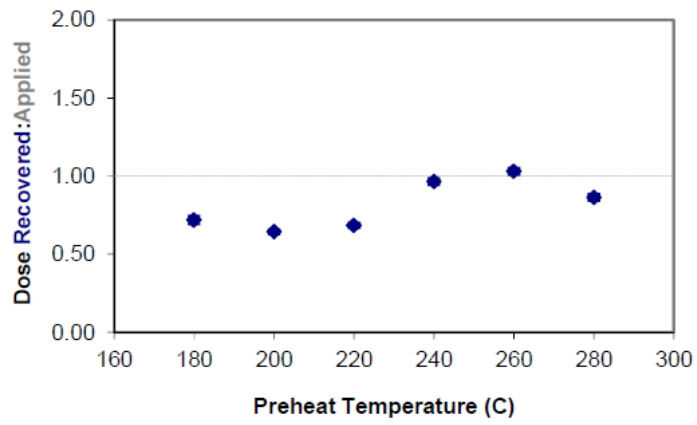
1



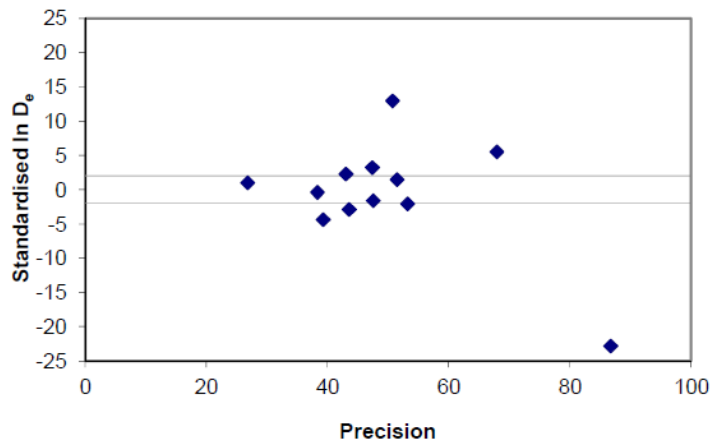
2



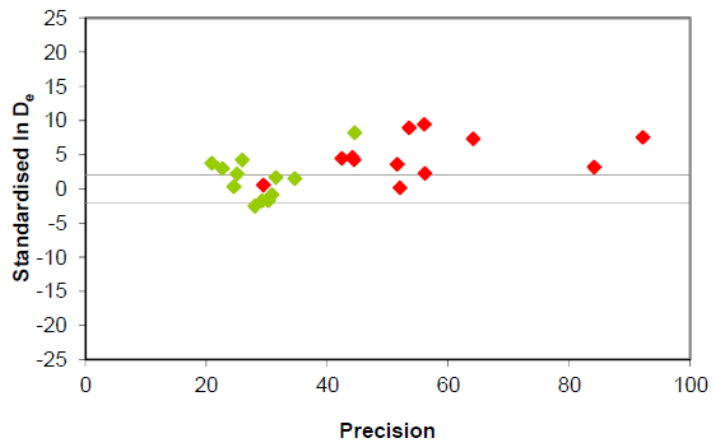
3



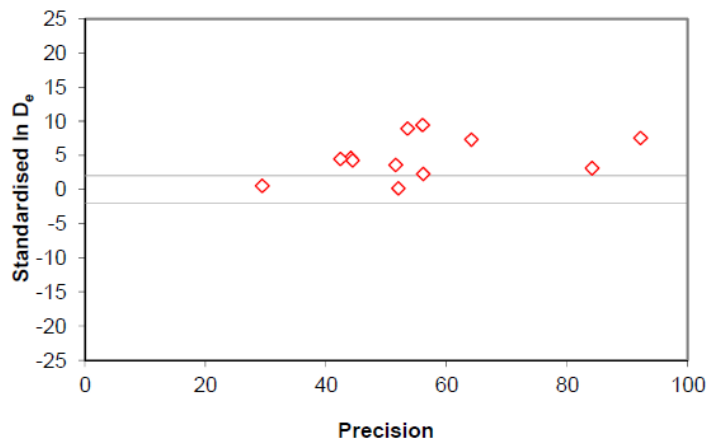
4



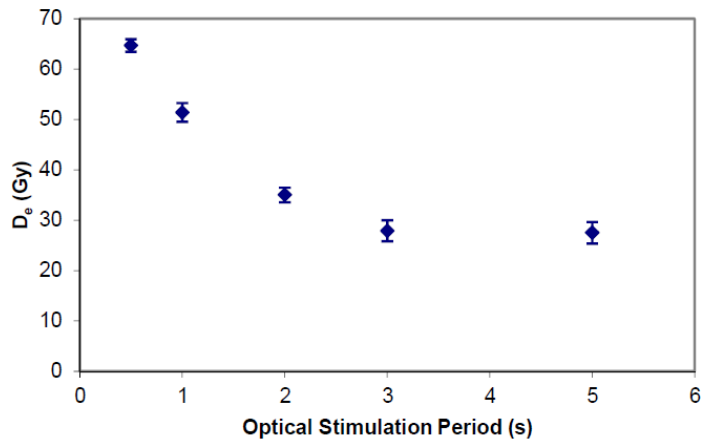
5



6

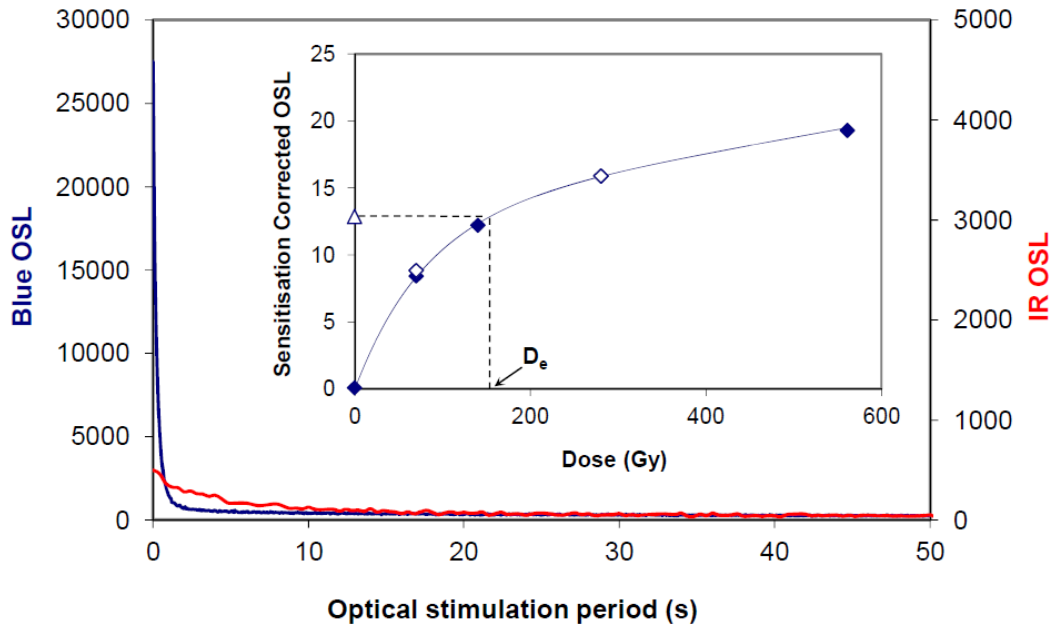


7

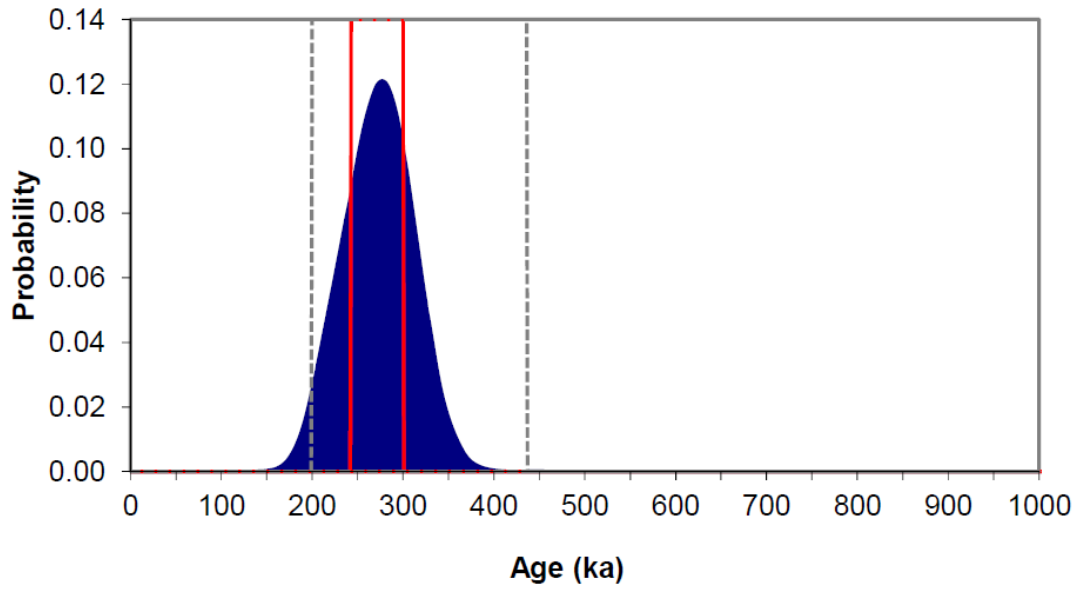


Ashley GL15035

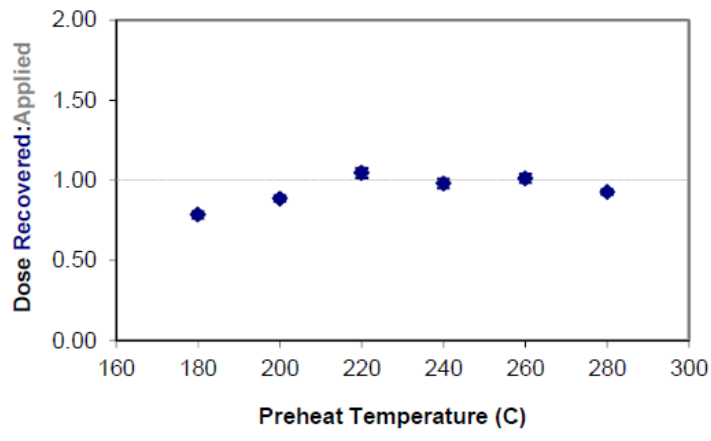
1



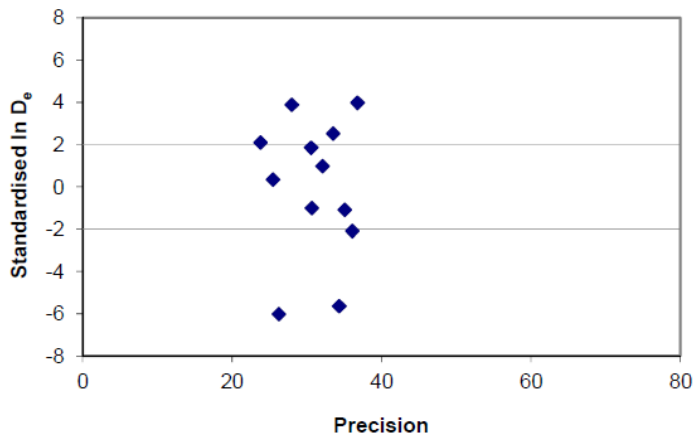
2



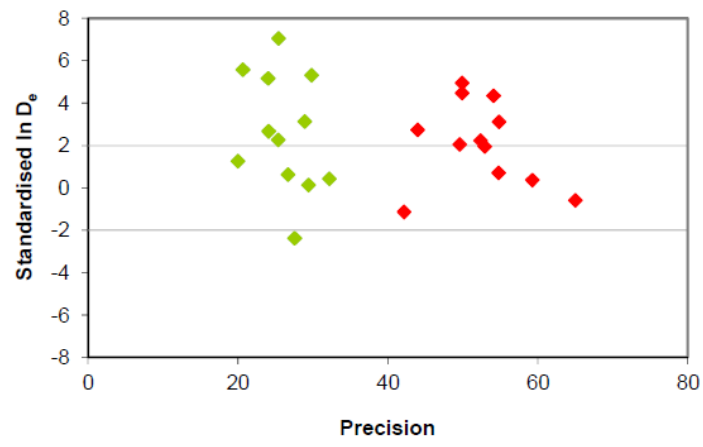
3



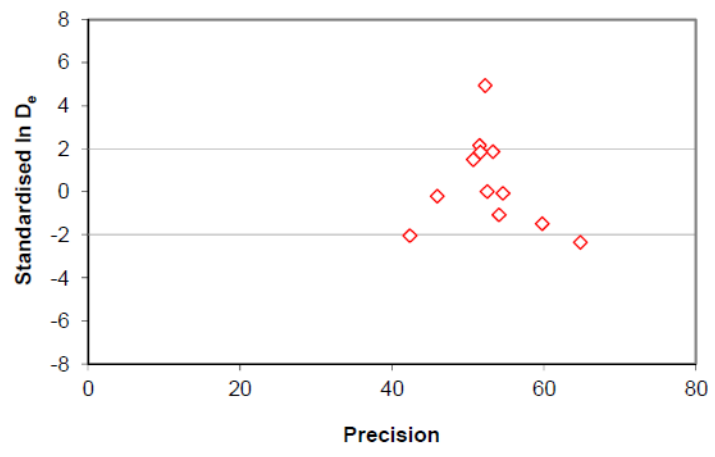
4



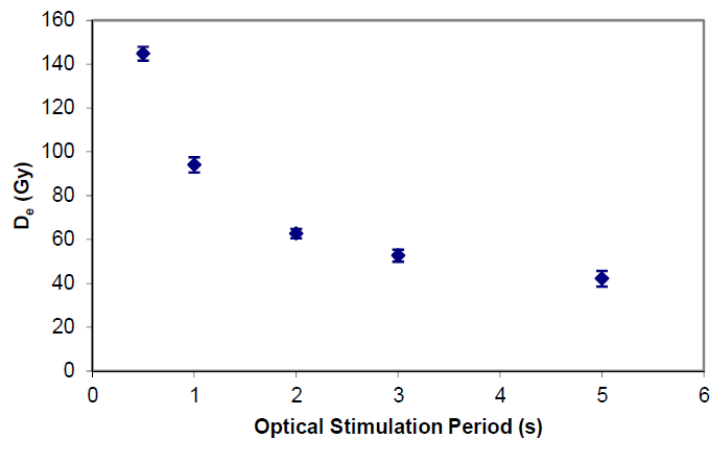
5



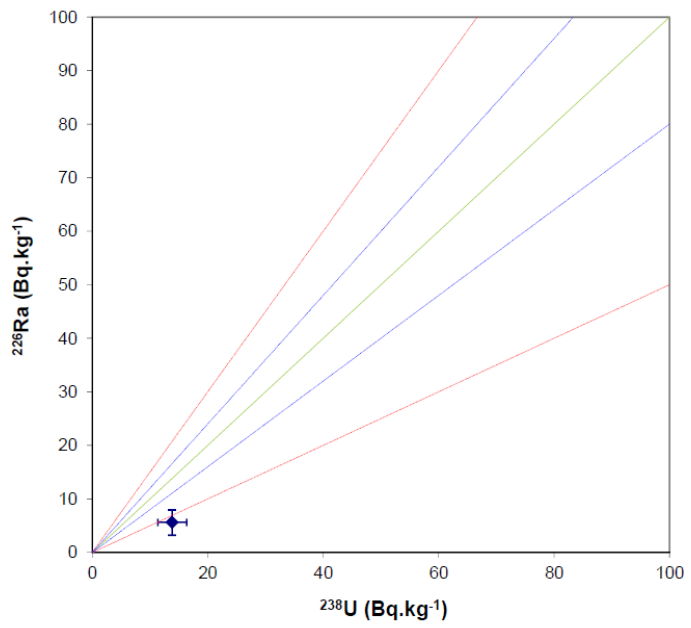
6



7

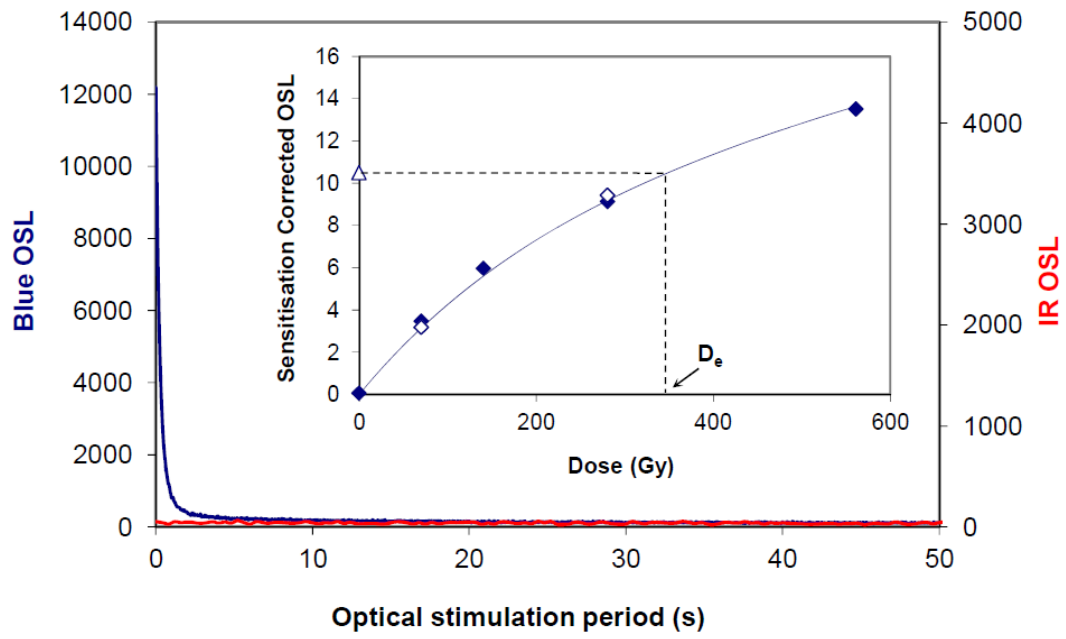


8

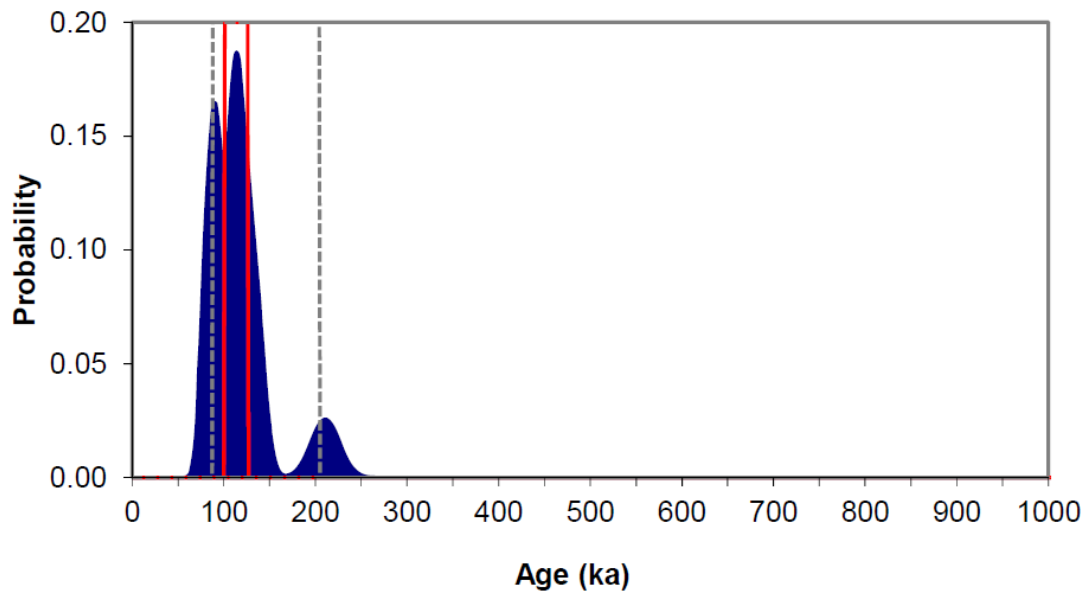


Ashley GL15036

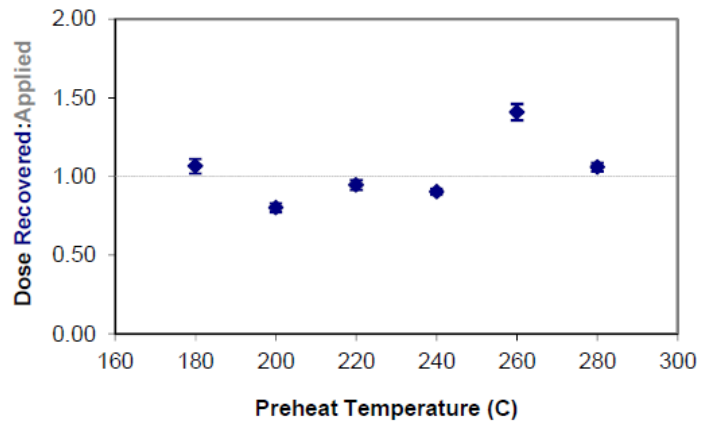
1



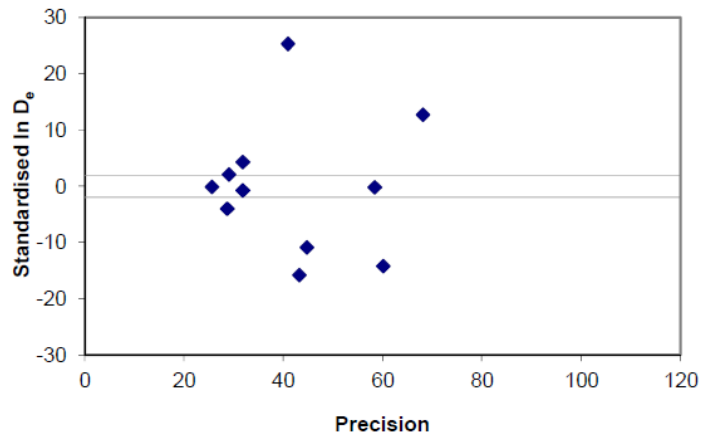
2



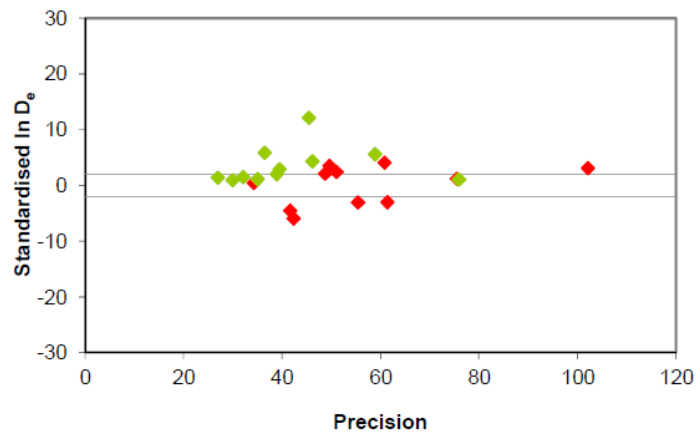
3



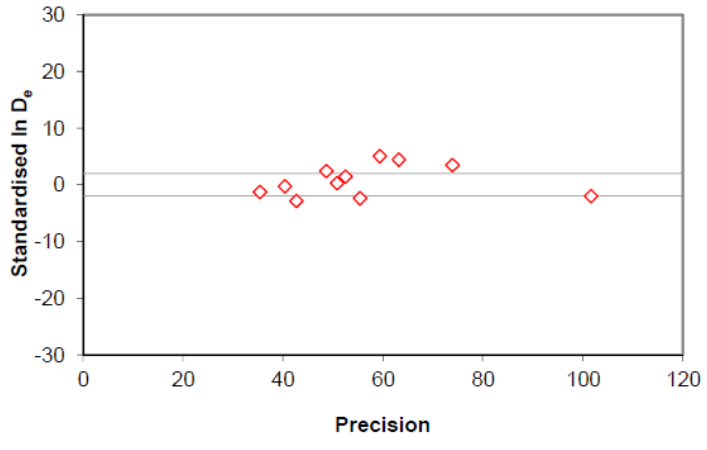
4



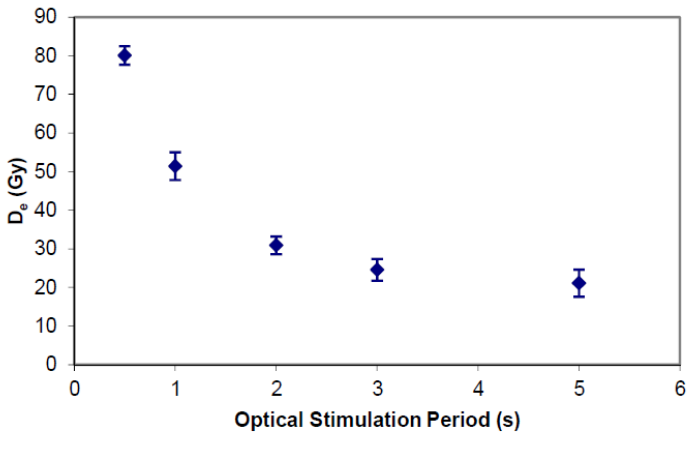
5



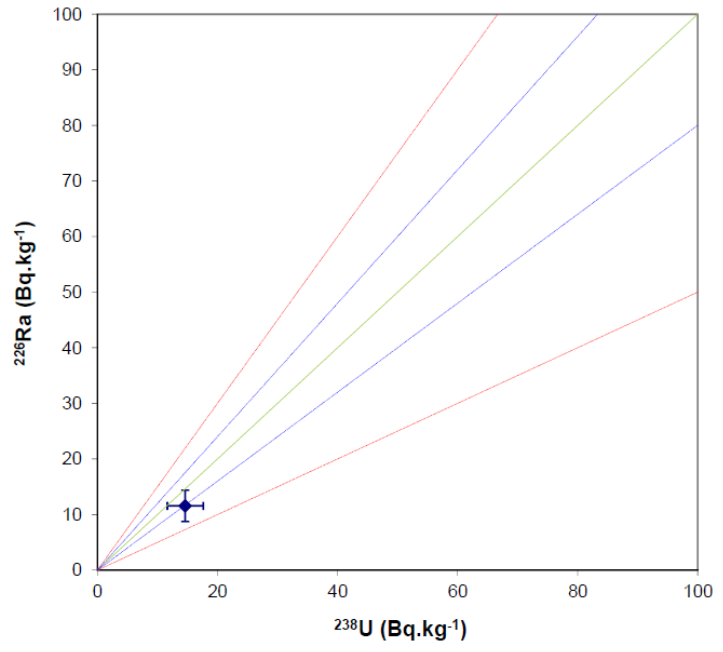
6



7

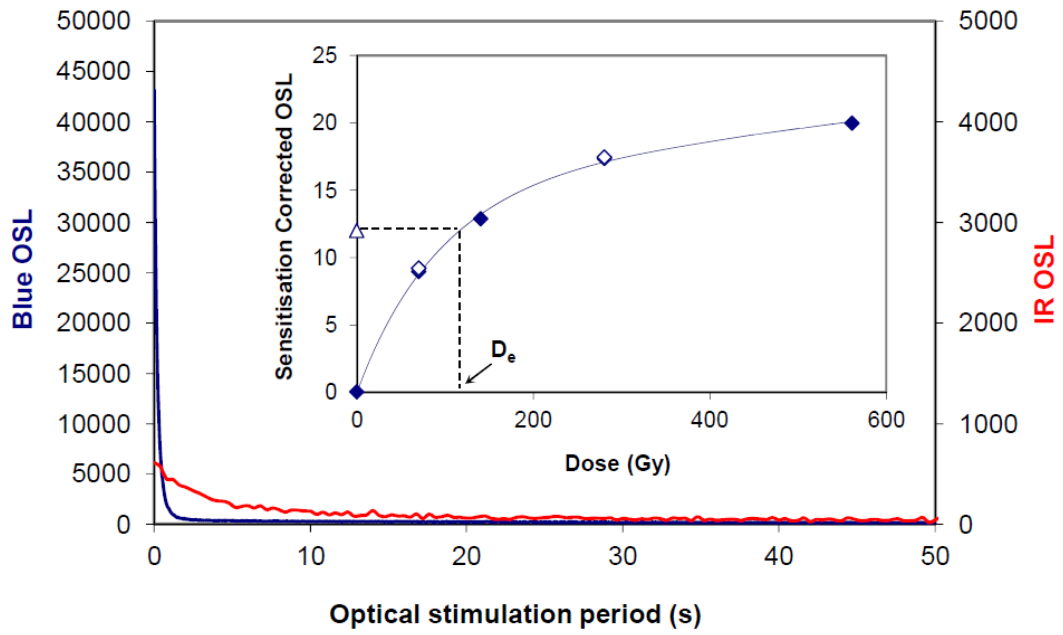


8

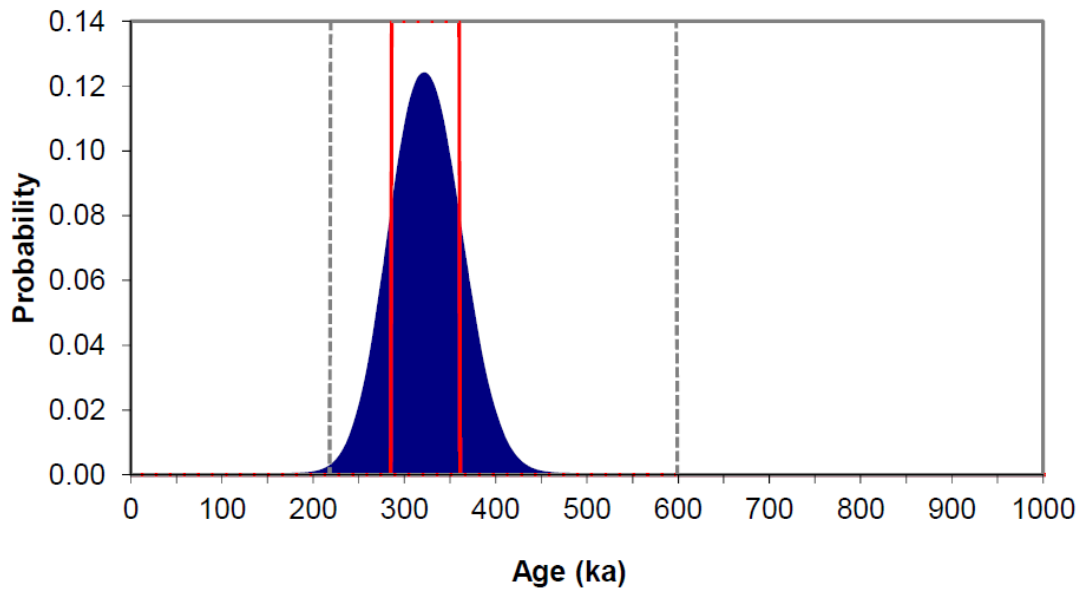


Ashley GL15037

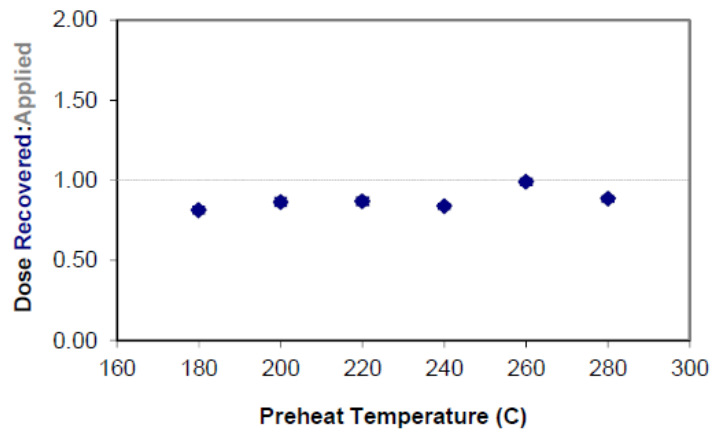
1



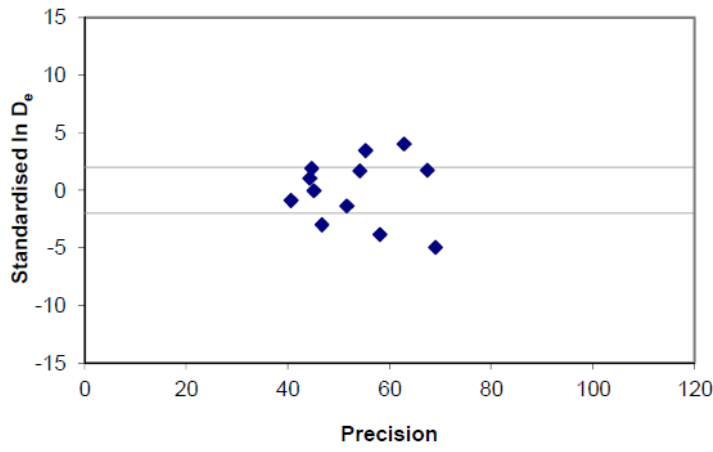
2



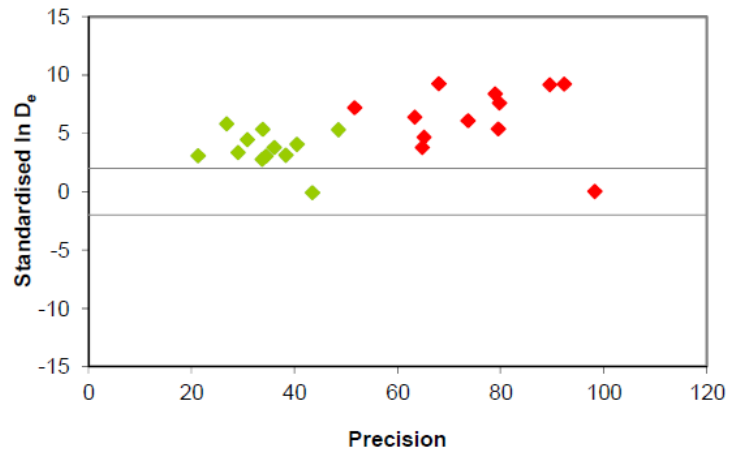
3



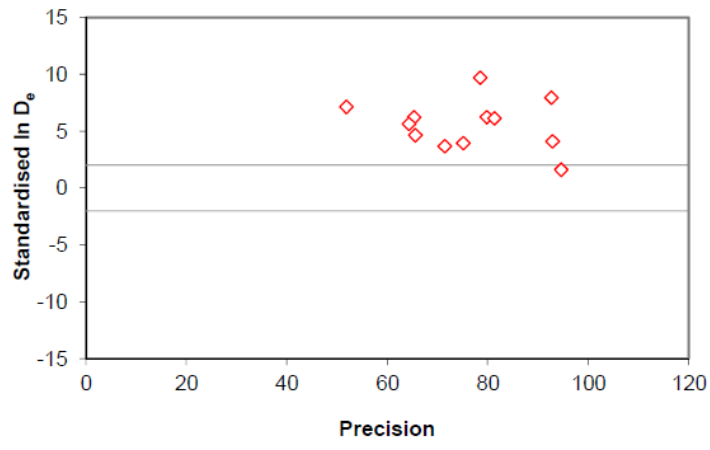
4



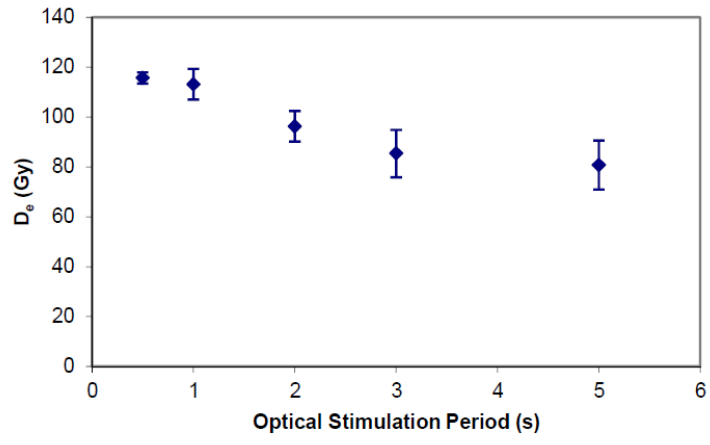
5



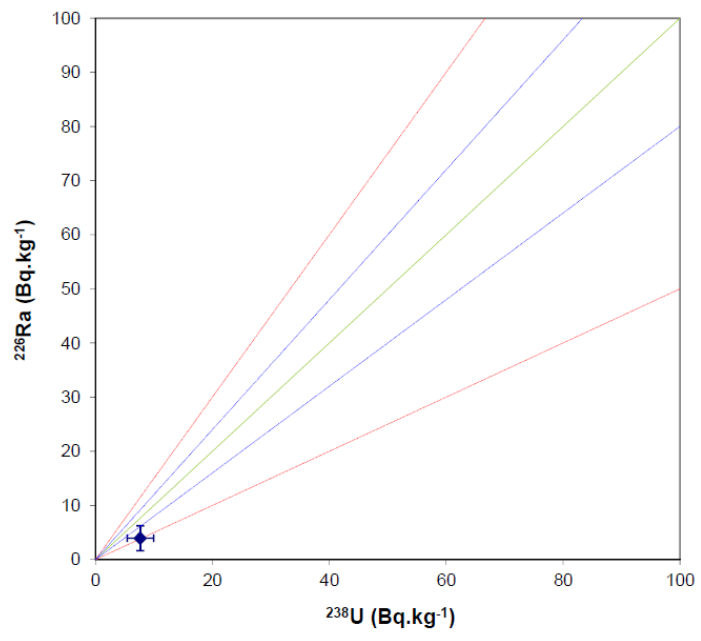
6



7

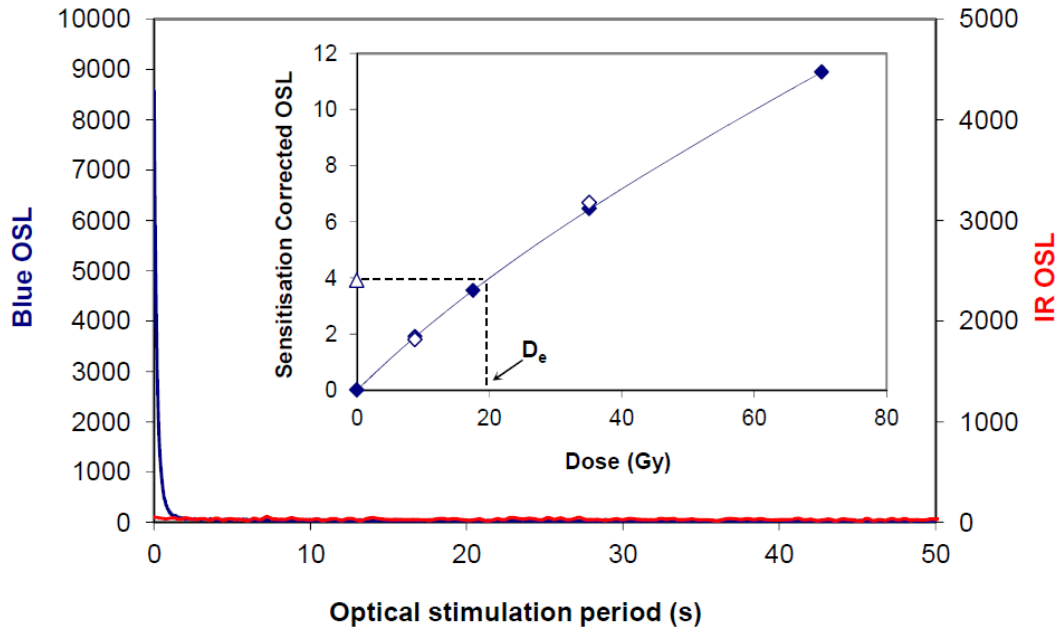


8

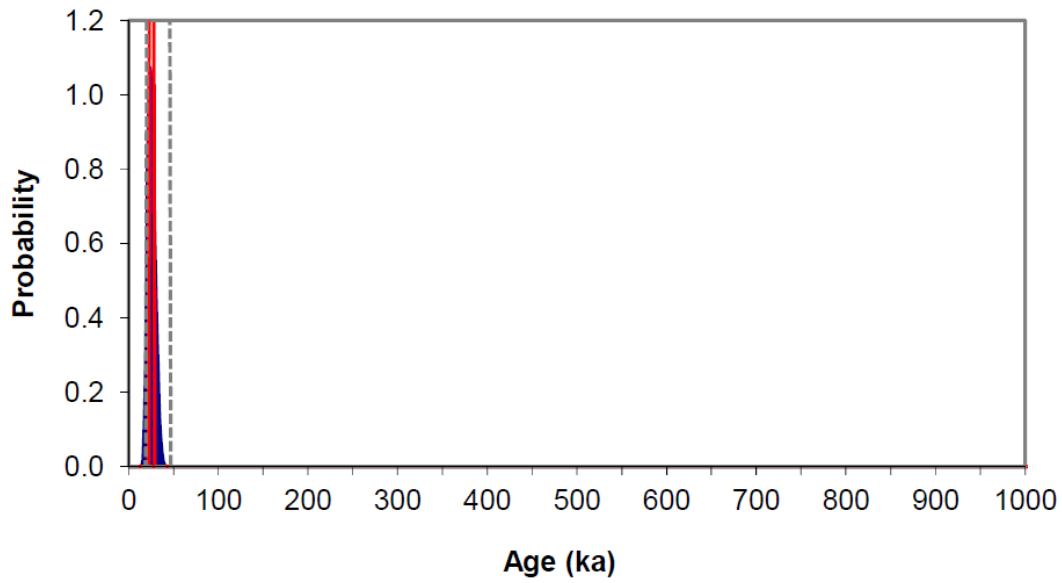


Bickton GL15075

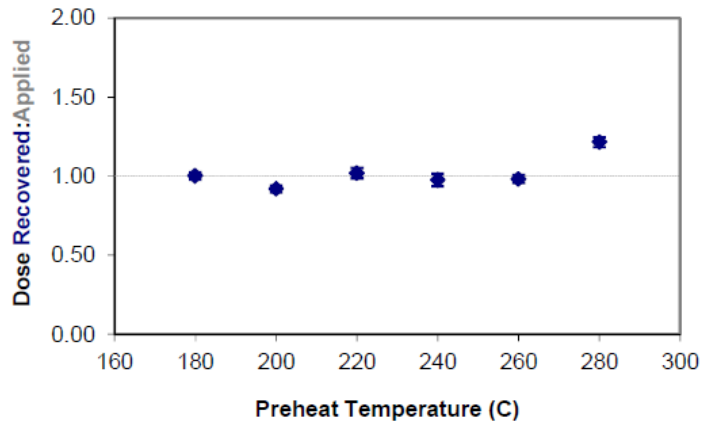
1



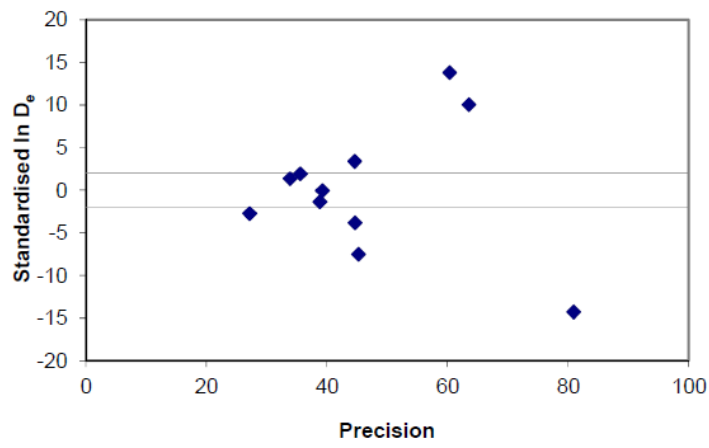
2



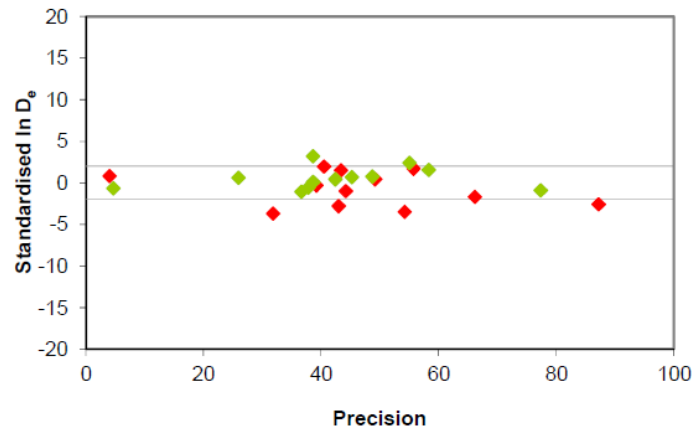
3



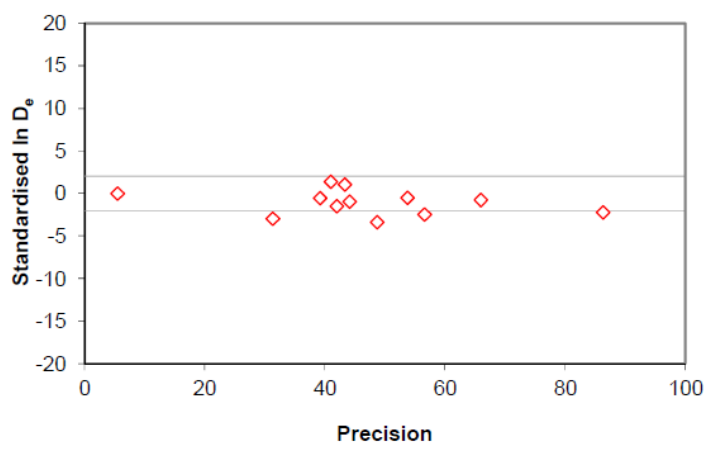
4



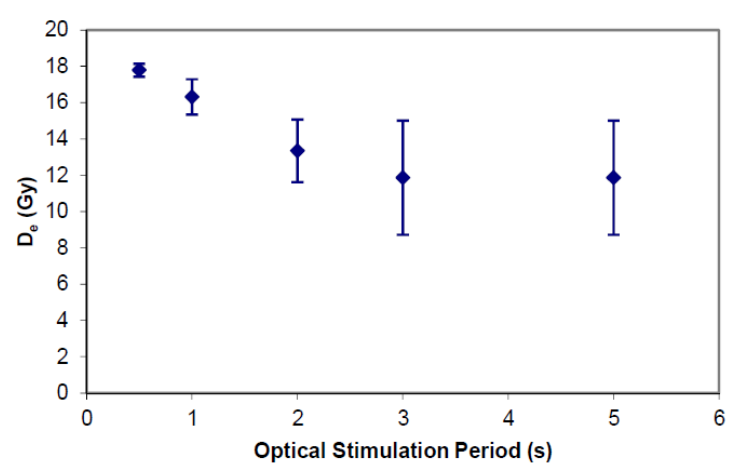
5



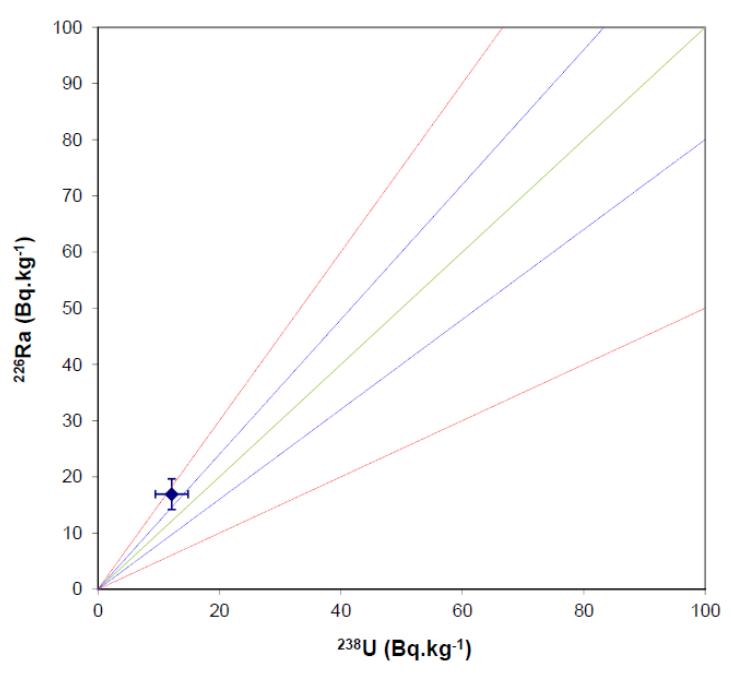
6



7

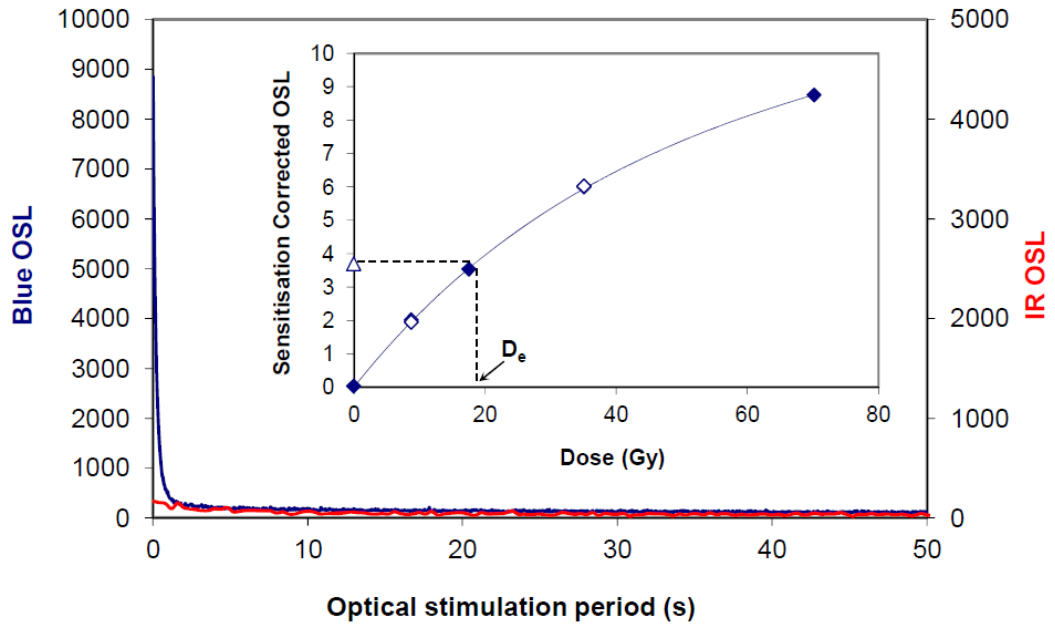


8

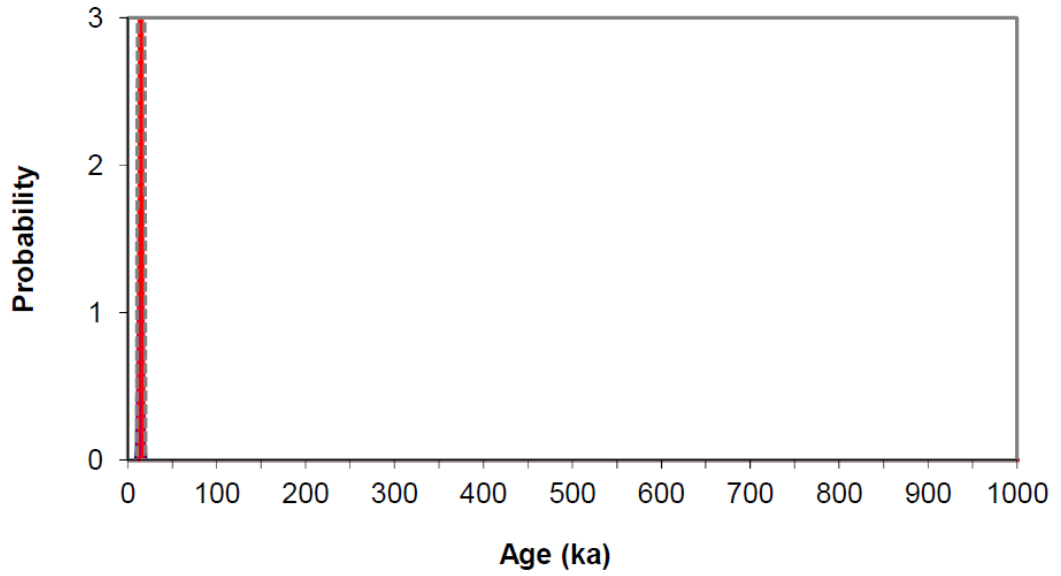


Bickton GL15076

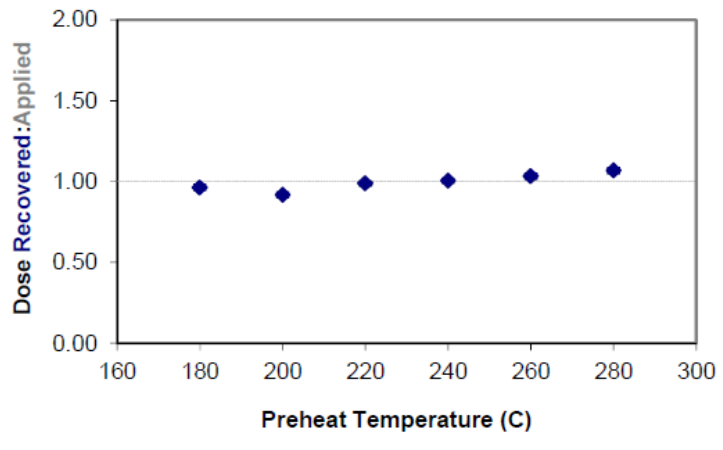
1



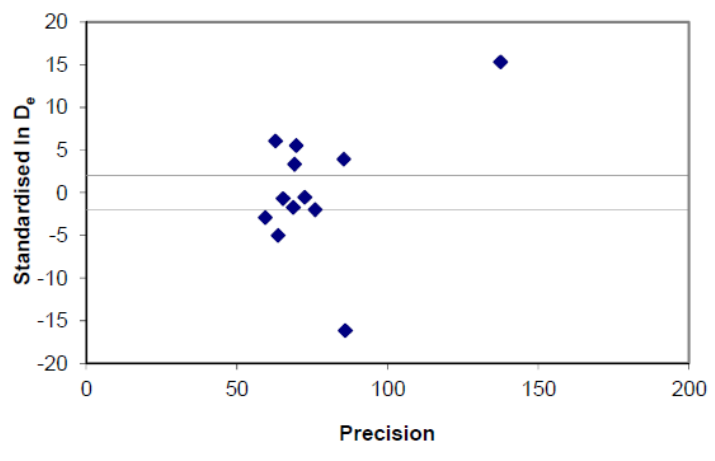
2



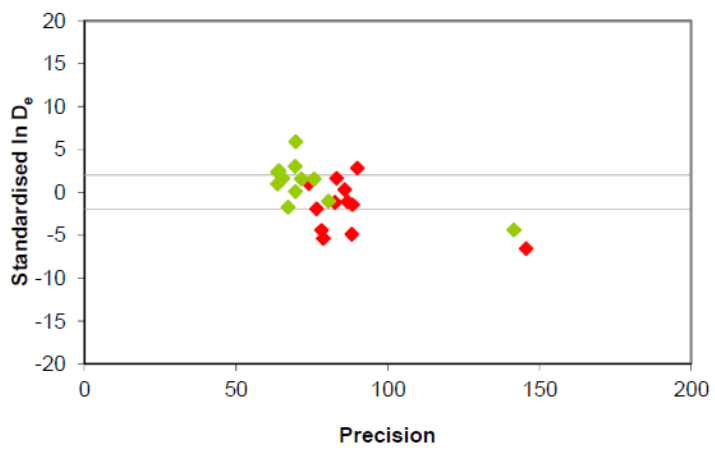
3



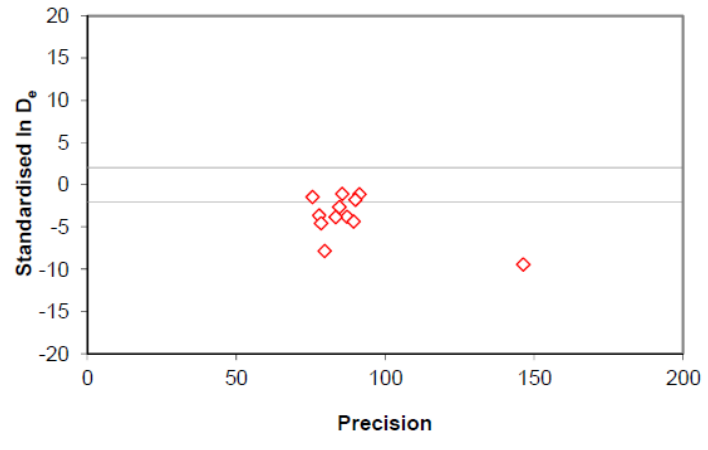
4



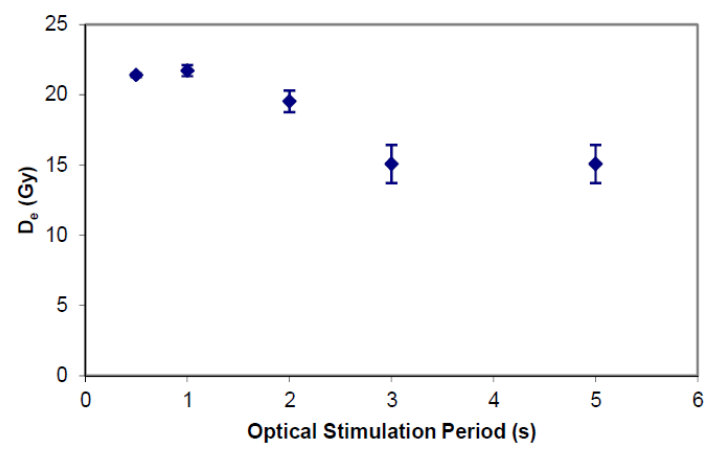
5



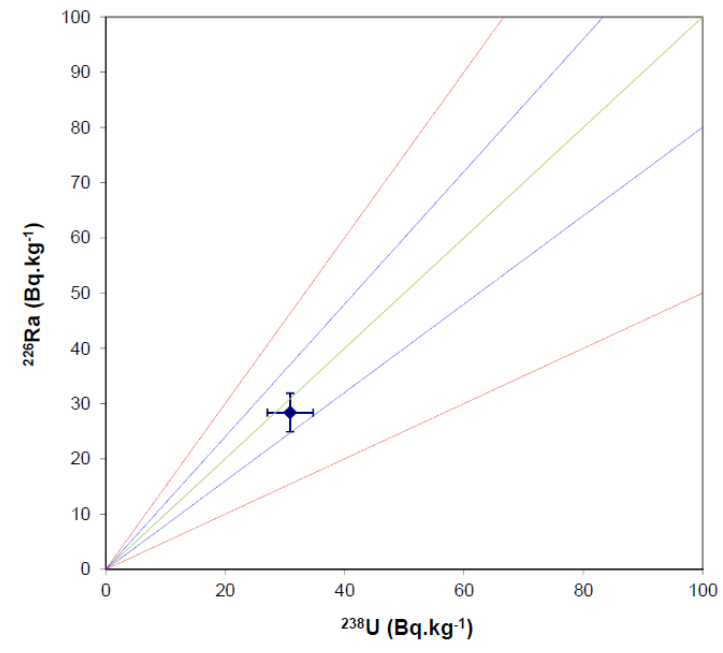
6



7

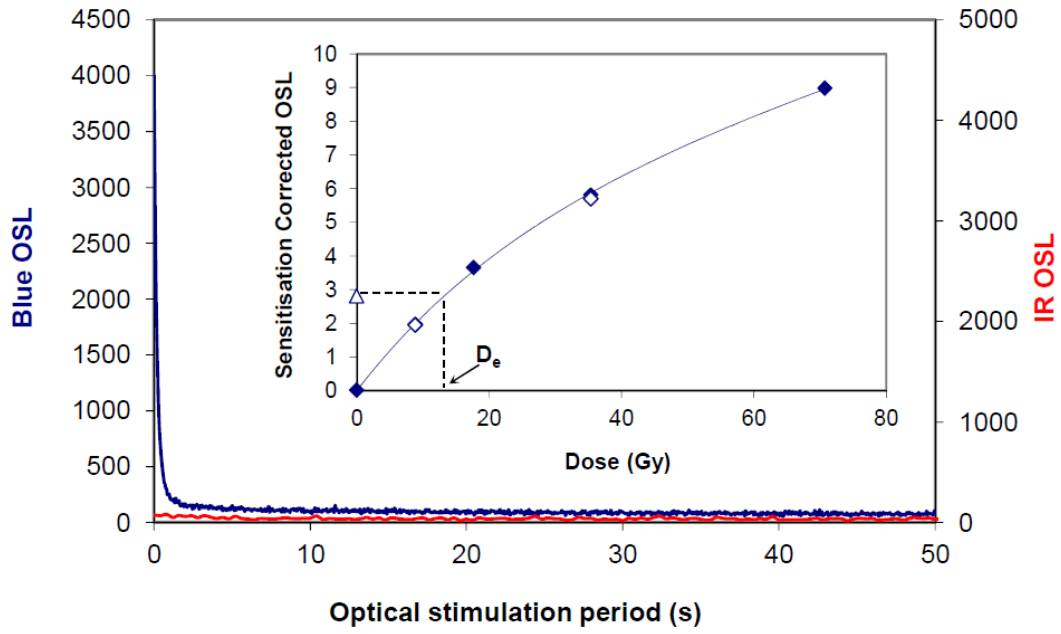


8

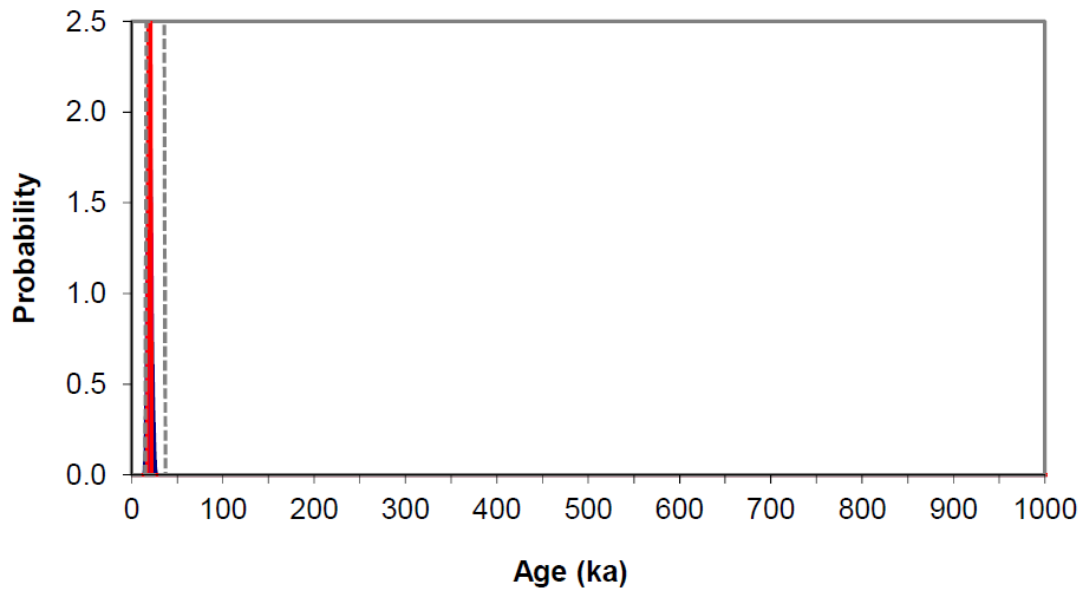


Bickton GL15077

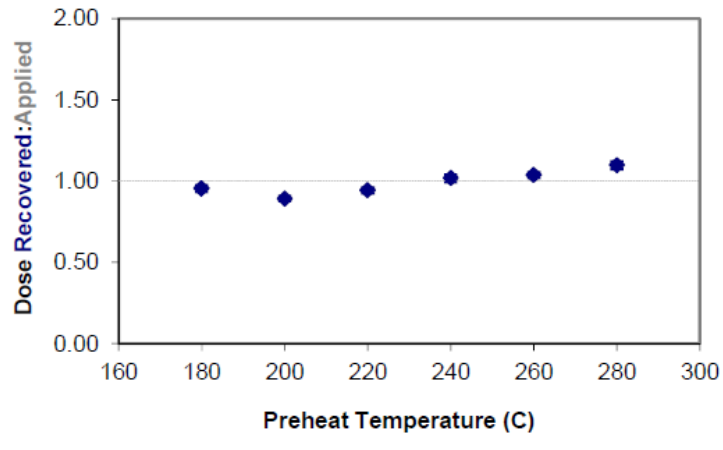
1



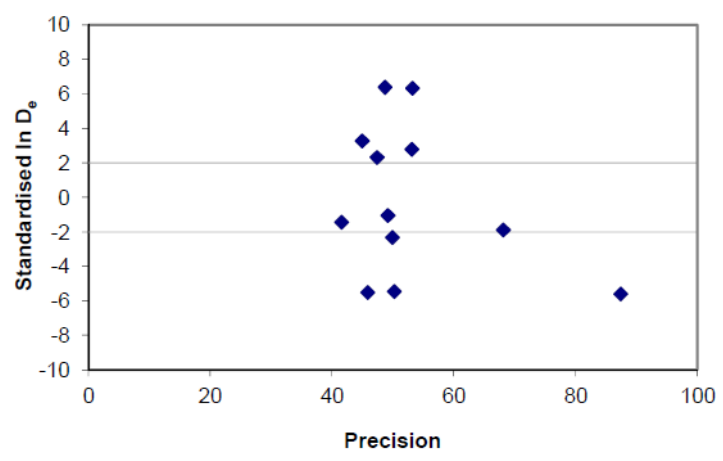
2



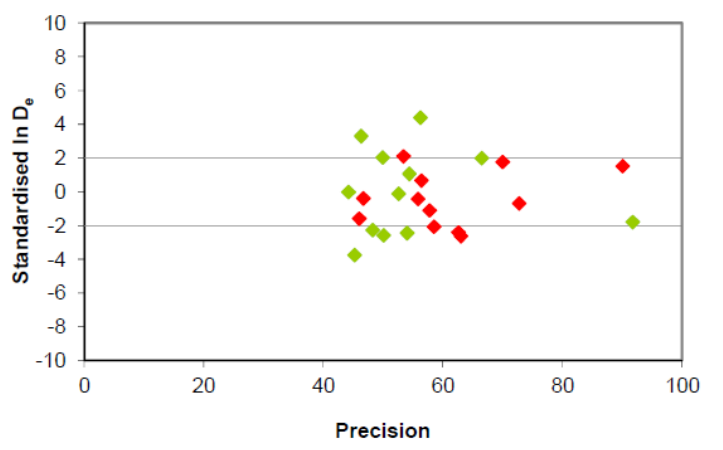
3



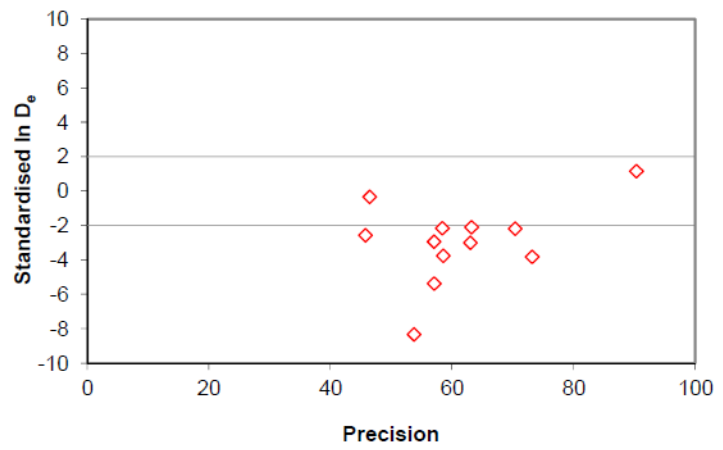
4



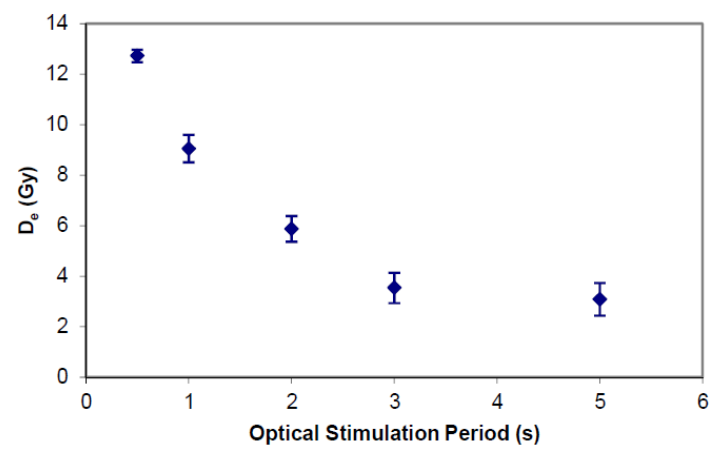
5



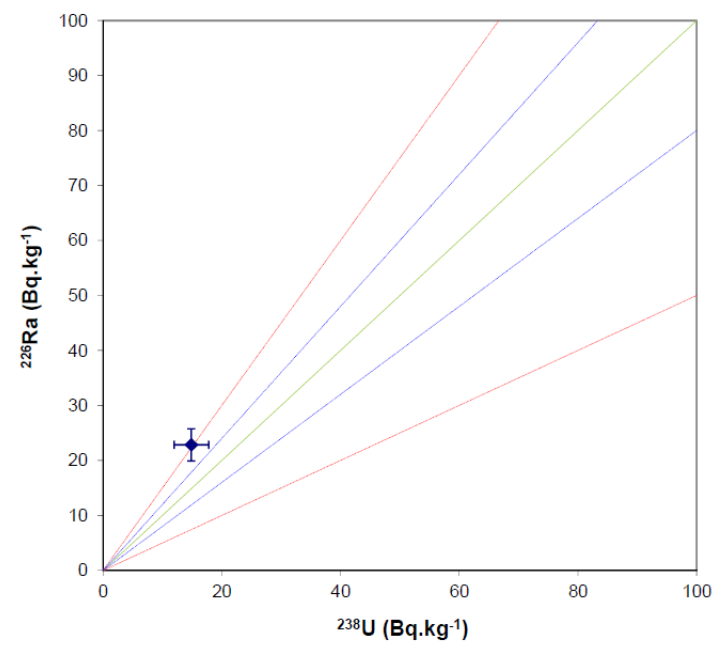
6



7

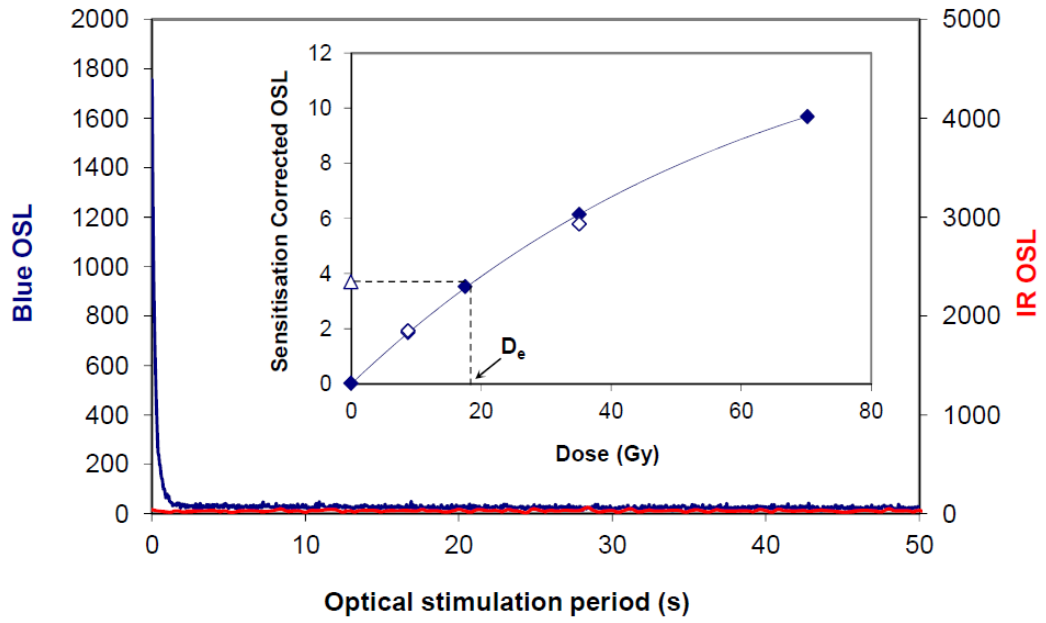


8

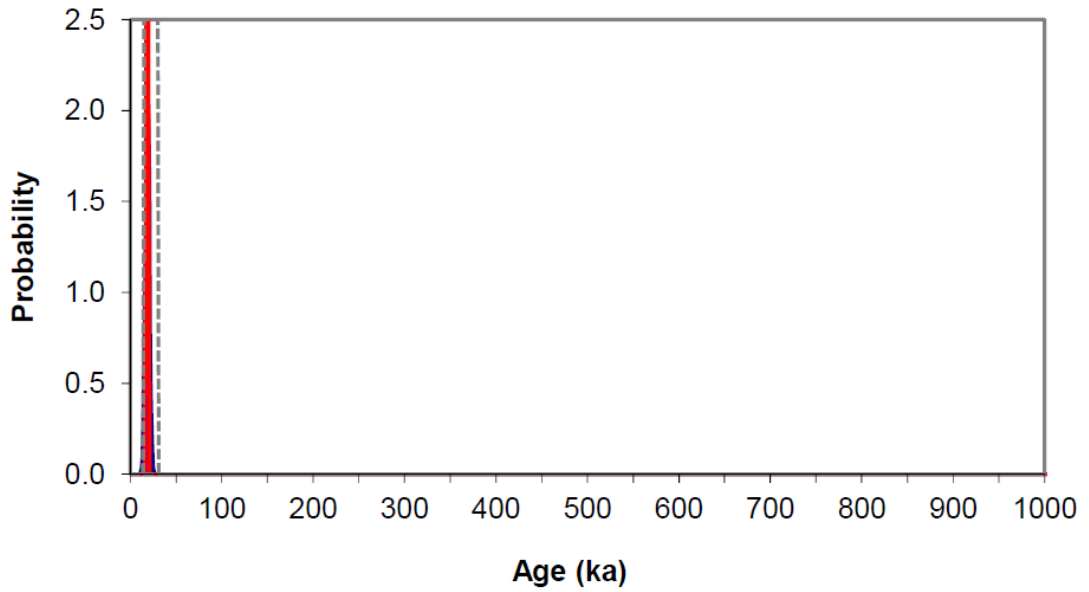


Bickton GL15078

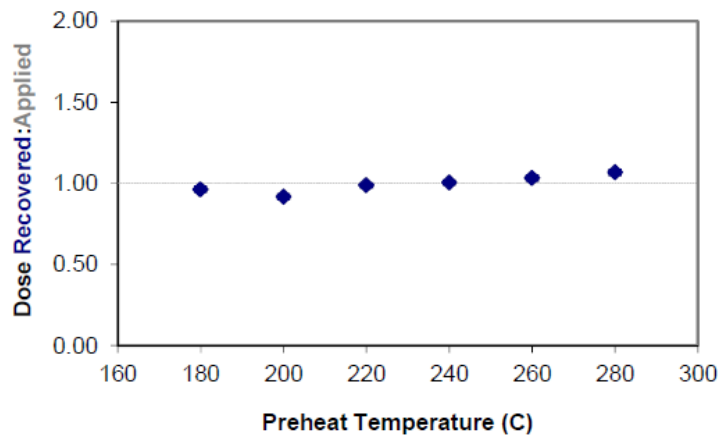
1



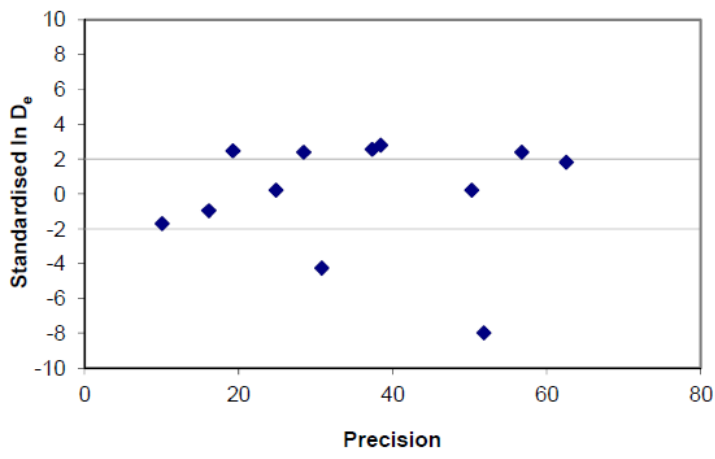
2



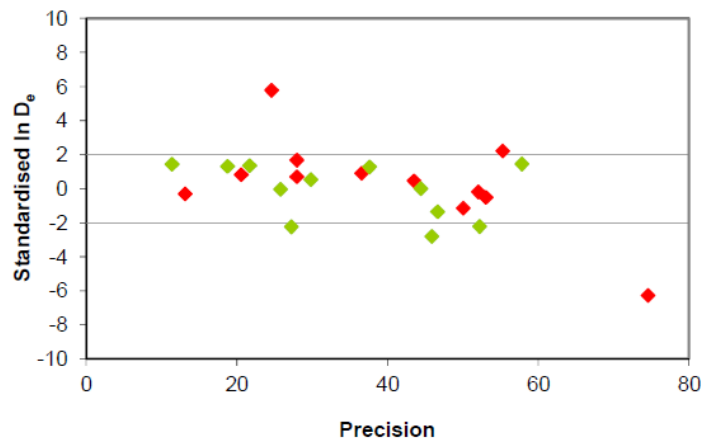
3



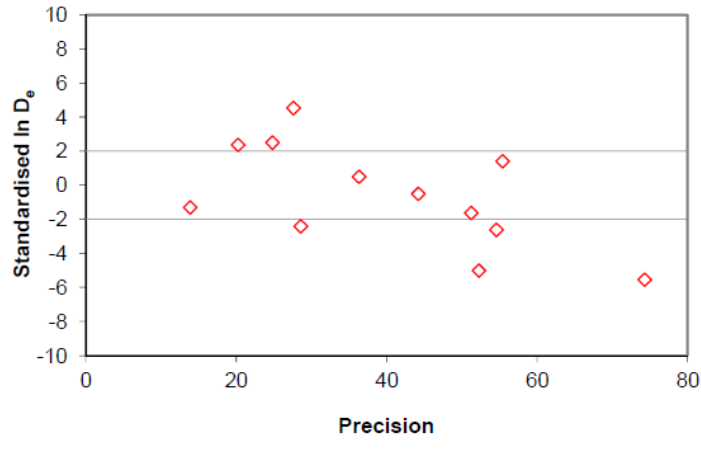
4



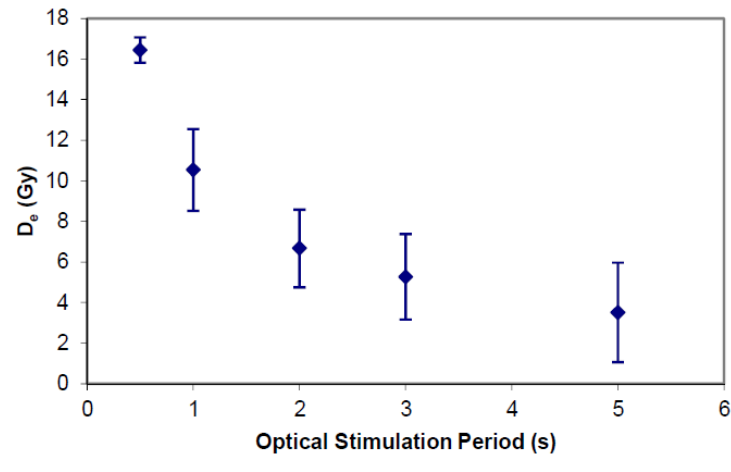
5



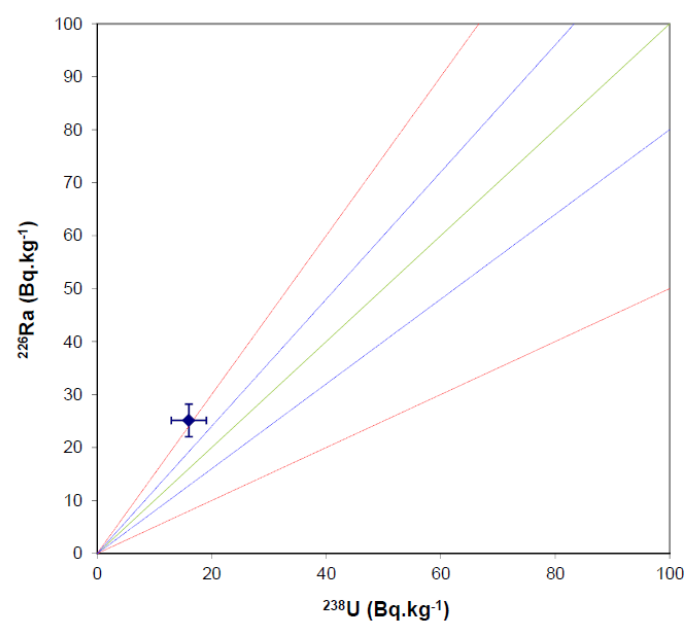
6



7



8



Appendix 37 Table summarising the number of artefacts studied per site and their current location.

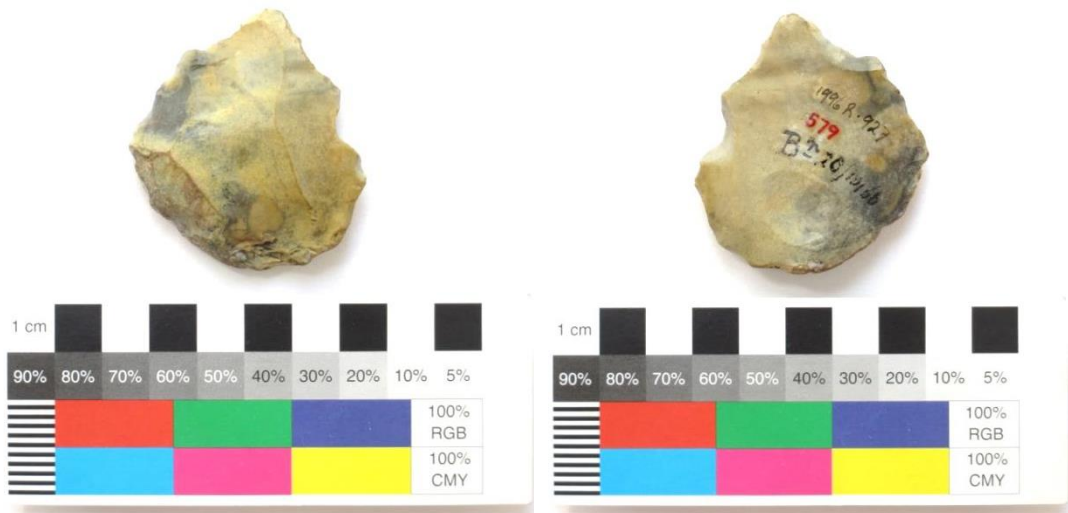
	Bemerton	Milford Hill	Woodgreen	Total
The Ashmolean Museum	1	12	0	13
Birmingham Museum	0	0	24	24
British Museum and art gallery	8	30	14	52
Bristol Museum and art gallery	0	0	51	51
National Museum Cardiff	1	3	3	7
Wiltshire Museum	3	34	0	37
Pitt Rivers Museum	1	11	0	12
Salisbury Museum	136	377	534	1047
Wells and Mendip Museum	1	0	9	10
Total	151	467	635	1253

Table A37.1 Table summarising the number of artefacts studied per site and their current location.

Appendix 38 Possible Levallois artefacts from Bemerton



Possible Levallois flake from Bemerton (artefact no. b6_21_94).

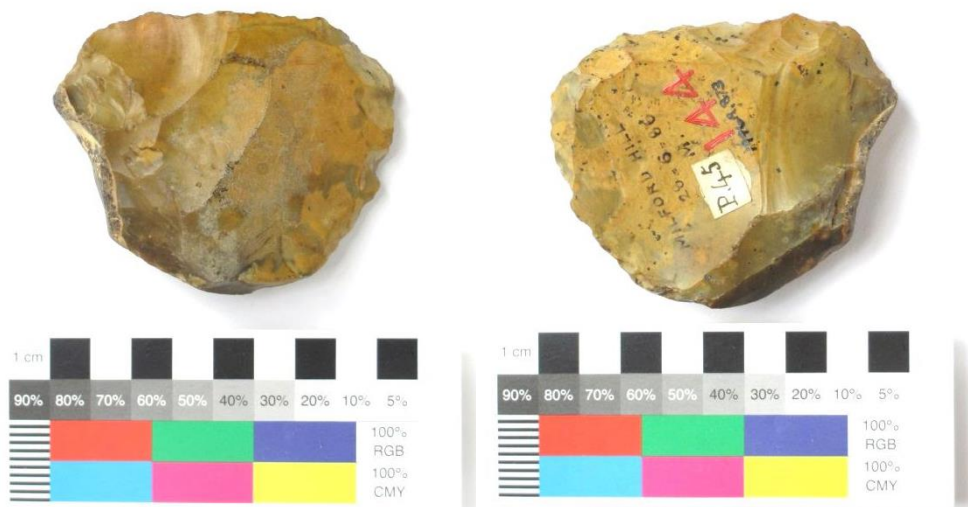


Possible Levallois flake from Bemerton (artefact no. b6_23_96).

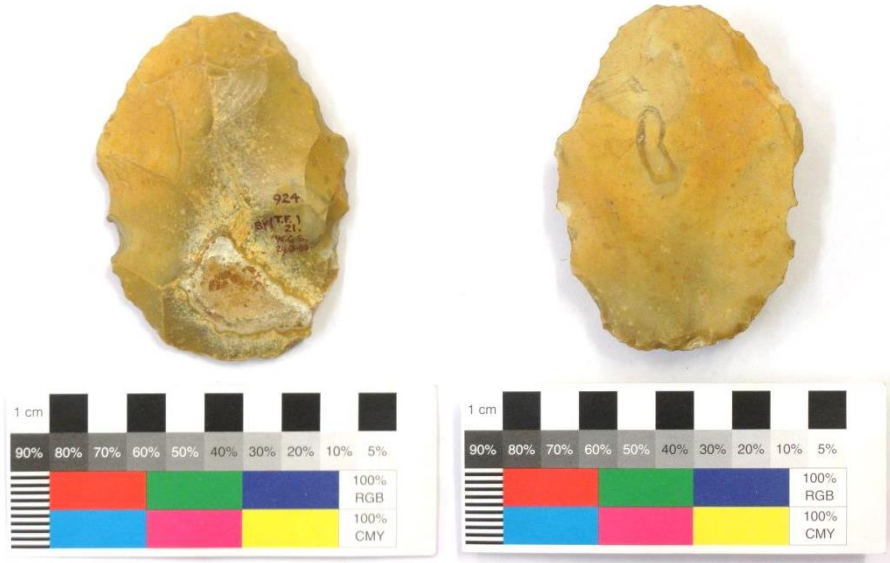
Appendix 39 Possible Levallois artefacts from Milford Hill



Possible Levallois flake from Milford Hill (artefact no. m7_13_300).

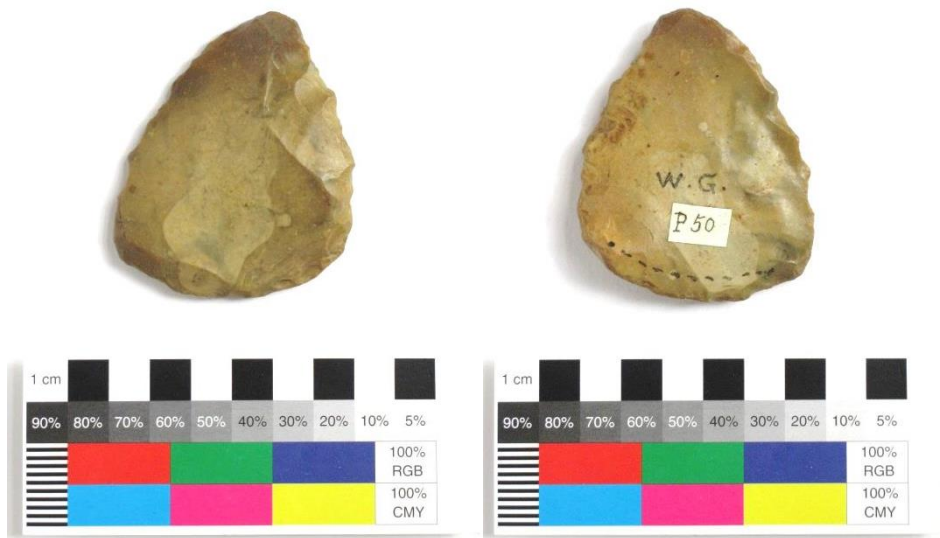


Possible Levallois core from Milford Hill (artefact no. m15_53_90).

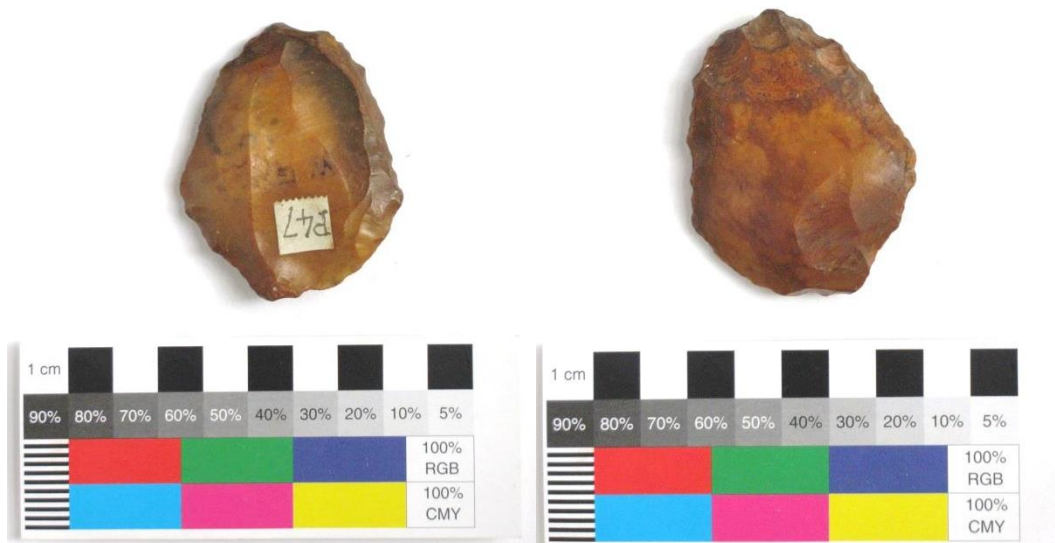


Possible Levallois flake from Milford Hill (artefact no. m1084).

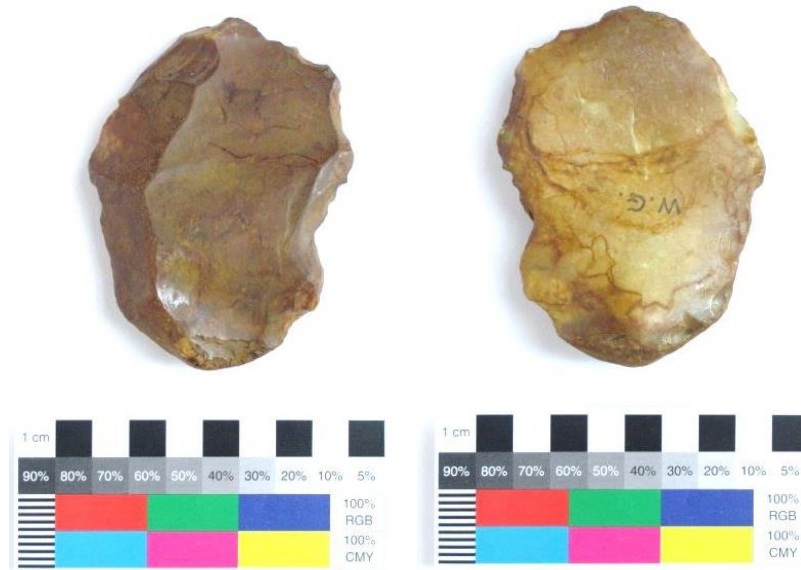
Appendix 40 Possible Levallois artefacts from Woodgreen



Possible Levallois Flake from Woodgreen (artefact no. w3_11_60).



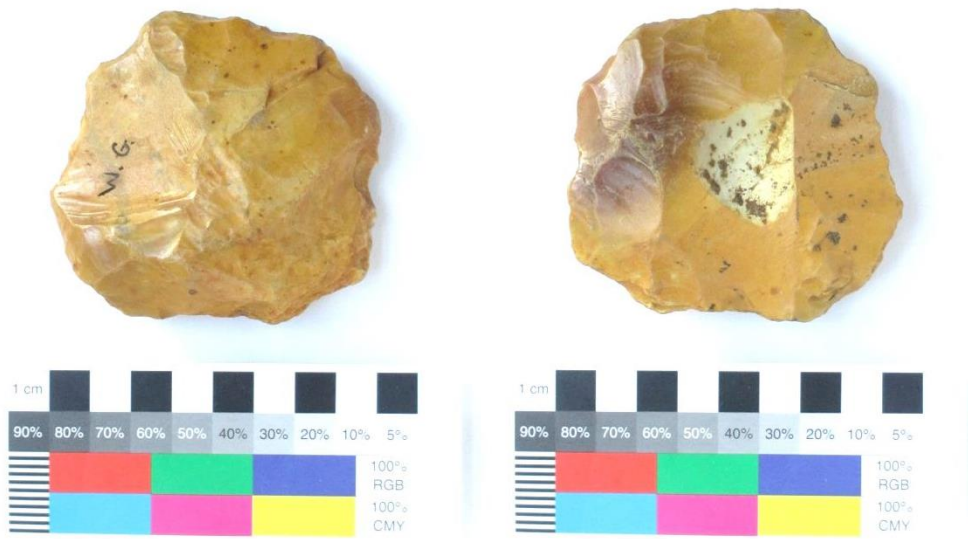
Possible Levallois flake from Woodgreen (artefact no. w4_4_136).



Possible Levallois flake from Woodgreen (artefact no. w5_38_229).



Possible Levallois flake from Woodgreen. Two 'pot lids' on the dorsal side are likely the result of frost damage (artefact no. w1_22_22).



Possible Levallois core from Woodgreen (artefact no. w7_24_341).

Appendix 41 Comparison of the condition of biface types

A comparison of the condition of the bifaces from Bemerton, Milford Hill and Woodgreen are presented in the following diagrams. For each site the condition of bifaces is visualised in histograms presenting the degree of patination, staining, abrasion and iron-manganese concretion.

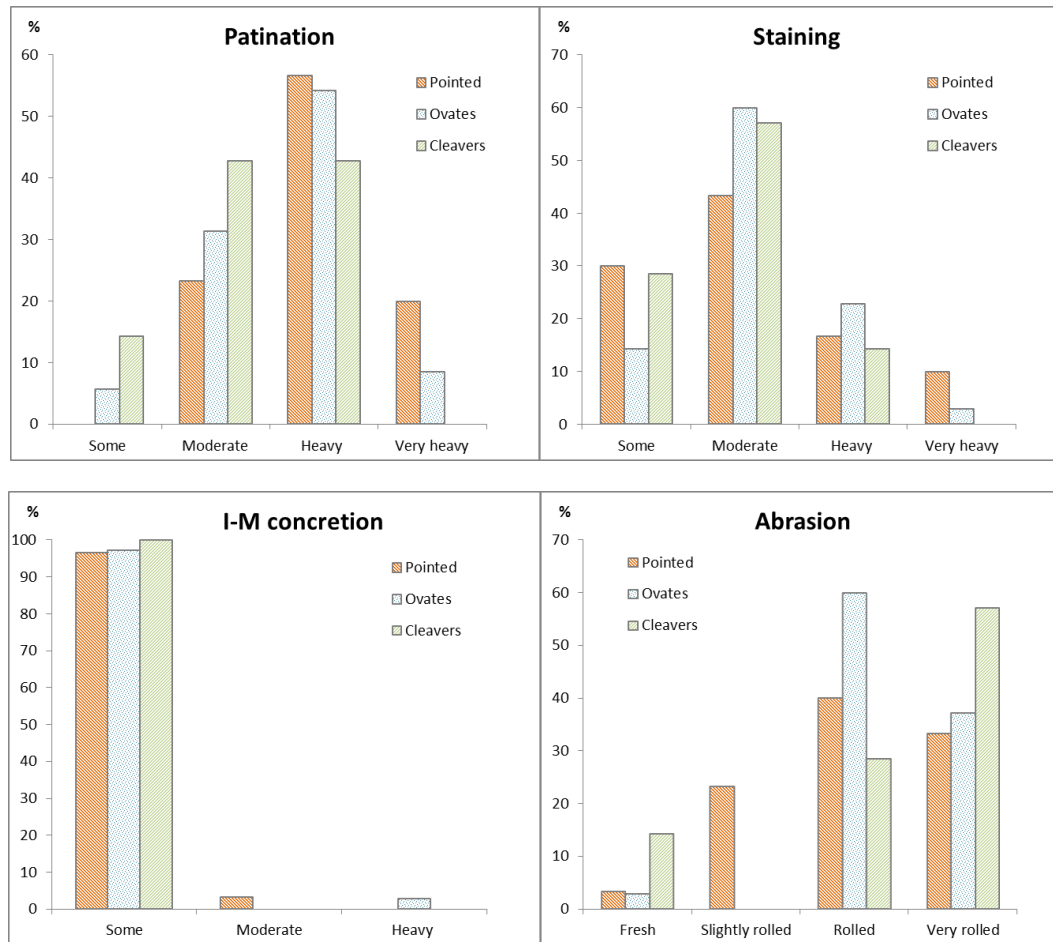


Figure A41.1 Patination, staining, abrasion and iron-manganese concretion of pointed, ovate and cleaver type bifaces from Bemerton.

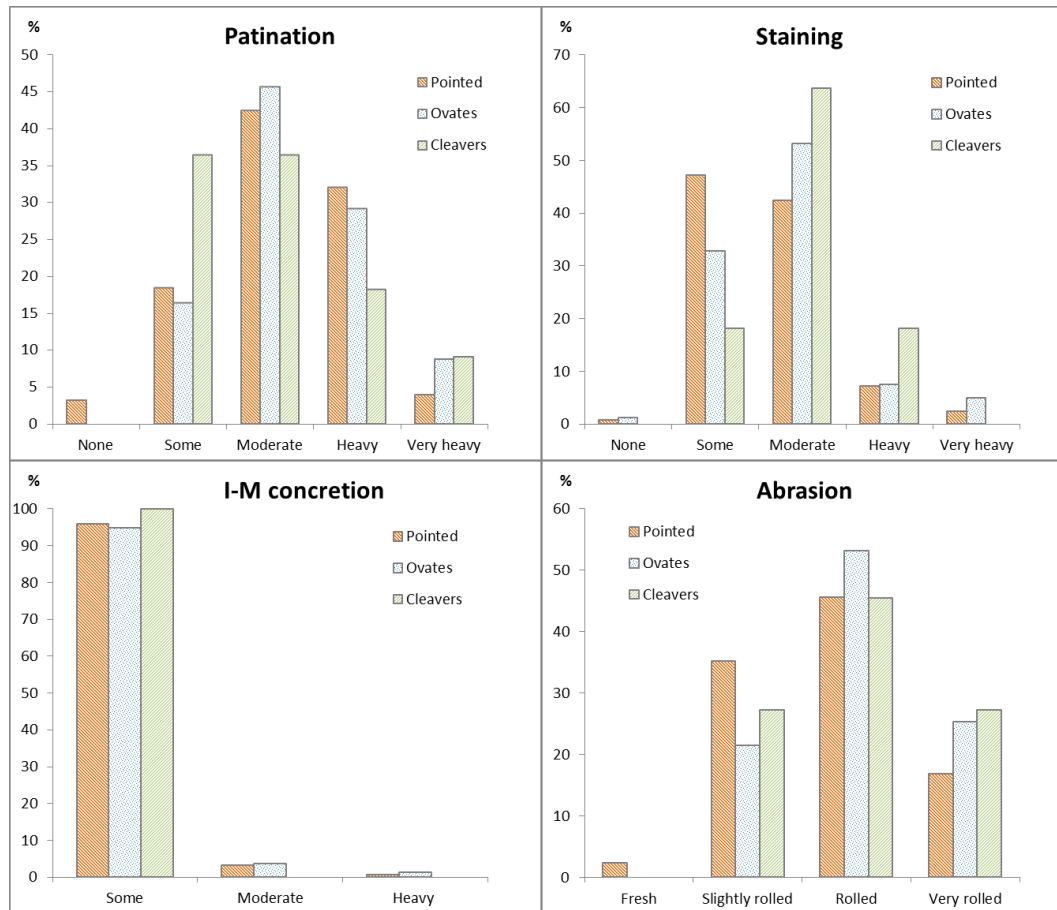


Figure A41.2 Patination, staining, abrasion and iron-manganese concretion of pointed, ovate and cleaver type bifaces from Milford Hill.

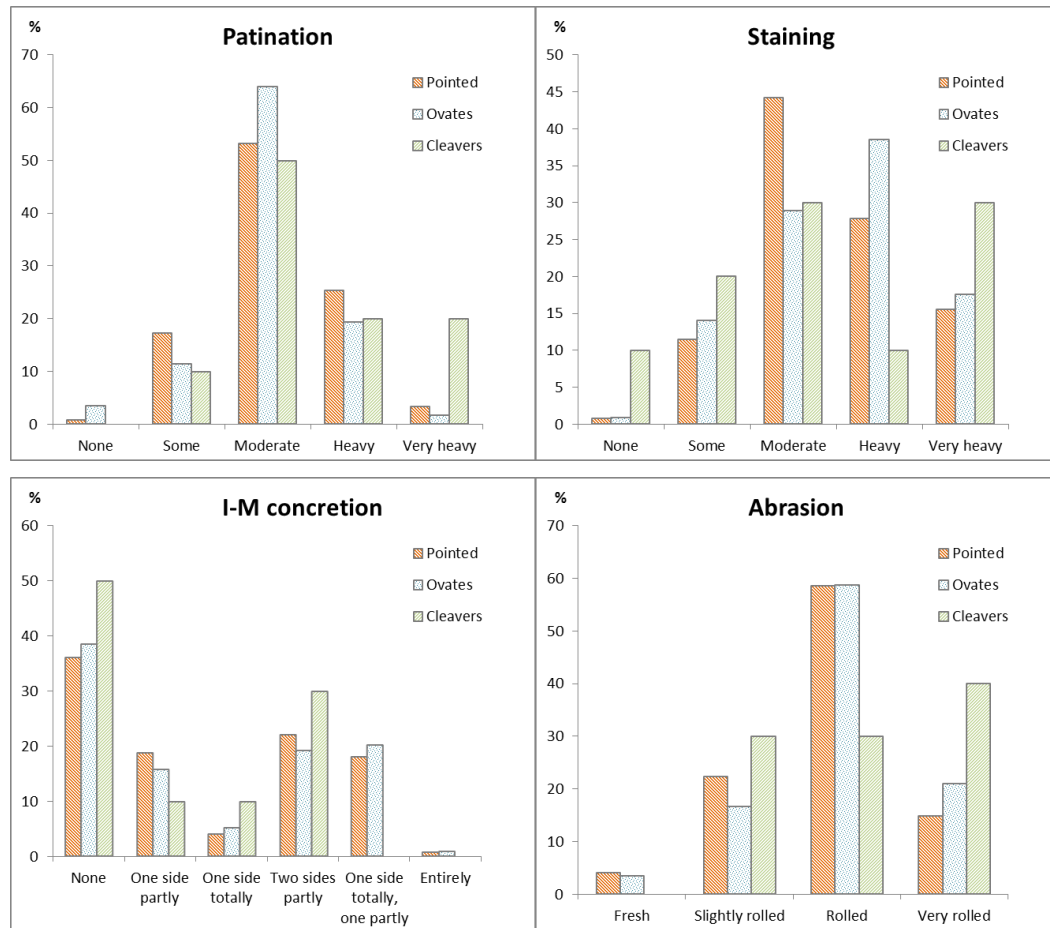


Figure A41.3 Patination, staining, abrasion and iron-manganese concretion of pointed, ovate and cleaver type bifaces from Woodgreen.

Appendix 42 Statistical analysis of artefact data for the comparison of the sites

The following tables present the results of the statistical analyses carried out for this research. The selection of methods was based on Dytham (2011). All categorical data was analysed using the Chi-square test (differences between the sites in e.g. the occurrence of artefact types, blank types, artefact condition). The differences in size and shape ratios between the sites were analysed using either One-way ANOVA or Kruskal-Wallis test. The former was used when data was approximately normally distributed, the latter was used when data failed the test of homogeneity of variance. When the one-way ANOVA indicated a significant difference between the sites, a test of least significant difference (LSD) was applied to identify which site(s) differed. When the Kruskal-Wallis test indicated significant differences between sites, this was further investigated through comparing the data per pair of sites using the Mann-Whitney U test.

Patina per site

			site			Total
			Bemerton	Milford Hill	Woodgreen	
Patination	none	Count	0	7	11	18
		Expected Count	2.2	6.7	9.1	18.0
	some	Count	8	83	109	200
		Expected Count	24.1	74.5	101.4	200.0
	moderate	Count	60	217	369	646
		Expected Count	77.8	240.8	327.4	646.0
	heavy	Count	69	134	125	328
		Expected Count	39.5	122.2	166.2	328.0
	very heavy	Count	14	26	21	61
		Expected Count	7.4	22.7	30.9	61.0
Total		Count	151	467	635	1253
		Expected Count	151.0	467.0	635.0	1253.0

Chi-Square Tests

	Value	df	Asymp. Sig. (2-sided)
Pearson Chi-Square	69.583 ^a	8	.000
Likelihood Ratio	71.713	8	.000
Linear-by-Linear Association	47.637	1	.000
N of Valid Cases	1253		

a. 1 cells (6.7%) have expected count less than 5. The minimum expected count is 2.17.

Staining per site

			site			Total
			Bemerton	Milford Hill	Woodgreen	
Staining	none	Count	0	6	6	12
		Expected Count	1.4	4.5	6.1	12.0
	some	Count	48	174	105	327
		Expected Count	39.4	121.9	165.7	327.0
	moderate	Count	76	230	255	561
		Expected Count	67.6	209.1	284.3	561.0
	heavy	Count	21	45	180	246
		Expected Count	29.6	91.7	124.7	246.0
	very heavy	Count	6	12	89	107
		Expected Count	12.9	39.9	54.2	107.0
Total		Count	151	467	635	1253
		Expected Count	151.0	467.0	635.0	1253.0

Chi-Square Tests

	Value	df	Asymp. Sig. (2-sided)
Pearson Chi-Square	150.865 ^a	8	.000
Likelihood Ratio	160.422	8	.000
Linear-by-Linear Association	91.986	1	.000
N of Valid Cases	1253		

a. 2 cells (13.3%) have expected count less than 5. The minimum expected count is 1.45.

Abrasion per site

			site			Total
			Bemerton	Milford Hill	Woodgreen	
worked	Fresh	Count	3	6	25	34
		Expected Count	4.1	12.7	17.2	34.0
	Slightly	Count	15	119	151	285
		Expected Count	34.3	106.2	144.4	285.0
	Rolled	Count	82	258	350	690
		Expected Count	83.2	257.2	349.7	690.0
	Heavily	Count	51	84	109	244
		Expected Count	29.4	90.9	123.7	244.0
Total	Count		151	467	635	1253
	Expected Count		151.0	467.0	635.0	1253.0

Chi-Square Tests

	Value	df	Asymp. Sig. (2-sided)
Pearson Chi-Square	38.188 ^a	6	.000
Likelihood Ratio	38.730	6	.000
Linear-by-Linear Association	20.352	1	.000
N of Valid Cases	1253		

a. 1 cells (8.3%) have expected count less than 5. The minimum expected count is 4.10.

Breakage per site

			site			Total
			Bemerton	Milford Hill	Woodgreen	
Broken	No	Count	116	323	462	901
		Expected Count	108.6	335.8	456.6	901.0
	Yes	Count	27	102	112	241
		Expected Count	29.0	89.8	122.1	241.0
	NID	Count	8	42	61	111
		Expected Count	13.4	41.4	56.3	111.0
Total		Count	151	467	635	1253
		Expected Count	151.0	467.0	635.0	1253.0

Chi-Square Tests

	Value	df	Asymp. Sig. (2-sided)
Pearson Chi-Square	6.266 ^a	4	.180
Likelihood Ratio	6.575	4	.160
Linear-by-Linear Association	.601	1	.438
N of Valid Cases	1253		

a. 0 cells (0.0%) have expected count less than 5. The minimum expected count is 13.38.

Cortex retention per site

			site			Total
			Bemerton	Milford Hill	Woodgreen	
Cortex retention	NA	Count	35	66	195	296
		Expected Count	35.7	110.3	150.0	296.0
	0-25%	Count	83	234	260	577
		Expected Count	69.5	215.1	292.4	577.0
	25-50%	Count	23	117	134	274
		Expected Count	33.0	102.1	138.9	274.0
	50-75%	Count	4	36	28	68
		Expected Count	8.2	25.3	34.5	68.0
	>75%	Count	3	14	18	35
		Expected Count	4.2	13.0	17.7	35.0
	NID	Count	3	0	0	3
		Expected Count	.4	1.1	1.5	3.0
	Total	Count	151	467	635	1253
		Expected Count	151.0	467.0	635.0	1253.0

Chi-Square Tests

	Value	df	Asymp. Sig. (2-sided)
Pearson Chi-Square	74.720 ^a	10	.000
Likelihood Ratio	67.681	10	.000
Linear-by-Linear Association	5.889	1	.015
N of Valid Cases	1253		

a. 4 cells (22.2%) have expected count less than 5. The minimum expected count is .36.

→ Not suitable for Chi-Square test.

Cortex location per site

			site			Total
			Bemerton	Milford Hill	Woodgreen	
C-location	NA	Count	36	66	197	299
		Expected Count	36.0	111.4	151.5	299.0
	Butt	Count	6	14	37	57
		Expected Count	6.9	21.2	28.9	57.0
	Tip	Count	3	2	6	11
		Expected Count	1.3	4.1	5.6	11.0
	Butt/tip	Count	0	0	1	1
		Expected Count	.1	.4	.5	1.0
	Side	Count	9	22	32	63
		Expected Count	7.6	23.5	31.9	63.0
	Body	Count	65	176	216	457
		Expected Count	55.1	170.3	231.6	457.0
	Multiple	Count	32	186	136	354
		Expected Count	42.7	131.9	179.4	354.0
	NID	Count	0	1	10	11
		Expected Count	1.3	4.1	5.6	11.0
Total		Count	151	467	635	1253
		Expected Count	151.0	467.0	635.0	1253.0

Chi-Square Tests

	Value	df	Asymp. Sig. (2-sided)
Pearson Chi-Square	87.110 ^a	14	.000
Likelihood Ratio	89.648	14	.000
Linear-by-Linear Association	19.129	1	.000
N of Valid Cases	1253		

7 cells (29.2%) have expected count less than 5. The minimum expected count is .12.

→ Not suitable for Chi-Square test.

Assemblage per site

			site			Total
			Bemerton	Milford Hill	Woodgreen	
artefact	Bifaces	Count	100	347	389	836
		Expected Count	100.7	311.6	423.7	836.0
	Flakes	Count	39	91	137	267
		Expected Count	32.2	99.5	135.3	267.0
	Cores	Count	0	5	5	10
		Expected Count	1.2	3.7	5.1	10.0
	Misc.	Count	12	24	104	140
		Expected Count	16.9	52.2	70.9	140.0
Total	Count		151	467	635	1253
	Expected Count		151.0	467.0	635.0	1253.0

Chi-Square Tests

	Value	df	Asymp. Sig. (2-sided)
Pearson Chi-Square	42.726 ^a	6	.000
Likelihood Ratio	45.822	6	.000
Linear-by-Linear Association	22.008	1	.000
N of Valid Cases	1253		

2 cells (16.7%) have expected count less than 5. The minimum expected count is 1.21.

Ranks

	site	N	Mean Rank	Sum of Ranks
artefact	Bemerton	151	328.43	49593.50
	Milford Hill	467	303.38	141677.50
	Total	618		

Test Statistics^a

	artefact
Mann-Whitney U	32399.500
Wilcoxon W	141677.500
Z	-1.916
Asymp. Sig. (2-tailed)	.055

Grouping Variable: site

Ranks

	site	N	Mean Rank	Sum of Ranks
artefact	Bemerton	151	369.30	55764.50
	Woodgreen	635	399.25	253526.50
	Total	786		

Test Statistics^a

	artefact
Mann-Whitney U	44288.500
Wilcoxon W	55764.500
Z	-1.688
Asymp. Sig. (2-tailed)	.091

Grouping Variable: site

Ranks

	site	N	Mean Rank	Sum of Ranks
artefact	Milford Hill	467	503.29	235036.50
	Woodgreen	635	586.96	372716.50
	Total	1102		

Test Statistics^a

	artefact
Mann-Whitney U	125758.500
Wilcoxon W	235036.500
Z	-5.185
Asymp. Sig. (2-tailed)	.000

Grouping Variable: site

Blank type of all artefacts per site

			site			Total
			Bemerton	Milford Hill	Woodgreen	
Blank type	NA	Count	77	141	326	544
		Expected Count	65.6	202.8	275.7	544.0
Possible cobble		Count	15	20	78	113
		Expected Count	13.6	42.1	57.3	113.0
Nodule		Count	56	296	212	564
		Expected Count	68.0	210.2	285.8	564.0
Flake		Count	3	10	19	32
		Expected Count	3.9	11.9	16.2	32.0
Total		Count	151	467	635	1253
		Expected Count	151.0	467.0	635.0	1253.0

Chi-Square Tests

	Value	df	Asymp. Sig. (2-sided)
Pearson Chi-Square	106.417 ^a	6	.000
Likelihood Ratio	108.179	6	.000
Linear-by-Linear Association	14.833	1	.000
N of Valid Cases	1253		

1 cells (8.3%) have expected count less than 5. The minimum expected count is 3.86.

Blank type of bifaces per site

			site			Total
			Bemerton	Milford Hill	Woodgreen	
Blank type	NA	Count	57	106	140	303
		Expected Count	43.6	150.8	108.6	303.0
Possible cobble		Count	6	13	18	37
		Expected Count	5.3	18.4	13.3	37.0
Nodule		Count	35	219	80	334
		Expected Count	48.1	166.3	119.7	334.0
Flake		Count	2	8	11	21
		Expected Count	3.0	10.5	7.5	21.0
Total		Count	100	346	249	695
		Expected Count	100.0	346.0	249.0	695.0

Chi-Square Tests

	Value	df	Asymp. Sig. (2-sided)
Pearson Chi-Square	65.877 ^a	6	.000
Likelihood Ratio	66.804	6	.000
Linear-by-Linear Association	3.900	1	.048
N of Valid Cases	695		

1 cells (8.3%) have expected count less than 5. The minimum expected count is 3.02.

Artefact shape per site

Test of Homogeneity of Variances

	Levene Statistic	df1	df2	Sig.
L	7.899	2	530	.000*
B	1.212	2	530	.298
T	.295	2	530	.745
Weight	9.031	2	530	.000*
Refinement (T/B)	3.322	2	530	.037*
Tip refinement (T2/L)	1.090	2	530	.337
Elongation(B/L)	1.012	2	530	.364
Edge Shape (B2/B1)	.291	2	530	.748
Profile shape (T2/T1)	.409	2	530	.665
pointedness (L1/L)	.069	2	530	.933

* Tested using Kruskal-Wallis

ANOVA

		Sum of Squares	df	Mean Square	F	Sig.
L	Between Groups	76032.198	2	38016.099	50.425	.000*
	Within Groups	399570.654	530	753.907		
	Total	475602.852	532			
B	Between Groups	4903.090	2	2451.545	13.551	.000
	Within Groups	95882.086	530	180.910		
	Total	100785.176	532			
T	Between Groups	4139.684	2	2069.842	24.525	.000
	Within Groups	44729.887	530	84.396		
	Total	48869.571	532			
Weight	Between Groups	1626685.386	2	813342.693	25.423	.000*
	Within Groups	16955816.476	530	31992.107		
	Total	18582501.862	532			
Refinement (T/B)	Between Groups	.265	2	.133	10.852	.000*
	Within Groups	6.481	530	.012		
	Total	6.746	532			
Tip refinement (T2/L)	Between Groups	.076	2	.038	19.822	.000
	Within Groups	1.019	530	.002		
	Total	1.096	532			
Elongation(B/L)	Between Groups	1.016	2	.508	40.399	.000
	Within Groups	6.667	530	.013		
	Total	7.684	532			

Edge Shape (B2/B1)	Between Groups	.440	2	.220	6.177	.002
	Within Groups	18.894	530	.036		
	Total	19.335	532			
Profile shape (T2/T1)	Between Groups	1.135	2	.568	16.399	.000
	Within Groups	18.344	530	.035		
	Total	19.479	532			
pointedness (L1/L)	Between Groups	.105	2	.052	4.658	.010
	Within Groups	5.949	530	.011		
	Total	6.053	532			

* Kruskal Wallis test

Ranks

site		N	Mean Rank
L	Bemerton	72	243.23
	Milford Hill	215	341.63
	Woodgreen	246	208.73
	Total	533	
Weight	Bemerton	72	251.58
	Milford Hill	215	324.41
	Woodgreen	246	221.33
	Total	533	
Refinement (T/B)	Bemerton	72	221.89
	Milford Hill	215	307.01
	Woodgreen	246	245.23
	Total	533	

Test Statistics^{a,b}

	Lenght	weight	Refinement (T/B)
Chi-Square	87.416	52.231	25.606
df	2	2	2
Asymp. Sig.	.000	.000	.000

a. Kruskal Wallis Test

b. Grouping Variable: site

Roe (1968) categories per site

			site			Total
			Bemerton	Milford Hill	Woodgreen	
ROE types	Pointed	Count	29	106	121	256
		Expected Count	34.6	101.9	119.5	256.0
	Ovate	Count	35	92	114	241
		Expected Count	32.6	95.9	112.5	241.0
	Cleaver	Count	7	11	10	28
		Expected Count	3.8	11.1	13.1	28.0
Total	Count		71	209	245	525
	Expected Count		71.0	209.0	245.0	525.0

Chi-Square Tests

	Value	df	Asymp. Sig. (2-sided)
Pearson Chi-Square	4.905 ^a	4	.297
Likelihood Ratio	4.467	4	.346
Linear-by-Linear Association	1.979	1	.159
N of Valid Cases	525		

1 cells (11.1%) have expected count less than 5. The minimum expected count is 3.79.

Blank type per biface type

			ROE			Total
			Pointed	Ovate	Cleaver	
Blank type	NA	Count	95	132	10	237
		Expected Count	115.6	108.8	12.6	237.0
Possible cobble		Count	10	14	4	28
		Expected Count	13.7	12.9	1.5	28.0
Nodule		Count	141	88	11	240
		Expected Count	117.0	110.2	12.8	240.0
Flake		Count	10	7	3	20
		Expected Count	9.8	9.2	1.1	20.0
Total		Count	256	241	28	525
		Expected Count	256.0	241.0	28.0	525.0

Chi-Square Tests

	Value	df	Asymp. Sig. (2-sided)
Pearson Chi-Square	28.102 ^a	6	.000
Likelihood Ratio	25.747	6	.000
Linear-by-Linear Association	8.323	1	.004
N of Valid Cases	525		

2 cells (16.7%) have expected count less than 5. The minimum expected count is 1.07.

Appendix 43 Average artefact size and shape of per abrasion category

	BEMERTON					Significance
	Fresh (N=3) Mean	Slightly rolled (N=7) Mean	Rolled (N=35) Mean	Very rolled (N=26) Mean	Total (N=71) Mean	
Length	128.04 ± 15.44	119.07 ± 31.45	95.00 ± 20.90	106.02 ± 24.34	102.80 ± 24.57	0.014
Breadth	74.89 ± 4.00	74.59 ± 10.84	66.38 ± 14.30	74.61 ± 13.21	70.56 ± 13.76	0.092
Thickness	39.11 ± 5.26	34.58 ± 10.30	28.82 ± 6.80	34.29 ± 9.06	31.83 ± 8.45	0.019
Weight	346.50 ± 40.08	291.33 ± 191.99	197.38 ± 119.47	318.18 ± 189.55	257.18 ± 163.09	0.011*
Refinement (T/B)	0.52 ± 0.06	0.46 ± 0.10	0.44 ± 0.08	0.46 ± 0.09	0.45 ± 0.09	0.418
Tip refinement (T1/L)	0.15 ± 0.05	0.13 ± 0.03	0.18 ± 0.04	0.21 ± 0.04	0.18 ± 0.05	< 0.001
Elongation (B/L)	0.59 ± 0.10	0.64 ± 0.09	0.71 ± 0.13	0.72 ± 0.11	0.70 ± 0.12	0.165
Edge Shape (B1/B2)	0.82 ± 0.15	0.59 ± 0.14	0.74 ± 0.19	0.83 ± 0.20	0.76 ± 0.20	0.027
Profile shape (T1/T1)	0.62 ± 0.05	0.57 ± 0.22	0.73 ± 0.18	0.82 ± 0.19	0.74 ± 0.20	0.015
Pointedness (L1/L)	0.45 ± 0.18	0.28 ± 0.05	0.39 ± 0.09	0.40 ± 0.11	0.39 ± 0.10	0.033

Table A43.1 Average size and shape of artefacts from Bemerton (the significance was tested using one-way ANOVA. Results with *are analysed using Kruskal-Wallis test).

	MILFORD HILL					Significance
	Fresh (N=4) Mean	Slightly rolled (N=59) Mean	Rolled (N=102) Mean	Very rolled (N=44) Mean	Total (N=209) Mean	
Length	148.32 ± 21.39	129.51 ± 30.36	123.20 ± 32.48	112.92 ± 29.23	123.30 ± 31.59	0.022
Breadth	82.70 ± 5.32	73.28 ± 12.53	73.54 ± 15.27	72.85 ± 12.65	73.50 ± 13.86	0.602
Thickness	40.10 ± 7.19	37.41 ± 7.38	38.27 ± 10.33	36.80 ± 10.00	37.75 ± 9.43	0.782
Weight	412.93 ± 105.89	331.56 ± 171.48	366.53 ± 228.80	333.41 ± 210.03	350.58 ± 208.00	0.628
Refinement (T/B)	0.49 ± 0.09	0.51 ± 0.08	0.52 ± 0.11	0.51 ± 0.12	0.52 ± 0.10	0.768
Tip refinement (T1/L)	0.12 ± 0.06	0.13 ± 0.03	0.16 ± 0.04	0.19 ± 0.04	0.16 ± 0.05	<0.001*
Elongation (B/L)	0.56 ± 0.05	0.58 ± 0.08	0.61 ± 0.10	0.67 ± 0.12	0.61 ± 0.10	<0.001*
Edge Shape (B1/B2)	0.55 ± 0.18	0.61 ± 0.17	0.70 ± 0.18	0.74 ± 0.19	0.68 ± 0.18	<0.001
Profile shape (T1/T2)	0.58 ± 0.33	0.56 ± 0.17	0.63 ± 0.18	0.70 ± 0.18	0.63 ± 0.19	<0.001
Pointedness (L1/L)	0.27 ± 0.09	0.32 ± 0.11	0.35 ± 0.11	0.36 ± 0.11	0.34 ± 0.11	0.044

Table A43.2 Average size and shape of artefacts from Milford Hill (the significance was tested using one-way ANOVA. Results with *are analysed using Kruskal-Wallis test).

WOODGREEN							Significance
	Fresh (N=10)	Slightly rolled (N=48)	Rolled (N=139)	Very rolled (N=47)	Total (N=245)		
	Mean	Mean	Mean	Mean	Mean		
Length	98.36 ± 30.45	100.39 ± 28.04	95.66 ± 24.22	102.90 ± 18.46	98.10 ± 24.35	0.304	
Breadth	63.80 ± 14.97	65.04 ± 14.08	67.53 ± 12.19	70.04 ± 11.12	67.37 ± 12.55	0.202	
Thickness	30.62 ± 7.61	32.25 ± 9.62	31.63 ± 9.60	32.72 ± 7.54	31.92 ± 9.13	0.861	
Weight	184.74 ± 119.84	225.04 ± 179.39	226.60 ± 154.05	266.56 ± 131.22	232.27 ± 154.41	0.315	
Refinement (T/B)	0.50 ± 0.14	0.50 ± 0.15	0.47 ± 0.12	0.47 ± 0.09	0.48 ± 0.12	0.681*	
Tip refinement (T1/L)	0.16 ± 0.05	0.17 ± 0.05	0.19 ± 0.04	0.20 ± 0.03	0.18 ± 0.04	0.002	
Elongation (B/L)	0.66 ± 0.10	0.67 ± 0.12	0.73 ± 0.12	0.69 ± 0.09	0.70 ± 0.12	0.006	
Edge Shape (B1/B2)	0.70 ± 0.29	0.66 ± 0.22	0.72 ± 0.19	0.75 ± 0.14	0.72 ± 0.20	0.094*	
Profile shape (T1/T2)	0.65 ± 0.30	0.65 ± 0.16	0.70 ± 0.18	0.77 ± 0.20	0.70 ± 0.19	0.011	
Pointedness (L1/L)	0.36 ± 0.15	0.33 ± 0.10	0.36 ± 0.10	0.39 ± 0.11	0.36 ± 0.11	0.040	

Table A43.3 Average size and shape of artefacts from Woodgreen (the significance was tested using one-way ANOVA. Results with *are analysed using Kruskal-Wallis test).

Appendix 44 Groups of artefacts from Bemerton, Milford Hill and Woodgreen in various conditions



Stained and abraded bifaces from Bemerton.



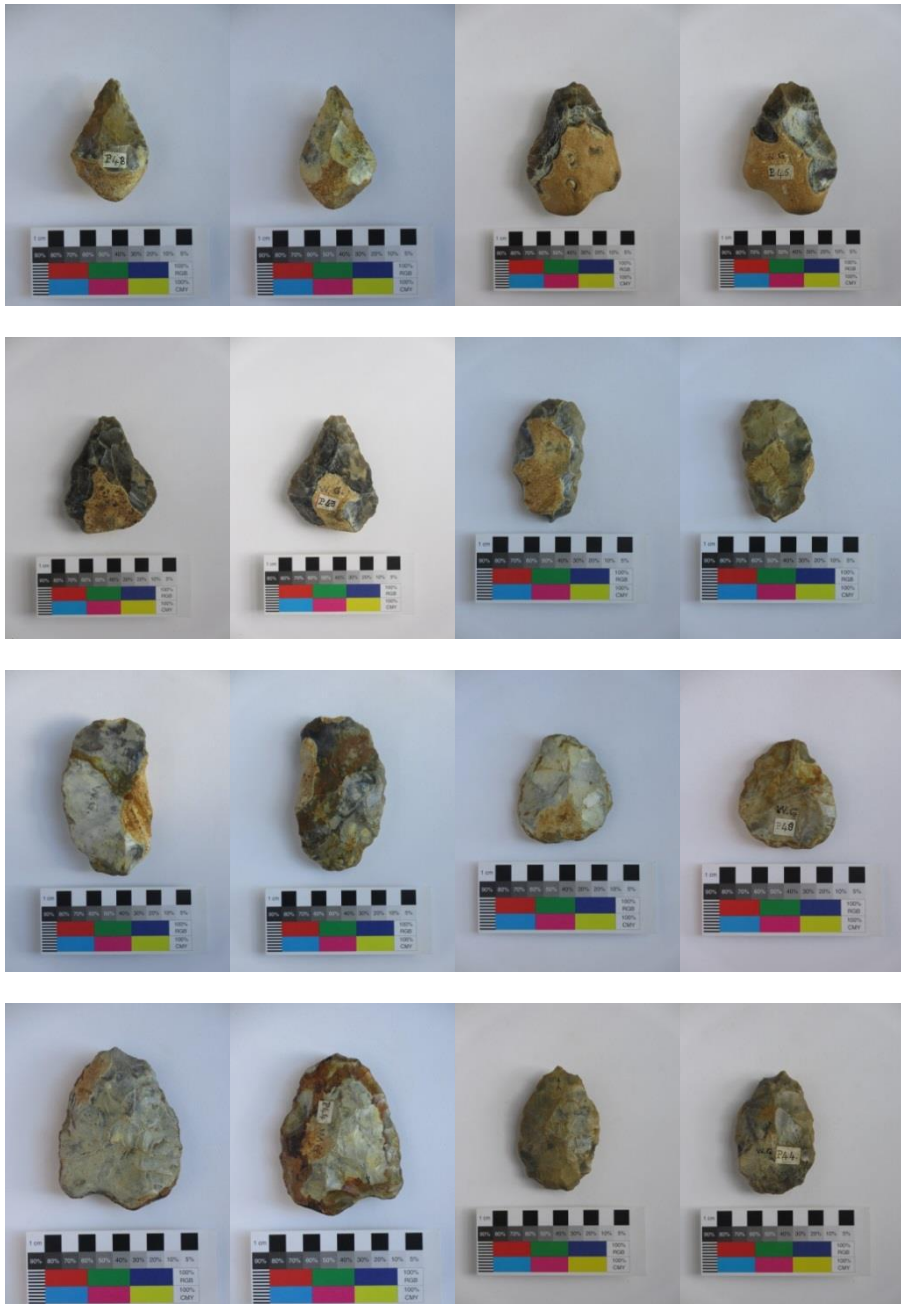
Moderately to heavily patinated bifaces from Bemerton.



Slightly to moderately patinated bifaces from Milford Hill



Stained bifaces from Milford Hill



Limitedly stained and moderately patinated bifaces from Woodgreen.



Patinated, stained and iron-manganese concreted bifaces from Woodgreen.